

NATURAL DAYLIGHT
AND
THE SIMULATION OF ITS EFFECTS UPON STOMATA

by
Jonathan Hughes, B.Sc.(Lond.)

Thesis submitted to the
University of Nottingham
for the degree of Doctor of Philosophy,
May, 1983.



CONTENTS

	Page
Abstract.....	iv
List of Principal Abbreviations.....	v
List of Tables.....	vii
List of Figures.....	ix
Acknowledgements.....	xiii
 <u>SECTION 1: Natural Daylight</u>	 1
1.1 Introduction and Literature Review.....	2
general.....	2
daytime.....	4
twilight.....	21
1.2 Materials and Methods.....	34
instrumentation.....	34
study areas.....	39
presentation.....	44
figures.....	47
1.3 Results and Discussion.....	52
(i) Incident light.....	52
general.....	52
daytime.....	53
twilight.....	59
tables.....	65
figures.....	76
(ii) Oak shadelight.....	90
light environment.....	90
canopy effects.....	98
tables.....	108
figures.....	110
(iii) Sugar beet shadelight.....	139
tables.....	147
figures.....	148
1.4 Conclusions.....	168

<u>SECTION 2: Stomatal development</u>	174
2.1 Introduction and Literature Review.....	175
epidermis.....	175
gaseous diffusion.....	176
stomatal morphogenesis and gas exchange.....	180
nastic stomatal responses.....	186
2.2 Materials and Methods.....	192
growth cabinet.....	192
gas exchange.....	199
experimental techniques.....	203
figures.....	207
2.3 Results.....	225
morphology.....	225
gas exchange.....	232
tables.....	236
2.4 Discussion.....	254
2.5 Conclusions.....	261
 <u>Section 3: Final Discussion and Conclusions</u>	 265
 Appendix I: FAWKES program.....	 274
Appendix II: CALIB and SUGAR programs.....	284
 Bibliography.....	 292

ABSTRACT

The spectral composition of natural daylight was examined using horizontal planar receptor surfaces. During the day, incident spectra were remarkably uniform. Particular attention was paid to physiologically important variables. The mean 660:730 nm photon fluence ratio (R:FR) was 1.15, corresponding to a phytochrome photoequilibrium of 0.53, but in late winter R:FR was lower than in late summer (ca. 1.0 and 1.25 respectively). The mean blue : red ratio (0.86) was strongly affected by cloud cover. The light environment of shade habitats was also examined. Under cloudy conditions in an oak woodland, R:FR fell to ca. 0.55 during the leafy phase, but higher values (ca. 0.8) were recorded in late summer as a result of the seasonal trend in incident R:FR. Reflectance and transmittance spectra and pigment content of the leaves and the transmittance of the canopy were measured. Beneath a dense sugar beet canopy, R:FR was well-correlated with canopy transmittance and fell to very low levels (ca. 0.06). However, even this would not sustain a classical "high irradiance response", so it is unlikely to be important under natural conditions.

In all three habitats, R:FR was lower and the blue : red ratio higher during twilight than during the day, but the latter was much less affected by the canopies. However, fluence rate was much more reliable as potential source of photoperiodic time signals. The involvement of phytochrome and other photoreceptors is discussed.

Leaf and stomatal morphogenesis in Chenopodium album L. was studied using a high irradiance growth cabinet. Reduced fluence rates of white or blue light produced larger leaves but had no effect on stomatal index (SI) while supplementary far-red reduced SI but had no effect on leaf area. Thus, both factors affect stomatal density. However, no differences in gas exchange characteristics were detected.

A flexible computer graphics program for data plotting is also described.

LIST OF PRINCIPAL ABBREVIATIONS

Roman

A	net photosynthetic rate; Amperes
ANOVAR	Analysis of variance
B:R	ratio of fluence rates of blue (410-500 nm) and red (610-700 nm) light
CD	epidermal cell density = density of undiffer- entiated epidermal cells + density of stomata
Ca	ambient concentration of water vapour
Ca'	" " " carbon dioxide
Ci	intercellular " " water vapour
Ci'	" " " carbon dioxide
E	transpiration rate
G	total diffusive conductance to water vapour
G'	" " " " carbon dioxide
GMT	Greenwich mean time
ga	atmospheric (boundary layer) conductance to water vapour
gc	cuticular conductance to water vapour
gs	stomatal " " " "
I	total photon fluence rate of incident light measured on horizontal plane
I _s	total photon fluence rate of incident light measured on a sphere
i	fractional incident fluence rate measured on horizontal plane
i'	fractional incident fluence rate measured perpendicularly to ray
k	extinction (absorption) coefficient
LAR	leaf area ratio (total leaf area : total biomass)
l	leaf area index

log R	common logarithm of fluence rate of red light (610-700 nm)
PAR	photosynthetically active radiation (400-700 nm)
Pr	the form of phytochrome predominantly absorbing red light
Pfr	the form of phytochrome predominantly absorbing far-red light
P _o	probability that the difference is due to chance alone (the null hypothesis)
RPA	relative pore area (ratio of maximum stomatal pore area to leaf area)
SD	stomatal density
SI	stomatal index
SLA	specific leaf area
SPD	spectral photon distribution
SPFR	spectral photon fluence rate
s	scattering coefficient
t	time

Greek

α	vertical angular distance of a point above the horizon
α_s	vertical angular distance of the sun above the horizon
β	horizontal angular distance of a point clockwise from due north
β_s	horizontal angular distance of the sun clockwise from due north
λ	wavelength
\mathfrak{z}	ratio of spectral photon fluence rates in 655-665 nm and 725-735 nm wavebands
ϕ	phytochrome photoequilibrium ([Pfr] : [Pr + Pfr], assuming maximum value of 0.75)
ϕ_c	calculated photoequilibrium

LIST OF TABLES

	PAGE
Table 1 Mean \overline{J} values for incident daylight	65
Table 2 " $\phi_c\%$ " " " "	67
Table 3 " B:R ratio " " " "	69
Table 4 Effect of cloud cover on PAR, \overline{J} and B:R ratio of incident light	71
Table 5 Effect of recording day and solar angle on \overline{J} , ϕ_c and B:R ratio of incident light during daytime	72
Table 6 Effect of recording day and solar angle on \overline{J} , ϕ_c and B:R ratio of incident light during twilight	73
Table 7 Mean log R values of incident daylight	74
Table 8 Leaf senescence of trees near shadelight recording station	108
Table 9 Effect of recording day and solar angle on \overline{J} , ϕ_c and B:R ratio of oak shadelight	109
Table 10 Effect of recording day and solar angle on \overline{J} , ϕ_c and B:R ratio of sugar beet shadelight	147
Table 11 Effect of differences in PAR fluence rate and supplementary far-red light on upper and lower epidermes of leaf 5 (Experiment I)	236
Table 12 Effect of differences in PAR fluence rate and supplementary far-red light on upper and lower epidermes of leaf 7 (Experiment I)	237

Table 13	Effect of differences in PAR fluence rate and supplementary far-red on leaf area, SLA and pigment content of leaves 5 and 7 (Experiment I)	238
Table 14	Effect of different levels of supplementary far-red light at high PAR fluence rate on upper and lower epidermes of leaf 9 (Experiment II)	239
Table 15	Effect of different levels of supplementary far-red light at high PAR fluence rate on leaf area, SLA, stomatal size and pigment content of leaf 9 (Experiment II)	241
Table 16	Effect of different levels of supplementary far-red light at low PAR fluence rate on leaf area and stomatal size and on upper and lower epidermes of leaf 3 (Experiment III)	242
Table 17	Effect of different levels of supplementary far-red light at low PAR fluence rate on leaf area and on upper and lower epidermes of leaf 5 (Experiment III)	244
Table 18	Effect of different levels of supplementary far-red light at low PAR fluence rate on leaf area and on upper and lower epidermes of leaf 7 (Experiment III)	246
Table 19	Effect of different fluence rates of blue light on upper and lower epidermes of leaf 6 (Experiment IV)	248
Table 20	Effect of different fluence rates of blue light on plant height, on petiole length, area, biomass and SLA of leaf 6, and on pigment content of leaf 8 (Experiment IV)	250
Table 21	Effect of dim blue and red light on the kinetics of stomatal opening; maxima, minima and stable values of stomatal conductance and other gas exchange parameters (Experiment V)	252
Table 22	Effect of light environment during growth on stable values of stomatal conductance and other gas exchange parameters (Experiment VI)	253

	LIST OF FIGURES	PAGE
Figure 1	Spherical geometry of natural radiation	47
Figure 2	Plan of Outwoods study area	49
Figure 3	Hemispherical photograph of bare oak canopy, 21 January, 1981; the grid describes the solar track for the whole year	49
Figure 4	Photograph of tree 4 from which sun and shade leaves were removed for pigment and optical assays	50
Figure 5	System used for determining optical properties of oak leaves	51
Figure 6	SPD recordings at Outwoods, 1980-81	77
Figure 7	" " " Sutton Bonnington, 1981	78
Figures 8 - 18	Relative SPFR surfaces describing incident light at Sutton Bonnington 1979-82	79 ~84
Figure 19	Relative SPD of incident light according to planar and spherical receptor geometry, 9 June 1982 (mean for $\alpha_s < 15^\circ$)	85
Figure 20	$\overline{3}$ vs. α_s for incident light (data from Outwoods and Sutton Bonnington)	86
Figure 21	$\overline{d_c}$ vs. α_s for incident light (data from Outwoods and Sutton Bonnington)	86
Figure 22	B:R ratio vs. α_s for incident light (data from Outwoods and Sutton Bonnington)	87
Figure 23	$\log R$ vs. α_s for incident light (data from Outwoods and Sutton Bonnington)	87
Figure 24	SPDs recorded on 12 April 1982 under broken cloud (normalised at 660 nm)	88
Figure 25	SPDs recorded on 7 July 1981 under cloudy and clear skies at $\alpha_s = 40^\circ$ and during twilight	88
Figure 26	Seasonal variation in red : far-red ratio	89
Figures 27 - 34	Relative SPFR surfaces describing shadelight in the oak woodland; April 1980 - January 1981	110 ~114
Figure 35	$\overline{3}$ vs. α_s for each day of recording in the oak woodland	116

Figure 36 ϕ_c <u>vs.</u> α , for each day of recording in the oak woodland	117
Figure 37 B:R ratio <u>vs.</u> α , for each day of recording in the oak woodland	118
Figure 38 log R <u>vs.</u> α , for each day of recording in the oak woodland	119
Figure 39 $\bar{\phi}$ (mean for $15^\circ < \alpha < 30^\circ$) <u>vs.</u> time during the canopy cycle in the oak woodland	121
Figure 40 ϕ_c (mean for $15^\circ < \alpha < 30^\circ$) <u>vs.</u> time during the canopy cycle in the oak woodland	121
Figure 41 B:R ratio (mean for $15^\circ < \alpha < 30^\circ$) <u>vs.</u> time during the canopy cycle in the oak woodland	123
Figure 42 log R (mean for $15^\circ < \alpha < 30^\circ$) <u>vs.</u> time during the canopy cycle in the oak woodland	123
Figure 43 Mean transmittance spectrum of leafless oak canopy, 25 April 1980	125
Figure 44 Mean transmittance spectrum of leafless oak canopy, 21 January 1981	125
Figures 45 & 46 Oak canopy and leaf transmittance and reflectance spectra, 28 May 1980	126
Figures 47 & 48 Oak canopy and leaf transmittance and reflectance spectra 4 July 1980	127
Figures 49 & 50 Oak canopy and leaf transmittance and reflectance spectra 13 August 1980	128
Figures 51 & 52 Oak canopy and leaf transmittance and reflectance spectra 16 September 1980	129
Figures 53 & 54 Oak canopy and leaf transmittance and reflectance spectra 21 October 1980	130
Figures 55 & 56 Oak canopy and leaf transmittance and reflectance spectra 11 November 1980	131
Figure 57 Seasonal changes in oak leaf mean pigment content, 1980	132
Figure 58 Seasonal changes in mean oak leaf and canopy transmittance at 680 nm, 1980	134
Figure 59 Seasonal changes in mean 660 : 730 nm transmittance ratio of oak leaves and canopy.	134

Figure 60	Shadelight $\overline{3}$ vs. canopy transmittance to red light (610-700 nm)	136
Figure 61	Seasonal changes in the mean B:R transmittance ratio of oak leaves, 1980	138
Figure 62	Seasonal changes in the mean B:R transmittance ratio of the oak canopy, 1980	138
Figures 63 - 69	Relative SPFR surfaces describing shade-light in the sugar beet crop, 1981	148 ~151
Figure 70	Relative spectral sensitivity of the spectroradiometers, 7 July 1980	153
Figure 71	Mean transmittance spectrum of sugar beet canopy, 28 July 1981	153
Figure 72	Mean transmittance spectrum of sugar beet canopy, 18 August 1981	154
Figure 73	Mean transmittance spectrum of sugar beet canopy, 16 September 1981	154
Figure 74	Mean transmittance spectrum of sugar beet canopy, 29 September 1981	155
Figure 75	Mean transmittance spectrum of sugar beet canopy, 21 October 1981	155
Figure 76	Mean transmittance spectrum of sugar beet canopy, 10 November 1981	156
Figure 77	Mean transmittance spectrum of sugar beet canopy, 2 December 1981	156
Figure 78	Transmittance spectrum of typical mature sugar beet leaf ($l=1$) and calculated spectra for 0.5, 2 and 3 leaf thicknesses according to Beer's Law (cf. Figs. 71 - 77)	157
Figure 79	$\overline{3}$ vs. α_r for shadelight beneath the sugar beet crop, 1981	159
Figure 80	ϕ_c vs. α_r for shadelight beneath the sugar beet crop, 1981	160
Figure 81	B:R ratio vs. α_r for shadelight beneath the sugar beet crop, 1981	161
Figure 82	$\log R$ vs. α_r for shadelight beneath the sugar beet crop, 1981	162
Figure 83	Mean PAR transmittance of sugar beet canopy vs. time, Summer 1981	164

Figure 84 Seasonal changes in mean \bar{J} beneath sugar beet crop	166
Figure 85 Seasonal changes in mean 660 : 730 nm transmittance ratio of sugar beet canopy	166
Figure 86 Shadelight \bar{J} <u>vs.</u> canopy transmittance to red (610-700 nm) light	167
Figure 87 SPDs of light output from metal halide and tungsten halogen lamps	208
Figure 88 Growth cabinet lighting module	210
Figure 89 Transmittance spectra of CuCl_2 solutions	212
Figure 90 Infra-red transmittance <u>vs.</u> aqueous pathlength	213
Figure 91 Growth cabinet	215
Figure 92 Light distribution over floor of growth chamber	216
Figure 93 Circuit diagram of growth cabinet (east side)	218
Figure 94 System used to study leaf gas exchange	220
Figure 95 Circuit diagram of astable switch	221
Figure 96 SI and SD along transects of upper and lower epidermes of a typical <u>Chenopodium album</u> leaf	223
Figure 97 Photograph of <u>Chenopodium album</u> plants grown under different levels of supplementary far-red light at low PAR fluence rate (Experiment III, at time of harvest)	224

ACKNOWLEDGEMENTS

Throughout this project I have received generous help from many people and it is my pleasure to acknowledge this and thank them. Dr. David Morgan, Mr. Peter ffoukes and Mr. Peter Lambton of the Department of Botany, University of Leicester, contributed large quantities of time, expertise, patience and good humour to the field work at Outwoods and Sutton Bonnington. The cooperation of Mr. Joseph Wright and the Estates Department of Charnwood Borough Council at Outwoods, and of Mr. John Topham at Sutton Bonnington is also gratefully acknowledged. The design and construction of the growth cabinet relied heavily on the knowledge and skill of Mr. Leslie Heathcote; I also thank Mr. Kenneth Bambridge for his valuable contribution to this part of the project. In the computing and statistical areas, I am indebted to the staff of the Computer Graphics Centre, University of Leicester, and of the Biometry Section at Sutton Bonnington for their valuable aid. I am also grateful to the Biometry Section and Dr. Andrew Taylor for allowing me to use the word-processors, and to Mr. Christopher Bates for his help with electronic difficulties. For their many long and usually thankless hours of epidermal cell counting, I am grateful to Ms. Teresa Bowles and particularly to Ms. Julia Todd; I also thank Dr. David Crawford for providing the projection microscope.

The financial support of the Natural Environment Research Council, the Society for Experimental Biology and, latterly, the Department of Health and Social Security and Mr. Frank Whatnall of "The West Leake Pit House" is gratefully acknowledged.

In a broader context, I am grateful to my supervisor at Sutton Bonnington, Dr. Colin Black, for his encouragement and advice throughout the project, and to Professors Harry Smith and "Dick" Whittington for cooperation and support generously given. I am also much indebted to the staff of the Departments of Botany and Zoology at Royal Holloway College, London. I thank my friends for many happy hours of argument and rancour over the years, and finally I thank my parents and sister for their unfailing support and affection for well over quarter of a century.

This dissertation is dedicated to all of these people.

Jon Hughes, April 1983

"Nothing is as simple as it is"

Leslie Heathcote

SECTION 1

Natural daylight

INTRODUCTION AND LITERATURE REVIEW

General

The development in plants of a capacity to absorb light and harness its energy anabolically was a fundamental event in natural history. This process of photosynthesis transformed the telluric atmosphere from a reducing to an oxidising one, and established an ozone layer in the upper atmosphere (ca. 1×10^9 years ago) which shielded the organisms from damaging high energy solar radiation.

Efficient utilisation of light has obvious selective advantages for phototrophs. Each species is differently adapted and genetically fairly plastic, but there is always an additional element of elasticity, allowing each individual to acclime to its own environment. Acclimation allows metabolism to proceed in a much wider variety of niches than could possibly be tolerated otherwise, and it is part of the gamut of responses which maintain homeostasis (in its broadest sense).

Any system can be controlled by monitoring its output and relating its appropriate variable features to this. A "negative feedback" scheme of this sort can ideally maintain a constant output, irrespective of the input. However, any time delay in the loop results in chronic system instability, and furthermore, even if the output is affected by more than one variable, the system always responds in the same way; thus only very crude responses to complex dynamic environmental factors can occur. There are advantages in transferring at least a part of the sensory capacity from the system output itself to separate, independent receptors. In a complex homeostatic system, control loops associated with various receptors and sophisticated interpreters act at appropriate points to evoke an effective array of responses.

Such a theoretical approach to a biological system is relevant because most organisms have been found to be remarkably tolerant of environmental change or, in other words, their niche parameters are very wide. In the literature, many factors are dismissed as "non-limiting", although very few "limited" resources can be wasted simply to allow the organism to become independent of them, especially in the face of constant competition from others. The various phenomena grouped together as

photomorphogenesis ("a non-directional developmental response to a non-directional, non-periodic light stimulus" - Smith [1975]) and phototropism ("a directional growth response to a directional light stimulus" - *ibid.*) serve primarily to regulate the absorption of light required for photosynthesis, although they may have other important functions. In the context of homeostasis, when plants are grown at a range of light levels similar to those of their native habitat, photomorphogenic control can buffer their growth rate (for example, Blackman and Rutter, 1948; Warrington and Mitchell, 1976). The factor limiting growth in the higher fluence rate treatments was not, for instance, leaf area since the leaves were able to grow larger in the other treatment; larger leaves might have allowed a higher rate of total photosynthesis, but, for whatever reason, this did not occur. It might be said that light was non-limiting; alternatively, one might advocate that growth was held constant by the photomorphogenic responses.

Apart from chlorophyll, which has an ill-defined and often forgotten photomorphogenic role (see Bjorkman, 1981), the existence in green plants of two receptor pigments has been established. Sensitive to light in the far-violet to blue region of the spectrum (300 - 500 nm), "cryptochrome" is active in phototropism and several photomorphogenic responses. "Phytochrome" on the other hand is sensitive to red and far-red light (600 - 800 nm) and is involved in photomorphogenesis and photoperiodism ("a non-directional developmental response to a non-directional, periodic light stimulus" - Smith [1975]).

There is evidence that these receptors have evolved to provide useful information about the natural light environment (see Smith, 1982). However, remarkably little meteorological information is available in a suitable form to define natural daylight, whereas most of the physiological research has been carried out with scant regard to the natural situation. It was the purpose of this research to provide suitable definitive information about the characteristics of daylight in several habitats, and to investigate the photomorphogenic control of the fundamental process of gas exchange (see Section 2).

It would seem appropriate, therefore, to review the literature concerning daylight phenomena in relation to plant photobiology and vice versa. Distinct categories of "daytime" and "twilight" were recognised.

Daytime

Environmental Phenomena

The physical literature on daylight has been reviewed by Robinson [1966], Henderson [1977] and Gates [1980], while Smith [1982] has considered those factors pertinent to plant development.

At the mean orbital distance of the Earth, the Sun generates a total electromagnetic irradiance of about 1.36 Kw m^{-2} , with a photon emission maximum at about 600 nm. The perfect "black-body" spectral distribution is somewhat distorted by atomic absorption and emission in the photosphere, but as the radiation penetrates the telluric atmosphere, a number of other processes are active. Molecular oxygen, nitrogen and ozone absorb most of those wavelengths below about 350 nm, while water vapour, oxygen and carbon dioxide absorb strongly above $1 \mu\text{m}$; between these lies the atmospheric "window" through which light penetrates. Even within this, light is scattered from the direct solar beam, causing the sky to appear luminous instead of dark; indeed, skylight contributes at least 10% of the radiation received at ground level. Small molecular particles ($<100 \text{ nm}$ diameter) scatter light in proportion to λ^{-4} (Strutt, 1871), while much larger particles or droplets ($>20 \mu\text{m}$ diameter) cause wavelength-independent scattering. Scattering by particles of intermediate size is problematical, but approximately proportional to $\lambda^{-1.3}$ (Gates, 1980).

Hence, at sea level a very clear unpolluted atmosphere gives rise to a deep blue sky, but as smoke and other particulate contamination increases, longer wavelengths become included, and the sky colour becomes paler. Clouds scatter light almost non-spectrally and therefore appear white or grey. Under most circumstances, the relative depletion of the direct beam correlates with enrichment of the scattered skylight, and so, although the quantity of direct and scattered daylight is different, the overall incident spectral distribution should scarcely be affected by scattering processes. Accordingly, very little difference has been reported between spectra under clear and overcast conditions (Taylor and Kerr, 1941; Hull, 1954; Vezina and Boulter, 1966; Robertson, 1966; Federer and Tanner, 1966; Holmes and Smith, 1977a; Goldberg and Klein, 1977). However, Hadfield [1974] reported relative increases in blue and red light under

overcast skies, and Guttman [1968] found that thin cirrus clouds tended to transmit longer wavelengths better than shorter ones. In contrast, cloud cover has very large effects upon the total fluence rate; dense storm clouds may transmit less than 5% of full daylight.

On a sloping site, daylight is affected by the aspect in relation to the solar track. Recordings may be taken with the sensor either horizontal or parallel to the slope, but the orientation will affect the relative contributions of direct and scattered light to the overall spectral photon distribution (SPD). No investigations of this problem have been reported in the literature, but Pope and Lloyd [1975] found a strong correlation between fluence rate integrated over a period and the aspect of the slope when detectors were mounted horizontally at ground level. Such a situation is equivalent to shading by an opaque object.

When spectral radiation is measured beneath a leafy canopy however, large differences in spectral quality accompany changes in fluence rate (see Holmes, 1981). Zederbauer [1908] was the first to measure the latter, while Salisbury [1916] identified the biphasic character of shadelight during the canopy cycle in deciduous woodland; this phenomenon was further quantified by Atkins, Poole, and Stanbury [1937]. However, these and other studies upto the late 1950s were severely limited by technical difficulties. Development of a leafy canopy is associated with reduced transmission of all wavelengths, but particularly those in the blue and red spectral regions. Transmission is usually somewhat greater in the green and very much greater in the far-red region above 700 nm. The spectral effect is less marked under coniferous canopies (Morgan and Smith, 1981; also Zavitsovski, 1982). These findings are predictable from the optical characteristics of chlorophyll-bearing leaves (Rabideau, French, and Holt, 1946; Woolley, 1971).

Tasker and Smith [1977] investigated the SPD in several deciduous woodlands during their canopy cycle. The initial burst of leaf emergence in spring was associated with a large drop in the red : far-red ratio. This subsequently increased, for some obscure reason. The ratio declined again in the beech wood, possibly owing to a secondary burst of leaf growth, whereas the oak canopy merely stabilised. However, these changes in the canopy were not apparent from the fluence rate data, which showed

large daily variations. Similarly, Hutchinson and Matt [1977] recorded no significant changes during the leafy phase of Liriodendron tulipifera.

The effect of a leafy canopy is complicated by gaps between leaves through which light can penetrate directly. Under overcast conditions these have no spectral effect per se, and merely increase the overall transmission. When the direct solar beam is present, however, transmission is strongly bimodal over a period of time because local sunflecks are formed when the solar disc aligns with a gap in the foliage. In light wind, leaf flutter causes coruscating sunflecks which exist for as little as 0.01 s (Norman and Tanner, 1969), but in still conditions the majority of even the smallest sunflecks have a lifetime of at least two minutes. The minimum diameter of a sunfleck is given by $2h \cdot \tan(d_s/2)$, where d_s is the angular diameter of the sun (ca. 0.5°) and h is the distance from the gap to the plane on which the solar image is projected. The fluence rate within the sunfleck is constant up to its edge and is proportional to the size of the gap. However, as the gap increases in size, the fluence rate falls more gradually towards the edge and, hence, the image becomes indistinct. When the gap size equals d_s , the entire direct solar beam is able to penetrate to the plane of projection; a further increase merely expands this area and has relatively little effect on the fluence rate within it.

Although it is the radiation available to plants which is of ecological significance, the optical properties of the canopy itself are of interest. When measured beneath an absorbing layer, light from an extended source such as the sky tends to be transmitted predominantly from the region overhead, because the path length increases rapidly towards the horizon; this simple model is to some extent applicable to vegetation canopies under overcast conditions (Evans, 1966). However, under clear skies transmittance ($=$ transmitted / incident fluence rates) becomes bimodal; however, if the solar track covers a representative band of the canopy, the mean transmittance should be similar on clear and cloudy days, unless the optical properties of the canopy actually change because of wilting or heliotropism, for instance. Sunflecks are associated with very high transmittance, so this must be compensated for by low transmittance at other times. A similar reciprocity will apply to the light quality beneath a leafy canopy on sunny days. Because of

their transient nature, however, sunflecks are often avoided when recording shade SPDs under clear skies. The sampling bias thus introduced probably explains the apparently different spectral quality of light beneath a canopy under clear and cloudy conditions (Holmes and Smith, 1977b); if light quality is measured representatively, the difference vanishes (Jordan, 1969). A further prediction is that if gaps are absent, transmittance should be independent of cloud cover.

Further difficulties arise in studying canopy transmittance because the fluence rate of the incident light is subject to large and rapid change (measurements at night using stable artificial light sources have not been reported). The SPD should, ideally, be measured simultaneously inside and outside the canopy in order to calculate the transmittance spectrum, but this has not been reported hitherto. When working on crop canopies, it is possible to measure the incident and shade SPDs in rapid succession (Yocum, Allen, and Lemon, 1964; Kasperbauer, 1971; McCartney, 1975) while, in a woodland, Goodfellow and Barkham [1974] were obliged to choose a single day with exceptionally constant atmospheric conditions, and check the SPD outside the wood occasionally. Unfortunately, no study has attempted to relate the changing optical properties of the canopy to the optical properties, abundance, or pigment content of the constituent leaves. Shell, Lane, and Lang [1976] reported that leaf heliotropism might reduce mean canopy transmittance appreciably.

Light in aquatic environments (see Spence, 1981) is additionally modified by surface reflection, suspended particles, phytoplankton and dissolved organic matter in the water, and the scattering and transmittance properties of water itself.

In ^{soil}terrestrial environments, light is able to penetrate to a depth of upto about 10 mm (Woolley and Stroller, 1978). Frankland [1981] and Smith [1982] reported that the attenuation in fine soil is not neutral, but somewhat greater at shorter wavelengths. There seem to have been no reports of the optical properties of natural undisturbed soils in the literature.

At this point it is appropriate to caution the treatment of a plant as a horizontal plane which absorbs light (see 2.2). Even at the microscopic level, shading

occurs and consequently the local light environment of each photoreceptor molecule will be affected by its position. Fukshanski [1981] recently reviewed developments in the area of light propagation within leaves.

In summary, the SPD of incident light is a function of incoming solar radiation, and the optical properties of gases, small particles and clouds in the Earth's atmosphere. Local factors such as slope and aspect, opaque and leafy shade, soil composition, and water transparency may be active too. Of these, only extra-terrestrial solar radiation can be regarded as constant (but see Henderson, 1977) and only cloud cover, opaque shade and slope can have a non-spectral effect. Leafy shade has the most marked effect on spectral distribution, especially in the blue and red regions.

Physiological responses

The physiological responses shown by plants to a changing aspect of their environment are most precisely studied in the laboratory where other factors can be held constant. The tacit philosophy is that individual responses are independent and additive. In photobiology, very little is known about specific interactions between variables and our understanding of the various systems is therefore much less complete than we might like to think. The reason is simple; even in isolation, the photoresponses have proved to be remarkably complex physiologically. Some of the more important of these in the life-cycle of higher plants are considered below.

Seeds

The photocontrol of seed germination has been reviewed recently by Frankland [1981], and Morgan and Smith [1981a]. It was in germinating seeds that the definitive phytochrome-mediated response was first discovered. In the 1930s, Flint and McAlister found that lettuce achenes (Lactuca sativa cv. Grand Rapids) germinate poorly when imbibed in darkness, but most can be induced to do so by a few minutes irradiation with white or red light; far-red has the opposite effect. Subsequently it was found that the most effective wavelengths for induction and inhibition were 660 nm and 730 nm (Borthwick, Hendricks, Toole and Toole, 1954). However, if an inductive pulse is followed by a pulse of far-red light, ~~the~~ germination occurs. The sequence can be

repeated many times with the same response to the terminal light pulse (Borthwick, Hendricks, Parker, Toole and Toole, 1952). This "red / far-red reversibility of induction" is considered to be a unique action of phytochrome.

Phytochrome is thought to be involved in the control of germination of many species. A far-red absorbing form (Pfr) is generated under red light and is associated with germination; conversely, a red absorbing form (Pr) is generated when Pfr absorbs far-red light, under which conditions germination is inhibited. Following a red pulse, the time required for the response to escape from reversibility varies and probably reflects the period over which Pfr is required to initiate the subsequent metabolic events. In some species Pfr tends to revert to Pr and so a single brief red pulse is insufficient to cause germination. Conversely, in species where germination in darkness can occur, the inhibitory effect of far-red light is not permanent, implying that Pfr is present from the start of imbibition and that it reappears after photoconversion to Pr (so-called inverse reversion).

It is generally thought that the concentration of Pfr is the important variable factor in these responses and that Pr is inactive (see Mohr, 1972), but Smith [1981a] suggested that it is the ratio of Pfr to Pr or total phytochrome which is significant. As the total amount of phytochrome in dormant imbibed seeds remains constant for prolonged periods, these two possibilities cannot be distinguished in the photoblastic response. In a homeostatic system, Smith's hypothesis might be preferable because the photoequilibrium (usually designated as $\phi = [Pfr] / [Pfr + Pr]$) established would be unrelated to phytochrome concentration and, hence, more reliable. However, the "Pfr as active form" hypothesis would seem to be more feasible mechanistically. Unfortunately, very little is known about the metabolic consequences of phytochrome photoconversion.

It has been suggested that the red / far-red antagonism seen in seeds is an adaptive feature, allowing the detection of leafy canopies (via their large relative attenuation of red light) and overlying soil (via its attenuation of all wavelengths) as both can have large effects on the Pfr level. This physiological behaviour is often associated with species which form persistent seed banks in the soil which await conditions favourable to

their opportunistic life-style (Gorski, Gorska and Nowick, 1977; Grime, 1981). Even photoreversibility can be considered adaptive, as it allows the seed to recover from induction resulting from the high level of red light in a transient sunfleck. Hence, phytochrome seems admirably suited to this putative role. Fenner [1980] found that when seeds are imbibed in daylight beneath a leafy canopy, dark germination is reduced relative to unirradiated controls. It has, furthermore, been suggested that the initial light requirement is mediated by phytochrome in the developing seed (McCullough and Shropshire, 1970; Creswell and Grime, 1981).

In some species, high fluence rates of white light inhibit germination (see Smith, 1975; Frankland, 1981; Bartley and Frankland, 1982). One explanation for this is that under conditions of rapid "cycling" (interconversion of Pr and Pfr), metastable intermediates accumulate and [Pfr] declines. This hypothesis can also explain "inverse dark reversion" as a slow appearance of Pfr from an intermediate rather than Pr itself. Another hypothesis (Hartmann, 1966) implicates Pfr destruction, but this has never been shown conclusively to occur in seeds.

Etiolated seedlings

When seeds germinate in darkness, as do those of most grasses and cultivated species, the morphogenesis of the seedlings is unusual until they are irradiated with light. Such etiolated seedlings synthesise very little chlorophyll and show extreme photo- and geotropic sensitivity. In dicotyledons the leaves are also reduced in size and hyponastic; the internodes extend rapidly while the initiation of leaf primordia is inhibited (Barsch-Gollnau, Ritterbusch and Mohr, 1980). It is thought to be an adaptive response to allow seedlings to grow up through the soil into daylight. It is associated with a massive de novo synthesis of Pr; Pfr formed photochemically from this is unstable and rapidly destroyed, in contrast to seed phytochrome which appears to be stable in either form (Kendrick, Spruit and Frankland, 1969). Reversion of Pfr to Pr was once thought to be important (Butler, Lane and Siegelman, 1963) but it has since become apparent that it is absent in etiolated seedlings of many species (Hopkins and Hillman, 1965; Kendrick and Hillman, 1971)

Because of its relatively high concentration, the

properties of seedling phytochrome have been extensively studied in vivo and in vitro. Pfr and Pr absorb most strongly at 730 nm and 660 nm respectively; both have secondary absorbance peaks in the blue region. A considerable overlap occurs in the red, and consequently the maximum achievable value of ϕ is about 80% (Butler, Hendricks and Siegelman, 1964; Pratt, 1978).

Although a light pulse induces some of the responses of dark grown seedlings, prolonged irradiation is often far more effective (Mohr, 1957, 1972). Action maxima arise in the far-red and blue regions, and often red light has a persistent effect (for example, Jose and Vince-Prue, 1977; Holmes and Schäfer, 1981). However, Hartmann's [1967] action spectrum for the inhibition of lettuce hypocotyl elongation by prolonged irradiation shows little activity in the red region, but this is simply because red light elicits opposing responses in different regions of the hypocotyl (Häcker, Hartmann and Mohr, 1964). A distinct feature of these responses is that they do not saturate until much higher fluence rates are reached; hence they are the so-called high irradiance responses (HIR) (Mohr, 1972).

There is no doubt that a separate photoreceptor for blue light exists in most etiolated seedlings. The best known response is that of phototropic curvature which shows a complex fluence rate dependent action in the far-violet to blue region (see Dennison, 1979). It has been shown on a number of occasions (see Thomas, 1981; Cosgrove, 1981) that several of the photomorphogenic responses to blue light are distinct from those to red and far-red. The photoreceptor involved has been named "cryptochrome", but little is known about its chemical nature (see Senger, 1980) other than that it seems able to photoreduce b-type cytochromes, at least in vitro.

In some systems (such as anthocyanin synthesis in Sinapis alba) however, the blue light response seems to be closely associated with the HIR to far-red (Wilderman, Drumm, Schäfer and Mohr, 1978). Consequently, as phytochrome in vitro is known to absorb in both these spectral regions, numerous attempts have been made to explain the HIR wholly in terms of phytochrome action (see Mancinelli, 1980). The most important of these are summarised below.

Hartmann [1966] proposed that HIR action reflected a

conflicting need for Pfr despite its constant destruction (and the consequent gradual depletion of total phytochrome). It was suggested that the optimal response in the long term corresponded to maximal [Pfr] x time. In an elegant experiment, he deduced that the optimal ϕ was 3% in the lettuce hypocotyl, and predicted the action spectrum of the response from in vitro absorbance data. This was similar to experimental data (Hartmann, 1967) but this was probably fortuitous as Hückler, Hartmann and Mohr [1964] had found previously that different regions of the hypocotyl showed opposing responses to red light, thus nullifying its overall effect. In addition, the simple model fails to predict the fundamental fluence rate dependence of the HIR. Hartmann suggested that an excited form of Pfr was formed initially which was more potent than the relaxed form into which it fell, and that more rapid photoconversion increased the relative proportion of the excited form. Unfortunately, there is no evidence for this hypothesis. Borthwick, Hendricks, and Schneider [1969] suggested an alternative, in which a bound form of Pfr was itself capable of photoconversion by far-red light, as some responses in this region appeared to be independent of phytochrome action per se. There is no further evidence in support of this suggestion, however.

In 1974, Schäfer and Mohr analysed mathematically the kinetics of phytochrome photoconversion, synthesis, and destruction. They successfully predicted the changes in Pfr concentration following light pulses, but unexpectedly demonstrated that under prolonged irradiation it was [Pr] which varied with wavelength and fluence rate, contradicting the idea of "Pfr as active form". Schäfer [1975] subsequently developed a model involving twelve simultaneous rate equations which predicted the required changes in concentration of various forms of Pfr. Unfortunately, this model relies upon rate constants of the pelletability effect (see Quail, Marme and Schäfer, 1973), now thought to be artifactual (see Watson and Smith, 1982).

A number of characteristics of phytochrome action imply that it is associated with membranes (see Raven, 1981; Hendricks and Borthwick, 1967); these form the basis of radically different models in which phytochrome destruction has no part. Smith [1970] suggested a conceptual model involving the action of phytochrome as a photochromic permease. As it is not a predictive scheme, it is difficult to devise critical experiments to test its

validity, but it is reasonable to assume that: fluence rate dependence would vary under different conditions, explaining the induction and HIR responses; Pr would have an active role, in close agreement with the prediction of Schäfer and Mohr [1972]; the response to many light treatments would increase with increasing numbers of permease molecules, that is, phytochrome concentration. Although Smith [1980] did not consider the latter to be a feature of his model, it has been found that the HIR declines when the phytochrome concentration is lowered (Mohr, Drumm, Schmidt and Steinitz, 1979; Beggs, Holmes, Jabben and Schäfer, 1980). However, this correlation does not prove causality.

Johnson and Tasker [1979] developed a somewhat similar model involving the transport and binding of substrate to Pfr, which predicts a strong fluence rate dependence in both the far-red and red regions via their effects on the Pr-Pfr cycling rate (Johnson, 1980). Wagner and Mohr [1966] reported such dependence to be absent from the HIR of Sinapis alba in the red region. Johnson [1980] confirmed this result, but concluded that the behaviour may have been due to the induction of chlorophyll accumulation. The fluence rate dependence in blue but not far-red light should also have been affected, but this possibility was not considered. In contrast, Holmes, Beggs and Schäfer [1982] found fluence rate dependence at all photoequilibria established by wavelengths from 640 to 740 nm, with chlorophyll tending merely to reduce the effectiveness of red light. However, although phytochrome cycling is maximal at about $\phi = 50\%$, there was no sign of a response peak in this region. Instead, the authors suggested that fluence rate dependence might result from the true photoequilibrium not being achieved at low fluence rates. In Chenopodium rubrum, hypocotyl elongation was independent of cycling rate in the red region, and was not related to chlorophyll synthesis (Ritter, Wagner and Holmes, 1981).

Bearing in mind that our knowledge of phytochrome relates almost exclusively to etiolated material, Smith [1981a] proposed that the variety of responses might arise from differences in the metabolic "perception" of the photoequilibrium itself, as there is no good reason for assuming Pr to be inactive. A mechanism which permits responses to photoequilibrium alone would have advantages in homeostatic control, but how such a dynamic ratio could act independently of the active phytochrome concentration

validity, but it is reasonable to assume that: fluence rate dependence would vary under different conditions, explaining the induction and HIR responses; Pr would have an active role, in close agreement with the prediction of Schäfer and Mohr [1972]; the response to many light treatments would increase with increasing numbers of permease molecules, that is, phytochrome concentration. Although Smith [1980] did not consider the latter to be a feature of his model, it has been found that the HIR declines when the phytochrome concentration is lowered (Mohr, Drumm, Schmidt and Steinitz, 1979; Beggs, Holmes, Jabben and Schäfer, 1980). However, this correlation does not prove causality.

Johnson and Tasker [1979] developed a somewhat similar model involving the transport and binding of substrate to Pfr, which predicts a strong fluence rate dependence in both the far-red and red regions via their effects on the Pr-Pfr cycling rate (Johnson, 1980). Wagner and Mohr [1966] reported such dependence to be absent from the HIR of Sinapis alba in the red region. Johnson [1980] confirmed this result, but concluded that the behaviour may have been due to the induction of chlorophyll accumulation. The fluence rate dependence in blue but not far-red light should also have been affected, but this possibility was not considered. In contrast, Holmes, Beggs and Schäfer [1982] found fluence rate dependence at all photoequilibria established by wavelengths from 640 to 740 nm, with chlorophyll tending merely to reduce the effectiveness of red light. However, although phytochrome cycling is maximal at about $\phi = 50\%$, there was no sign of a response peak in this region. Instead, the authors suggested that fluence rate dependence might result from the true photoequilibrium not being achieved at low fluence rates. In Chenopodium rubrum, hypocotyl elongation was independent of cycling rate in the red region, and was not related to chlorophyll synthesis (Ritter, Wagner and Holmes, 1981).

Bearing in mind that our knowledge of phytochrome relates almost exclusively to etiolated material, Smith [1981a] proposed that the variety of responses might arise from differences in the metabolic "perception" of the photoequilibrium itself, as there is no good reason for assuming Pr to be inactive. A mechanism which permits responses to photoequilibrium alone would have advantages in homeostatic control, but how such a dynamic ratio could act independently of the active phytochrome concentration

seems obscure; even Smith's [1970] model seems to imply some dependence on phytochrome concentration. Interestingly, it would then predict that responses would be dependent on both ϕ and Pfr concentration.

None of the models of phytochrome action fits all the available experimental data. Smith [1970, 1975, 1981a] has argued that the simple concept of Pfr being the active form is untenable because of the sometimes paradoxical (Chon and Briggs, 1966; Hillman, 1966a; Fox and Hillman, 1967; Hillman, 1967; Klein, Edwards and Shropshire, 1967; Hopkins, 1971; Hillman, 1972; Smith, 1981b) and generally variable relationship between Pfr concentration and the known HIRs of higher plants. (Mohr [1972] documents both threshold and proportional responses to Pfr concentration). Even in 1965, Butler and Lane raised similar doubts and proposed that two different populations of phytochrome might exist, one associated with induction and the other with the HIR. This proposal has received support on several occasions as a possible explanation of various paradoxical phenomena (Wagner and Mohr, 1966; Hillman, 1967; Kendrick et al., 1969; Wetherell and Koukkari, 1970; Smith, 1975; Jose and Vince-Prue, 1977a; Mohr et al., 1979; Beggs et al., 1980).

De-etiolation

Photomorphogenesis in etiolated seedlings is physiologically complex and considerably different from that in seeds, largely as a result of a distinct HIR. This disappears quickly after irradiation with red or white light as the seedlings deetiolate and synthesise chlorophyll. Beggs et al. [1980] studied this behaviour in detail. These workers first derived a normal HIR action spectrum for the inhibition of hypocotyl extension in Sinapis alba, showing peaks in the far-red, blue, and red regions. They then investigated the effect of lowering the concentration of phytochrome by pre-irradiating with red light and allowing some Pfr destruction to occur before giving an effective reversal pulse of far-red. Such pretreatments led to a massive and simultaneous drop in the effectiveness of blue and far-red light, while that of red remained constant. Pretreatment with continuous light banished the blue and far-red effects completely, while chlorophyll accumulation was shown to be responsible for a shift in the action maximum from 660 nm to 640 nm. They concluded that the typical HIR action spectrum seen in etiolated seedlings had two components. The action of blue

and far-red light was associated with the form of phytochrome synthesised during etiolation (probably involving labile Pfr in the manner of Hartmann's [1966] hypothesis), while in the red region a response to multiple induction occurred, seemingly independent of etiolation. Mohr et al [1979] reported similar results for anthocyanin synthesis and phenyl ammonia lyase activity, except that the effectiveness of red light was enhanced by the pretreatments. Thus Butler and Lane's [1965] hypothesis may be correct in that the HIR phytochrome seems to be restricted to etiolated tissue. Results from lettuce hypocotyls (for example, Turner and Vince, 1969; Hartmann, 1967) are in conflict with this notion only because of the peculiar effects of red light on this system (see H~~ä~~cker et al., 1964).

Mature plants

The action of light in modulating the growth of green plants has received remarkably little attention despite its obvious importance. Research in this area is technically difficult because the fluence rate of natural daylight is high compared to that which can be easily generated in the laboratory (see 2.2). Although most species can grow at these lower fluence rates they are often morphologically and physiologically remote from their natural habit. It would be strange indeed if this had no effect on their photoresponses. It is difficult, therefore, to compare results from different laboratories, and the fashionable extrapolation to "the field" is unjustified in most cases.

In fact, only during the last decade has it become possible to predict relative rates of photosynthesis from simple measurements of fluence rate, and hence to balance assimilation rates under different spectral regimes. McCree [1972b] showed that when plants were grown under equal quantum fluence rates in the region between 400 and 700 nm, their rates of biomass accumulation were relatively independent of the spectral composition of the light source; this definition of photosynthetically active radiation (PAR) has been generally accepted, as other definitions appeared to be biased against shorter wavelengths. Only if the spectral distribution of the light source and the spectral quantum sensitivity of the photodetector is known, can unbiased estimates of relative photosynthetic rates be made. Stolwijk reached a similar conclusion in 1954. Gaastra [1959] provided tables of

conversion factors for various light sources and photodetectors, while McCartney [1975] found that for natural daylight the irradiance (W m^{-2}) as measured by tube solarimeters could be converted to $\mu\text{mol m}^{-2}\text{s}^{-1}$ by the multiplication factor 4.56. Differential photosynthetic rates can confound most other light effects (for example in the otherwise excellent work of van der Veen and Meijer [1959]).

Morgan and Smith [1981a] recently reviewed the literature on photomorphogenesis in green plants. Most studies have concentrated on the promotive effect of far-red light on stem elongation. Roodenburg [1940] was probably the first to suggest that far-red was important, and in 1957, Downs, Hendricks, and Borthwick demonstrated that phytochrome controlled the end-of-day photostimulation of internode elongation. In Fuchsia, a far-red pulse given immediately after the end of the photoperiod was more effective than at any other time during the night; the later the pulse was given, the smaller was the response. Also, when an end-of-day dichromatic pulse comprising various proportions of red and far-red light was given, internode extension was closely correlated with the fluence ratio (Vince-Prue, 1977).

Although these were not "daytime" responses, the results are of great significance in understanding the photocontrol of development and growth in green plants; they imply that the Pfr level established during the period of irradiation continues to exert an effect throughout the dark period. Such an inductive response is only consistent with stable photochromicity, and is in accord with the results of Beggs et al. [1980], in that the HIR per se seems to be associated with the labile Pfr of etiolated seedlings and is absent from green plants. Unfortunately, it is impossible to measure the concentrations of Pfr and Pr in green plants because the routine spectrophotometric procedures are useless in the presence of chlorophyll fluorescence, so it is not yet possible to verify these conclusions. Pratt [1982] has reviewed the recent encouraging development of alternative radioimmunoassays.

Vince-Prue [1977] also showed an essentially linear relationship between internode extension and the end-of-day phytochrome photoequilibrium as measured in etiolated tissue. However, far-red light is also effective during the photoperiod itself (Fitter and Ashmore, 1974; Holmes

and Smith, 1975, 1977c; Krizek and Ormrod, 1980). In Chenopodium album, the relationship between stem extension and photoequilibrium during the photoperiod was also linear (Morgan and Smith, 1978a). The latter workers questioned the relevance of end-of-day light treatments to events in the natural environment after finding that such regimes were much less effective than treatments applied throughout the photoperiod. They have also reported that the response is species-dependent, being very pronounced in ruderal sun plants, but almost absent in shade tolerant species (Morgan and Smith, 1979).

Supplementary far-red light given during the photoperiod has rapid effects on stem extension (Morgan and Smith, 1978b; Lecharney and Jacques, 1982) and is antagonised by red light (Morgan, O'Brien and Smith, 1980). Moreover, fluence rate does not seem to have any specific effect on the almost linear relationship which exists between stem extension and photoequilibrium (Morgan, Child and Smith, 1981), strongly implying that phytochrome is not acting in its HIR mode, but in a manner analogous to the induction response. More importantly, it indicates that phytochrome is able to sense the red : far-red ratio in a manner which is irradiance compensated.

Several other responses are thought to be mediated by phytochrome in green plants of certain species. Supplementary far-red light increased the ratios of leaf area to plant biomass, leaf area to leaf biomass, and leaf biomass to stem biomass (Young, 1975; Frankland and Letandre, 1978). The leaf morphology of the aquatic plant Hippuris vulgaris seems to be extraordinarily sensitive to far-red light (Bodkin, Spence and Weeks, 1980). Apical dominance is also affected (Tucker and Mansfield, 1972).

The good correlation between photoequilibrium and response generally observed in green plants requires that if [Pfr] alone is responsible for the action of phytochrome, [Pfr + Pr] must be constant in the different light treatments. Although spectrophotometric assay is impossible in green tissue, chlorophyll accumulation can be prevented by the herbicide norfluorazon and normal assays can be carried out. The phytochrome system of plants grown under such conditions is thought to resemble that of normal etiolated material (Jabben and Deitzer, 1979). Norfluorazon treated plants can be grown heterotrophically under normal lighting conditions. Using such techniques, it was found that after growth in

continuous light for several days, the phytochrome concentration increased substantially during a 24 hour dark period (Jabben and Deitzer, 1980). In a similar manner, Smith [1981b] investigated Pfr and Pr concentration changes in bleached maize plants grown under continuous low fluence rate white light with various levels of supplementary far-red. [Pfr + Pr] was not constant but was linearly correlated with ϕ , while Pfr became independent of ϕ . Moreover, a good correlation between photoresponse (leaf length) and ϕ was apparent. Thus it would appear that while ϕ , [Pr] or [Pr + Pfr] could control the response, [Pfr] could not. Although these controversial results accord with the original predictions of Schaffer and Mohr [1974], it is still generally accepted that Pfr is the active form.

It is becoming increasingly recognised that these responses are of adaptive value (see Smith, 1982). As the incident spectrum is remarkably constant (Goldberg and Klein, 1977), changes in the red : far-red ratio of natural daylight light are almost entirely a product of leafy canopies. The symbol ζ (zeta) has been suggested to represent the fluence ratio at the absorption maxima of phytochrome (660 and 730 nm) (Sinclair and Lemon, 1973; Monteith, 1976). This and similar ratios have been shown to be closely correlated with leaf area index (Jordan, 1969; Kasperbauer, 1971; Holmes and Smith, 1977b).

Smith and Holmes [1977] showed that the photoequilibrium established in etiolated tissue was closely correlated with ζ , but it has been pointed out that the screening effect of chlorophyll is likely to shift the action peak from 660 nm to shorter wavelengths (Borthwick, Hendricks and Parker, 1948b; Kasperbauer, 1971; Jose and Schaffer, 1979). There is little doubt that the red : far-red ratio is physiologically significant for many ruderal species adapted to rapidly exploiting exposed sites. After germination, such plants respond vigorously to shading from nearby competitors, whereas in contrast, understorey species which are tolerant of shade seem to be indifferent to the red : far-red ratio (Fitter and Ashmore, 1974; Morgan and Smith, 1979).

A more sophisticated approach was developed by Tasker [1978]. Hartmann [1966] showed that the photoequilibrium of phytochrome under dichromatic irradiation could be predicted on theoretical grounds from the actinic wavelengths and relative fluence rates, the

continuous light for several days, the phytochrome concentration increased substantially during a 24 hour dark period (Jabben and Deitzer, 1980). In a similar manner, Smith [1981b] investigated Pfr and Pr concentration changes in bleached maize plants grown under continuous low fluence rate white light with various levels of supplementary far-red. [Pfr + Pr] was not constant but was linearly correlated with ϕ , while Pfr became independent of ϕ . Moreover, a good correlation between photoresponse (leaf length) and ϕ was apparent. Thus it would appear that while ϕ , [Pr] or [Pr + Pfr] could control the response, [Pfr] could not. Although these controversial results accord with the original predictions of Schäfer and Mohr [1974], it is still generally accepted that Pfr is the active form.

It is becoming increasingly recognised that these responses are of adaptive value (see Smith, 1982). As the incident spectrum is remarkably constant (Goldberg and Klein, 1977), changes in the red : far-red ratio of natural daylight light are almost entirely a product of leafy canopies. The symbol ζ (zeta) has been suggested to represent the fluence ratio at the absorption maxima of phytochrome (660 and 730 nm) (Sinclair and Lemon, 1973; Monteith, 1976). This and similar ratios have been shown to be closely correlated with leaf area index (Jordan, 1969; Kasperbauer, 1971; Holmes and Smith, 1977b).

Smith and Holmes [1977] showed that the photoequilibrium established in etiolated tissue was closely correlated with ζ , but it has been pointed out that the screening effect of chlorophyll is likely to shift the action peak from 660 nm to shorter wavelengths (Borthwick, Hendricks and Parker, 1948b; Kasperbauer, 1971; Jose and Schäfer, 1979). There is little doubt that the red : far-red ratio is physiologically significant for many ruderal species adapted to rapidly exploiting exposed sites. After germination, such plants respond vigorously to shading from nearby competitors, whereas in contrast, understorey species which are tolerant of shade seem to be indifferent to the red : far-red ratio (Fitter and Ashmore, 1974; Morgan and Smith, 1979).

A more sophisticated approach was developed by Tasker [1978]. Hartmann [1966] showed that the photoequilibrium of phytochrome under dichromatic irradiation could be predicted on theoretical grounds from the actinic wavelengths and relative fluence rates, the

absorbance spectra of Pr and Pfr, and the quantum efficiency ratio for photoconversion. Of course, wavelengths other than those involved in the calculation of Φ can be used. Tasker expanded Hartmann's equation to account for polychromatic irradiation, so that ϕ could be calculated* for any light source. The procedures take no account of possible differences between in vivo and in vitro absorbance, or of pigment screening effects.

Nonetheless, such correlations are scarcely an adequate basis for an eco-physiological theory of phytochrome function. We have no knowledge of Pfr levels or photoequilibria in green tissue, and the molecule itself may be different from that extracted from etiolated material (see Pratt, 1982). For instance, it is difficult to explain the effectiveness of different far-red regimes (Morgan and Smith, 1980a) on the basis of simple proportionality to [Pfr] x time; indeed, the ratio of leaf to stem biomass appears proportional to the dose of far-red given.

There have been innumerable reports describing photomorphogenic responses to fluence rate, but very few distinguish between the effects of a separate photoreceptor (such as cryptochrome) and those of photosynthesis. In light grown seedlings there is little doubt that cryptochrome is active (Meijer, 1968; Black and Shuttleworth, 1972; Gaba and Black, 1979; Thomas and Dickenson, 1979). In wholly phototrophic plants, it is difficult to stimulate cryptochrome without affecting photosynthesis; the only possibility is to change the proportion of blue light relative to green, as these wavebands have fairly similar activity in photosynthesis (McCree, 1972a); variations in the red region would affect phytochrome too. Such treatments are technically difficult to arrange, especially at high fluence rates comparable to those in nature, and there are no reports of such work in the literature. Other reports of responses to blue light (Popp, 1926; Meijer, 1959; van der Veen and Meijer, 1959) are therefore confounded by photosynthetic effects, but it seems likely from their data that cryptochrome is active in light grown plants. Morgan and Smith [1981b] observed that in Chenopodium album, PAR and Φ interacted strongly in their effects on stem extension rate and leaf to stem biomass ratio. A further problem is the possibility that cryptochrome may itself be photochromic in the red and blue regions (Lüser and Schäfer, 1980). Shuttleworth and Black [1977] found that blue and red light act

* as ϕ_c

synergistically in phototropic bending in deetiolated Helianthus seedlings.

In summary, the principal known photomorphogenic responses of higher plants are evoked by changes in the relative proportions of red and far-red light. Often, the response is not instantaneous, and none occurs if the status quo is restored within a few minutes. The largest spectral changes seen in nature (those associated with leafy shade) are precisely those which elicit the photoresponses mediated by phytochrome. The general function of phytochrome may be to detect leafy shade. Probably, a fluence rate dependent response to far-red light is confined to etiolated seedlings, whereas a response of this type to blue light is generally distributed, even though it is little understood.

Unfortunately, the published data on the daytime SPD do not exclude the possibility that other environmental factors confuse the detection of leafy shade. Hence, during this project it was intended further to characterise the spectrum of natural daylight in order to answer the following questions:

- 1) What variation exists in the daytime spectrum at unshaded locations?
- 2) How does the spectral transmittance of a canopy vary during its leafy phase?
- 3) Do changes in the optical properties and pigment content of the constituent leaves have a significant effect upon the transmittance spectrum?
- 4) Is \bar{z} a good indicator of leafy interception over a prolonged period?

Twilight

Environmental Phenomena

In marked contrast to daytime, conspicuous changes in fluence rate and spectral distribution occur during twilight when the sun is near the horizon. Rozenburg [1966] provided the most recent extensive survey of the phenomena associated with twilight.

The maximum fluence rate of PAR at noon under a cloudless sky is typically $2 \text{ mmol m}^{-2} \text{ s}^{-1}$ in temperate latitudes, but cloud cover can reduce this to perhaps $50 \text{ } \mu\text{mol m}^{-2} \text{ s}^{-1}$, although the mean is about $500 \text{ } \mu\text{mol m}^{-2} \text{ s}^{-1}$. At night, the brightest moonlight and starlight give values for PAR of around $2 \text{ pmol m}^{-2} \text{ s}^{-1}$ and $2 \text{ fmol m}^{-2} \text{ s}^{-1}$, respectively; cloud cover might reduce these by an order of magnitude.

Hence, during twilight, fluence rate changes by about nine orders of magnitude in as little as two hours; during this period the rate of change is almost exactly exponential. The time at which a given fluence rate is reached during the progress of twilight consequently varies by less than 15 minutes as a result of cloud cover, whereas the equivalent seasonal change is around 4.5 hours in temperate latitudes; Holmes and Smith [1977a] were presumably referring to earlier events when they concluded that cloud cover had an overwhelming effect. Cloud cover has more significant effects upon the spectral nature of the changes. Unfortunately, much of the literature on this aspect of twilight concerns the colour of different regions of the sky, rather than their integral contribution to the spectral photon distribution of incident light. The sequence of events at dusk is described below (it is reversed at dawn).

In the late afternoon, under a clear sky, the fluence rate begins to drop rapidly at the start of "civil twilight" when the sun subtends an angle of about $+7^\circ$ to the horizon; this phase ends after sunset when the angle reaches -6° . Human visual acuity is retained during most of this period, but during the subsequent "nautical twilight", only large objects remain visible. This phase corresponds to solar angles of -6° to -12° , and fluence rates of about 50 and $0.5 \text{ pmol m}^{-2} \text{ s}^{-1}$, respectively. The period of exponential decline runs approximately from sunset to the point when the solar angle reaches -12° ;

thereafter, during "astronomical twilight", the fluence rate stabilises at its night-time level, usually at about an angle of -18° .

Towards sunset, the fluence rate becomes increasingly unrelated to the direct solar beam as a result of the rapidly increasing path length through the atmosphere and the decreasing angle of incidence to a horizontal surface. The sun and adjacent sky appear red during this period as a result of the spectral absorbance characteristics of the lower atmosphere and not, as has often been claimed, increased scattering (Rozenburg, 1966). The contribution of the direct beam is negligible at sunset, and consequently the event is imperceptible from a horizontal surface. Apparent sunset occurs at least two minutes later than geometrical or true sunset, because the atmosphere refracts the direct beam by about 0.5° . According to Rozenburg [1966], and contrary to Morgan and Smith [1981], the spectral effect of refraction is negligible.

After sunset, the halo of red light remains, separated by a white band (and sometimes, high in the sky, a purple patch) from the rest of the sky. The blue of the sky overhead starts to become enhanced at this stage by two factors. Firstly, the increasing path length through the ozone layer leads to lower transmittance in the green and red spectral regions, where the Chappuis absorbance band lies. Secondly, the scattering profile (the frequency distribution of scattering events versus altitude) shifts to higher altitudes, where particle scattering is relatively much less common than molecular scattering. At the horizon opposite to the sun, the dull shadow of the Earth, surrounded by a red glow known as the "Belt of Venus", appears. As the shadow rises, it rapidly becomes indistinct as the projected edge occupies more of the sky.

During the exponential phase of twilight the red area above the solar horizon slowly disappears. The scattering profile moves into increasingly unpolluted air in the upper atmosphere, accentuating the blue colour of the sky, as the lower, denser regions of the atmosphere come within the Earth's shadow. As the density of air declines exponentially with height, and scattering is proportional to density, the fluence rate at the Earth's surface declines exponentially too.

Multiple scattering in the lower layers gradually

gains in importance relative to that of simple scattering in the tenuous stratosphere. This phase corresponds to the end of nautical twilight, when the exponential decline ends. The high order relationship between wavelength and the probability of multiple scattering renders the sky deep blue, while the somewhat lighter blue of the singly scattered light becomes restricted to the solar horizon. This finally disappears at a solar angle of about -19° when true night begins.

Even under clear skies, this orderly progression of events is disturbed. In the absence of Chappuis absorption, the shorter wavelengths within the visible region would tend to increase relative to longer ones as twilight progresses. However, increasing absorbance in the ozone layer often leads to the opposite effect in the red and far-red regions during much of the twilight period (Goldberg and Klein, 1971; Sinclair and Lemon, 1973; Holmes and McCartney, 1976). However, Shropshire [1973] observed a transient drop in the red : far-red ratio soon after dawn. Holmes and McCartney [1976] and Johnson, Salisbury and Connor [1967] reported analogous events in the same region and the blue and red regions, respectively. The transient "reversal effect" has long been known in meteorology and is thought to result from a shift in the relative positions of the scattering profile and the ozone layer (Rozenburg, 1966). The effect varies from day to day in both extent and timing; seasonal and longer term trends may also exist.

Clouds are largely restricted to the lower regions of the atmosphere and so have important spectral effects only around sunrise and sunset, when they attenuate the scattered light from the upper atmosphere, and reflect downwards red light from the direct solar beam. These effects are highly variable. Similarly, particle scattering in other parts of the atmosphere can introduce further complexity to the spectral phenomena.

Unfortunately, much of this information is of little direct relevance to photobiology because it principally documents changes in the visible spectrum and fails to provide quantitative information about the changes in irradiation to which plants respond. Direct measurement of the SPD incident upon a planar surface during the twilight period is difficult, because of the rapidly declining fluence rate. Salisbury [1981a, 1981b] included a series of spectral energy distributions recorded around the time

of sunset. These indicated a drop in orange light relative to both blue and far-red, as twilight proceeded. The red : far-red ratios reported were much higher than those commonly encountered (Smith, 1982). The apparatus used required a prolonged period (10 minutes) to scan the entire spectrum, and the change in fluence rate during this was corrected for arithmetically, assuming a linear rather than logarithmic fall in fluence rate. Goldberg and Klein [1977] showed similar trends during twilight at a number of geographical locations.

In summary, whereas the changes in fluence rate associated with twilight are generally large and quite consistent, the spectral changes are small, rather variable and poorly documented. It was considered a vital aspect of this project to remedy this deficiency and provide adequate information about the crepuscular change in light quality and quantity occurring in natural daylight.

Physiological Responses

In the 1920s, daylength was found to have a potent effect on flowering in a number of species; some were induced to flower by short days and others by long days. Such a response requires the participation of both a photoreceptor and a timer. Hamner and Bonner [1938] concluded from their work on Xanthium strumarium that the length of the night, rather than the day, was the critical factor since a brief pulse of light between two dark periods (a night break) inhibited flowering just as strongly as if a full day had separated them. Thus, much effort has been expended in attempting to reveal a "darkness timing" mechanism. Unfortunately, it is now known that both day and night length are important in the response. Indeed, the complex interactions of the photoreceptor and timer have confounded the majority of physiological investigations of photoperiodic control. The most recent reviews of the field are those of Vince-Prue [1975], Evans [1975], Vince-Prue [1979], and Salisbury [1981b].

The perception of dawn and dusk has been studied in several species both in the field (Takimoto and Ikeda, 1960, 1961; Katayama, 1964) and the laboratory (see Salisbury, 1981b). The threshold fluence rate (below which

no distinction is made between the light and total darkness) at dusk and at dawn, and the critical night length (that which induces 50% of maximum flowering) all seem to show great variability even within a single species. The genetics of this aspect have not been studied, although it seems likely that complex polymorphisms maintained by natural selection pressure may be responsible.

The role of phytochrome

Many attempts have been made to characterise the photoreceptor involved, but the variability of the material and the complexity of the photoperiodic system as a whole have led to numerous misconceptions. Red seems to be the most active spectral region controlling flowering. Using a spectrograph, Borthwick and co-workers identified precisely the wavelengths involved, by giving four species pulses of monochromatic light after twelve hours of a sixteen hour dark period, when the sensitivity was greatest. The consequent light dose versus flowering response curves were used to construct the four action spectra (see Shropshire, 1972) still regarded as definitive of the photoperiodic response. In the short day flowering Glycine max (Parker, Hendricks, Borthwick and Scully, 1945) and in the long day flowering Hordeum vulgare (Borthwick, Hendricks and Parker, 1948a) and Hyoscyamus niger (Parker, Hendricks and Borthwick, 1950), the peak of sensitivity lay at 610 - 620 nm, while that for Xanthium strumarium (Parker, Hendricks, Borthwick and Scully, 1946) was about 20 nm higher. The sensitivity in the red region for all four species was quite similar, but large differences were apparent in the less effective blue region. This variation has been largely ignored but may be an important clue to the photoreceptor involved in the sensing of daylength. Using Xanthium, the involvement of phytochrome was demonstrated by the complete reversibility of the effects of a red pulse by a far-red one (Borthwick, Hendricks and Parker, 1952).

Any light source establishes an equilibrium between the two forms of phytochrome which is largely dependent upon its spectral distribution and the absorption spectra of Pr and Pfr. The plant responds physiologically to the level of Pfr; this would be relatively high in daylight, but much lower under monochromatic far-red light. Moreover, in darkness any Pfr present might slowly disappear non-photochemically, and this might be the

origin of the photoperiodic response (Borthwick, Hendricks and Parker, 1952). Subsequently, it was found that the Pr absorbance maximum in vitro lay at 660 nm (Butler, Hendricks and Siegelman, 1964), but discrepancies between this and the observed action maximum have been satisfactorily explained by the absorbance of much of the light in this region by chlorophyll (Borthwick, Hendricks and Parker, 1948b; Cathey and Borthwick, 1964).

It is largely on the basis of these results that many workers have concluded that phytochrome alone controls photoperiodic phenomena. Indeed, Borthwick, Hendricks and Parker [1952] suggested that a slow loss of relatively unstable Pfr during the dark period could constitute the timing mechanism itself (in the manner of sand draining from an hour glass). This opinion is now untenable as it has been shown that night breaks do not simply reset the dark timing system. A much more likely explanation of the timing mechanism is that of Bünning [1936] which envisages an oscillating metabolic system as a timing standard (in the manner of a clock's pendulum). The crucial evidence for this is that when the periodicity of light - dark cycles is experimentally increased beyond 24 hours, the timing system often resonates again at approximate multiples of 24 hours (Nanda and Hamner, 1958; Pittendrigh, 1980). So what, then, is the role of phytochrome?

Close examination of flowering responses has revealed an intricate system which is far from understood. In Chenopodium rubrum, a short day flowering species, Kasperbauer, Borthwick and Hendricks [1963] investigated phytochrome involvement intensively. They concluded that inhibition of flowering occurred when the Pfr level remained above a certain low threshold for at least one hour. The effectiveness of a red pulse was thought to be because Pfr was thereby raised to a high level and the rate of its "decay" was sufficiently slow to allow the process of inhibition to begin. Although a far-red pulse could reverse the effects of red light, far-red light itself could inhibit flowering if maintained for a sufficient period. The inference was that the threshold Pfr level was even lower than that established by far-red light. The authors were cautious in their interpretation of the data, and recognised that other factors could be involved.

The effect of temperature on the minimum night

length required for flowering supports the tentative hypothesis described above. The rate of Pfr destruction in etiolated seedlings is temperature dependent (Kendrick, Spruit and Frankland, 1969), whereas one of the principal features of the metabolic timer is its capacity to compensate for thermal change, homeostasis being an essential characteristic of circadian timing (Pittendrigh and Caldarola, 1973). Thus one might predict on the basis of the hypothesis of Kasperbauer et al. [1963] that only the initial period (of Pfr "decay") in the timing process would be temperature sensitive; this was found to be the case in Xanthium (Salisbury, 1963).

Attractive though the scheme appears, complications and objections remain. The fairly straightforward, phytochrome mediated response corresponds to the period of maximum sensitivity to white or red light given as a night break. However, this belies the situation during the rest of the night. In plants of Pharbitis nil (a short day flowering species) grown in daylight, the period of hypersensitivity to red light is transient (Takimoto and Ikeda, 1960). Moreover, Cumming, Hendricks and Borthwick [1965] showed that, in Chenopodium rubrum plants grown in continuous light, periods of hypersensitivity to red light recurred at circadian intervals during a 72 hour dark period. This is easily explained by a rhythmical change in sensitivity to Pfr; what is difficult to explain is why the sensitivity to far-red light showed no such rhythmicity in either system. Takimoto and Hamner [1965b] obtained similar results using Pharbitis.

A further weakness is that we have no knowledge of phytochrome transformations in green plants and, as very few plants have ever been induced to flower while in the etiolated state, any conclusions drawn by extrapolation from the physiology of such tissue to green plants is, at best, premature. Vince-Prue (in preparation) has shown that in Pharbitis nil a series of closely spaced red pulses extending the photoperiod are not far-red reversible. Thus, outside the night break phenomenon, the involvement of phytochrome in photoperiodism is largely hypothetical.

To avoid the problem of detecting Pfr in green tissue, Cumming et al. [1965] developed a subtle technique to investigate the involvement of Pfr in the timing system. Other factors remaining equal, the proportion of phytochrome molecules in the Pfr form can be controlled,

within limits, by varying the proportions of red and far-red given during a saturating dichromatic light pulse. Hence, a fixed proportion of Pfr can be set-up by providing a certain proportion of red light in the pulse. If changes in the proportion of Pfr control the physiological response, then it should be possible to monitor them by finding at intervals the proportion of red light which does not disturb the system. These so-called "null methods" have yielded strange results, usually implying an initial decline in Pfr, often followed by its apparent reappearance in darkness (Cumming *et al.*, 1965; Evans and King, 1969; King and Cumming, 1972). Recently it has been suggested that the quantum efficiency of phytochrome photoconversion may vary rhythmically in addition to the light - dark rhythm itself (King, Schäfer, Thomas and Vince-Prue, 1982). If this is true, many experiments, including those using null methods, may have been carried out below saturating fluence rates.

Care should be taken not to interpret these findings as if they related to other systems such as etiolated seedlings where, although the physiology of phytochrome is better understood, it may be totally different. In green plants there is no apparent reason why Pfr should not be stable or appear during darkness; both have analogues in seed phytochrome where Pfr is stable (Kendrick *et al.*, 1969) and can appear in darkness (Boissard, Spruit and Rollin, 1968). On the other hand, the null technique is only informative if light effects are solely mediated by Pfr concentration; this is itself hypothetical. Indeed, it has been suggested that cycling between Pr and Pfr may have a specific role (Jose and Vince-Prue, 1978).

If the involvement of phytochrome in short day flowering species is paradoxical, further complications are introduced when long day flowering species are considered: firstly, the well defined period of hypersensitivity to red light is uncommon in these species; secondly, the promotion of flowering is usually proportional to the fluence rate and duration of the nocturnal pulse; and thirdly, reversibility is the exception rather than the rule (Vince-Prue, 1975). Moreover, not only does far-red fail to reverse the effect of a red pulse, it actually enhances it when long pulse lengths are used or if the treatment is given close to the end of the photoperiod. Under these conditions, the maximal spectral response shifts to a narrow peak at 710 nm (Schneider, Borthwick and Hendricks, 1967), even in

the presence of a background of red light (Borthwick et al., 1969). This has variously been interpreted as a result of absorbance by a bound form of phytochrome (ibid.), an effect of cyclic photophosphorylation (Schneider and Stimson, 1971; 1972; Ginkel and Hammans, 1980a, 1980b), or even a specific effect of cycling (Vince-Prue, 1975; Jose and Vince-Prue, 1978), but there is very little evidence to support any of these notions. Although the response is similar to the HIR of photomorphogenesis, there is evidence that the latter is confined to etiolated seedlings. According to null experiments, the level of Pfr declined gradually during darkness in the long day flowering Lolium temulentum (Evans, 1976).

It seems that, until Pfr can be assayed in green plants, little progress beyond the work of King, Vince-Prue and Quail [1978] is likely in this area. They carried out null experiments on Pharbitis nil in parallel with spectrophotometric assays using photobleached, heterotrophic plants. Both implied that a continuous loss of Pfr occurred, but the rates indicated were different.

Despite the contradictions, it is possible to reach some general conclusions about the physiology of light / dark timing. Part of the confusion may result from ambiguous signals being given to the timing system by apparently simple light treatments. A brief pulse of red light given during a dark period (a typical night break treatment) seems to be interpreted as "dawn", but a subsequent red pulse (for example, Takimoto and Hamner, 1965a) as "dusk", even though there has been no intervening photoperiod (hence, the term skeleton photoperiod). When the second pulse is replaced by the true photoperiod, the "dusk" signal occurs when ^{the photoperiod} ends. If the "dawn" signal is given as a pulse, the end of the pulse is not seen as "dusk", and furthermore, a subsequent "dawn" signal is ignored. However, substitution of the night break by prolonged irradiation is perceived as a photoperiod (that is, "dawn" and "dusk"); the system has apparently become reset.

Hoshizaki and Hamner [1969] suggested that separate circadian oscillators are entrained by "dawn" and "dusk" signals, and that it is the phasing of these oscillators that determines the response. This internal coincidence model does not, however, account for how both signals seem to be ignored under certain circumstances. A more widely

held view is that the effect of a light treatment depends on its relationship to an endogenous rhythm (that is, whether the system is in a "photophile" or "skotophile" phase). In order to explain entrainment, this external coincidence model has an accessory feature which allows prolonged irradiation to re-phase the rhythm. Although neither model is satisfactory in its present form, they suggest that many peculiar photoperiodic effects may be quite simple manifestations of Nanda-Hamner resonances (Nanda + Hamner, 1952).

Over and above these problems is the unknown action of the photoreceptor. Does a simple "Pfr threshold" hour-glass system actually exist alongside the clock itself? Perhaps attempts to understand both photoreceptor and timer simultaneously are over-ambitious.

In the context of the natural radiation environment, it is interesting that the light received during the photoperiod itself has distinct effects on photoperiodism (Vince-Prue, 1975, 1979, 1981; Evans, 1975; Kadman-Zahvi and Ephrat, 1976; Salisbury, 1981a, 1981b). (Photosynthetic rate differences do not seem to be important (Takimoto and Naito, 1962) and it is generally thought that phytochrome is involved.) These ^{effects} have been termed "dynamic mode" responses to distinguish them from "static mode" or induction responses such as those to night breaks (Jose and Vince-Prue, 1978).

The red : far-red ratio seems to become inhibitory to flowering when much above unity in several species, although lower ratios have little effect (Lane, Cathey and Evans, 1965). Conversely, flowering in Lolium temulentum seems to be inhibited by ratios both above and below unity (Evans, Borthwick and Hendricks, 1965). Indeed, it is thought that long day flowering species are generally more sensitive to light quality during the photoperiod (Vince-Prue, 1975). However, this is not the case in short and long day flowering grasses, both of which are stimulated to flower by far-red light (Kadman-Zahvi and Ephrat, 1976).

The end of day Pfr level seems to affect the start of dark timing in several species (Borthwick et al., 1952b; Al-Hattab, 1968; Holland and Vince, 1971), but the evidence is equivocal (Salisbury, 1981a, 1981b). Rhythmical changes in sensitivity to red : far-red ratios may have an adaptive value in allowing the system to ignore the effects of leafy shade during the day.

Nonetheless, Holmes and Wagner (1980) have argued on theoretical grounds that such a change in the red : far-red ratio (and hence Pfr) is a more likely "zeitgeber" (cue) than fluence rate change alone. The idea of a change in Pfr being effective rather than its actual level is consistent with most published data. Under continuous light interrupted only by an inductive dark period, a supplementary far-red light pulse can either inhibit or stimulate flowering in short day species, depending upon the interval between the pulse and the start of the dark period (King, 1974). Deitzer, Hayes and Jabben [1979] found that plants of Hordeum vulgare (cv. "Wintex") grown under 12 hour photoperiods flowered after a long inductive period of uninterrupted light. During this, supplementary far-red pulses alternately stimulated and inhibited flowering with a persistent circadian rhythm; sensitivity minima coincided with the times when the photoperiod would have occurred.

Other photoreceptors

In addition to these effects related exclusively to red and far-red light, presumably mediated by phytochrome, there is good evidence implicating other wavelengths and indeed other photoreceptors.

There have been numerous reports of the effects of blue light on flowering. Often it is relatively impotent, but, for example, in Hyoscyamus niger, long days consisting of red light alone do not induce flowering, whereas blue light has the same effect as white or red plus far-red light in inducing flowering (Stolwijk and Zeevaart, 1955). Blue light was also more effective than red in Salvia occidentalis; both far-red and blue were antagonised by red light (Meijer, 1959). In similar experiments on the short day flowering Pharbitis nil, seedlings grown in blue or far-red light for 2 days failed to flower after a long inductive night, but if red or white light was used, most plants flowered. Again, red antagonised far-red and blue, but the effects of these two wavelengths were distinct; a terminal red pulse lead to flowering only after the far-red treatment (Takimoto and Naito, 1962), whereas in Lemna perpusilla the colour of the light given during the photoperiod greatly affected the reversibility of red night breaks (Hillman, 1966b). In some species sensitivity to blue light is even greater than that to far-red when given at the end of the photoperiod. These include Callistephus chinensis (Wichrow

and Benedict, 1936), Lolium temulentum (Evans, Borthwick and Hendricks, 1965), Chenopodium rubrum (Sawnhey, 1977a, 1977b, 1977c) and many members of the Cruciferae (Funke, 1948; Stolwijk, 1954; Hanke, Hartmann and Mohr, 1969; Brown and Klein, 1971).

Blue light seems to be active in night break phenomena. In Pharbitis nil at least, the responses to blue, red or far-red night break pulses seem independent (Takimoto and Ikeda, 1960; Takimoto and Hamner, 1965b). In Salvia occidentalis blue light has been shown to be as effective as far-red in reversing the effect of a red night break (Meijer, 1959), while far-red and blue night breaks were equally effective in Hyoscyamus niger (Schneider, Borthwick and Hendricks, 1967). The original action spectra for night breaks derived by Borthwick and co-workers demonstrated a consistent high sensitivity in the red region, but the effectiveness of blue light varied considerably between species.

From the absorbance spectra of phytochrome in vitro, Hartmann [1966] calculated that ϕ in blue, red and far-red light would be about 40%, 80% and <2%, respectively. If the absorbance in vivo is similar, according to most hypotheses the activity of blue and red light should be similar, but this is not found. Instead the effect of blue light is usually similar to that of far-red light, as in the HIR. However, this analogy is unhelpful because the HIR is itself the subject of controversy. Some of the variation in the effectiveness of blue light is undoubtedly due to screening by chlorophyll, which is itself affected by nyctinastic movements of leaves (Bünning and Moser, 1969) and intracellular chloroplast movements. It should be noted that Everett and Briggs [1970] concluded that the absorbance of blue light by phytochrome in vivo was substantially different from that in vitro; consequently, ϕ in blue light may be closer to that in far-red.

Most of the experiments carried out to compare the efficacy of different spectral regions have used irradiance (power per unit area) to compare treatments (see Vince-Prue, 1975). This practice is erroneous because photochemical action is a function of photon absorption and not power per se. Thus, in most of the action spectra and other studies the efficacy of blue is about half its true value relative to far-red. Furthermore, if the dose-response curves are not parallel in all regions, gross

and Benedict, 1936), Lolium temulentum (Evans, Borthwick and Hendricks, 1965), Chenopodium rubrum (Sawnhey, 1977a, 1977b, 1977c) and many members of the Cruciferae (Funke, 1948; Stolwijk, 1954; Hanke, Hartmann and Mohr, 1969; Brown and Klein, 1971).

Blue light seems to be active in night break phenomena. In Pharbitis nil at least, the responses to blue, red or far-red night break pulses seem independent (Takimoto and Ikeda, 1960; Takimoto and Hamner, 1965b). In Salvia occidentalis blue light has been shown to be as effective as far-red in reversing the effect of a red night break (Meijer, 1959), while far-red and blue night breaks were equally effective in Hyoscyamus niger (Schneider, Borthwick and Hendricks, 1967). The original action spectra for night breaks derived by Borthwick and co-workers demonstrated a consistent high sensitivity in the red region, but the effectiveness of blue light varied considerably between species.

From the absorbance spectra of phytochrome in vitro, Hartmann [1966] calculated that ϕ in blue, red and far-red light would be about 40%, 80% and <2%, respectively. If the absorbance in vivo is similar, according to most hypotheses the activity of blue and red light should be similar, but this is not found. Instead the effect of blue light is usually similar to that of far-red light, as in the HIR. However, this analogy is unhelpful because the HIR is itself the subject of controversy. Some of the variation in the effectiveness of blue light is undoubtedly due to screening by chlorophyll, which is itself affected by nyctinastic movements of leaves (Bünning and Moser, 1969) and intracellular chloroplast movements. It should be noted that Everett and Briggs [1970] concluded that the absorbance of blue light by phytochrome in vivo was substantially different from that in vitro; consequently, ϕ in blue light may be closer to that in far-red.

Most of the experiments carried out to compare the efficacy of different spectral regions have used irradiance (power per unit area) to compare treatments (see Vince-Prue, 1975). This practice is erroneous because photochemical action is a function of photon absorption and not power per se. Thus, in most of the action spectra and other studies the efficacy of blue is about half its true value relative to far-red. Furthermore, if the dose-response curves are not parallel in all regions, gross

distortions can result (see Shropshire, 1972).

Hence, despite the possible involvement of other photoreceptors, the conclusion that "all photoperiodic phenomena can be explained in terms of phytochrome" may be correct, but the problem remains, are the explanations correct? Furthermore, if phytochrome serves to detect the red : far-red ratio of natural daylight while cryptochrome is the fluence rate receptor (Smith, 1982), why do plants use phytochrome to measure photoperiod?

In summary, photoperiodic control is most potent in the red region, with blue and far-red light generally acting antagonistically to red, although many exceptions are known. In most cases, fluence rate changes alone can elicit the response. Since the available data on the crepuscular changes in SPD are an inadequate basis for the hypotheses which have been advanced in explanation of photoperiodism, it was intended during the course of this investigation to discover:

- 1) What changes in phytochrome-related parameters of light quality occur during twilight?
- 2) Are such potential zeitgebers sufficiently accurate to explain photoperiodic control?
- 3) Does shading interfere with these?
- 4) Are changes in fluence rate more or less accurate than spectral changes?
- 5) Do other potential zeitgebers exist?

MATERIALS AND METHODS

Instrumentation for light measurements

A spectroradiometer was used to measure spectral photon fluence rate (SPFR; the number of photons within a given waveband incident upon a surface of a certain area during a unit of time) throughout the 400 - 800 nm wavelength range at various field sites. The instruments comprised i) a receptor surface, ii) a dispersing spectral filter, iii) a light sensitive surface, iv) an amplifier and v) a recorder. In this study two instruments belonging to the Department of Physiology and Environmental Science at Sutton Bonington and the Department of Botany, University of Leicester, were used. All the components were manufactured by Gamma Scientific Inc. (San Diego, USA), unless otherwise stated. They are described critically below.

i) The receptor surface of any radiometer should transmit light from different angles of incidence according to Lambert's Cosine Law. A simple surface fails to do this because of specular reflection, but specially shaped opalescent materials can be approximately "cosine corrected" to mimic the ideal planar surface, and these are in general use. Fluence rate, however, is defined to include non-planar surfaces too, and plants are not planar.

In nature, irradiation is always multidirectional, as illustrated in Figure 1. The point C is irradiated from all directions; the radiating sources may be projected at infinity and represented by a sphere. Z is the zenith, the point directly above C, and N is the direction of north. Any point P on the sphere is identified by its altitude and azimuth angles, α and β . If a small area at P irradiates a horizontal plane at C

$$i' = i \cdot | \cos (90^\circ - \alpha) | \quad \dots(1)$$

where i' is the fluence rate at C and i is the fluence rate when measured perpendicularly to the beam.

If the angular area is ($\delta\alpha \cdot \delta\beta$), then integrating for the whole sphere

1.2 instrumentation

$$I = \int_{-90^{\circ}}^{90^{\circ}} \int_0^{360^{\circ}} i \cdot |\cos(90^{\circ} - \alpha)| \cdot d\beta \cdot d\alpha \quad \dots(2)$$

where I is the total fluence rate at C .

The component of I from the lower hemisphere has generally been ignored in photobiology, but it is not inconsiderable. A horizontal cosine-corrected planar receptor surface, sensitive to the upper radiating hemisphere alone is generally assumed to estimate reliably the fluence rate to which a plant is exposed in the field; however, assuming plants to be spherical might be a more realistic approximation. In this case ZC would be just one of an infinite number of rays perpendicular to the surface of the receptor, making i' independent of α . A sphere has four times the area of a circle of equal radius, hence Eq.2 simplifies to

$$I_s = \int_{-90^{\circ}}^{90^{\circ}} \int_0^{360^{\circ}} (0.25 \cdot i) \cdot d\beta \cdot d\alpha \quad \dots(3)$$

A receptor head with such isotropic sensitivity would not easily be designed to have good cosine correction over its surface, but the underestimate resulting from specular reflection of grazing rays of light would be a constant proportion from all directions and would be accounted for when the instrument was calibrated. Whether this approach is an improvement over convention is unknown, but the difference would be greatest when α is small or negative. Richardson [1959] found that in woodlands a photometer fitted with a spherical receptor was more sensitive to canopy differences and less sensitive to meteorological effects than a planar one. A non-spherical shape might be a closer approximation to the light absorbed by a certain plant, but it would have to be cosine-corrected in some way, as i' would again be a function of α . The principles apply equally to light quality (see 1.1).

Nonetheless, in order to permit comparison with other

1.2 instrumentation

workers' results, receptors with planar cosine correction were used generally in this work. The Sutton Bonington instrument was fitted with a 33 mm fused silica head fixing directly onto the filter, whereas the Leicester instrument utilised a 2.5 mm quartz head coupled via a 500 mm glass fibre optic. For one experiment, however, a crude spherical receptor was fashioned from an intensely scattering 40 mm diameter solid sphere of high density expanded polystyrene in which the fibre optic was embedded. The material effectively randomised the light incident anywhere on the surface, so that directional sensitivity varied by less than 5%. An approximate calibration was carried out in the normal manner (see below). Data obtained in the field using the Leicester spectroradiometer fitted with this receptor ~~were~~ compared with that from the Sutton Bonington instrument operated simultaneously with the conventional planar receptor.

ii) The filter essentially disperses the collimated light from the receptor into its component spectral parts by means of either diffracting or refracting optics. In a monochromator system where only one sensor is used, the spectrum must be shifted across it mechanically; thus the SPD is examined serially. The size of the exposed sensor surface (see below) and the precision of collimation determine the bandwidth of the instrument.

The Sutton Bonington instrument used a type 700-31 monochromator operated manually, while the type NM-3H used in the Leicester instrument was operated entirely by a remote controller (type SC-1). Both provide a digital readout of the wavelength between 380 and 820 nm and an electrical analogue output for recording purposes. The instruments automatically scan through the spectrum by slowly rotating their internal diffraction grating. Accuracy was better than 5 nm and the bandwidth was about 4 nm; scanning rate was about 30 nm s⁻¹.

iii) Relative signal levels are conveniently expressed in decibels (dB), where

$$X_{dB} = 10 \log_{10} (\text{level}_1 / \text{level}_2) \quad \dots(4)$$

The maximum usable sensitivity of any sensor is reached when its signal-plus-noise : noise ratio falls much below 10 dB. In the instruments used here, photomultiplier detectors were employed (types PI-6 and D46, in Sutton Bonington and Leicester instruments respectively.) In such

1.2 instrumentation

a tube, electrons are liberated photoelectrically from the phosphor surface and are amplified exponentially. Although the sensitivity is very high, the efficiency of the phosphor is wavelength dependent, and even in darkness a small anode current flows. This is caused by thermal electrons in the tube, and the slight conductivity between cathode and anode which is strongly dependent on humidity. Sensitivity was controlled by setting the anode voltages appropriately for the conditions.

iv) The output current of a photomultiplier is small and must be amplified. The amplifiers used incorporate precision power supplies for the photomultipliers; the voltage steps selected gave about 5 dB differences in sensitivity and a total range of about 15 dB. The Sutton Bonington instrument (using type 2020-100 amplifier) had the greater sensitivity of $10 \text{ pmol m}^{-2} \text{ s}^{-1} \text{ nm}^{-1}$ at 500 nm and 7 dB less at the wavelength extremes. Integrating between 400 and 700 nm for PAR, this corresponds to about $30 \text{ nmol m}^{-2} \text{ s}^{-1}$. The Leicester instrument (using type DR-2) was about 6 dB less sensitive. In addition, attenuation steps of 0, 10, 20, and 30 dB were available. Using different combinations of anode voltage and attenuation, SPDs of daylight or other sources could be measured within a range of PAR up to $2 \text{ mmol m}^{-2} \text{ s}^{-1}$ in about twelve sensitivity steps.

With the shutter closed, amplifier null was adjusted electronically at maximum attenuation, then at minimum attenuation the dark current was balanced out. In the field, rapid humidity changes occurred at dawn and dusk; as high sensitivity was required at these times, the changes in dark current were compensated for frequently.

v) The data might ideally have been recorded digitally onto magnetic tape, but facilities for this were not available. Instead, x-y chart recorders (type 24000, Bryans Ltd., Mitcham, U.K.) were used, plotting the relationship between wavelength and output onto paper as the monochromator scanned through the spectrum. During this process, machine settings and other details could be noted beside the trace and so the flexibility offered by the analogue method was of some value under field conditions. Although frequently checked during operation, the correspondence between increments along the x-axis and the wavelength setting of the monochromator varied slightly with the gain of the recorder amplifiers, largely because of changes in ambient temperature. The error

1.2 instrumentation

increased with wavelength, but this was generally less than 3 nm at 800 nm.

The sensitivity of the instruments at each anode voltage used was wavelength dependent and did not remain constant over long periods. Consequently, after each day in the field, they were calibrated against a standard source delivering known spectral irradiance; this consisted of a tungsten halogen lamp supplied by the National Physical Laboratory (Teddington, U.K.). The required current of 8.33 A ($\pm 0.1\%$) was provided by a stabilised power supply (type TSV 70 Mk.II, Farnell Instruments Ltd., Wetherby, U.K.) and measured using a Pye Instruments Ltd. (Cambridge, U.K.) type 7556 potentiometer across a 0.01 ohm standard resistance. Source and receptor head were fixed 0.5 m apart on an optical bench, as directed by the N.P.L. The procedure for deriving the SPD of an unknown light source from its plotted spectral scan and that of the calibration lamp with its known spectral output is described in the computing Appendix II.

Quantitative measurement of SPFR is notoriously difficult; even the primary standards have a consistency worse than $\pm 1\%$ (Arnold, 1975). McCartney [1975] and Kummur [1981] give equations which attempt to define the uncertainty. Here, however, the problem of potential error was approached pragmatically. Errors in the measurement of an SPD resulting from a change in fluence rate during the scan were always less than 2% (see below). Random errors resulting from inaccuracy in setting-up the instruments were estimated to be less than 3% by calibrating with a deliberate 2 volt anode voltage error (that usually accepted under field conditions). A similar error between calibration sessions was deduced by repeating the calibration procedure several times. Systematic errors resulting from aging of the lamp could have been the largest, but facilities were only available for measuring total irradiance, and spectral changes would have remained obscure. Errors in wavelength were generally less than 5 nm, although heating effects occasionally increased this to 8 nm.

1.2 instrumentation

increased with wavelength, but this was generally less than 3 nm at 800 nm.

The sensitivity of the instruments at each anode voltage used was wavelength dependent and did not remain constant over long periods. Consequently, after each day in the field, they were calibrated against a standard source delivering known spectral irradiance; this consisted of a tungsten halogen lamp supplied by the National Physical Laboratory (Teddington, U.K.). The required current of 8.33 A ($\pm 0.1\%$) was provided by a stabilised power supply (type TSV 70 Mk.II, Farnell Instruments Ltd., Wetherby, U.K.) and measured using a Pye Instruments Ltd. (Cambridge, U.K.) type 7556 potentiometer across a 0.01 ohm standard resistance. Source and receptor head were fixed 0.5 m apart on an optical bench, as directed by the N.P.L. The procedure for deriving the SPD of an unknown light source from its plotted spectral scan and that of the calibration lamp with its known spectral output is described in the computing Appendix II.

Quantitative measurement of SPFR is notoriously difficult; even the primary standards have a consistency worse than $\pm 1\%$ (Arnold, 1975). McCartney [1975] and Kummar [1981] give equations which attempt to define the uncertainty. Here, however, the problem of potential error was approached pragmatically. Errors in the measurement of an SPD resulting from a change in fluence rate during the scan were always less than 2% (see below). Random errors resulting from inaccuracy in setting-up the instruments were estimated to be less than 3% by calibrating with a deliberate 2 volt anode voltage error (that usually accepted under field conditions). A similar error between calibration sessions was deduced by repeating the calibration procedure several times. Systematic errors resulting from aging of the lamp could have been the largest, but facilities were only available for measuring total irradiance, and spectral changes would have remained obscure. Errors in wavelength were generally less than 5 nm, although heating effects occasionally increased this to 8 nm.

Study areas

Because of the cost and delicacy of the instrumentation and the volume of data required for realistic statistical comparisons, quantitative information about the differences between the light regimes of different habitats is sadly lacking. As two spectroradiometers were available for this work, it was decided to record the SPDs simultaneously beneath and outside vegetation canopies, so that any significant differences between shaded and open regimes could be expressed as a specific effect of the canopy at each time of recording. Analogous to a dual-beam spectrophotometer, the technique is an improvement over previous work where changes outside the canopy are superimposed on those beneath it.

As the climax vegetation of this phyto-climatic zone, oak woodland was an obvious choice for investigation. Beneath this canopy the shadow cast is not dense and a rich ground flora can be supported. In contrast, commercial pressures on land use dictate that the individuals comprising a crop canopy must be closely spaced and so an intense shadow is usually cast. Sugar beet was chosen as a suitable species for investigation, on account of its extremely dense canopy (see Morgan and Smith, 1981 for comparisons).

A significant factor in deciding upon suitable locations was the possibility of damaging the instruments during transport and use under field conditions. Because of humidity changes, dark current always increased rapidly after removal from the laboratory to the field, so the instruments had to be set up the evening before the photoperiod to be recorded. Consequently, they required protection from rainfall and, when remote from the University, could never be left unattended. Another factor was the paradoxical need to record light completely in the open, yet at the same point as the shade light was recorded; where large trees are involved, even approximating to this ideal state is logistically difficult.

The Oak Woodland

The best preserved oak woodland in the Leicester-Nottingham area is Swithland Wood (NGR = SK540125), described by Tasker [1977], but although direct comparison

1.2 study areas

with his work would have been interesting, this area was rejected because Leicestershire County Council were not enthusiastic about such a project being carried out there, and more importantly, the best locations in the wood are remote both from usable roads and from unshaded locations where the incident light could be recorded. Unfortunately, most of the other oakwoods in the area have been entirely replanted by Man and, hence, are unlikely to represent a close approximation to their natural state.

The Outwoods (NGR = SK516157 HAMSL = 140 m) however, like Swithland, are a formerly extensive relic of the ancient Charnwood Forest, and while much of the interior was cut and reafforested fairly recently, there remains an outer belt of naturally seeded oaks. Part of this, along the south-west edge of the wood, was selected as the study area. Charnwood Borough Council welcomed the proposed work, and easy access was provided by the road alongside.

The trees in the study area were mature Quercus robur L. individuals, with a mean height of about 18 m and trunk diameter of 0.52 m at breast height. Two individuals felled since the study show 80 and 120 growth rings. The mean gradient of the land is about 10%. Probably as a result of trampling and the related erosion of the very acid (pH 3.5) brown earth soil, the ground flora is impoverished and contrasts markedly with Swithland. Festuca rubra L. is abundant, with a mean June cover of 57% as indicated by optical point quadrat sampling at 1 m intervals along a 150 m transect through the wood. Pteridium aquilinum (L.) Kuhn, Teucrium scorodonia L. and Endymion non-scriptus (L.) Garcke occur occasionally.

The Sutton Bonington spectroradiometer was located at a fixed position selected at random within a 2 m radius of a point in the wood subjectively judged to be representative. Within this area the June mean cover of Festuca was 52%, giving a DOMIN rating of 8. As the monochromator drive could not be operated remotely, the operator had to be within reach of it, yet not physically shade the receptor head; hence, the assembly was fixed such that the receptor was 0.6 m above ground level and could be operated from beneath. The adjacent area was surveyed using a theodolite, and the trees numbered (Fig. 2). Correspondingly, Figure 3 is a hemispherical photograph taken in January 1981 from the exact position of the receptor head. The zenith ($\alpha = 90^\circ$) is approximately at the centre, and the horizon ($\alpha = 0^\circ$) is along the edge.

1.2 study areas

Using random arrays of points placed over the photograph, the interception of light in the absence of leaves was found to be 44% (+1%) with no significant difference between $60^\circ > \alpha > 30^\circ$ and $90^\circ > \alpha > 60^\circ$ estimates ($t=0.89$, $p_0 > 5\%$).

North-east of this site is a small ridge which, while not appreciably interfering with shadelight recording, afforded a convenient site for the recording of incident light (that is, global daylight unscreened by vegetation). The Leicester instrument was deployed on the crest of this ridge with its receptor head fixed above a 2.5 m support. Logistically straightforward, this location had all the advantages of close proximity to the woodland site. The quantum sensor (type Li-190s) of a light meter (type Li-18s; Li-Cor, Lincoln, USA) was fixed next to the spectroradiometer receptor head to provide a measure of PAR (which could be compared later with the 400 - 700 nm integral from the spectroradiometer) and any irradiance change during the course of recording the SPD. The data from both stations were discarded if this exceeded 2%. At the incident light recording station, notes were made regarding the cloud type and cover (0/8 for a clear sky to 8/8 for fully overcast conditions) for each SPD. Power for the machines was provided by a small petrol generator.

In order to characterise the canopy which gave rise to the recorded shadelight regime, a number of variable factors were measured after each day of recording. Leafy twigs were cut from a low branch of tree number 4 and brought down from the highest branch using a shotgun (Fig. 4). Leaf pigment content was then determined for the sun and shade leaves by McKinney's method (see Sestak, Catski and Jarvis, 1971). The twigs were first placed in darkness for an hour with their cut ends in water to restore full turgor. A leaf was cut and its area and fresh weight measured before two 9 mm discs were cut from the lamina and themselves weighed. They were rapidly homogenised with cold 80% (aq.) acetone, and extracted on ice in darkness for 20 minutes in 10.0 cm³ of the solvent. The suspension was centrifuged for 5 minutes to remove the cell debris, before assaying at 663, 645, and 480 nm in a spectrophotometer (type SP1800, Pye Unicam, Cambridge, U.K.) Chlorophyll a and b and carotenoid content were calculated from their extinction coefficients on fresh weight and unit area bases. Leaf biomass was also measured. The whole procedure was carried out on ten leaves from each twig.

1.2 study areas

The spectral properties of the leaves themselves were measured using a spectroradiometer (see Fig. 5). Differences in angular reflection and transmission are not accounted for by this procedure, but no integrating optics were available. The transmittance control was the direct beam, while that for reflectance was found by substituting a magnesium oxide plate, with a total reflectance of approximately 97%, for the leaf.

A total of eight photoperiods were recorded in the oak woodland; 25th April 1980 before bud break, 28th May 1980, 4th July 1980, 13th August 1980, 16th September 1980, 21st October 1980 when the canopy was senescing, 11th November 1980 during leaf fall, and 21st January 1981 when the branches were bare. A record was kept of the condition of the leaves borne by the nearby trees during senescence.

The Sugar Beet Crop

A small plot (4 x 3 m) was prepared on Experimental Field 12 at the School of Agriculture (NGR = SK506262, HAMSL = 46 m) for the cultivation of an erectophyll sugar beet cultivar (Beta vulgaris L. cv "Monoire"). This crop was grown for two purposes; the first was to provide a shadelight regime as intense as any likely to arise in agriculture or in nature, and to investigate the variation in its optical properties with time (see 1.3(iii)). Secondly, the radiation environment beneath the canopy was used as a treatment in a parallel study of the photocontrol of seed germination in natural daylight. If the canopy density had shown considerable spatial variation, the light recordings made at one point would inadequately describe others, so many more data would be required to define the shadelight regime. To avoid the problem an attempt was made to create a particularly homogeneous canopy; even so, this study comprised nearly 50,000 light measurements.

Normal seed drilling in rows was rejected as the variation in the distance, and hence competition, between nearest neighbours may be quite large. The optimal arrangement to minimise such differences is a triangular grid whereby each plant is surrounded by six equidistant nearest neighbours; however, planting seeds in such a pattern is inadequate because of the poor germination and

1.2 study areas

establishment of sugar beet. Instead, young field-grown plants were transplanted into the plot in mid-May, at a density of 6.7 plants m^{-2} . A very homogeneous canopy was produced, but transplanting checked seedling growth for 1 - 2 weeks, and hence maximum light interception was reached towards the end of September, rather than late August - early September in a conventionally drilled crop (Jaggard, Lawrence, and Biscoe, 1982).

Ignoring two guard rows, a point equidistant from three plants and 0.1 m above soil level was selected at random for the positioning of the receptor head of the Leicester spectroradiometer. 4 m from this, outside the canopy, the Sutton Bonington instrument was deployed with its receptor head 0.6 m above soil level. This arrangement was justified on the grounds that, although the less sensitive Leicester instrument did not allow reliable measurements to be made around dawn and dusk once the canopy had developed, the higher sensitivity available for recording the incident light allowed SPDs to be recorded long before dawn, at the times when some photoperiodically sensitive plants are thought to sense "beginning-of-day". Mains power was used. The PAR estimate from a Li-Cor quantum meter was recorded on a chart recorder; instrument settings, time and meteorological data were noted on the spectral chart as before.

Eight photoperiods were studied; 7th July 1981 before the plants had expanded enough to form the canopy, 28th July 1981, 18th August 1981, 16th September 1981, 29th September 1981, 21st October 1981, 10th November 1981, and 2nd December 1981. During July and August two quantum meters were used on four occasions to measure the mean transmittance of the developing canopy; one was manoeuvred between the rows (approximately 30 mm above soil level), the other positioned outside the canopy.

Also at Sutton Bonington, three photoperiods were studied in which only the incident light was recorded; 29th August 1979, 12th May 1982, and 9th June 1982. On the latter, data were gathered using both planar and spherical receptor heads. Thus, in all, nineteen complete photoperiods were investigated; the dates were not selected for "good weather" (although recording was not attempted at times of heavy rain) and hence the data are largely unbiased in this respect.

Presentation

Each spectral photon distribution (SPD) was handled as a block of forty-one SPFR bands. Each of these was 10 nm in width, starting from 395-405 nm etc. Computers were used extensively in the processing, storage, presentation, and analysis of this information; some of the main algorithms are described in Appendices I and II.

One way of reducing the data to more manageable proportions is to extract from ~~them~~ various parameters which might be physiologically potent (see 1.1) rather than consider the SPDs themselves. The program SUGAR assembles each SPD from the raw data and derives a number of such parameters from it. Subsequently, FAWKES was developed to plot each parameter as a conventional graph, and statistical analysis followed. Direct application of statistics to data is often unsatisfactory because a blind a priori approach risks leaving important trends within ~~them~~ completely obscure.

When comparing data gathered on different dates, time is an unsatisfactory control variable. As the times of sunrise and sunset vary with the season, so does the path length of the direct solar beam through the atmosphere at any time. This largely determines the quantitative and qualitative changes in the incident SPD. Referring to Figure 1, the solar position is defined by α_s , the solar angle, and β_s , the solar azimuth. Relative path length is largely a function of α_s (Robinson, 1966). Mean time is related to the average apparent movement of the sun around the celestial poles and not directly to α_s or β_s ; the discrepancy results from the tilt of the Earth's axis and its orbital motion. α_s and β_s may, however, be calculated according to the following principles.

Chronologically, the day is roughly defined by the return of the sun to due north (that is, $\beta_s = 0^\circ$) but as an orbit progresses, as seen from the Earth the sun moves against the distant starry background (although direct observation of this is prevented by the glare of daylight). Because of the orbital effect, a solar day is 1/365 longer than the actual rotation time of the Earth (the sidereal day). Sidereal and solar times are in phase only at the Autumnal Equinox; thereafter, the former runs about four minutes per day faster. At any instant, the sidereal time defines the relative position of the

celestial sphere. Siderial time at Greenwich (GST) can be calculated from GMT if the date is known, and is tabulated for 0000 GMT in the Ephemeris. By extrapolation, GST can be calculated from GMT during that day. East or west of Greenwich, the local siderial time is similarly derived from local mean time (four minutes ahead of GMT for every degree east). The apparent solar position on this celestial sphere is accurately predictable from the complex orbital motion of the Earth. The Ephemeris tabulates it for 0000 GMT in the polar coordinates of Right Ascension (RA, analogous to terrestrial longitude) and Declination (analogous to latitude). The small shift in solar RA during the day can be compensated for by extrapolation. Knowing these three variables, the relative solar position is fixed for any known latitude. α_s and β_s can now be calculated. Consider the spherical triangle formed by the zenith, Z, the celestial pole, N, and the sun at P, according to Figure 1. The time elapsed since the sun was due south (the zenith-pole-sun "hour angle") is calculated by subtracting RA from siderial time. The angle subtended by pole and zenith is 90° minus the latitude, while that subtended by the sun and the pole is 90° minus the declination. Thence, spherical trigonometry yields the pole-zenith-sun angle (β_s) and the angle subtended by the zenith and the sun ($90^\circ - \alpha_s$).

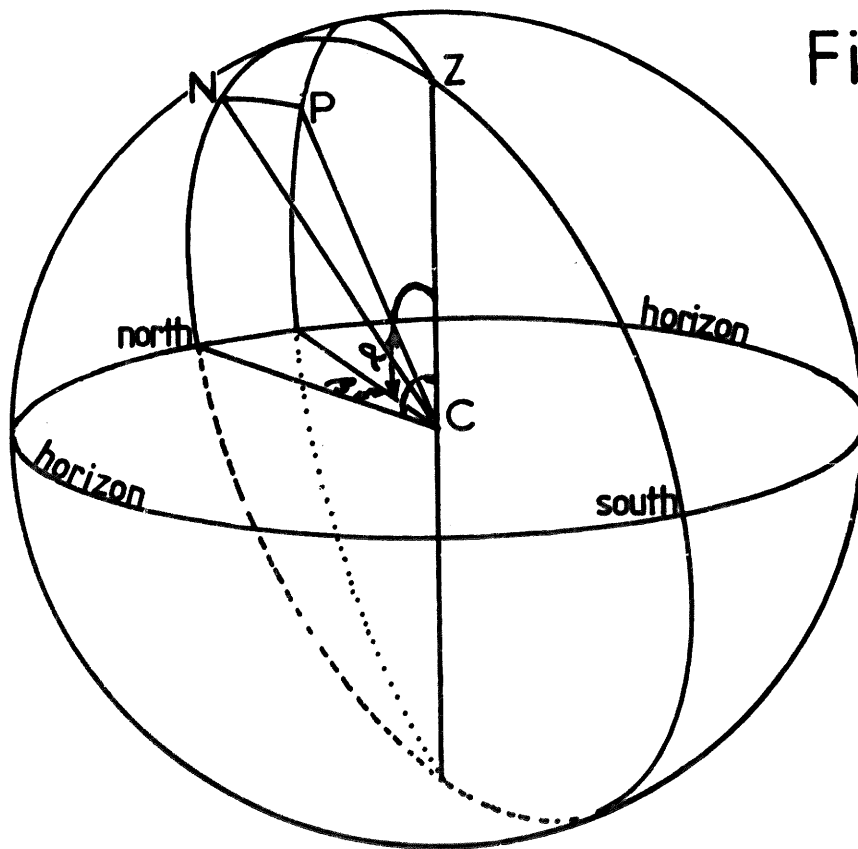
True solar angle and azimuth were calculated in this way by the algorithm ALAZ (see Appendix II). The error introduced by atmospheric refraction is not entirely predictable, but is quite large at low solar angles (when the apparent α_s is 0.5° greater - about a sun's breadth). No account was taken of the local horizon or correction made for non-geocentric observation.

It is quite possible that features of the SPDs, not related to any of the nine parameters derived from them, could have unsuspected physiological significance, but presenting the mass of data in a suitable form to reveal such features is difficult. The method adopted in this work was to express each SPD relative to the total fluence rate at that moment, and so construct a "surface" to represent the variation of light quality with time during each photoperiod. The normalising procedure is necessary because the change in the total irradiance during each photoperiod is many orders of magnitude greater than the variation within the instantaneous SPD. This disparity should serve to temper argument concerning the role of spectral changes in nature.

1.2 presentation

However, some technique was required to represent the three dimensions (time, wavelength, and relative SPFR) of this surface on paper in a clear manner. Contour mapping procedures for surfaces of this complexity were found to be too difficult to interpret and lacked the required precision, while simple graphical projections of a mesh connecting the data points was unsatisfactory as all the lines were drawn, including those conceptually hidden behind other parts of the surface. However, conventional surface drawing routines (which compute the position of hidden areas) use an algorithm which requires height coordinates of the surface to occur at points corresponding to regular distances along each of the two controlling axes. In this project, SPDs were not recorded at regular intervals, so using the algorithm directly gave a distorted time axis. Alternatively, when the irregular matrix was mathematically fitted to a regular one, the smoothing effect was found to be often excessive and unpredictable. Eventually, drawings of the relative SPD surfaces were plotted using a new algorithm (subroutine JØ6HEF) under development at the Computer Graphics Centre of Leicester University. Uniquely, this accepts irregularly spaced matrices. The conceptual viewing position was chosen to eliminate perspective and to preserve a "left-to-right" sense for increasing time and wavelength.

Fig.1



Spherical geometry of natural radiation

C is a point surrounded by sources of light; projected at infinity, these comprise the radiating sphere.

Z is the zenith, the point vertically above C

P is any point on the sphere

α is the angular altitude of P above the horizon ($-90^\circ < \alpha < +90^\circ$)

β is the angular azimuth of P clockwise from north ($0^\circ < \beta < 360^\circ$)

CN is the Earth's axis of rotation

N is the northern celestial pole

Figures 2 and 3

The Outwoods shadelight recording site.

Large Arabic numeral labels refer to nearby trees

On the overlay, the bearing of true North (and South, East & West) is indicated alongside magnetic North. The grid indicates solar position throughout the year:-

Arabic numerals indicate local solar time in hours after noon (morning hourly positions are also indicated);

Roman numerals indicate the month of the year

- (i = January and November
- ii = February and October
- iii = March and September
- iv = April and August
- v = May and July
- vi = June
- xii = December)

Fig. 2

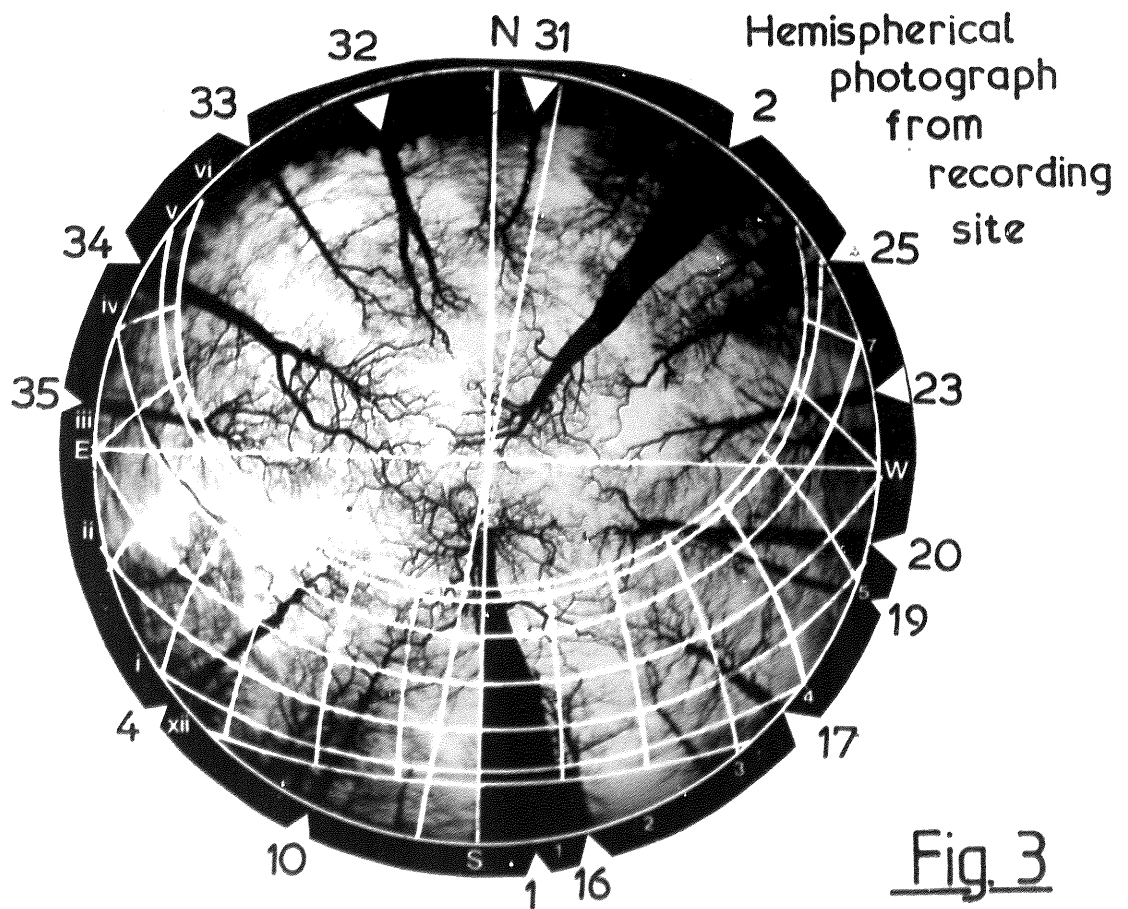
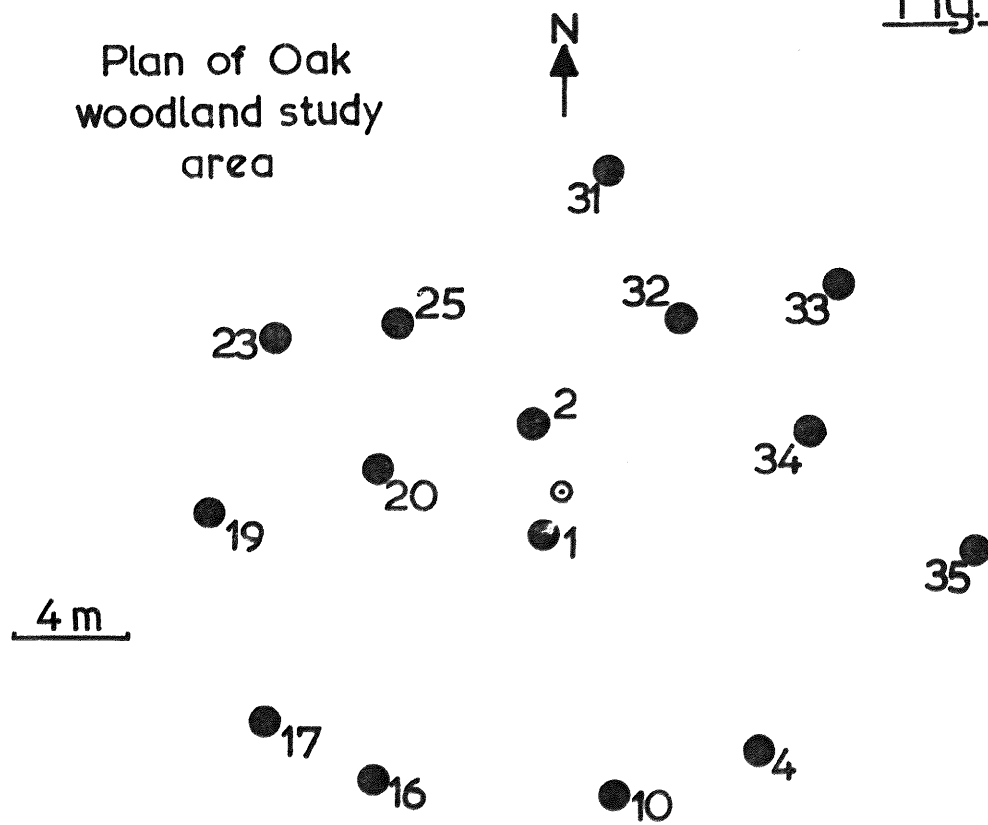


Fig. 3

Fig. 2

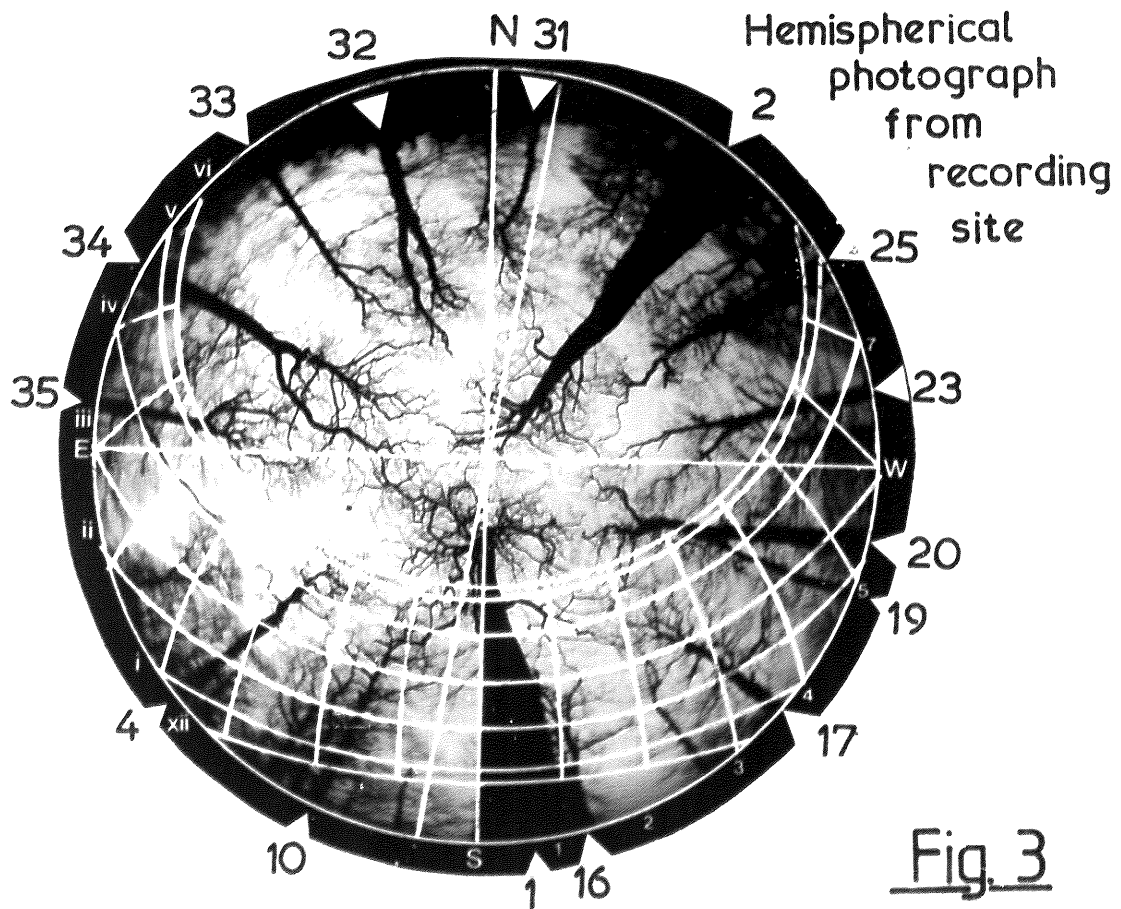
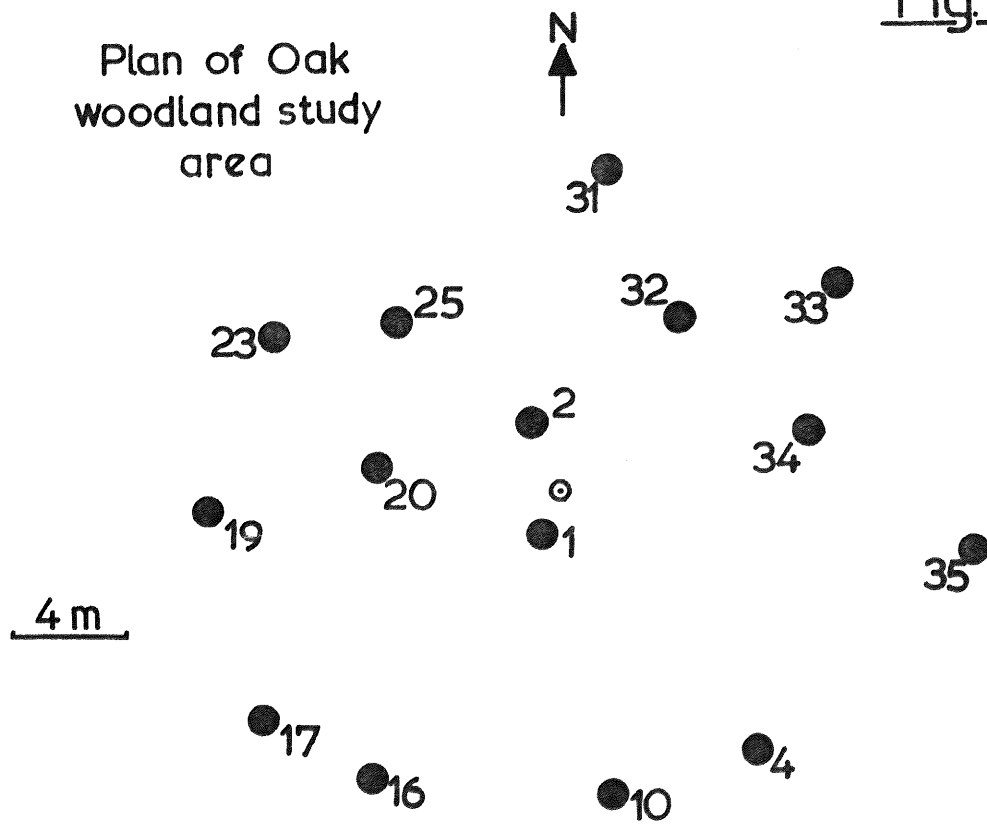


Fig. 3

Fig. 2

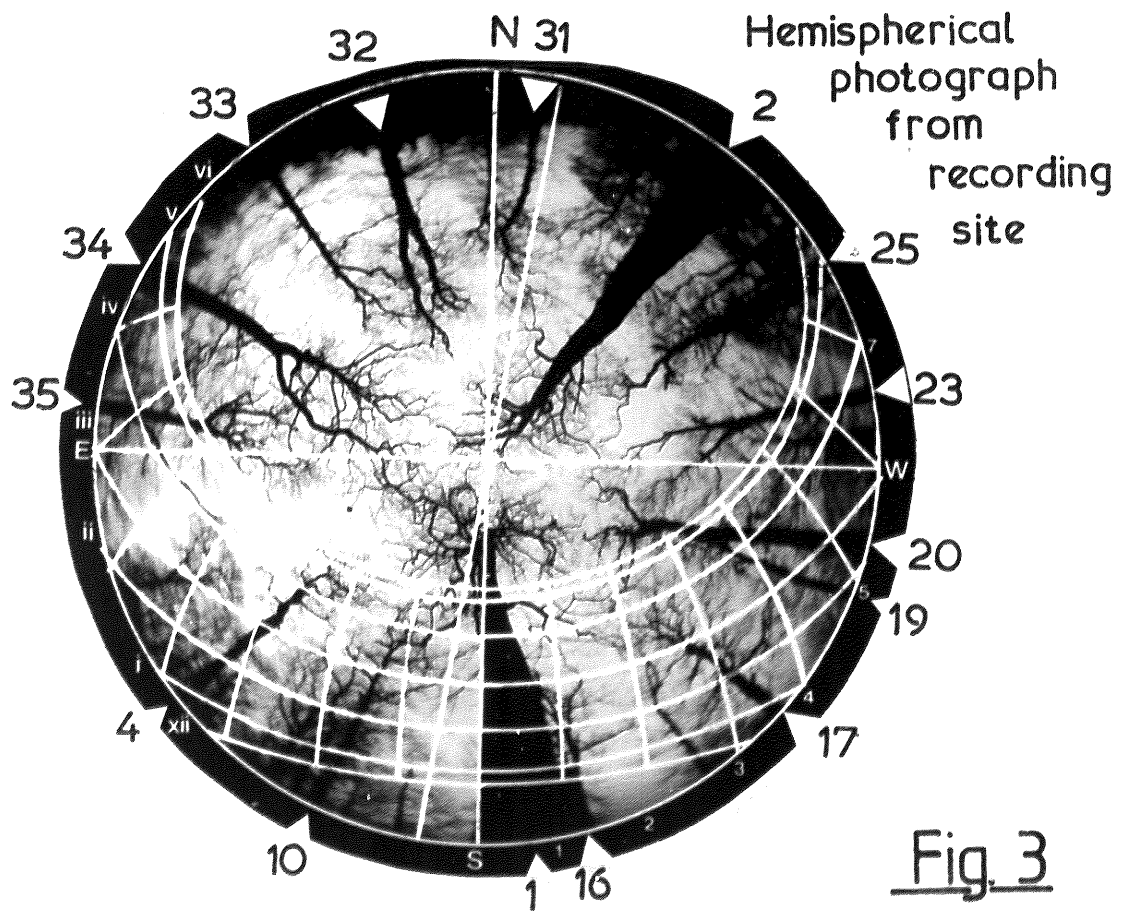
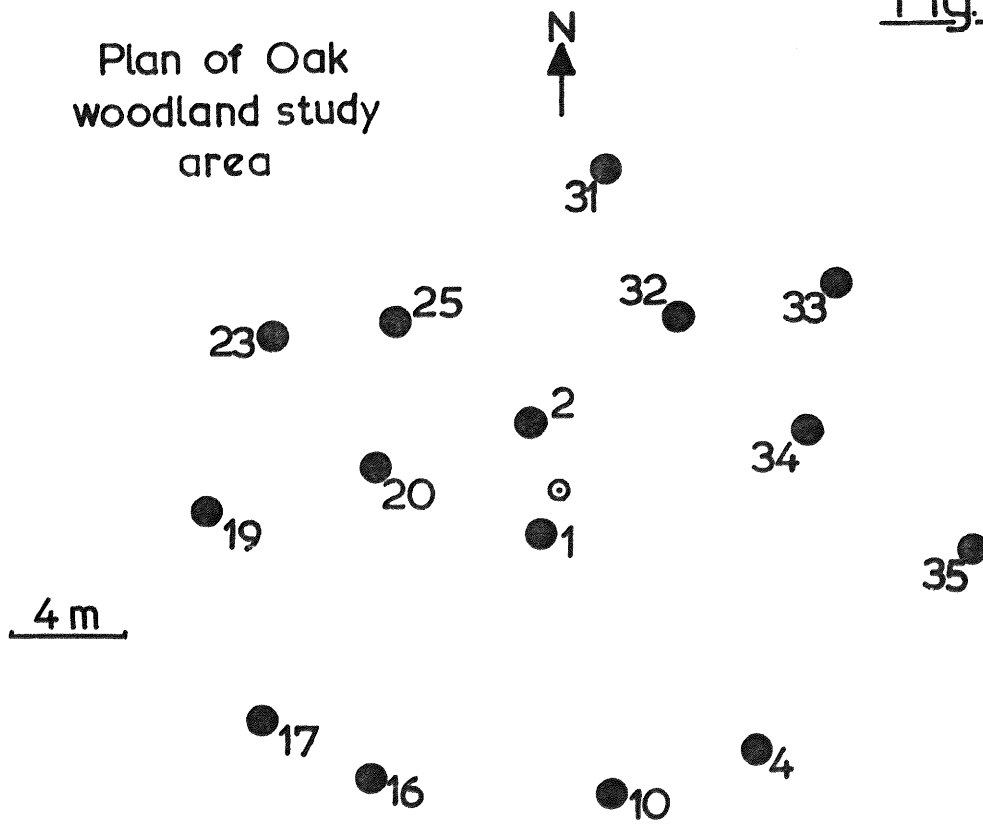
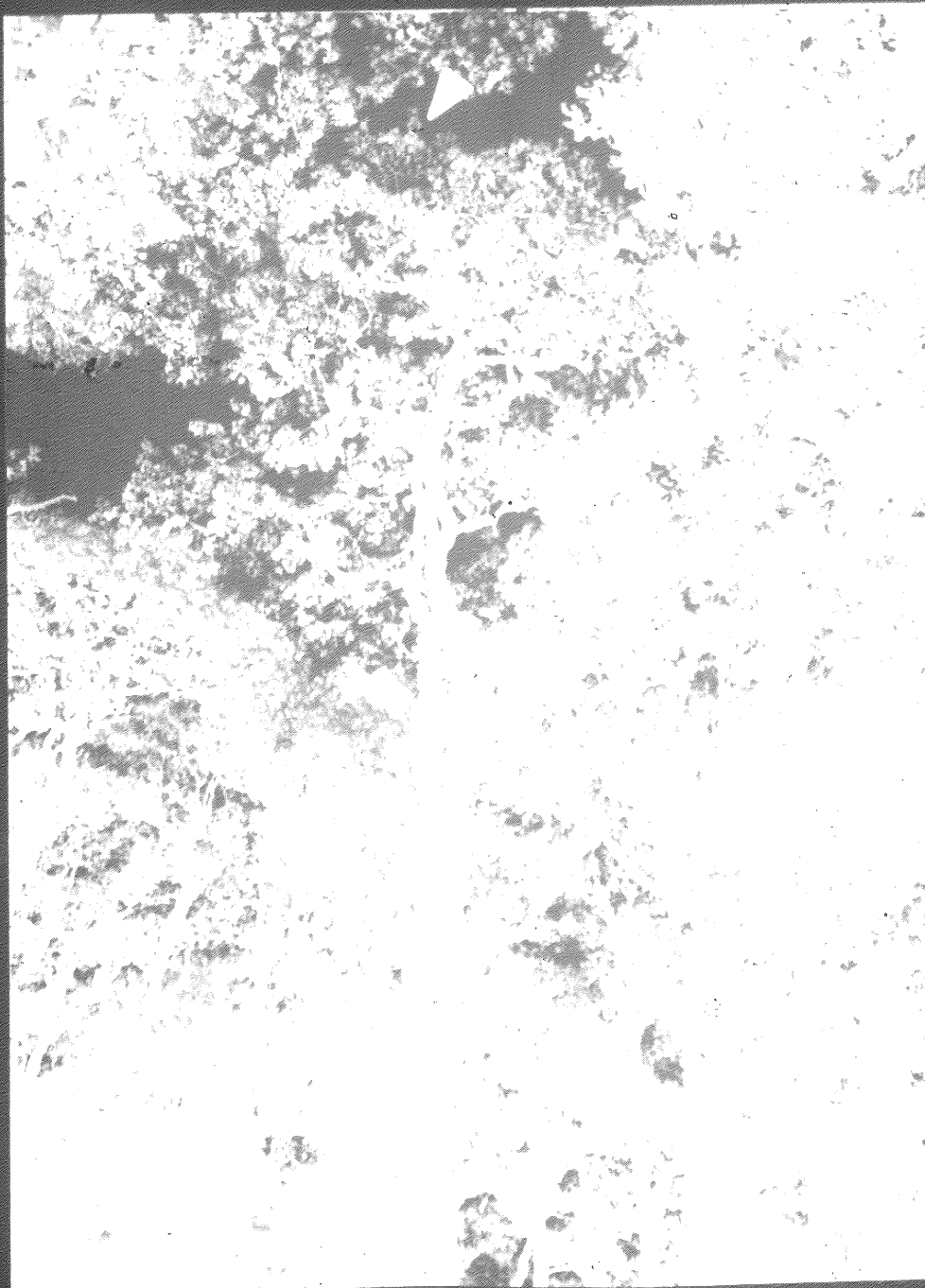


Fig. 3

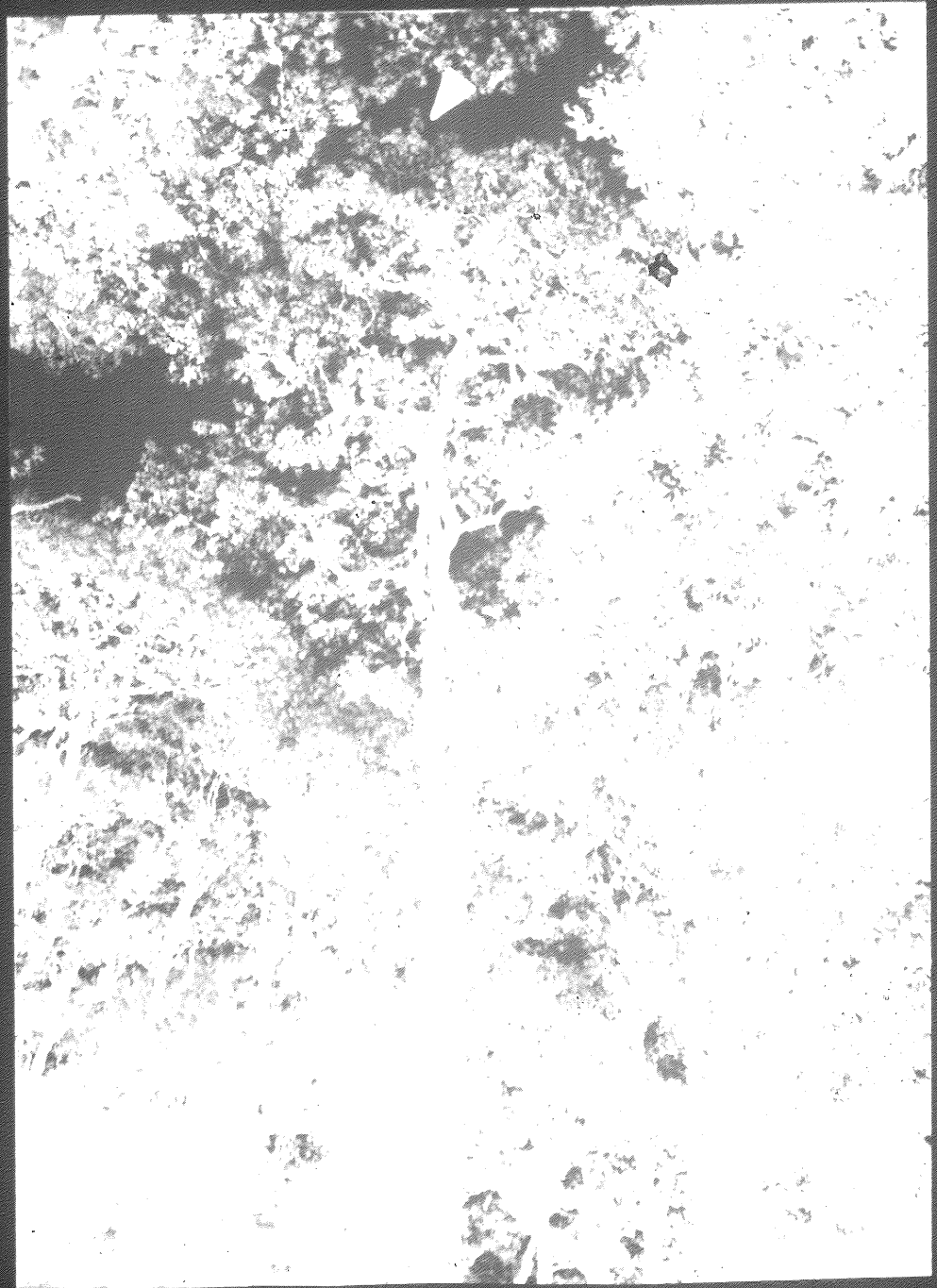
Fig. 4



Outwoods, August 1980. Tree No. 4

The branches from which sun and shade leaves
were taken are indicated by arrows.

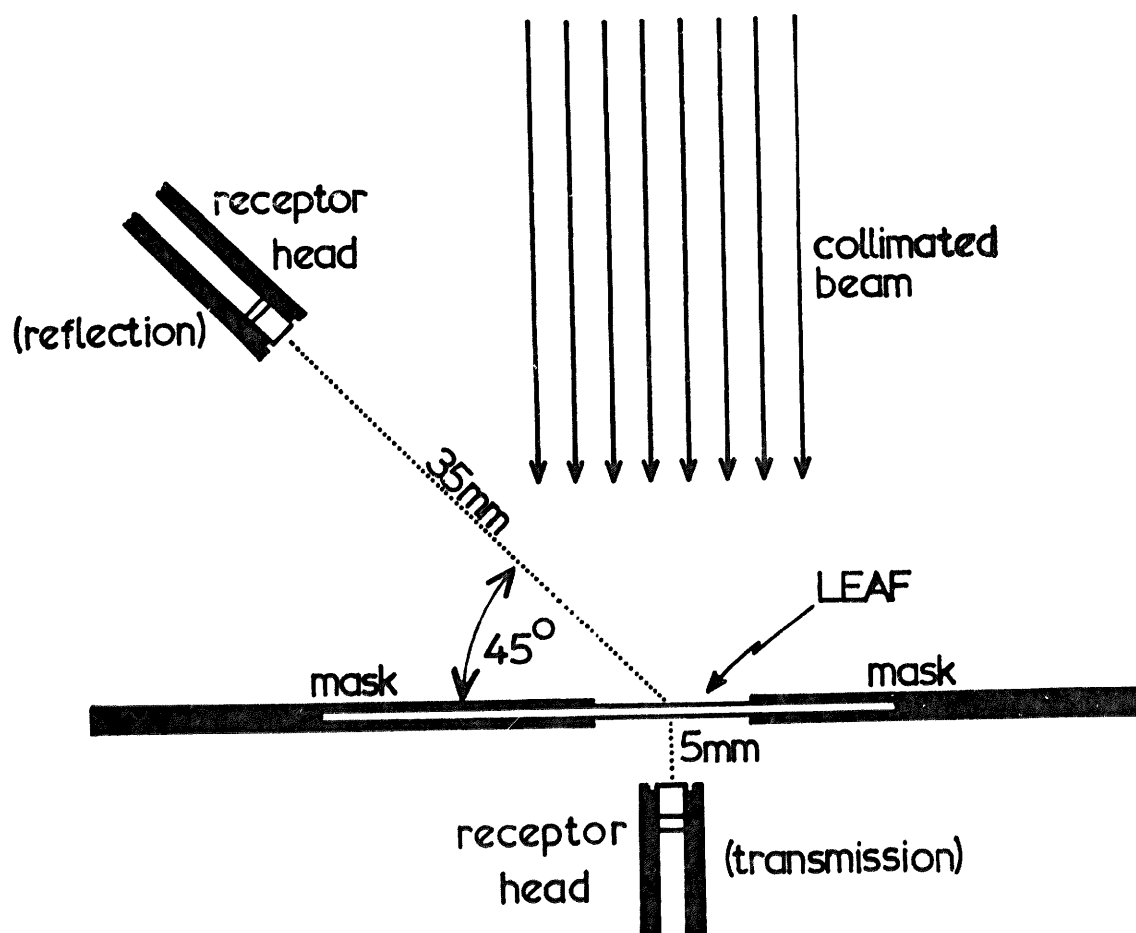
Fig. 4



Outwoods, August 1980. Tree No. 4

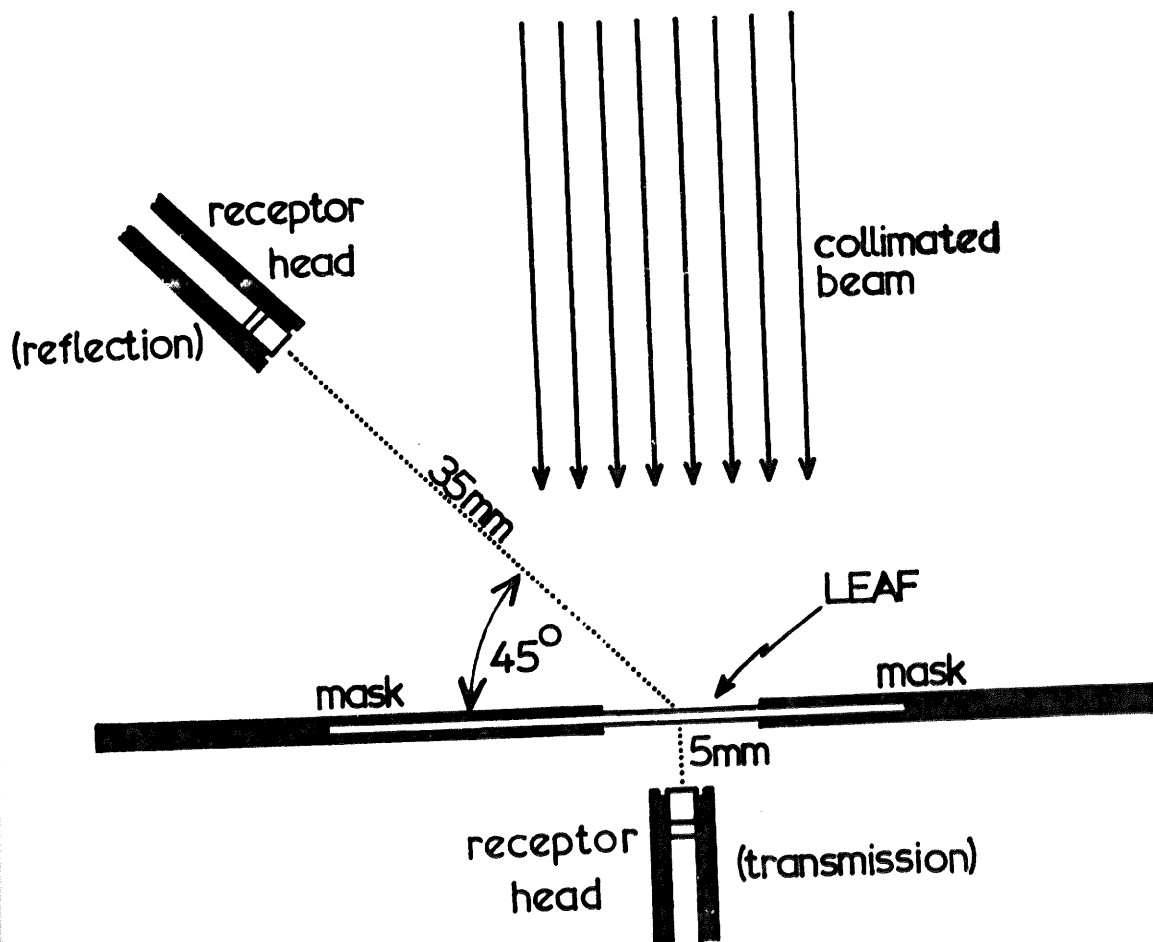
The branches from which sun and shade leaves were taken are indicated by arrows.

Fig.5



System for measuring spectral reflectance and transmittance of oak leaves.

Fig. 5



System for measuring spectral reflectance and transmittance of oak leaves.

RESULTS AND DISCUSSION

1) INCIDENT LIGHT

General

The dates and times at which SPD data were recorded at Outwoods (in 1980) and Sutton Bonington (in 1981) are illustrated in Figures 6 and 7 respectively. The dotted and broken lines indicate the times at which α was equal to 0° (sunrise and sunset) and 30° respectively. The upper and lower bars along each of the year day lines represent the PAR fluence rate and cloud cover respectively at the time of each SPD recording.

Considering the form of the SPDs in general, the results obtained are in general agreement with earlier work. Three typical scans recorded on 7th July 1981 are presented in Figure 25, but it was considered desirable to show the rate and extent of change throughout different photoperiods. Thus, Figures 8 - 18 show the relative SPD surfaces corresponding to photoperiods studied at Sutton Bonington on 29th August 1979 and between July 1981 and June 1982 (see Fig. 7). They serve to illustrate the variation in light quality during the photoperiod which can be expected in open situations throughout the year. The equivalent data for Outwoods show entirely similar features.

All the surfaces show a number of grooves running perpendicular to the wavelength axis; in the blue and green regions these are caused by relatively low energy atomic absorption in the photosphere of the sun. Such absorption by various elements leads to a massive reduction in fluence rate in a large number of very narrow (ca. 0.1 nm) wavebands, first discovered and catalogued by Fraunhofer. The groove at 430 nm results from Fraunhofer G (iron/calcium) and G1 (hydrogen) absorption bands, while that at 490 nm is caused by Fraunhofer F (hydrogen) alone. The complex b1, b2 and b4 (magnesium) gives rise to the groove at 520 nm. In the red and far-red, however, molecular absorption in the Earth's atmosphere becomes increasingly intense and is responsible for the dominant grooves in this region. Those at 655 nm and 735 nm are due to water vapour, although the Fraunhofer c (hydrogen α) absorption band contributes substantially to the former. Molecular oxygen is responsible for the grooves at 630, 695 and 765 nm. The Chappuis band of ozone absorption in

the green - red region is too shallow and broad to be distinguishable.

However, the relative SPFR at each wavelength is not constant; there is some variation within the main part of the day, and a major redistribution around sunrise and sunset. The calculated values for \mathcal{F} (Fig. 20), ϕ_c (Fig. 21) and B:R ratio (Fig. 22) bear this out. The equivalent data for the logarithmic fluence rate of red light ($\log R$) are given in Figure 23. The ranges of solar position where $\alpha_s > 7.5^\circ$ and $\alpha_s < 7.5^\circ$ will be considered separately.

Daytime ($\alpha_s > 7.5^\circ$)

Results

The most striking feature of the relative SPFR surfaces (Figs. 8 - 18) is their remarkable smoothness between 460 and 690 nm (all the more so because local irregularities of the surface appear prominent when data are plotted in this way). The fall-off at shorter wavelengths is quite uniform, but in the far-red considerably more noise is apparent. Although there is little difference between the potential SPFR errors in the far-red and violet, some of the variation in the former is due to the potentially greater wavelength error in this region (see 1.2) interacting with intense atmospheric absorbance near 735 and 765 nm. Thus, within the 5 nm wavelength error, considerable redistribution of the apparent fluence rates in the adjacent wavebands was possible. The most extreme example is seen on 28th July 1981 (Fig. 10) at 9.75 h and 10.53 h when subsequent inspection of the recorded position of the 765 nm absorbance band revealed errors of +7 nm and -8 nm respectively; these were the result of an electronic fault. However, the apparent high proportion of far-red between 13.5 and 16.5 h on 16th September 1981 (Fig. 12) cannot be accounted for on this basis, and was probably a direct result of the unusual weather conditions at that time; the heavy rain-bearing clouds had reduced PAR to about $100 \mu\text{mol m}^{-2} \text{s}^{-1}$.

\mathcal{F} , ϕ_c , and B:R ratio were calculated from the data shown in Figures 8 - 18 and those gathered at the Outwoods in 1980 (see Fig. 6). These are presented graphically versus the calculated solar angle (α_s) in Figures 20, 21 and 22 respectively. The horizontal bars indicate the mean value of the parameter over that range

the green - red region is too shallow and broad to be distinguishable.

However, the relative SPFR at each wavelength is not constant; there is some variation within the main part of the day, and a major redistribution around sunrise and sunset. The calculated values for β (Fig. 20), ϕ_c (Fig. 21) and B:R ratio (Fig. 22) bear this out. The equivalent data for the logarithmic fluence rate of red light ($\log R$) are given in Figure 23. The ranges of solar position where $\alpha_s > 7.5^\circ$ and $\alpha_s < 7.5^\circ$ will be considered separately.

Daytime ($\alpha_s > 7.5^\circ$)

Results

The most striking feature of the relative SPFR surfaces (Figs. 8 - 18) is their remarkable smoothness between 460 and 690 nm (all the more so because local irregularities of the surface appear prominent when data are plotted in this way). The fall-off at shorter wavelengths is quite uniform, but in the far-red considerably more noise is apparent. Although there is little difference between the potential SPFR errors in the far-red and violet, some of the variation in the former is due to the potentially greater wavelength error in this region (see 1.2) interacting with intense atmospheric absorbance near 735 and 765 nm. Thus, within the 5 nm wavelength error, considerable redistribution of the apparent fluence rates in the adjacent wavebands was possible. The most extreme example is seen on 28th July 1981 (Fig. 10) at 9.75 h and 10.53 h when subsequent inspection of the recorded position of the 765 nm absorbance band revealed errors of +7 nm and -8 nm respectively; these were the result of an electronic fault. However, the apparent high proportion of far-red between 13.5 and 16.5 h on 16th September 1981 (Fig. 12) cannot be accounted for on this basis, and was probably a direct result of the unusual weather conditions at that time: the heavy rain-bearing clouds had reduced PAR to about $10 \mu\text{mol m}^{-2} \text{s}^{-1}$.

β , ϕ_c , and B:R ratio were calculated from the data shown in Figures 8 - 18 and those gathered at the Outwoods in 1980 (see Fig. 6). These are presented graphically versus the calculated solar angle (α_s) in Figures 20, 21 and 22 respectively. The horizontal bars indicate the mean value of the parameter over that range

of α_s and the small vertical bars indicate the corresponding standard error. The data were classified according to the day of recording and three classes of solar angle ($7.5^\circ < \alpha_s < 15^\circ$, $15^\circ < \alpha_s < 30^\circ$, and $30^\circ < \alpha_s < 60^\circ$) and the mean and standard error calculated for each. The results are given in Tables 1, 2 and 3.

Further statistical analysis of the sources of variation is not straightforward. It is in the nature of these data that, for each parameter, differences between the mean values for different days cannot be separated from the effect of solar angle; there are two reasons for this. Firstly, it is possible that the relationship between a parameter and α_s changes. Therefore, after the main factors (days and solar angles) have been accounted for, a source of variation due to the interaction itself must be separated from the residual variation. Secondly, the number of recordings made within each class on each day was not constant, and problems arise from the consequent unequal replication within the factorial matrix. Conventional procedures would be unable to treat the sub-classes uniformly, and wildly inaccurate, even negative, variances would be generated. Superficially, this could have been avoided by recording a fixed number of SPDs within the periods corresponding to the α_s classes, but although a normal feature of experimental design, it cannot be achieved in this case. Around mid-summer α_s exceeds 30° during most of the day, while around mid-winter α_s is always less than 30° (see Figs. 6 and 7), leaving the corresponding sub-classes empty. It is possible for empty sub-classes to be fitted into the pattern of the others by treating them as "missing values", but this is not justified here, in essence because only things which can exist can be missing.

Therefore, the data are inherently "non-orthogonal" and the sources of variation can never be completely separated; those accounted for earlier in any analysis will steal variability from the later ones. Table 5 shows the results of a non-orthogonal ANOVAR of the \mathcal{F} , ϕ_c , B:R ratio and log R data; the sum-of-squares was partitioned firstly between the nineteen days, then between the three solar angle classes, followed by the interaction and finally the residue. For \mathcal{F} , ϕ_c and log R the insignificance of the interaction ($p_0 > 5\%$) implies that the factors act independently, but the differences between days and between solar angle classes are highly significant ($p_0 < 0.1\%$). For the B:R ratio, interaction

between days and angles is significant ($p_o < 5\%$) implying that the solar angle affects the ratio differently on different days. The origin of this effect is unknown, but it is in any case minute. Above the interaction there is a significant difference between days ($p_o < 1\%$) but not between solar angle classes ($p_o > 5\%$).

The coefficients of sample variation (standard deviation expressed as a percentage of the mean) for \bar{J} , ϕ_c , B:R and log R subclasses are approximately 5%, 0.5%, 10% and 10% respectively. It is possible that cloud cover may have been responsible for some of this variability. Figure 25 illustrates two relative SPDs from Figure 9 both corresponding to a solar angle of 40° ; one was recorded in the morning when the sky was overcast, and the other in the afternoon under a clear sky. A difference is apparent, although it is small compared with that associated with twilight. Figures 6 and 7 show that the most radical change in cloud cover in the solar angle class $30^\circ - 60^\circ$ occurred on that day (7th July, 1981). The statistical significance of the effect of cloud cover on PAR, \bar{J} and ϕ_c was examined. The data for $30^\circ < \alpha_s < 60^\circ$ were divided into three classes according to cloud cover (0/8 - 1/8, 3/8 - 5/8 and 7/8 - 8/8) and subjected to a simple ANOVA (Table 4). As would be expected, PAR was strongly affected by cloud cover ($p_o < 0.1\%$). Similarly, cloud cover had highly significant effects on the B:R ratio ($p_o < 0.1\%$), but the effect on \bar{J} was not significant ($p_o > 5\%$). The correlation coefficients of B:R and \bar{J} versus cloud cover were +0.87 and -0.26 respectively. Thus, it seems unlikely that cloud cover can be held responsible for much of the variation in \bar{J} , although it is probably a potent factor in modifying the B:R ratio.

All the results presented above relate to the down-coming radiation incident upon a horizontal plane (that is, where $\alpha > 0^\circ$). As this convention is open to some criticism, SPDs were recorded using a spherical receptor head for comparison (see 1.2). Tables 1 - 3 include a summary of the data gathered using this receptor, and Figure 19 shows the mean spectral fluence rate received by the spherical receptor relative to the planar receptor during the main part of the day.

Discussion

During daytime, while the total irradiance varies greatly with atmospheric conditions, the relative SPDs show a remarkable consistency in the face of considerable climatic variation. This may be explained, however, by the effect of cloud upon incident light.

In the absence of clouds or aerosols, Rayleigh scattering is responsible for the intensity of the sky remote from the solar disc, and as the effect is inversely proportional to the fourth power of the wavelength, these regions appear predominantly blue (maximum SPFR is at 460 nm). The contribution of this skylight to the global fluence rate is considerable, but the spectral shift is reduced by the concomitant loss of the same wavelengths from the direct beam. When an isotropic cloud layer intervenes, however, the direct solar beam is scattered much more strongly. Because the proportionality of scattering to wavelength is small, so are the spectral differences under clear and cloudy conditions. As cloud cover increases the intensity of the skylight increases initially but subsequently falls as more of the light is back-scattered. Hence, clear conditions would be expected to differ substantially from overcast ones only in total fluence rate (because of massively increased back-scattering of the direct beam and, in the presence of dense cloud, skylight) and in the proportion of each wavelength contributed by different areas of the sky. Figures 8 - 18 and the results of the ANOVAR for \bar{J} and PAR in Table 4 are in broad agreement with this.

The changes in B:R ratio associated with cloud cover (Fig. 25, Table 4) are in agreement with previous work (Taylor and Kerr, 1941; Hull, 1954; Robertson, 1966; Holmes and Smith, 1977a) but difficult to explain. The absorbance band of water vapour at 655 nm and the slight spectral dependence of scattering by water droplets might contribute to the difference. A further factor might be that part of the predominantly blue back-scattered light from lower parts of the atmosphere would be reflected downwards again from a cloud layer, enhancing the relative contribution of this waveband.

Accordingly, larger spectral shifts would be expected during the passage of broken cloud, when the global spectrum would tend towards that of Rayleigh skylight alone or the direct beam alone when the solar

disc was obscured or exposed respectively. Extreme cases of either are transient and therefore difficult to record, but the attempt made on 12th April 1982 gives an indication of their potential (see Fig 24). These results are not entirely in agreement with those of Holmes and Smith [1977a] who found the spectral difference between clear and fully overcast conditions to be greater than that between completely clear and "sun obscured" conditions. A complicating factor is that haze or relatively tenuous cloud at high altitude (as on 12th April 1982) may accompany lower cloud; cirrus clouds would be expected to increase $\bar{3}$ a little (Guttman, 1966). Even an approximate "Rayleigh sky" is very rare.

The correspondence between the mean $\bar{3}$ values reported in Table 1 and those of Holmes and Smith [1977a] is almost uncanny. These workers derived a mean of 1.15 ± 0.02 for clear skies at high solar angles using horizontal planar receptors; for various reasons (for instance, differences in receptor geometry or orientation, wavebands measured), none of the other published data are entirely comparable. As the variation about mean $\bar{3}$ is very small, it was not expected to be significantly related to either the day of recording or the class, but Table 5 ascribes significance to both factors. Because the factors are non-orthogonal, the order in which they are accounted for influences the variance estimate for each, although the total variability remains constant. However, when the sequence is reversed, the variance ratios become 8.4 and 38 (instead of 11 and 38), so the difference does not affect the conclusion drawn from the data.

There have been reports of seasonal variation in a far-red : red ratio of incident daylight at sunset (Gorski, 1976) and of the direct solar beam at various solar angles under clear sky (Gorski, 1980). However, as no information was included concerning the variability of the data, the value of the work is limited. Table 1 indicates that the data recorded in this work incorporate little seasonal trend. The mean values in the $7.5^\circ < \alpha < 15^\circ$ class for the months between June and September and between December and April inclusive were subjected to a small sample t - test. The insignificant difference ($t=1.8$, $p_0 > 5\%$) casts doubt upon Gorski's extrapolation to the natural environment.

However, the early months of the year (corresponding to the putative maximum far-red:red ratio) were sampled on

few occasions in this project. Tasker [1977] reported $\bar{\alpha}$ values in woodlands prior to leaf emergence somewhat lower than the mean of those in Table 1 and of Holmes and Smith [1977a]. Moreover, he found significant differences between days but attributed these to the relatively greater proportion of light transmitted by the bare canopy from the zenith region of the sky. This seems unlikely, as a comparison of the data recorded at Outwoods on 25th April 1980 outside (Table 1) and beneath the leafless canopy (Fig. 35) shows that $\bar{\alpha}$ was closely similar ($\pm 1\%$) at both sites during daytime. For purposes of comparison, the data of Tasker [1977] for $10^\circ < \alpha_s < 40^\circ$, unpublished data of A. Webb for $\alpha_s = 10^\circ$ (recorded at Sutton Bonington in 1983), the reciprocal of Gorski's [1980] data for $\alpha_s = 10^\circ$ and those reported here for $7.5^\circ < \alpha_s < 15^\circ$ are presented together in Figure 26. The pooled English data show highly significant differences between summer and winter periods ($t=7.3, p_0 < 0.1\%$). In view of the different techniques used and assuming the Polish data to have a similar variability to the rest, the three sets are not inconsistent. However, in view of the day to day variability of the data in relation to the size of the putative annual trend, it is unlikely that the latter is of much ecological significance.

Light reflected from beneath is likely to modulate the growth of plants above, as leaves generally reflect at least as much light as they transmit. As the absorbance of far-red is relatively small, both transmitted and reflected light show a low ratio of red to far-red (Moss and Loomis 1952). When considering light from the whole radiant sphere (Fig. 1), the effect of a leafy canopy on the light environment beneath it (see below) must be greater than on that above it; however, most plant parts directly exposed to this reflected light will be significantly screened from downwardly directed incident light. In this connection, the relatively high proportion of far-red received by the spherical head while $\alpha_s > 30^\circ$ is interesting (Fig. 19). The irradiance incident upon the sphere (I_s) illuminated by diffuse skylight alone is lower than that upon the horizontal plane (I); hence I_s is approximately 70% I in the PAR region (400 - 700 nm). However, since the grass sward beneath the receptor heads at the recording site reflected a considerable quantity of far-red light, I_s is greater in this region, and approximately equal to I . Differences are also apparent from Tables 1 - 3.

Twilight ($\alpha < 7.5^\circ$)

Results

In contrast to the constancy of the spectrum during the main part of the day (see above), extensive shifts in the distribution are apparent around sunrise and sunset (Figs. 8 - 18 and Fig. 25). Following the lines parallel to the time axis through the day shows that the contribution of the blue wavelengths falls as dawn approaches and continues to do so for up to an hour after sunrise; thereafter, their contribution changes abruptly to a fairly constant level which persists through the day, until a similarly sudden increase associated with sunset begins; this effect is maximal at 460 nm. At somewhat longer wavelengths the transition becomes less marked until, at about 550 nm (yellow-green) there is little change. Thence, in the orange and red, the opposite change is seen, the contribution rising at dawn and falling at dusk. The maximum change occurs at about 600 nm, but again the effect becomes less marked at longer wavelengths until, at about 710 nm in the far-red, there is little twilight change. At longer wavelengths still, the contribution declines once more at dawn and increases at dusk in much the same manner as for blue light.

These crepuscular changes are, however, not shown in all cases. Figures 11 - 17 show prominent peaks at 590 nm superimposed on the initial and terminal SPDs. These result from sodium street lighting (D1 and D2 Fraunhofer emission) back-scattered towards Earth by cloud. Figs. 16 and 17 also show the characteristic mercury emission at 580 nm and 435 nm caused by faint light from distant discharge lamps. None of these sources contributed a large proportion of the recorded fluence rate (and they always contained less than $50 \text{ pmol m}^{-2} \text{ s}^{-1}$). On several days, the usual major shifts in the distribution failed to occur. Around dawn on 28th July 1981 (Fig. 10) the normal smooth drop in blue light was interrupted by a secondary peak at the expense of both red and far-red. This was correlated with a period of broken cloud cover. Similar aberrant blue peaks occur on other plots, and were generally associated with broken or layered clouds near the sun. In contrast, Figure 16 shows a normal high proportion of far-red during twilight, but a fairly constant level of blue. Figure 18 shows a similar phenomenon at dawn, but a normal change at dusk. These were associated with fog, in the

presence of which daylight often appears yellowish.

As would be expected from Figures 8 - 18, the B:R ratio generally drops rapidly at dawn and rises at dusk, except in the presence of fog. Figure 22 shows this parameter plotted versus solar angle for all the incident daylight SPDs recorded in this study. The equivalent rise and fall in \bar{J} (Fig.20) and ϕ_c (Fig.21) is less marked. The mean values recorded on each day during the twilight period ($-7.5^\circ < \alpha_s < -2.5^\circ$, $-2.5^\circ < \alpha_s < 2.5^\circ$, and $2.5^\circ < \alpha_s < 7.5^\circ$) are given in Tables 1, 2 and 3 respectively. Statistical analysis of the data for the twilight period involved a non-orthogonal procedure similar to that adopted for daytime. The subclasses were as above (3 classes of α_s , 19 days) and the results are given in Table 6. The interaction term is significant ($p_o < 1\%$) for all three light quality parameters, due largely to the effects of fog. However, even in relation to the interaction, the main factors have highly significant effects upon \bar{J} and ϕ_c ($p_o < 0.1\%$). The B:R ratio shows the largest interaction between factors; above this α_s is predominant ($p_o < 0.1\%$) while the variation between days is barely significant ($p_o < 5\%$). Figure 23 shows, for comparison, the logarithmic fluence rate of red light ($\log R$) for the incident daylight data. The data are summarised in Table 7, from which it is apparent that large differences exist between days and solar angle classes. A non-orthogonal analysis of variance of this parameter (Table 6) shows that interaction between the main factors is insignificant and, although the difference between days is highly significant ($p_o < 0.1\%$), it is small in relation to the effect of solar angle.

Discussion

Both in the laboratory and the field it is apparent that critical night length can be estimated precisely ($\pm 1\%$) by individuals of certain species at their optimal physiological age (see Salisbury, 1981b). Unfortunately, the zeitgeber, photoreceptor and timing mechanism are all largely obscure. Various experimental procedures have led to conflicting suggestions regarding the action of the photoreceptor. It is of course essential that these must be consistent with the potential zeitgebers in the natural environment.

It is apparent that phytochrome is involved in photoperiodism, and that the red:far-red ratio has large

effects upon ϕ_c . Figure 20 indicates that phytochrome is likely to be affected by the spectral changes associated with twilight, the photoequilibrium falling with declining solar angle. Such a fall is predicted when the whole SPD is related to the phototransformation in vitro (Fig. 21). Although there is a significant effect of date upon the relationship between the parameters and solar angle, the effect of solar angle itself is much more significant statistically; the variation between days is smaller. It seems likely that such changes do have the required accuracy relative to solar angle to provide the zeitgeber for photoperiodic time measurement.

The opinion that Pfr concentration above a certain threshold prevents dark timing is widely held and is in agreement with much of the experimental data. However, although [Pfr] is probably lower during twilight than during the main part of the day, the photoequilibria established are likely to be much higher than those which commonly result from end-of-day spectral treatments in the laboratory. It is possible that at even lower solar angles, the red : far-red ratio may be further depressed, as reported by Goldberg and Klein [1977]. However, from the data in Figures 20 and 21, this seems unlikely to be common, as the decline in both \overline{P} and ϕ_c seems to level out or even become reversed between -5° and -10° .

A further objection was raised by Holmes and Wagner [1980]. The fluence rate of moonlight is sufficient to saturate many of the photomorphogenic responses of etiolated tissue and, as its spectral distribution is similar to daylight, they concluded that the photoequilibrium established during the night might often be similar to that of daytime. On these occasions, a low photoequilibrium would be confined to twilight, and would persist throughout the night in the absence of moonlight. The characteristic feature of twilight would thus be a decline in the photoequilibrium established, and it was suggested that the fall in [Pfr] might initiate dark timing. The hypothesis is consistent with much of the earlier experimental data, and offers a particularly attractive explanation of the results of King [1974] who found that far-red pulses towards the end of the photoperiod could stimulate flowering. Nonetheless, there is no specific evidence in support of the hypothesis.

In this context, the report by Shropshire [1973] of

a transient fall in the red:far-red ratio of direct sunlight soon after dawn is of significance. Analogous but much smaller events during twilight were frequently recorded during the work reported here. However, their timing in relation to solar angle was very variable, and consequently, the data as a whole do not show a distinct fluctuation in the region 0° to 5° . It seems likely, therefore, that this reversal effect is more marked in the spectrum of the direct solar beam than in total incident daylight, and probably has little relevance to photoperiodism.

Holmes and Wagner [1980] assumed that phytochrome in green plants behaves similarly to that in etiolated seedlings. However, the fluence rate required for photoconversion in green plants is unknown along with other important variable factors, and consequently the efficacy of different treatments in establishing photoequilibria is purely a matter for conjecture at the present time. Unfortunately this assumption is not a unique weakness as it underlies both the other principal hypotheses regarding the detection of dawn and dusk. Figure 23 shows the relationship between fluence rate in the region 600 - 700 nm and solar angle. During the twilight period, the decline is almost exactly exponential, and a critical fluence rate offers at least as accurate a zeitgeber as the spectral change. Moreover, it should always be remembered that good photoperiodic responses can be evoked without any change in light quality. The critical fluence rate seems to vary widely between species and individual plants, but it is nonetheless likely to be an important factor in photoperiodism.

According to the Pfr threshold hypothesis, the critical fluence rate is related to the rate of Pfr decay; at low fluence rates, [Pfr] is depressed and true photoequilibrium is not established. Instead, a "photostationary state" is set up in which the proportion of Pfr is much lower. Hence, [Pfr] can decline with changes in light quality, quantity, or both. Some experiments have indicated that the null proportion of red in a dichromatic pulse usually declines during the initial period of darkness, implying that the level of Pfr does indeed fall rapidly as a result of decay, and thus that dark reactions could compete significantly with photochemical reactions at fluence rates similar to those around sunset and sunrise. They also have indicated on a

number of occasions a less convenient "inverse reversion" of Pr to Pfr, as the null proportion of red subsequently undergoes a transient but dramatic increase. This implies that the system is more complex than that envisaged by the Pfr threshold hypothesis.

Moreover, there is good evidence from photomorphogenic studies that Pfr decay is very slow in green plants (Vince-Prue, 1977) and light grown plants treated with norfluorazon (Jabben and Deitzer, 1979). Very low fluence rates can provide effective night breaks, implying that photochemical conversion of phytochrome is efficient and hence that competition from these dark reactions is likely to be significant only at very low fluence rates. However, caution should be exercised in this assumption, as such high sensitivity to light is transient, if it occurs at all (Vince-Prue, 1975). Therefore, at present little can be concluded regarding the true level of Pfr at the fluence rates observed during twilight.

An alternative explanation involves a specific effect of cycling between Pfr and Pr, distinct from that of Pfr concentration or photoequilibrium (Jose and Vince-Prue, 1977; Johnson and Tasker, 1979). The "dynamic mode" of phytochrome action via cycling rate should show strong fluence rate dependence and thus would be capable of detecting a zeitgeber of this type. The action spectrum of cycling rate (Kendrick and Spruit, 1973; Johnson and Tasker, 1979) shows a peak at about 680 nm, falling gradually towards shorter wavelengths but rapidly towards longer ones. However, although the rate of cycling should be greater when far-red is mixed with red, such regimes have rarely been found to act as particularly effective photoperiod extensions (Salisbury, 1981a; Cumming et al, 1965; Evans and King, 1969; King and Cumming, 1972). Thus there is little justification for invoking a role for cycling.

Although it may be possible that the action of blue light is mediated by phytochrome photoconversion, it is equally possible that a distinct receptor such as cryptochrome is involved. This might act independently or via phytochrome. Sarkar and Song [1982] showed that energy transfer from flavine mononucleotide to phytochrome occurred under blue irradiation in vitro, promoting photoconversion of Pr to Pfr and inhibiting the reverse process. This may be significant in vivo, as cryptochrome

is thought likely to be a flavin or flavoprotein. The work of Lüser and Schäfer [1980] indicates that cryptochrome may itself have photochromic properties. As so little work has been reported on the action of cryptochrome, speculation about the possible mechanism of blue light action in photoperiodic control is futile.

Nonetheless, the results in Figure 22 and Tables 3 and 6 indicate that a large change in the relative fluence rates of red and blue light occurs during twilight. As a potential zeitgeber this is probably as accurate as the γ change. This finding contradicts that of Johnson et al. [1967] who reported a transient increase in the B:R ratio at the moment of apparent sunset, followed by a slow decline. However, these workers aimed their receptor at the sun, rather than mounting it horizontally, and consequently the contribution of the direct beam is exaggerated. Table 3 shows that there is no significant difference between the mean B:R ratios for $-7.5^\circ < \alpha < -2.5^\circ$ recorded using planar and spherical receptor heads ($t=0.85$, $p_0 > 5\%$).

outside
- Dubrovnik
P 58

TABLE 1 INCIDENT LIGHT \bar{x} VALUES

Date	$-7.5^{\circ} < \alpha, < -2.5^{\circ}$			$-2.5^{\circ} < \alpha, < +2.5^{\circ}$			$+2.5^{\circ} < \alpha, < +7.5^{\circ}$		
	mean	SEM	n	mean	SEM	n	mean	SEM	n
29. 8.79	1.00	.02	(17)	1.21	.03	(24)	1.27	.03	(13)
25. 4.80	.72	.01	(9)	.89	.02	(9)	.99	.01	(4)
28. 5.80	.67	.01	(7)	.83	.02	(9)	.99	.02	(4)
4. 7.80	.85	.03	(10)	.93	.03	(14)	1.01	.02	(7)
13. 8.80	1.02	.02	(6)	1.19	.04	(10)	1.32	.07	(9)
16. 9.80	.88	.03	(6)	1.06	.02	(11)	1.27	.03	(8)
21.10.80	.87	.02	(10)	.97	.01	(14)	.99	.01	(9)
11.11.80	.69	.01	(12)	.93	.02	(13)	.98	.02	(5)
21. 1.81	1.05	.04	(6)	1.22	.02	(13)	1.30	.09	(4)
7. 7.81	.95	.01	(21)	1.15	.04	(10)	1.31	.06	(4)
28. 7.81	1.00	.01	(12)	1.07	.04	(10)	1.29	.05	(5)
18. 8.81	.90	.01	(21)	1.05	.02	(18)	1.22	.05	(3)
16. 9.81	.89	.02	(21)	1.03	.03	(18)	1.23	.03	(11)
29. 9.81	.90	.02	(19)	.98	.04	(16)	1.15	.11	(4)
21.10.81	.79	.01	(17)	.96	.03	(13)	1.08	.01	(6)
10.11.81	.97	.02	(20)	1.07	.01	(18)	1.11	.02	(4)
2.12.81	.84	.01	(23)	1.02	.03	(18)	1.20	.05	(6)
12. 4.82	.69	.02	(23)	.84	.02	(25)	1.01	.01	(14)
9. 6.82	.91	.03	(11)	.96	.02	(24)	1.12	.03	(8)
MEAN	.87			1.02			1.15		
S.E.M.	.03			.03			.03		
N	19			19			19		
Spherical receptor 9. 6.82	.72	.04	(7)	.71	.02	(24)	.82	.03	(8)

TABLE 1 (contd.)

$7.5^\circ < \alpha_j < 15^\circ$			$15^\circ < \alpha_j < 30^\circ$			$30^\circ < \alpha_j < 60^\circ$		
mean	SEM	n	mean	SEM	n	mean	SEM	n
1.23	.01	(8)	1.21	.01	(7)	1.14	.01	(10)
1.00	.02	(4)	1.04	.01	(7)	1.04	.01	(14)
1.00	.04	(4)	1.01	.02	(4)	1.02	.01	(16)
1.07	.01	(6)	1.09	.05	(7)	1.08	.01	(18)
1.34	.05	(6)	1.26	.01	(7)	1.24	.03	(11)
1.22	.04	(3)	1.25	.01	(7)	1.22	.01	(10)
1.05	.01	(4)	1.05	.01	(10)	--	-	(0)
1.05	.01	(5)	1.09	.01	(8)	--	-	(0)
1.29	.03	(6)	1.25	.02	(6)	--	-	(0)
1.30	.03	(4)	1.26	.03	(6)	1.18	.02	(16)
1.29	.02	(3)	1.24	.05	(5)	1.19	.03	(12)
1.19	.04	(4)	1.27	.04	(3)	1.26	.03	(8)
1.11	.03	(4)	1.18	.02	(7)	1.12	.02	(6)
1.10	.07	(2)	1.17	.04	(5)	1.08	.06	(4)
1.08	.01	(2)	1.08	.01	(6)	--	-	(0)
1.16	.02	(4)	1.18	.02	(4)	--	-	(0)
1.11	.03	(5)	1.19	-	(1)	--	-	(0)
1.00	.01	(6)	1.02	.02	(6)	0.98	.01	(10)
1.26	.02	(5)	1.29	.03	(3)	1.21	.03	(6)
1.15	.02	19	1.15	.02	19	1.13	.02	13
.94	.03	(5)	.89	.05	(3)	.92	.03	(5)

TABLE 2 INCIDENT LIGHT ϕ_c (%) VALUES
 $-7.5^\circ < \alpha_r < -2.5^\circ$ $-2.5^\circ < \alpha_r < +2.5^\circ$ $+2.5^\circ < \alpha_r < +7.5^\circ$

Date	mean	SEM	n	mean	SEM	n	mean	SEM	n
-----	-----	---	--	-----	---	--	-----	---	--
29. 8.79	49.1	.1	(17)	52.2	.2	(24)	53.2	.1	(13)
25. 4.80	46.7	.2	(9)	49.2	.3	(9)	51.2	.1	(4)
28. 5.80	45.7	.3	(7)	48.1	.5	(9)	51.1	.3	(4)
4. 7.80	47.6	.1	(10)	49.3	.3	(14)	51.2	.2	(7)
13. 8.80	49.3	.1	(6)	51.7	.3	(10)	53.1	.3	(9)
16. 9.80	47.8	.2	(6)	50.0	.2	(11)	51.9	.1	(8)
21.10.80	48.7	.1	(10)	50.9	.2	(14)	52.0	.1	(9)
11.11.80	45.8	.2	(12)	50.3	.2	(13)	51.5	.3	(5)
21. 1.81	50.1	.2	(6)	52.0	.2	(13)	53.1	.5	(4)
7. 7.81	48.4	.1	(21)	51.4	.3	(10)	53.4	.4	(4)
28. 7.81	48.2	.1	(12)	49.9	.5	(10)	52.6	.4	(5)
18. 8.81	47.7	.2	(21)	49.8	.2	(18)	51.9	.3	(3)
16. 9.81	48.5	.2	(21)	50.4	.3	(18)	52.7	.2	(11)
29. 9.81	48.2	.2	(19)	48.7	.7	(16)	52.3	.6	(4)
21.10.81	46.8	.1	(17)	49.8	.4	(13)	51.7	.2	(6)
10.11.81	49.3	.2	(20)	50.7	.1	(18)	51.7	.3	(4)
2.12.81	46.5	.2	(23)	50.3	.3	(18)	52.4	.3	(6)
12. 4.82	45.5	.4	(23)	48.2	.4	(25)	51.2	.2	(14)
9. 6.82	47.9	.6	(11)	48.8	.3	(24)	51.4	.3	(8)
-----	-----	---	--	-----	---	--	-----	---	--
MEAN	47.8			50.1			52.1		
S.E.M.	.3			.3			.2		
N	19			19			19		
-----	-----	---	--	-----	---	--	-----	---	--
Spherical receptor 9. 6.82	46.3	1.0	(7)	46.5	.4	(24)	49.1	.3	(8)

-7.5°

n
--

(13)

(4)

(4)

(7)

(9)

(8)

(9)

(5)

(4)

(4)

(5)

(3)

(11)

(4)

(6)

(4)

(6)

(14)

(8)

.1

(8)

TABLE 2 (contd.)

 $7.5^{\circ} < \alpha_1 < 15^{\circ}$ $15^{\circ} < \alpha_2 < 30^{\circ}$ $30^{\circ} < \alpha_3 < 60^{\circ}$ mean SEM n
-----mean SEM n
-----mean SEM n

53.4 .1 (8)

53.9 .1 (7)

53.8 .1 (10)

51.8 .2 (4)

52.6 .1 (7)

52.6 .1 (14)

51.6 .6 (4)

52.0 .2 (4)

52.4 .1 (16)

52.2 .1 (6)

52.9 .2 (7)

53.0 .1 (18)

53.8 .1 (6)

53.8 .1 (7)

53.6 .1 (11)

52.9 .1 (3)

53.5 .1 (7)

53.7 .1 (10)

53.0 .1 (4)

53.3 .1 (10)

-- - (0)

52.6 .1 (5)

53.1 .1 (8)

-- - (0)

53.8 .1 (6)

53.9 .1 (6)

-- - (0)

53.5 .2 (4)

53.9 .1 (6)

53.7 .1 (16)

53.3 .2 (3)

53.9 .3 (5)

53.7 .2 (12)

52.6 .3 (4)

53.4 .2 (3)

53.5 .2 (8)

52.4 .2 (4)

53.4 .1 (7)

53.1 .2 (6)

52.4 .5 (2)

53.2 .4 (5)

53.2 .6 (4)

52.4 .4 (2)

53.0 .1 (6)

-- - (0)

52.7 .2 (4)

53.1 .1 (4)

-- - (0)

52.7 .1 (5)

53.2 - (1)

-- - (0)

51.9 .2 (6)

52.7 .2 (6)

52.4 .1 (10)

53.0 .1 (5)

53.2 .2 (3)

53.5 .1 (6)

52.7

53.2

53.2

.1

.1

.1

19

19

13

51.1 .3 (5)

50.6 .6 (3)

51.5 .3 (5)

TABLE 3

INCIDENT LIGHT B:R RATIO VALUES

Date	$-7.5^{\circ} < \alpha_s < -2.5^{\circ}$			$-2.5^{\circ} < \alpha_s < +2.5^{\circ}$			$+2.5^{\circ} < \alpha_s < +7.5^{\circ}$		
	mean	SEM	n	mean	SEM	n	mean	SEM	n
29. 8.79	1.52	.05	(17)	1.38	.03	(24)	1.00	.04	(13)
25. 4.80	2.00	.08	(9)	1.53	.04	(9)	1.17	.09	(4)
28. 5.80	1.90	.16	(7)	1.19	.06	(9)	.91	.04	(4)
4. 7.80	2.40	.13	(10)	1.44	.75	(14)	.98	.06	(7)
13. 8.80	2.06	.20	(6)	1.37	.04	(10)	1.22	.10	(9)
16. 9.80	1.68	.31	(6)	.94	.09	(11)	.92	.08	(8)
21.10.80	1.68	.17	(10)	1.29	.09	(14)	.95	.03	(9)
11.11.80	.93	.05	(12)	1.10	.03	(13)	1.10	.07	(5)
21. 1.81	1.27	.14	(6)	1.24	.09	(13)	1.01	.26	(4)
7. 7.81	1.79	.11	(21)	1.09	.04	(10)	1.01	.04	(4)
28. 7.81	1.64	.17	(12)	1.01	.07	(10)	.99	.11	(5)
18. 8.81	1.82	.10	(21)	1.24	.06	(18)	1.14	.05	(3)
16. 9.81	1.66	.06	(21)	1.05	.04	(18)	1.16	.06	(11)
29. 9.81	2.00	.14	(19)	1.17	.14	(16)	1.00	.14	(4)
21.10.81	1.50	.05	(17)	1.15	.02	(13)	.90	.07	(6)
10.11.81	1.86	.05	(20)	1.39	.07	(18)	.96	.01	(4)
2.12.81	.66	.03	(23)	.85	.05	(18)	.88	.10	(6)
12. 4.82	2.02	.08	(23)	1.14	.02	(25)	.90	.02	(14)
9. 6.82	2.52	.25	(11)	1.21	.04	(24)	1.09	.06	(8)
MEAN	1.73			1.20			1.01		
S.E.M.	.10			.04			.02		
N	19			19			19		
Spherical receptor 9. 6.82	2.20	.25	(7)	1.12	.03	(24)	1.03	.05	(8)

+7.5°

TABLE 3 (contd.)

	7.5° < α _s < 15°			15° < α _s < 30°			30° < α _s < 60°		
n	mean	SEM	n	mean	SEM	n	mean	SEM	n
(13)	.75	.01	(8)	.79	.01	(7)	.80	.01	(10)
(4)	1.05	.05	(4)	.90	.04	(7)	.90	.02	(14)
(4)	.85	.02	(4)	.85	.02	(4)	.86	.01	(16)
(7)	1.03	.02	(6)	1.28	.17	(7)	.90	.03	(18)
(9)	1.18	.15	(6)	1.03	.05	(7)	.95	.01	(11)
(8)	.95	.11	(3)	.89	.06	(7)	.88	.01	(10)
(9)	.92	.02	(4)	1.02	.07	(10)	--	-	(0)
(5)	.99	.05	(5)	.93	.04	(8)	--	-	(0)
(4)	1.03	.05	(6)	.85	.02	(6)	--	-	(0)
(4)	.87	.09	(4)	.74	.01	(6)	.77	.01	(16)
(5)	.87	.14	(3)	.78	.02	(5)	.82	.01	(12)
(3)	.90	.02	(4)	.80	.01	(3)	.84	.01	(8)
(11)	.83	.03	(4)	.83	.02	(7)	.76	.02	(6)
(4)	.78	.08	(2)	.73	.04	(5)	.81	.04	(4)
(6)	.67	.05	(2)	.72	.01	(6)	--	-	(0)
(4)	.92	.01	(4)	.84	.02	(4)	--	-	(0)
(6)	.81	.03	(5)	.85	-	(1)	--	-	(0)
(14)	.68	.02	(6)	.77	.05	(6)	.76	.02	(10)
(8)	.95	.09	(5)	.82	.05	(3)	.75	.02	(6)
-----				-----			-----		
	.90			.86			.83		
	.03			.03			.02		
	19			19			13		
-----				-----			-----		
(8)	.86	.07	(5)	.81	.09	(3)	.77	.05	(5)

Table 4
ANOVAR of cloud cover effect
7th July 1981 $30^\circ < \alpha < 60^\circ$

Parameter - PAR fluence rate

<u>Source</u>	<u>Df</u>	<u>Sum-of-squares</u>	<u>Variance</u>	<u>V.R.</u>
CLOUD COVER	2	1.57×10^6	7.86×10^5	6
Residue	12	1.71×10^6	1.43×10^5	
Total	14	3.29×10^6		

Parameter - β

<u>Source</u>	<u>Df</u>	<u>Sum-of-squares</u>	<u>Variance</u>	<u>V.R.</u>
CLOUD COVER	2	.034	.017	3
Residue	12	.067	5.58×10^{-3}	
Total	14	.101		

Parameter - B:R ratio

<u>Source</u>	<u>Df</u>	<u>Sum-of-squares</u>	<u>Variance</u>	<u>V.R.</u>
CLOUD COVER	2	.0273	.0136	10
Residue	12	.0160	1.34×10^{-3}	
Total	14	.0433		

TABLE 5 NON-ORTHOGONAL ANALYSIS OF VARIANCE

INCIDENT LIGHT : DAYTIME ($\alpha_s > 7.5^\circ$)

<u>SOURCE</u>	<u>Df</u>	<u>Sum-of-Squares</u>	<u>Variance</u>	Error <u>V.R.</u>	D x A <u>V.R.</u>
Parameter - β					
DAYS	18	2.880	.160	38	
ANGLES	2	0.092	.046	11	
D x A	30	0.194	6.4×10^{-3}	1.5	
Residue	278	1.170	4.2×10^{-3}		
Parameter - ϕ_c					
DAYS	18	9.28×10^{-3}	5.15×10^{-4}	22	
ANGLES	2	1.57×10^{-3}	7.83×10^{-4}	34	
D x A	30	6.00×10^{-4}	2.00×10^{-5}	.86	
Residue	278	6.44×10^{-3}	2.32×10^{-5}		
Parameter - B:R ratio					
DAYS	18	4.84	.269	---	6.9
ANGLES	2	0.19	.093	---	2.4
D x A	30	1.17	.039	2.7	
Residue	278	3.92	.014		
Parameter - log R					
DAYS	18	24.24	1.35	23	
ANGLES	2	23.76	11.88	205	
D x A	30	2.37	.079	1.36	
Residue	278	16.18	.058		

TABLE 6 NON-ORTHOGONAL ANALYSIS OF VARIANCE

INCIDENT LIGHT : TWILIGHT ($\alpha, < 7.5^\circ$)

<u>SOURCE</u>	<u>Df</u>	<u>Sum-of-Squares</u>	<u>Variance</u>	<u>Error V.R.</u>	<u>D x A V.R.</u>
---------------	-----------	-----------------------	-----------------	-------------------	-------------------

Parameter - β

DAYS	18	8.3	.459	---	23
ANGLES	2	6.9	3.45	---	173
D x A	36	.71	.02	2.2	
Residue	629	5.7	9.06×10^{-3}		

Parameter - ϕ_c

DAYS	18	0.0862	4.79×10^{-3}	---	10
ANGLES	2	0.1708	0.0854	---	178
D x A	36	0.0172	4.78×10^{-3}	3.9	
Residue	629	0.0774	1.23×10^{-3}		

Parameter - B:R ratio

DAYS	18	38.4	2.13	---	3.1
ANGLES	2	42.8	21.4	---	31
D x A	36	24.5	.68	7.2	
Residue	629	59.8	.095		

Parameter - log R

DAYS	18	59.5	3.31	12
ANGLES	2	595	297	1095
D x A	36	9.36	.260	.95
Residue	629	171	.271	

TABLE 7 INCIDENT LIGHT log R VALUES

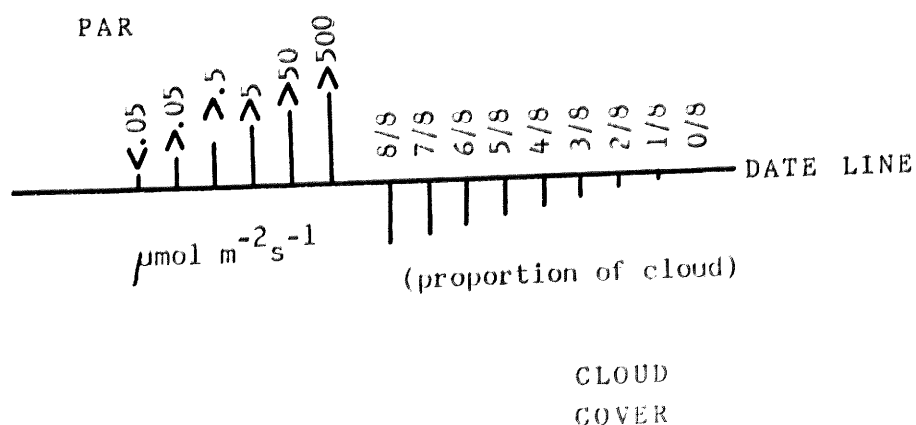
Date	$-7.5^{\circ} < \alpha_s < -2.5^{\circ}$			$-2.5^{\circ} < \alpha_s < +2.5^{\circ}$			$+2.5^{\circ} < \alpha_s < +7.5^{\circ}$		
	mean	SEM	n	mean	SEM	n	mean	SEM	n
28. 8.79	-1.13	.16	(17)	.57	.07	(24)	1.31	.04	(13)
25. 4.80	-1.62	.20	(9)	.21	.11	(9)	1.05	.09	(4)
28. 5.80	-1.08	.23	(7)	.42	.12	(9)	1.39	.10	(4)
4. 7.80	-1.37	.13	(10)	.03	.11	(14)	1.02	.09	(7)
13. 8.80	-1.16	.27	(6)	.56	.10	(10)	1.26	.08	(9)
16. 9.80	-1.30	.30	(6)	.29	.16	(11)	.65	.08	(8)
21.10.80	-1.10	.20	(10)	.58	.11	(14)	1.37	.04	(9)
11.11.80	-0.95	.21	(13)	.40	.06	(13)	.93	.09	(5)
21. 1.80	-1.24	.16	(6)	-0.20	.13	(13)	.49	.18	(4)
7. 7.81	-0.63	.14	(21)	.86	.09	(10)	1.48	.04	(4)
28. 7.81	-1.02	.17	(12)	.43	.14	(10)	1.09	.12	(5)
18. 8.81	-1.47	.14	(21)	.01	.15	(18)	.84	.09	(3)
16. 9.81	-1.51	.16	(21)	.30	.06	(18)	1.01	.06	(11)
29. 9.81	-1.50	.18	(19)	.25	.16	(16)	1.36	.20	(4)
21.10.81	-1.33	.18	(17)	.64	.10	(13)	1.44	.11	(6)
10.11.81	-1.62	.15	(20)	.00	.09	(18)	.78	.09	(4)
2.12.81	-1.12	.16	(23)	.59	.07	(18)	1.38	.05	(6)
12. 4.82	-1.30	.14	(23)	.57	.08	(25)	1.37	.04	(14)
9. 6.82	-1.41	.16	(11)	-0.03	.08	(24)	.66	.11	(8)
MEAN	-1.25			.34			1.05		
S.E.M.	.06			.06			.07		
N	19			19			19		
Spherical receptor 9. 6.82	-1.30	.16	(7)	-0.14	.09	(24)	.55	.12	(8)

TABLE 7 (contd.)

7.5°	7.5° < α_s < 15°			15° < α_s < 30°			30° < α_s < 60°		
n	mean	SEM	n	mean	SEM	n	mean	SEM	n
(13)	1.87	.03	(8)	2.19	.06	(7)	2.60	.02	(10)
(4)	1.40	.12	(4)	2.00	.07	(7)	2.36	.04	(14)
(4)	1.53	.27	(4)	1.81	.18	(4)	2.33	.07	(16)
(7)	1.33	.08	(6)	1.61	.07	(7)	2.22	.05	(18)
(9)	1.74	.09	(6)	2.09	.12	(7)	2.25	.04	(11)
(8)	1.31	.27	(3)	1.80	.16	(7)	2.01	.04	(10)
(9)	1.90	.08	(4)	2.18	.07	(10)	--	-	(0)
(5)	1.38	.07	(5)	1.64	.12	(8)	--	-	(0)
(4)	1.05	.12	(6)	1.45	.07	(6)	--	-	(0)
(4)	1.93	.07	(4)	2.39	.04	(6)	2.61	.04	(16)
(5)	1.72	.22	(3)	2.20	.13	(5)	2.45	.06	(12)
(3)	1.49	.07	(4)	1.79	.23	(3)	2.26	.08	(8)
(11)	1.48	.08	(4)	1.94	.07	(7)	2.29	.09	(6)
(4)	1.77	.29	(2)	2.19	.19	(4)	2.34	.07	(4)
(6)	1.98	.04	(2)	2.42	.03	(6)	--	-	(0)
(4)	1.26	.13	(4)	1.78	.07	(4)	--	-	(0)
(6)	1.69	.03	(5)	1.72	-	(1)	--	-	(0)
(14)	1.94	.07	(6)	2.31	.07	(6)	2.37	.06	(10)
(8)	1.47	.17	(5)	1.56	.37	(3)	2.38	.16	(6)
	1.59			1.95			2.34		
	.06			.07			.04		
	19			19			13		
(8)	1.39	.18	(5)	1.43	.41	(3)	2.14	.18	(5)

Figures 6 and 7. SPD recordings during 1980 (at Outwoods) and 1981 (at Sutton Bonnington).

The main vertical axis represents the date (1 January = year day 0). Each day studied is marked by a horizontal date line, itself representing the time of day from left to right. Each SPD recorded is represented by a small vertical bar: above the date line, this represents PAR fluence rate; below the date line cloud cover is represented.



(...) $\alpha_s = 0^\circ$
 (---) $\alpha_s = 30^\circ$

Fig. 6

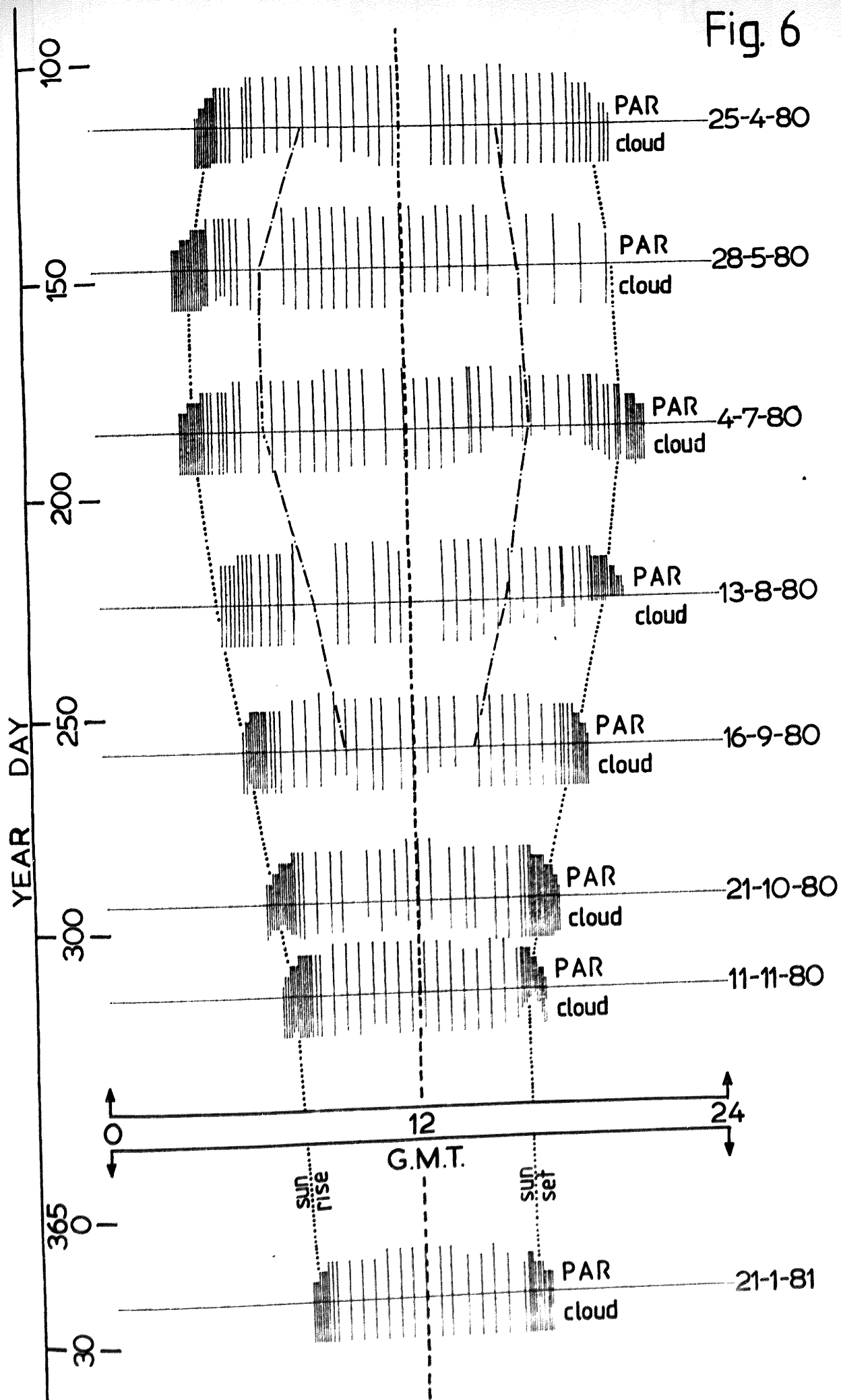
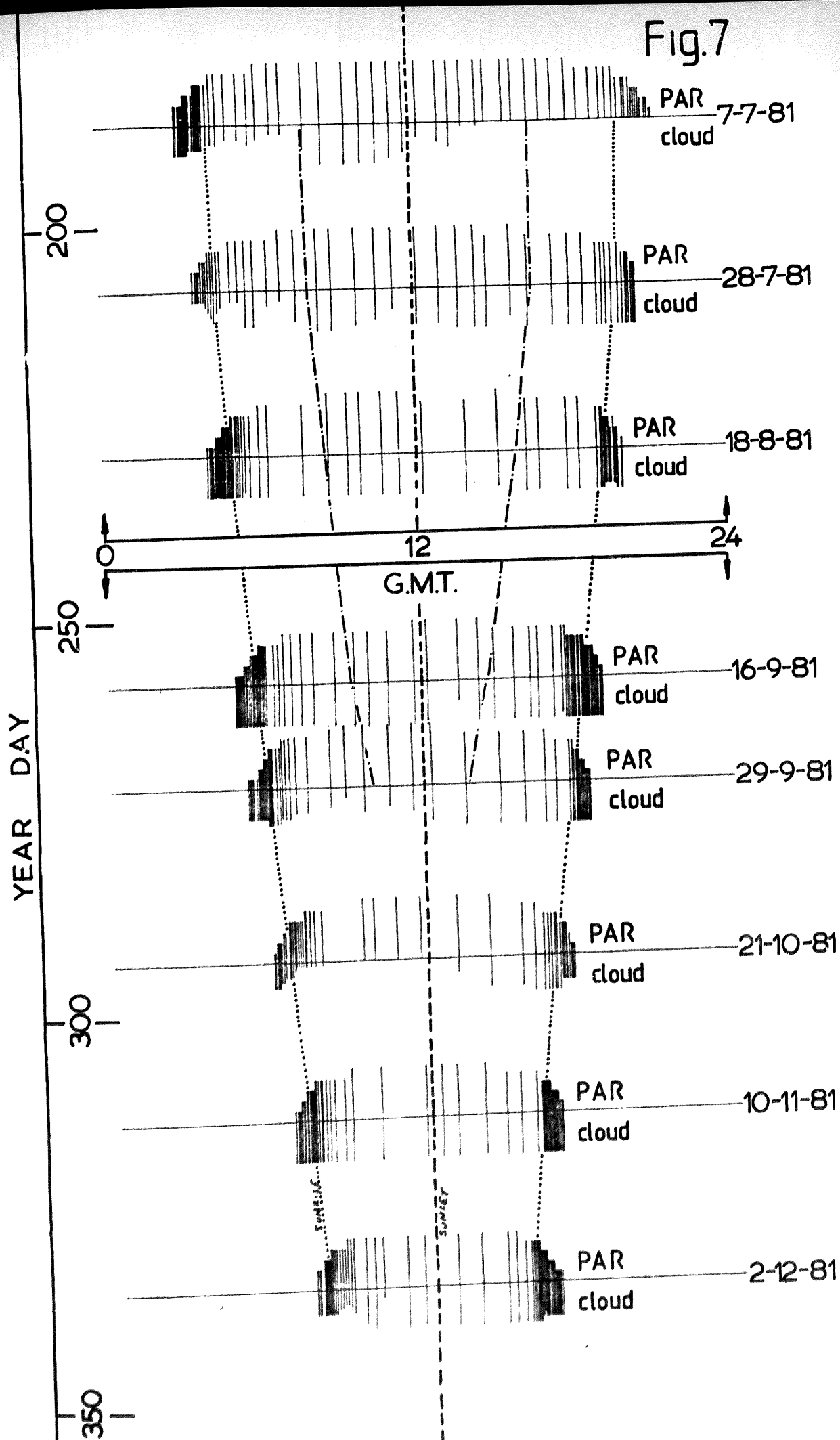


Fig.7



Figures 8 - 18.

Relative SPFR surfaces of incident daylight at Sutton Bonnington 1979-82.

The dashed lines represent the times of sunrise and sunset; wavelength is in nanometers.

Figure 8: 29 August, 1979

Figure 9: 7 July, 1981

Figure 10: 28 July, 1981

Figure 11: 18 August, 1981

Figure 12: 16 September, 1981

Figure 13: 29 September, 1981

Figure 14: 21 October, 1981

Figure 15: 10 November, 1981

Figure 16: 2 December, 1981

Figure 17: 12 April, 1982

Figure 18: 9 June, 1982

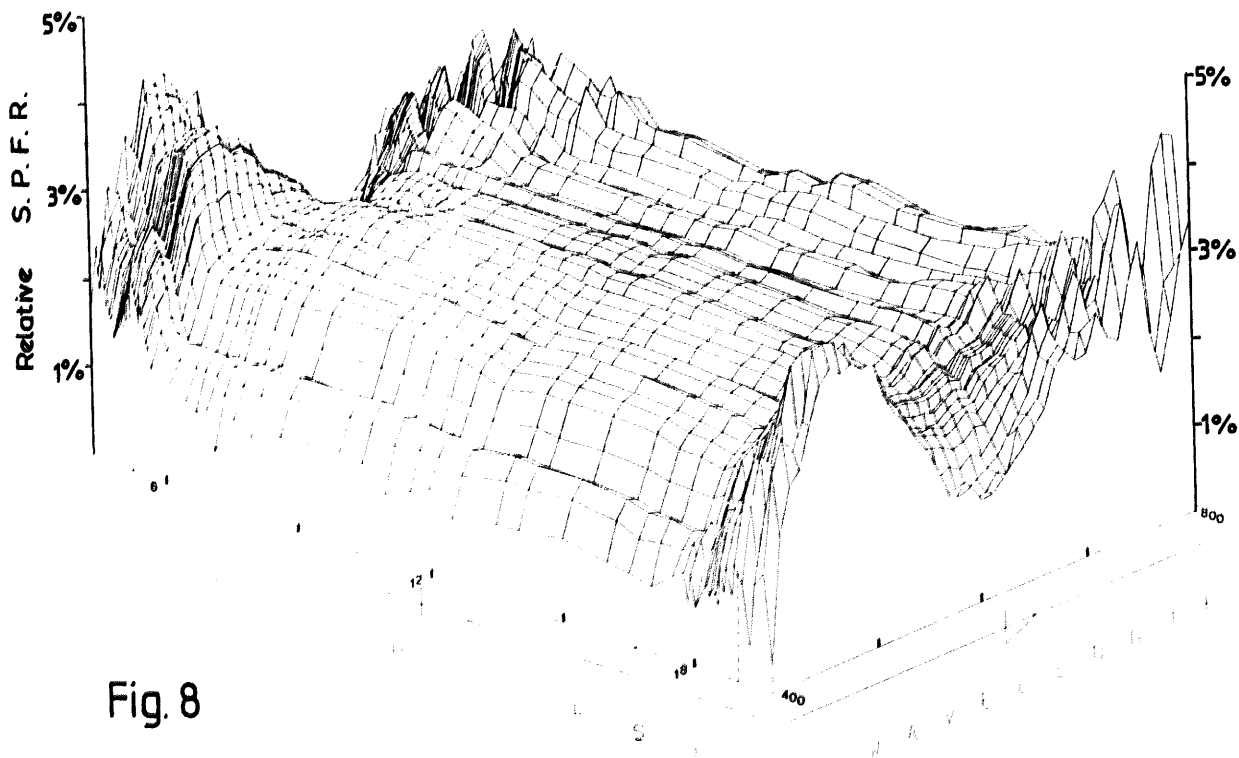


Fig. 8

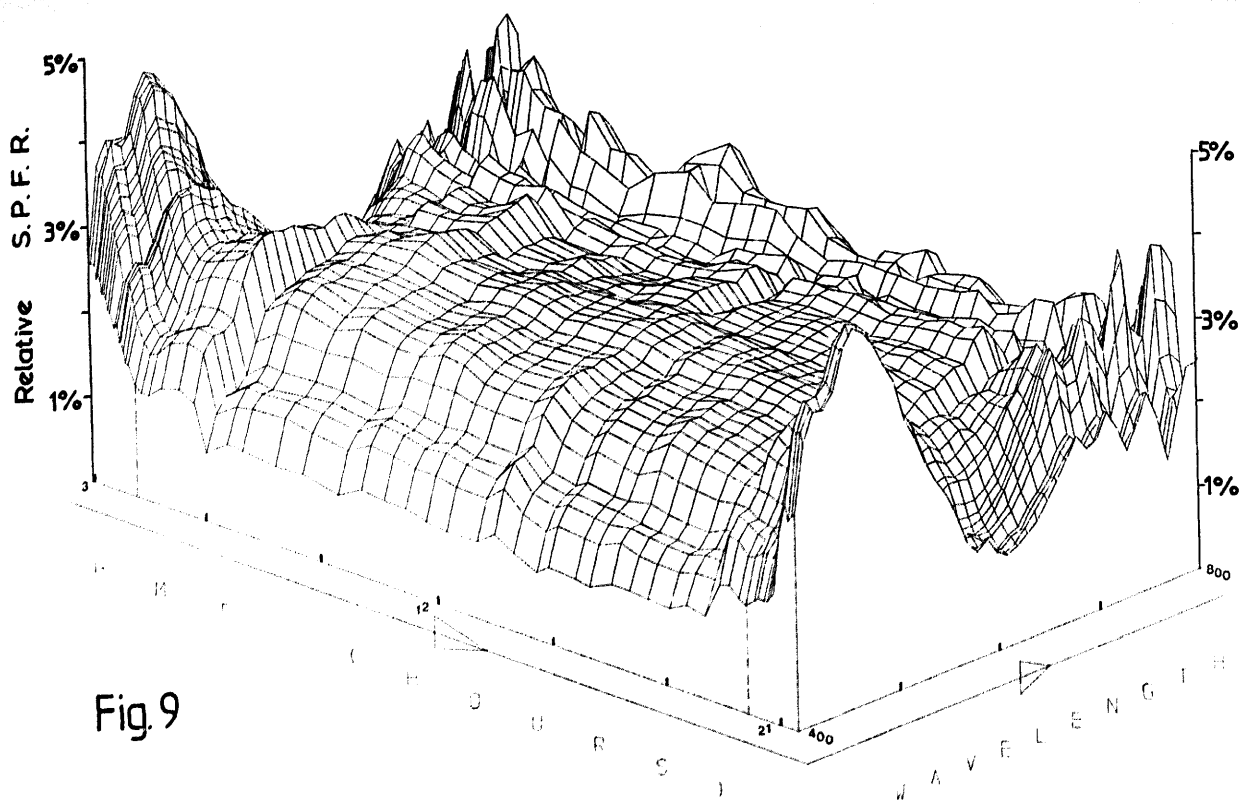


Fig. 9

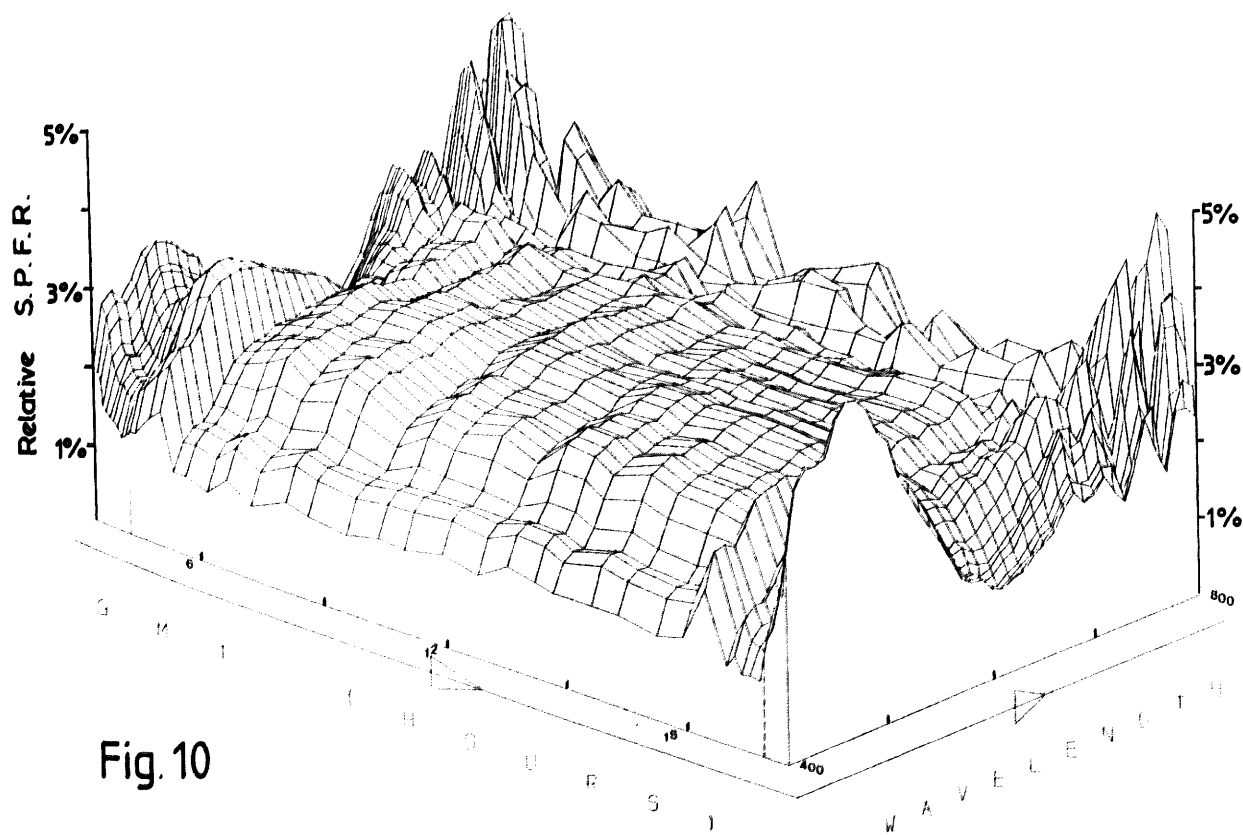


Fig. 10

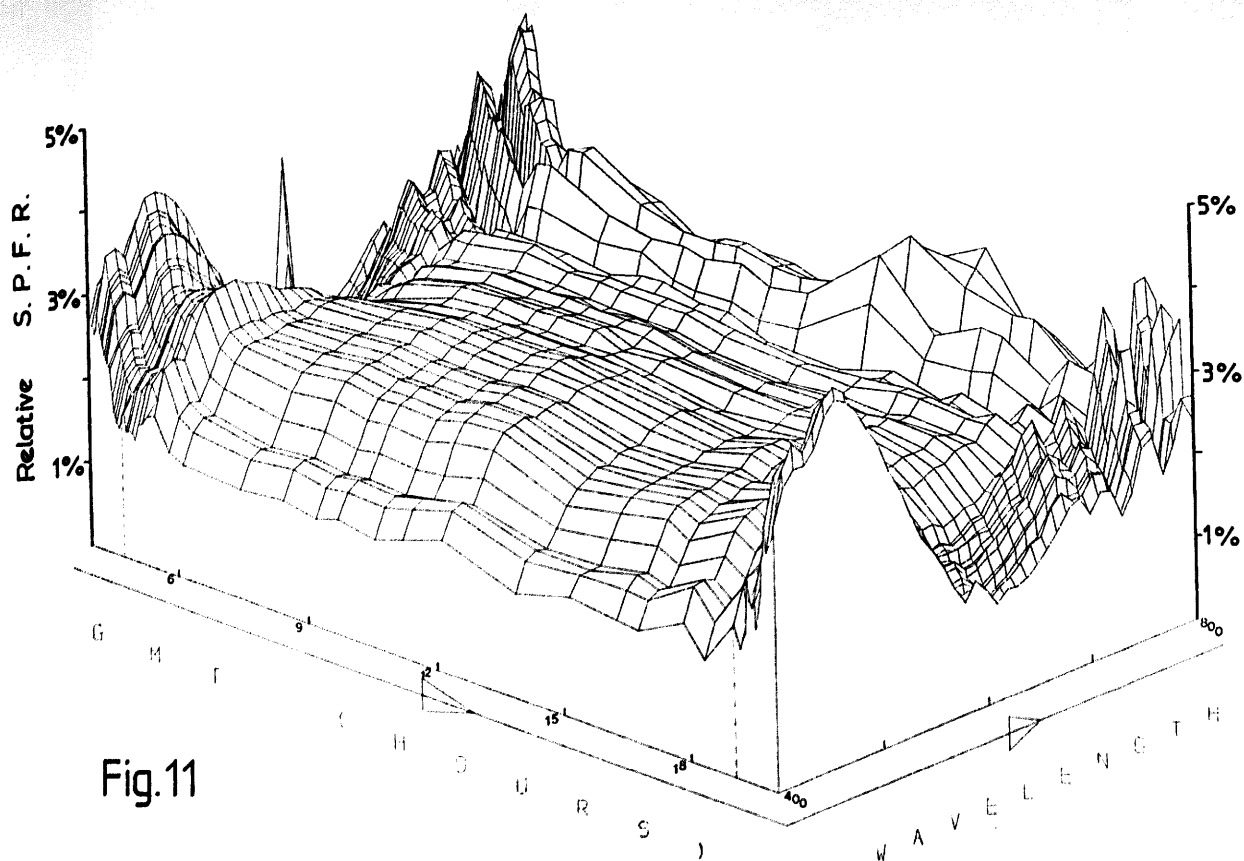


Fig.11

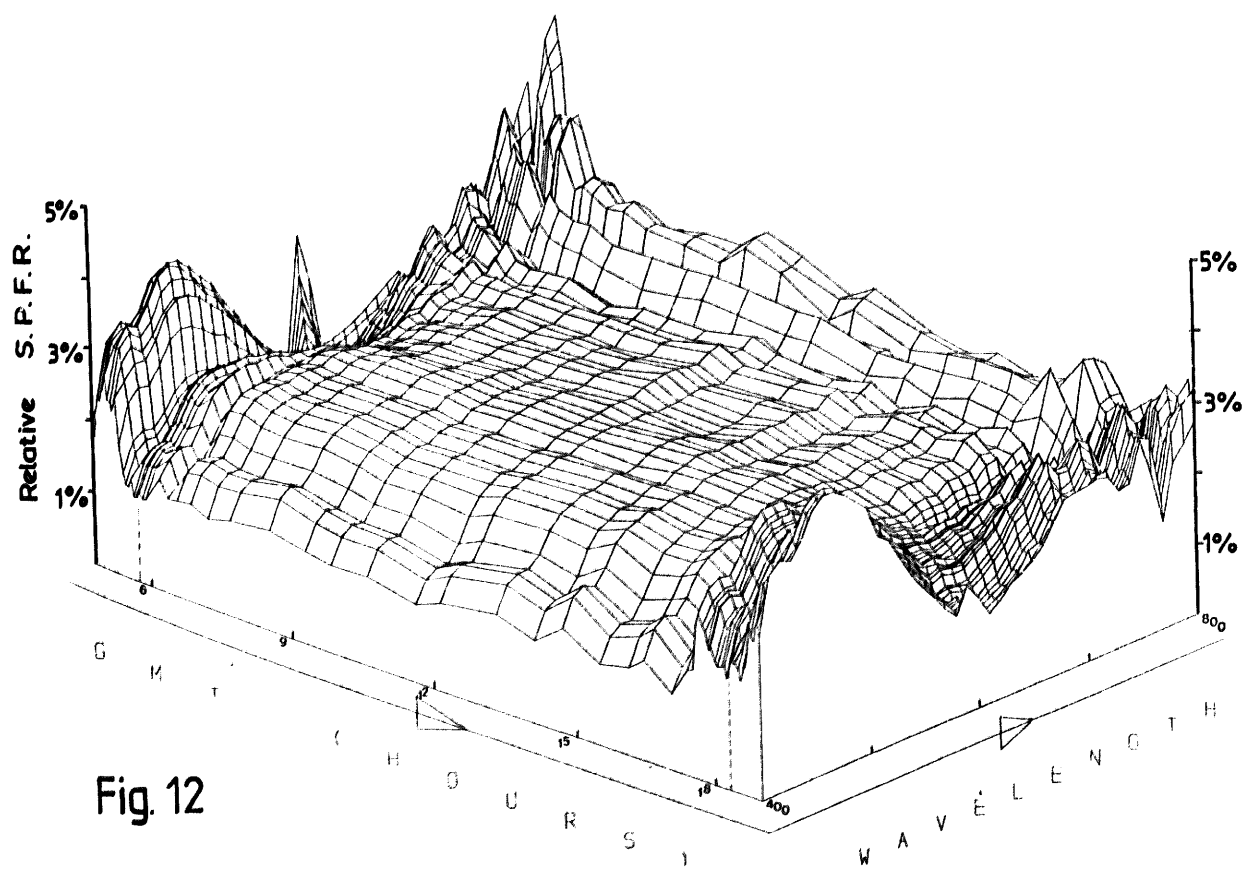


Fig. 12

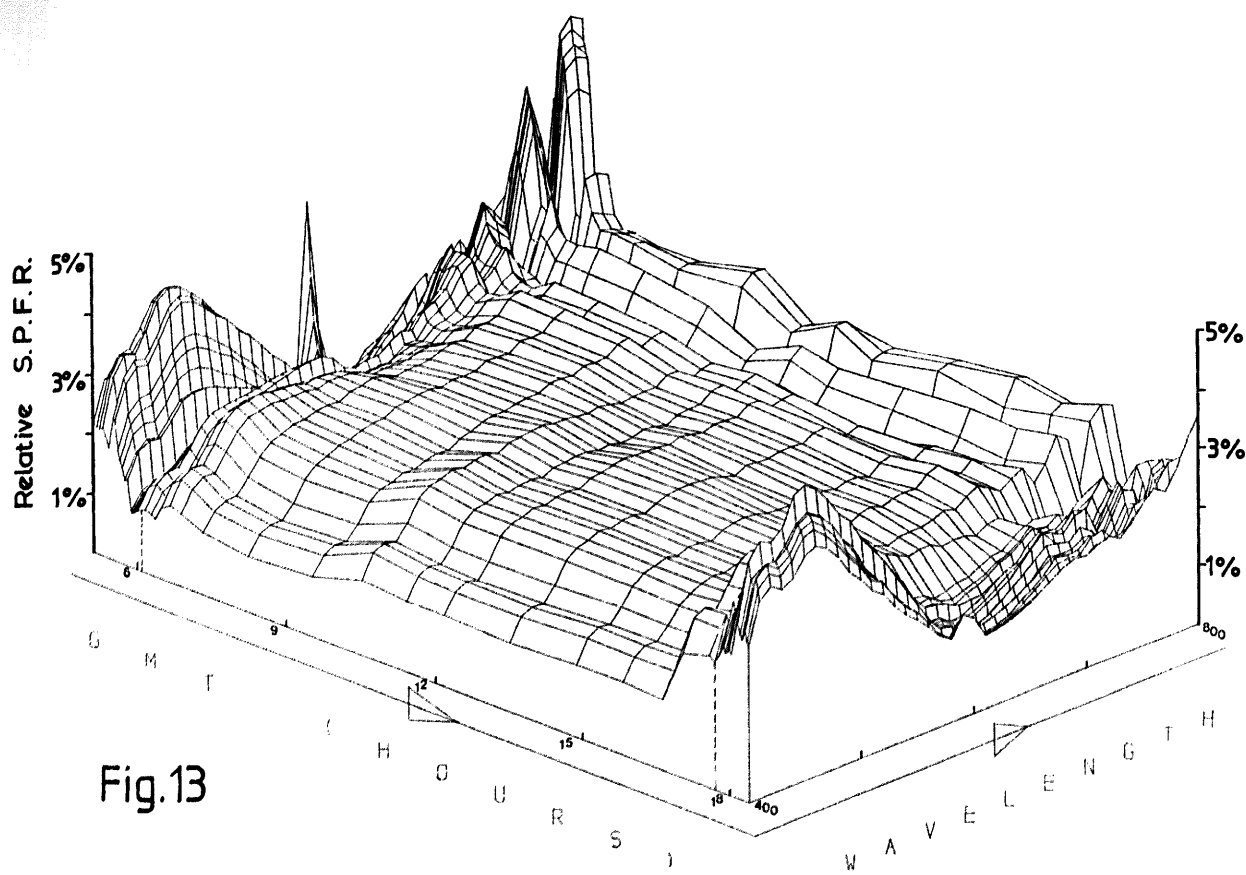


Fig.13

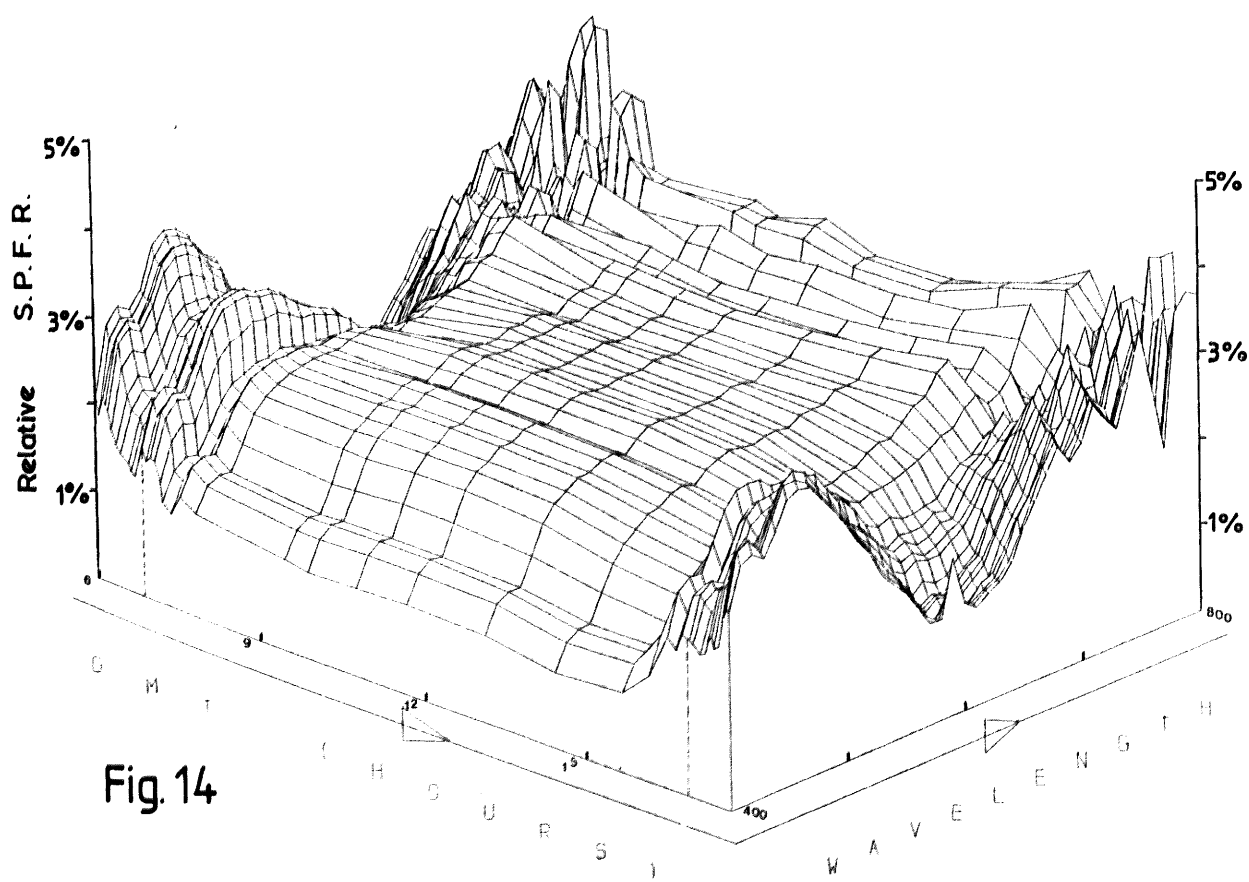


Fig.14

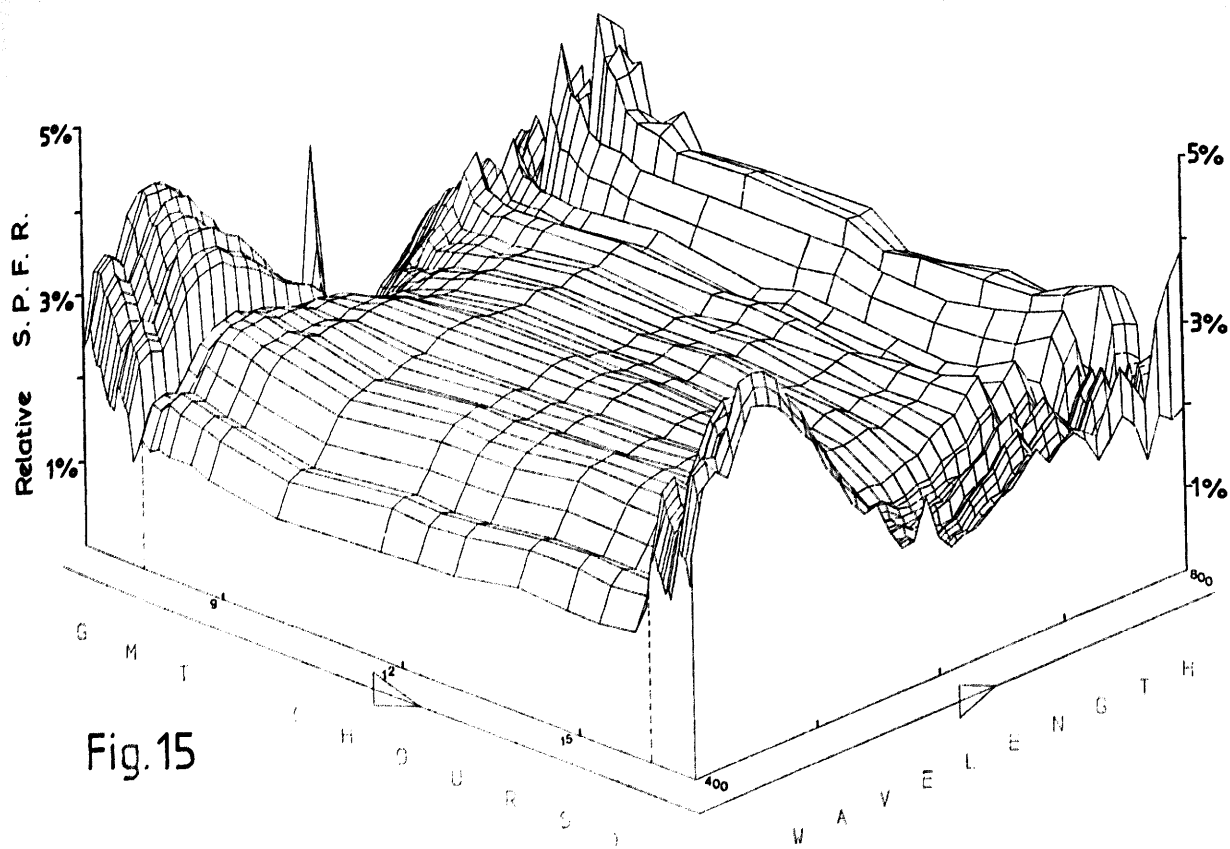


Fig.15

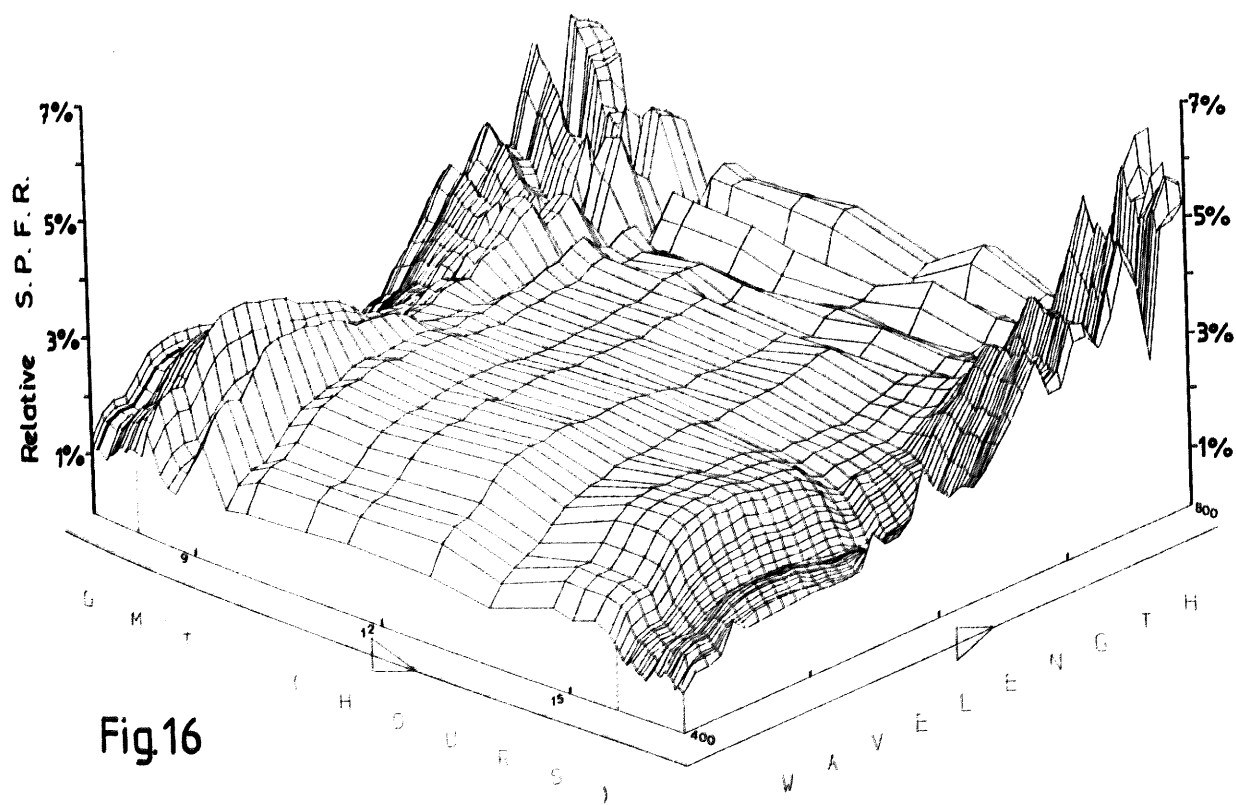


Fig.16

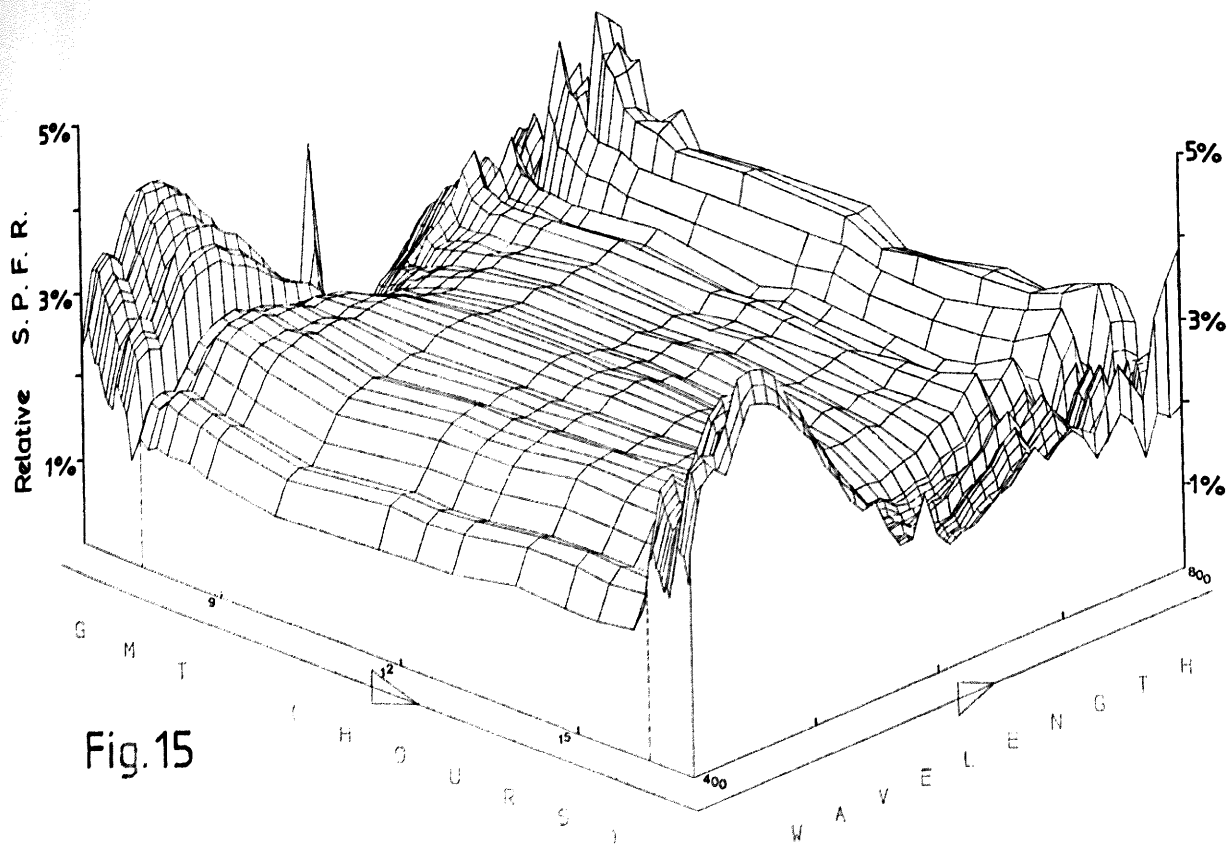


Fig.15

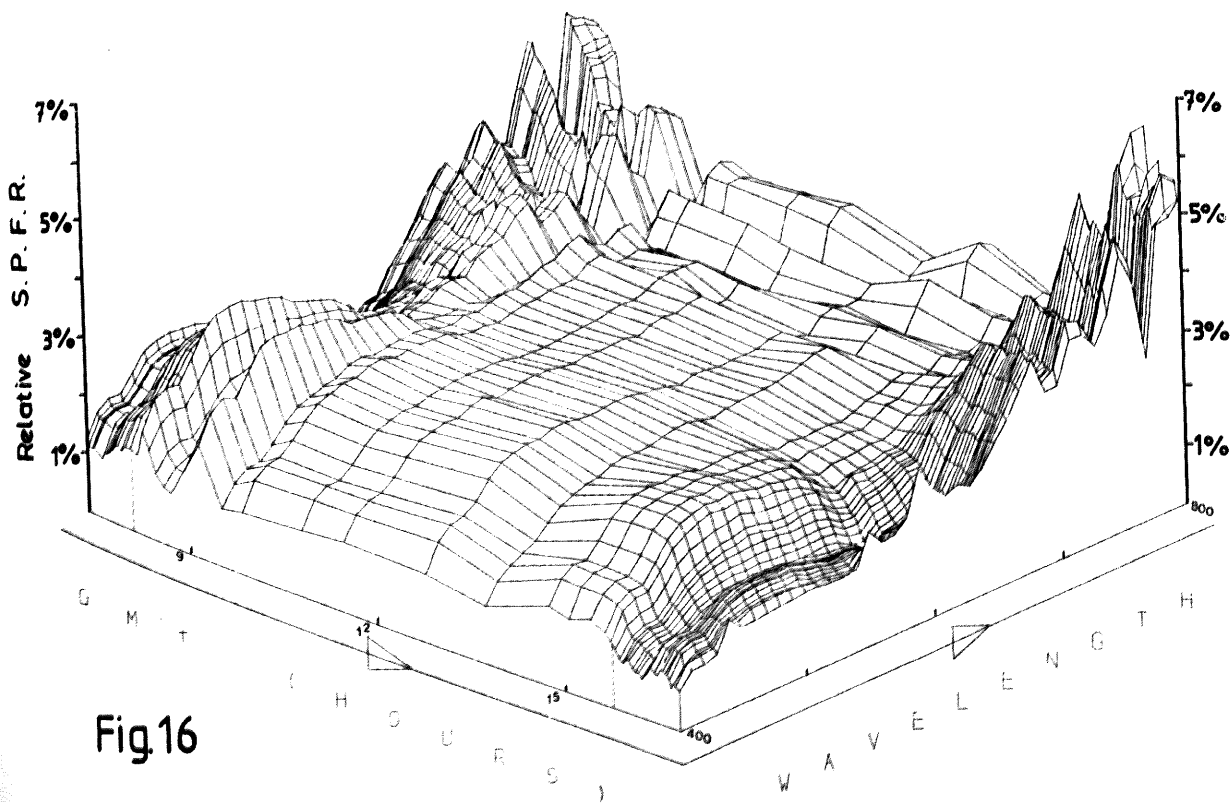


Fig.16

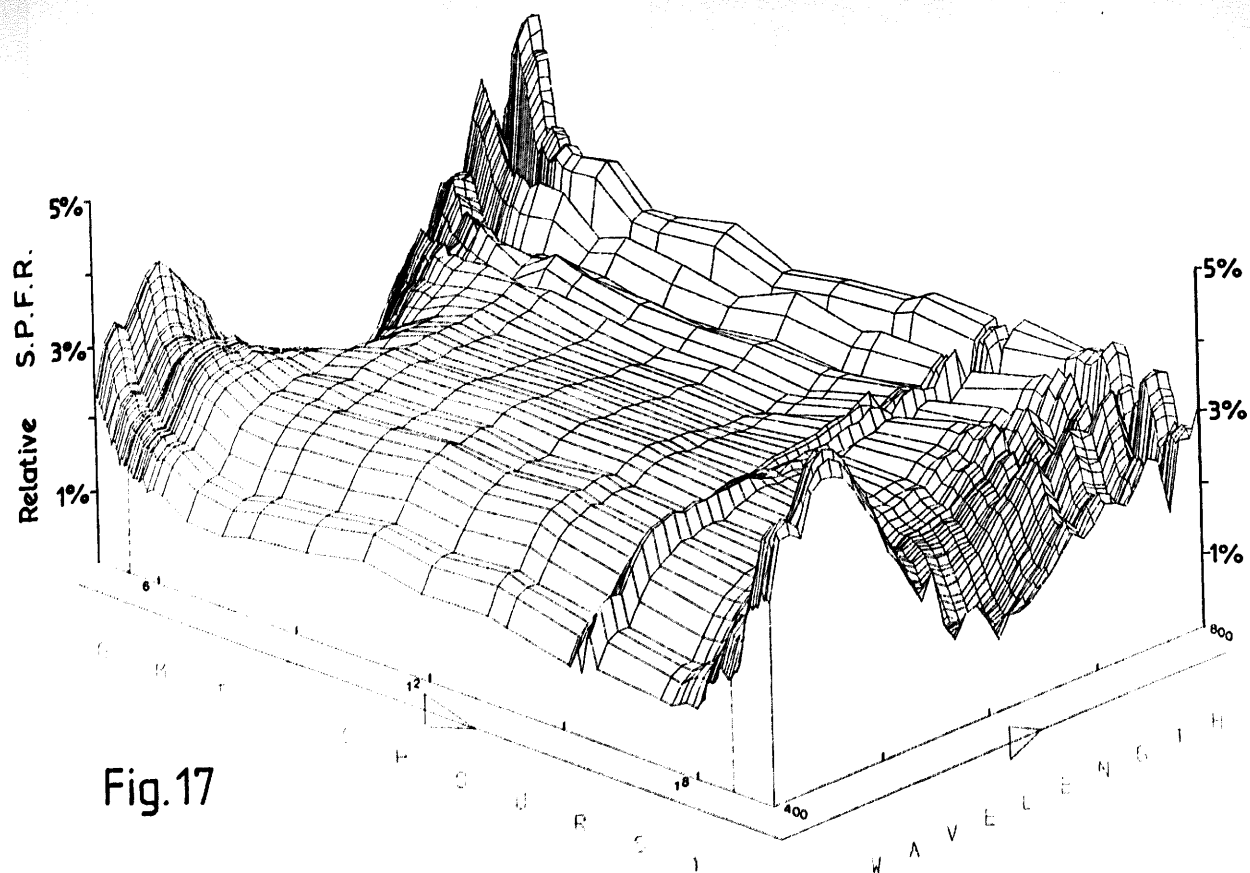


Fig.17

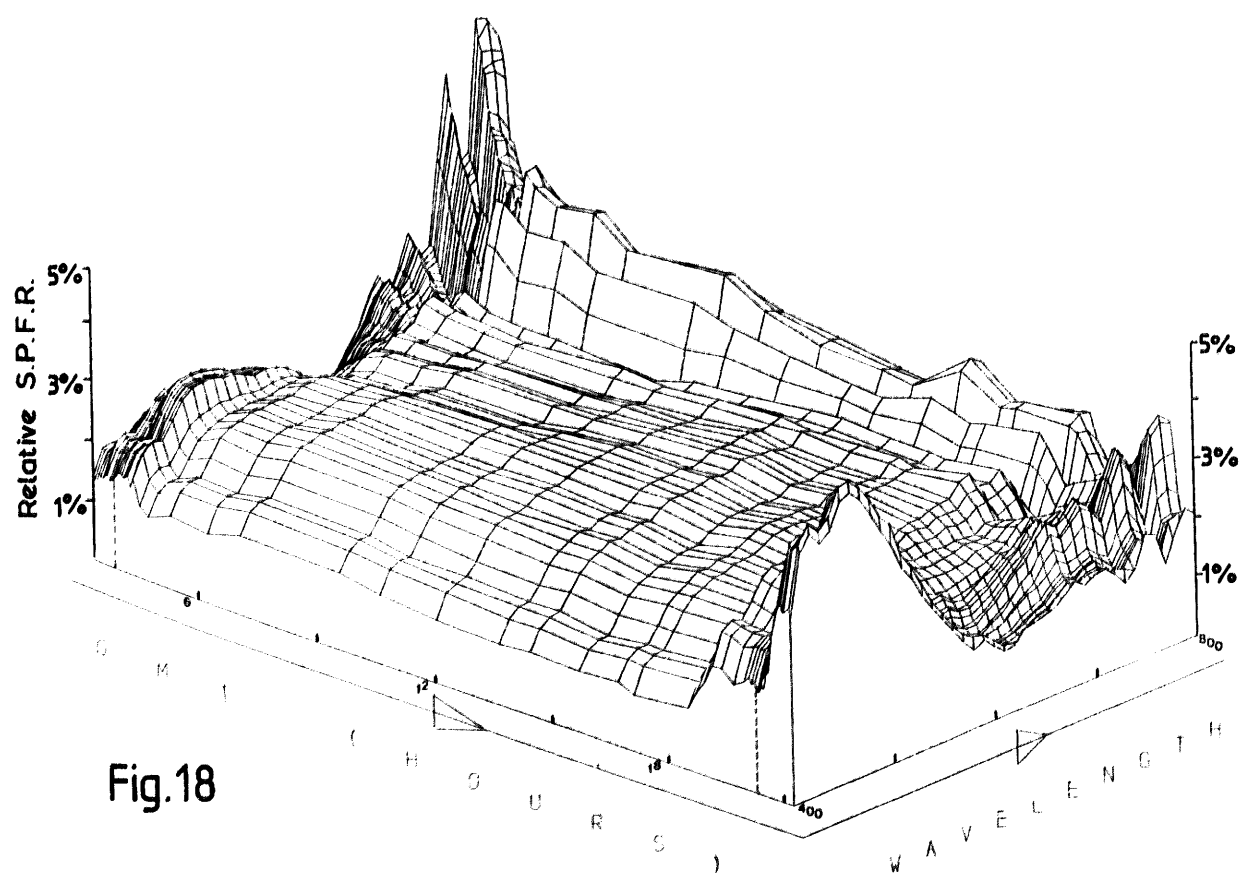


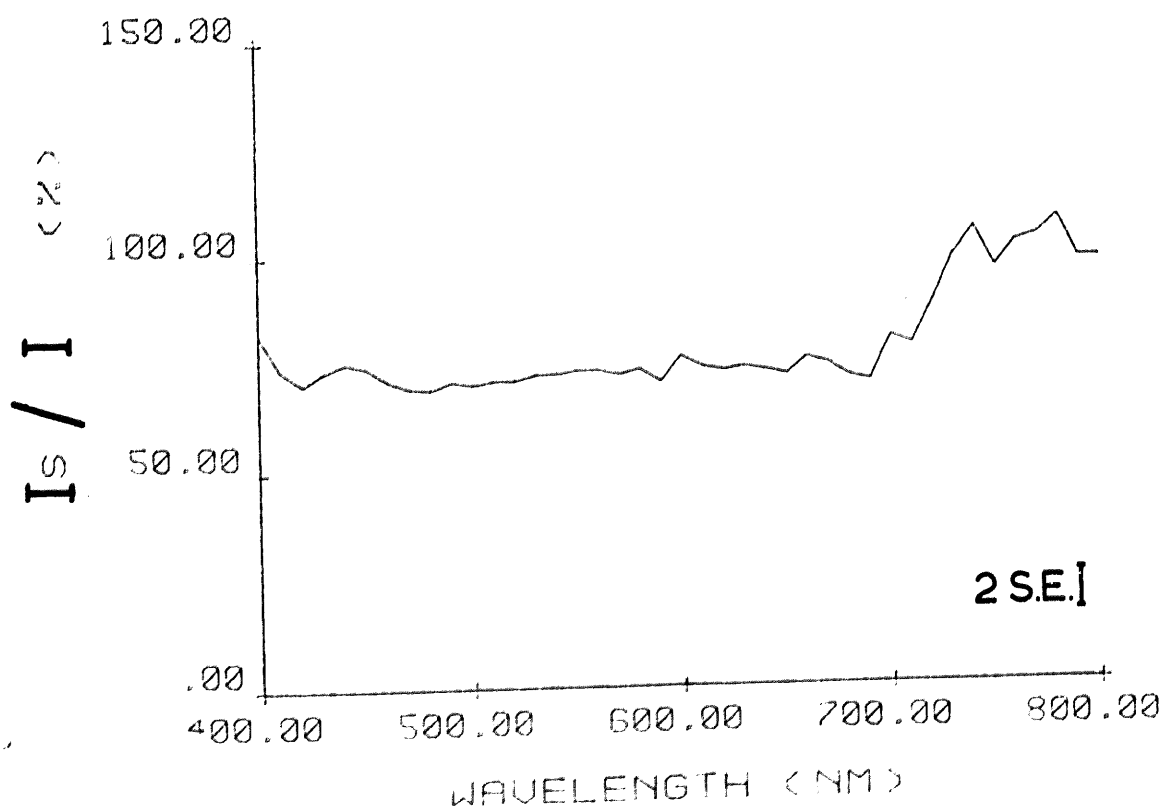
Fig.18

FIG.19

Relative SPD of incident light according to
planar and spherical receptor geometry

9 June 1982

(mean for $\alpha_0 > 15^\circ$)



Relative 240 of incident light according to
 planar and spherical microtopography
 9 June 1965

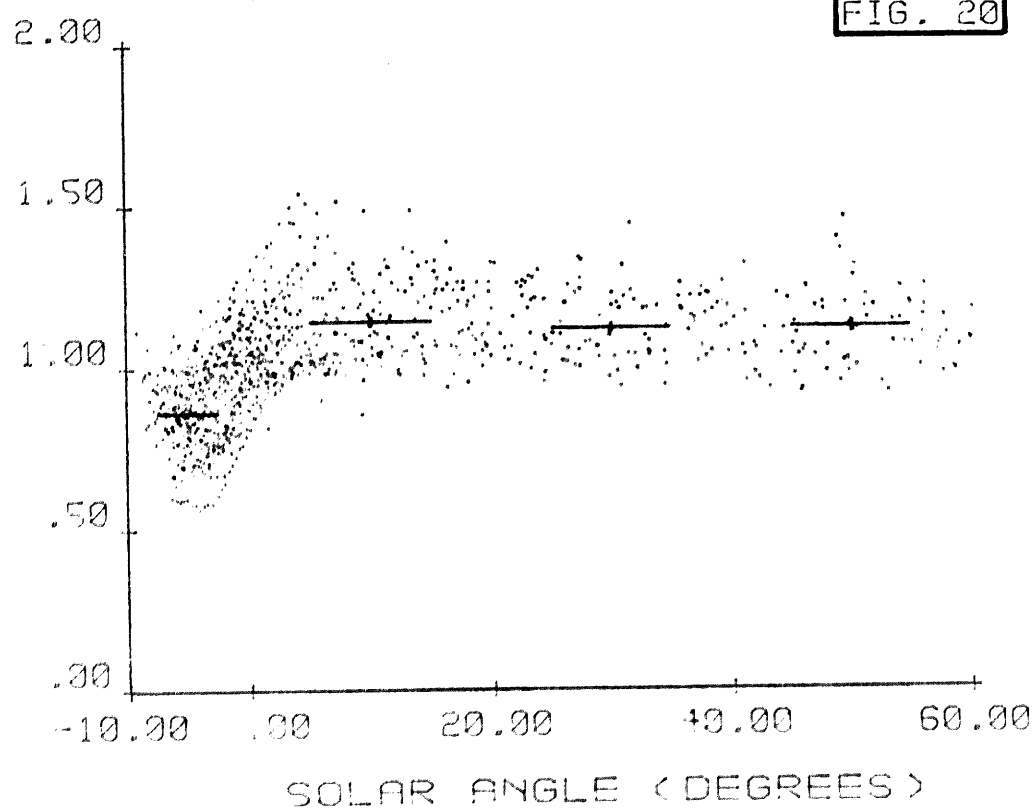
Each horizontal bar indicates the mean over that range of λ

1225

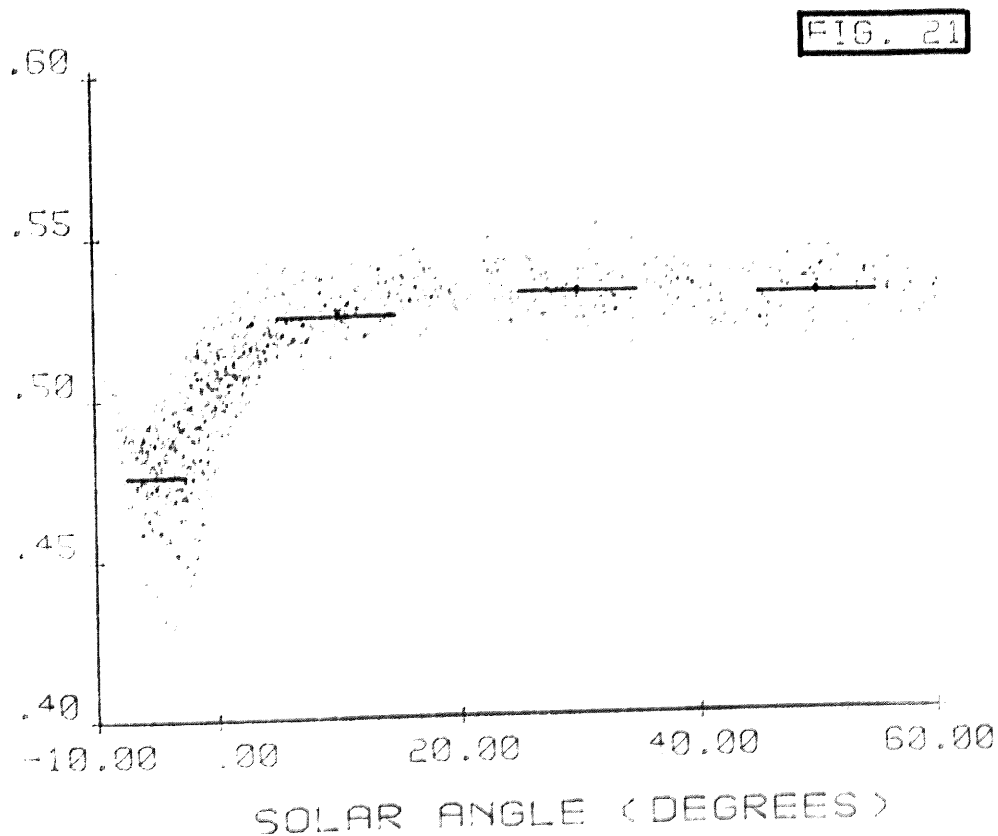
00.000 00.000 00.000 00.000 00.000

00.000 00.000 00.000 00.000 00.000

ZETA



PHI-C



Each horizontal bar indicates the mean over that range of α_s

R
B

LOG R

FIG. 22

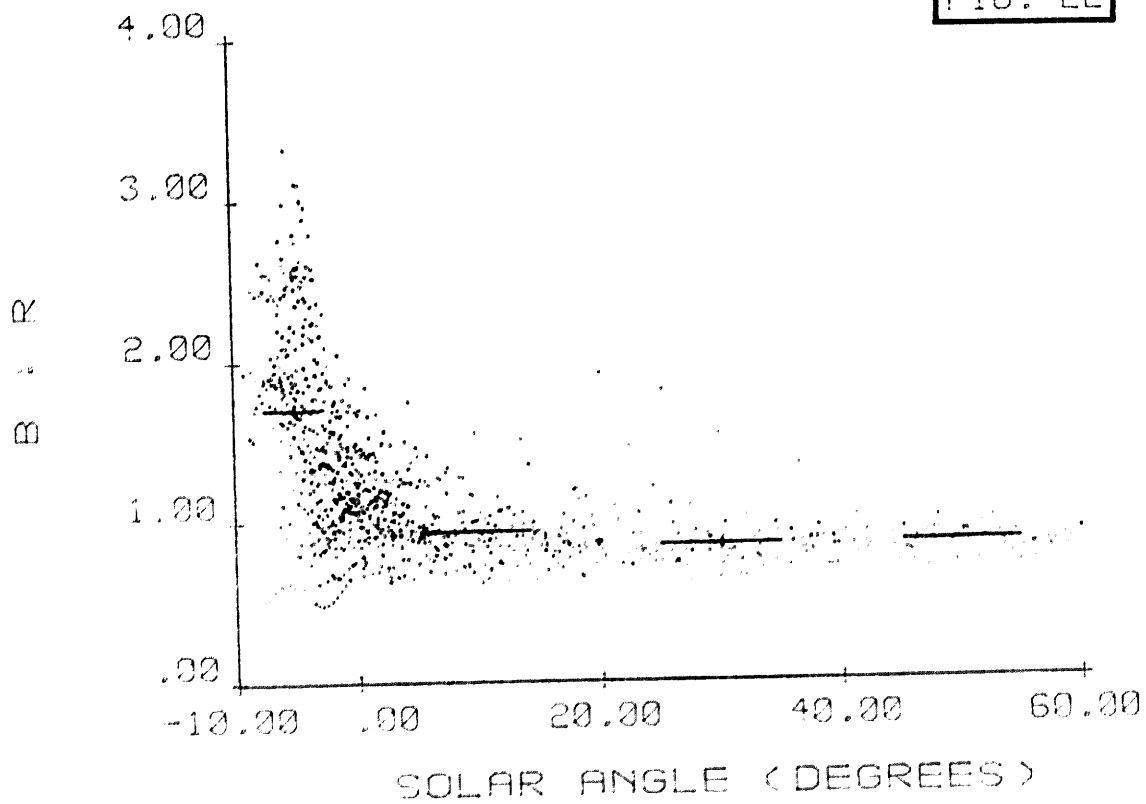


FIG. 23

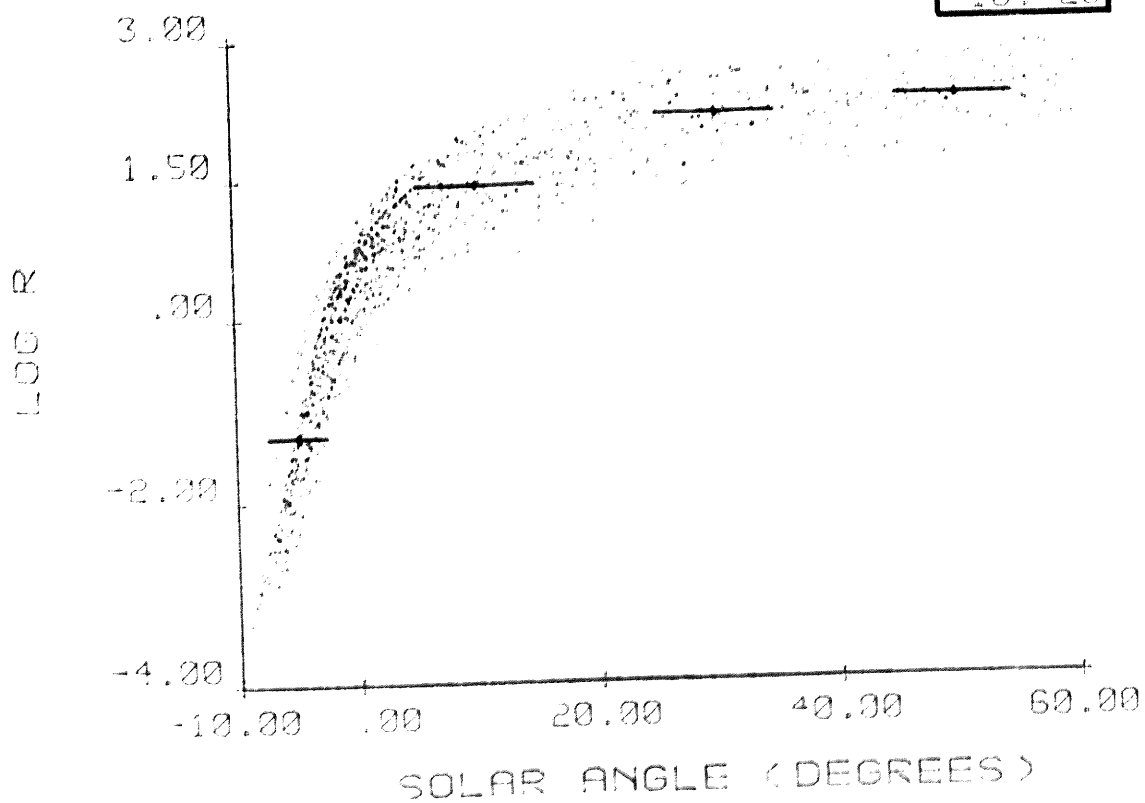


Figure 24.

Effect of broken cloud on light quality.

9 July 1982

Normalised to 100% at 660 nm.

Figure 25.

Effect of cloud cover in relation to crepuscular
change in light quality.

7 July 1981

Clear and cloudy SPDs recorded at $\alpha_s = 40^\circ$
twilight SPD recorded at -5°

Normalised to 100% at 660 nm.

1
1
RELATIVE SPFR (%)

2
1
1
RELATIVE SPFR (%)

Fig. 24

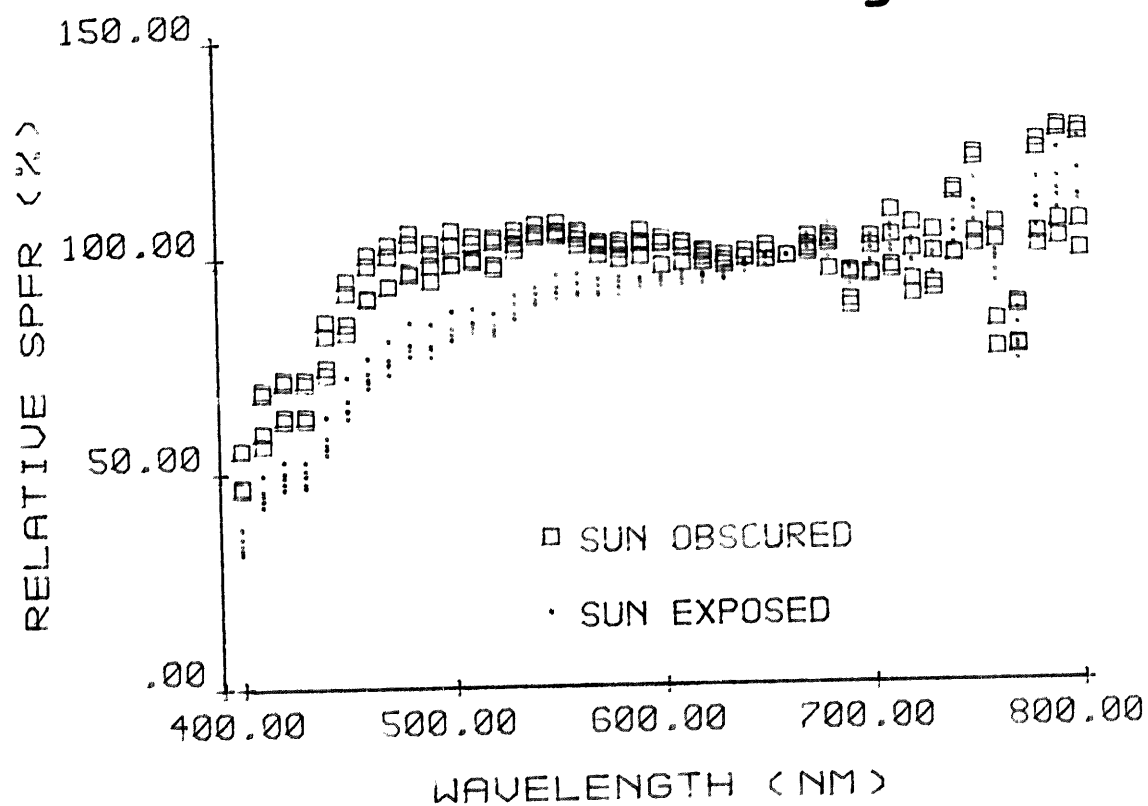
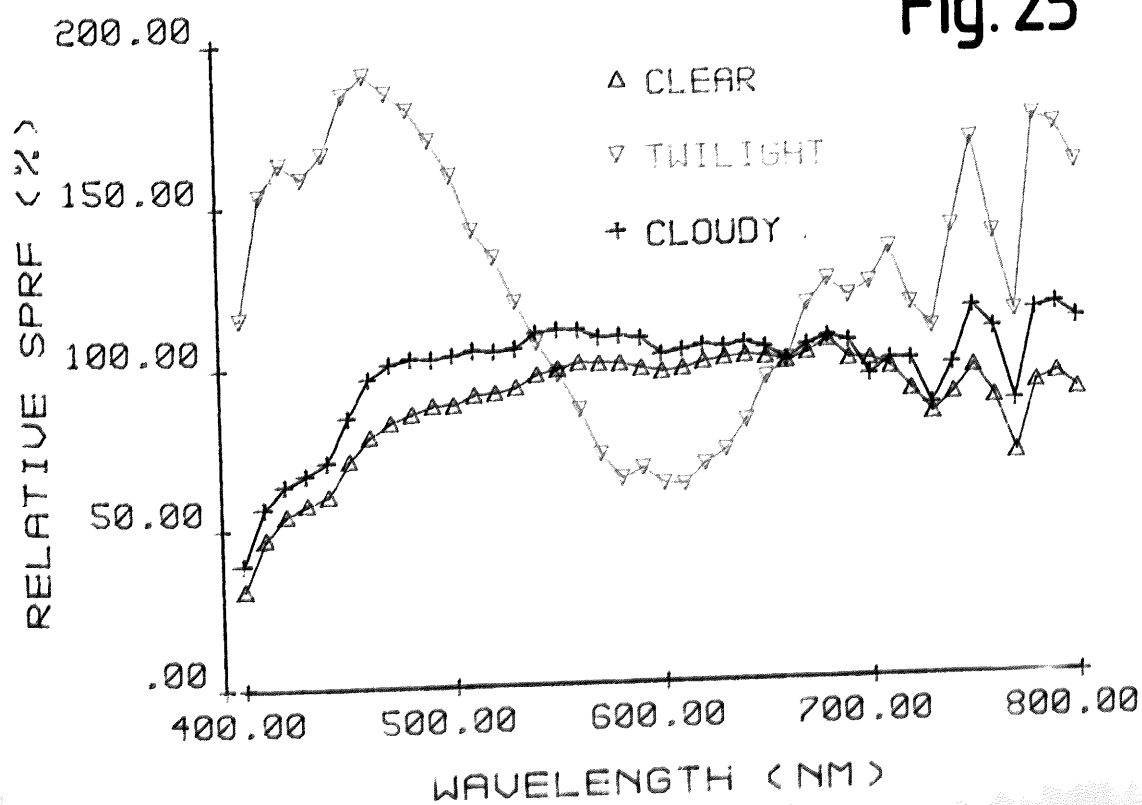


Fig. 25



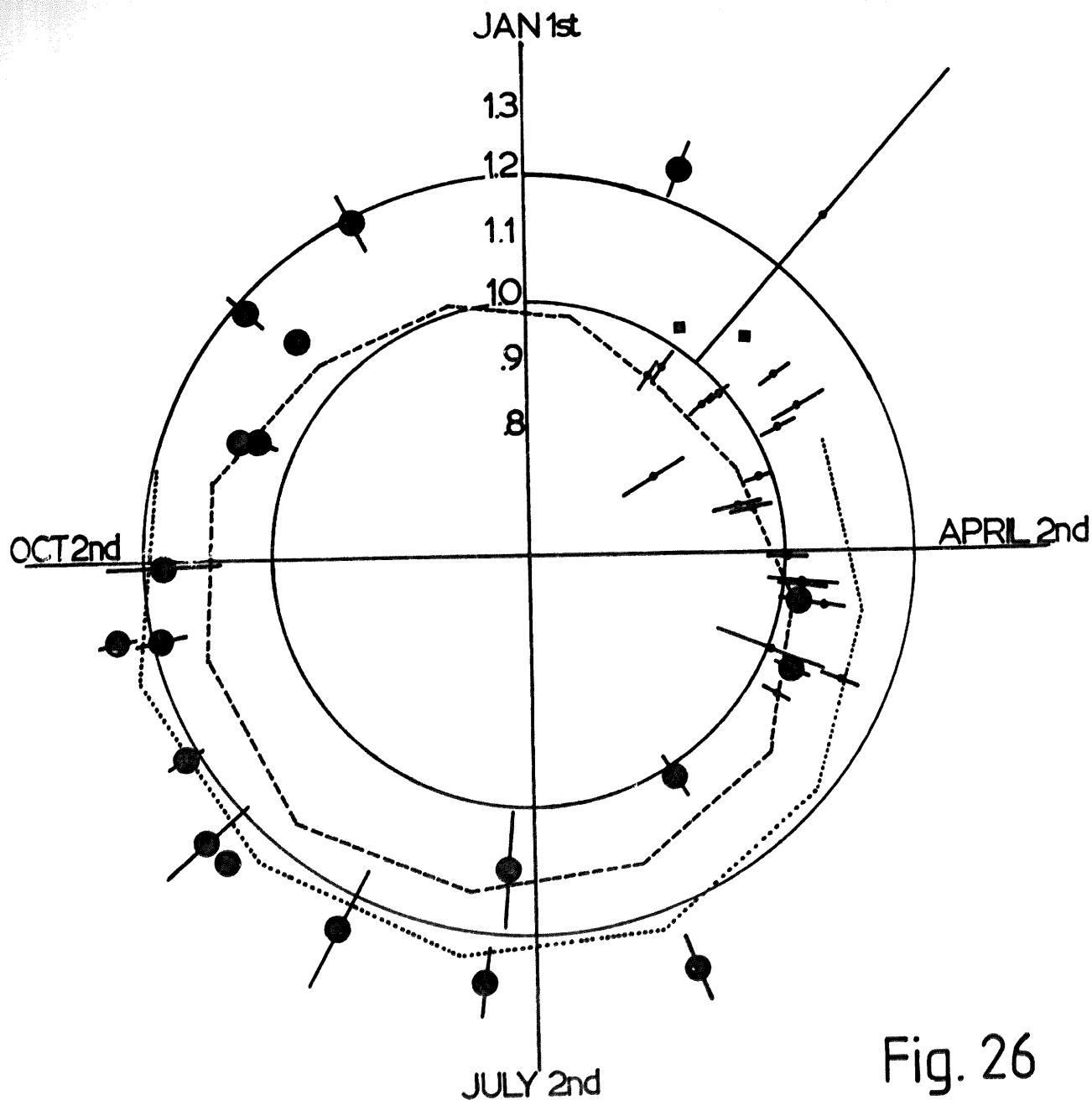


Fig. 26

Seasonal variations in mean $\bar{\alpha}$ of incident daylight

(1 day $\approx 1^\circ$; error bars = ± 2 SE)

(●) this study $7.5^\circ < \alpha_s < 15^\circ$

(•) Tasker [1977] $\alpha_s > 10^\circ$

(■) A. Webb (unpublished data) $\alpha_s = 10^\circ$

(...) Gorski [1980] $\alpha_s = 30^\circ$

(---) Gorski [1980] $\alpha_s = 10^\circ$

11) SHADELIGHT WITHIN THE OAK WOODLAND

The light environment

Results

Between April 1980 and January 1981 the light environment within the oak woodland was intensively studied on eight occasions (see Fig. 6). From these data, relative SPFR surfaces were constructed using the J06HEF algorithm in order to describe the changes in light quality during each day and between days. In addition, the parameters \mathfrak{J} , ϕ_c , B:R ratio and log R were calculated for each SPD (Figs. 35 - 38 respectively). Almost invariably, each shadelight SPD was recorded simultaneously with one outside the wood; it was therefore possible to calculate transmittance spectra for the canopy itself. On each occasion, leaves were taken from one of the trees in order to estimate their pigment content and optical properties.

On all occasions the fluence rate within the oak woodland was lower than that outside because of absorption and reflection of incident light by the leaves and branches of the trees. Prior to leaf emergence, the reduction was spectrally neutral because the twigs and branches are opaque and their reflectance is very small. Hence, the relative SPFR surface corresponding to recordings taken in Outwoods on 25th April 1980 (about ten days prior to leaf emergence in the most precocious oak trees in the area) is entirely similar to those in Figures 8 - 18 recorded in the open.

The general features of the surface (Fig. 27) are a remarkably consistent SPFR during the main part of the day between wavelengths of about 450 and 700 nm, with a fairly smooth decline in the violet region and a series of deep grooves in the far-red. During twilight the contribution of blue light relative to orange was considerably greater, whereas the level of far-red was largely unchanged. Hence, the red : far-red ratio declined as the blue : red ratio increased. The variation is apparent from Figures 35 - 38 where the corresponding values of \mathfrak{J} , ϕ_c , B:R ratio and log R respectively are shown versus solar angle.

In 1980, oak leaf emergence in Outwoods began in the second week of May, and most of the initial leaf expansion was complete before the end of the month. Although, as a result of chlorophyll absorbance of blue and red light, a

1.3(ii) light environment

typical leaf appears green to the human eye, transmittance and reflectance in this spectral region is modest in comparison to that in the far-red where chlorophyll does not absorb significantly. Thus, by the end of May the light regime within the woodland had changed dramatically.

The relative SPFR surface in Figure 28, corresponding to the photoperiod investigated on 28th May, illustrates this change. Although several features of the incident daylight spectrum are apparent in the shadelight (for instance, the grooves at 430 and 760 nm) the leafy canopy massively depleted the PAR region (400 - 700 nm), so that the residual far-red light becomes a dominant feature of the surface. A small ridge is apparent in the green region, centred at 550 - 560 nm.

During the morning twilight period, the fluence rate of both blue and far-red light increased relative to that of orange, as generally observed in incident daylight. However, because of inclement weather conditions, there are no equivalent data for the evening twilight period. Indeed, the last two SPDs were recorded despite moderate rain, making operation of the spectroradiometer difficult and potentially hazardous. Moreover, rainwater rapidly accumulated on the receptor heads, presumably disturbing their optical properties, while the high humidity increased the photomultiplier leakage current considerably. Consequently, the last two SPDs are of dubious validity and recording was abandoned shortly before sunset when weather conditions worsened. The parameters of this SPFR surface are plotted versus solar angle in Figures 35 - 38. It is apparent that while $\bar{\phi}$ and ϕ_c were much lower under the leafy canopy, log R was less severely affected while the B:R ratio was almost untouched. The crepuscular changes typical of the unshaded spectrum persisted in all four parameters.

Except between 15 and 20 h, the relative SPFR surface for the 4th July (Fig. 29) is essentially similar to that for the previous sampling day, with grooves at 430 and 760 nm, a small ridge at 550 nm and a dominant ridge of residual far-red light. A relatively higher proportion of blue and far-red light occurred during twilight. The sky was uniformly overcast, except between 15 and 20 h (see Fig. 6) when the cloud cover became broken, alternately exposing and obscuring the solar disc. These phenomena had large effects on the SPD within the woodland. On four occasions SPDs were recorded showing

relatively high levels of far-red light; these were separated by SPDs in which the relative contribution of far-red was more typical. Some time before sunset, however, complete cloud cover was restored.

The four parameters of the data are presented versus solar angle in Figures 35 - 38. All four show considerable perturbations associated with the time of broken cloud, but the crepuscular change in the B:R ratio and log R is large in relation to these, whereas the reverse is true of \bar{J} and ϕ_c .

Most of the SPFR surface corresponding to recordings made on the 13th August (Fig. 30) is similar to that recorded on the previous two occasions, except that the ridge in the green region is perhaps less marked. A modest increase in blue and far-red light relative to orange is apparent during the evening twilight, but because of technical difficulties, recordings were not started sufficiently early in the morning to reveal any equivalent change before sunrise. The four parameters of the data are included in Figures 35 - 38.

The SPD recorded at 7.48 h^(Fig. 30) is aberrant, showing a high fluence rate in the red relative to the blue and far-red. This was the result of the direct solar beam penetrating a gap in the foliage (between trees 4 and 35) and forming a sunfleck. The form of this SPD is a product of the transmission of the canopy plus an overwhelming contribution from the direct beam. Inspection of Figure 6 reveals, however, that cloud cover at the time of the recording was 8/8. The paradox is explained by notes made beside the raw trace indicating that the cloud cover, although uniform, was "thin cirrus" permitting a substantial proportion of the direct beam to pass without scattering. This was confirmed by the high fluence rate of PAR outside the wood ($>1600 \mu\text{mol m}^{-2}\text{s}^{-1}$) according to both the quantum meter reading and the spectroradiometer record. Conversely, at 6.18 h an SPD was recorded showing an abnormally high proportion of far-red, corresponding to "8/8 thin hazy cloud", but on this occasion the solar disc was not aligned with a gap in the canopy. Such a difference is to be expected if the mean transmittance of the canopy is to remain constant under different cloud conditions.

At the beginning of autumn (16th September), the relative SPFR surface (Fig. 31) is essentially similar to

those defined earlier in the leafy phase of the canopy cycle. In the evening twilight, the normal increase in blue and far-red relative to orange is apparent, but in the morning twilight, although the relative contribution of far-red is higher, there is no equivalent shoulder in the blue region. The B:R ratio data (Fig. 37) are in accord with this, and the SPDs recorded simultaneously outside the wood show similar trends around sunrise. It seems likely that the low proportion of blue light in the morning was a consequence of the fine mist at that time; the effect may also have been enhanced by the presence of broken cumulus cloud.

The lower cloud thinned temporarily between 7 and 9 h, revealing a fine layer of high altitude cirrus cloud. When the solar disc again aligned with the foliage gap between trees 4 and 35, a sunfleck was recorded (7.80 h) with a characteristically high level of red light. In accordance with the hypothesis that sunflecks are compensated for by lower transmittance at other times when the solar disc is not obscured by cloud, the adjacent SPDs show a slightly lower than average red : far-red ratio. These differences are apparent from the data in Figures 35 and 36.

When the light environment was investigated again (21st October) many of the trees in the wood were carrying senescent leaves. Table 8 shows the senescence estimate for the trees nearest the receptor head. They were scored as 0 for normal uniformly summer-green leaves, 2 for moderate senescence where the chlorophyll had been withdrawn from the lamina except near the major veins, and 4 for dead, brown leaves still attached to the tree. None of the trees had shed a significant proportion of their leaves. The onset of canopy senescence is not apparent from the light quality surface (Fig. 32) which is generally similar to those derived earlier in the leafy phase (Figs. 28 - 31); the parametric data in Figures 35 - 38 are in agreement with this. However, between about 10 and 14 h the cloud cover was reduced to a broken cirrus layer. During this period any estimate of the exposure of the solar disc was purely arbitrary because the disc was visible at all times, but scattering of the direct beam varied considerably according to the quantum meter reading. Recording the SPD under these conditions was difficult as the fluence rate was subject to gradual change. Nonetheless, it was possible during this period to record eight spectra which differed from the retrace by

1.3(ii) light environment

less than 2% (see 1.2). It is apparent from the table below that the information recorded alongside the SPDs is not sufficient to explain fully the variation in \bar{z} values recorded on the floor of the oakwood.

Time	Cloud cover	Solar disc alignment		\bar{z}
		Cloud	Canopy	
-----	-----	-----	-----	---
10.05	3/8 cirrus	exposed	foliage	.55
10.57	6/8 cirrus	exposed	foliage & trunk	.38
11.13	3/8 cirrus	obscured	foliage	.57
11.62	4/8 cirrus	obscured	foliage	.64
12.05	5/8 cirrus	obscured	foliage & trunk	.44
12.52	4/8 cirrus	exposed	foliage & trunk	.43
12.28	6/8 cirrus	exposed	foliage & trunk	.53
12.88	6/8 cirrus	exposed	sunfleck	.90

Three weeks later (11th November) the canopy had become extensively senescent and several trees had shed their leaves entirely. Table 8 shows that most of the green colouration of the remaining leaves had been lost by this stage; the trees were scored according to their leaf complement: A = intact; B = largely intact; C = partly intact; D = bare.

The light quality surface (Fig. 33) shows that the differential transmission of far-red light relative to shorter wavelengths is much smaller than earlier in the leafy phase, and the molecular absorbance bands at 630, 655 and 690 nm are again conspicuous, while the ridge in the green region is less marked. The contribution of blue light did not change appreciably during the twilight periods, although a normal high level of far-red relative to orange is apparent. As the sky was uniformly overcast for the whole day except around sunrise and sunset (see Fig. 6), no special complications are introduced into the transmission surface. All these features are consistent with the parametric data illustrated in Figures 35 - 38.

The light in the oakwood was recorded for the last time on 21st January 1981, when all the trees were bare. Accordingly, during the main part of the day the relative SPFR surface (Fig. 34) is similar to that in Figure 27 for April of the previous year, as the leafless canopy was spectrally neutral. During the morning and evening twilight the contribution of blue light relative to orange was high, although in the morning there is no

1.3(ii) light environment

less than 2% (see 1.2). It is apparent from the table below that the information recorded alongside the SPDs is not sufficient to explain fully the variation in \bar{z} values recorded on the floor of the oakwood.

Time	Cloud cover	Solar disc alignment		\bar{z}
		Cloud	Canopy	
-----	-----	-----	-----	---
10.05	3/8 cirrus	exposed	foliage	.55
10.57	6/8 cirrus	exposed	foliage & trunk	.38
11.13	3/8 cirrus	obscured	foliage	.57
11.62	4/8 cirrus	obscured	foliage	.64
12.05	5/8 cirrus	obscured	foliage & trunk	.44
12.52	4/8 cirrus	exposed	foliage & trunk	.43
13.28	6/8 cirrus	exposed	foliage & trunk	.53
13.88	6/8 cirrus	exposed	sunfleck	.90

Three weeks later (11th November) the canopy had become extensively senescent and several trees had shed their leaves entirely. Table 8 shows that most of the green colouration of the remaining leaves had been lost by this stage; the trees were scored according to their leaf complement: A = intact; B = largely intact; C = partly intact; D = bare.

The light quality surface (Fig. 33) shows that the differential transmission of far-red light relative to shorter wavelengths is much smaller than earlier in the leafy phase, and the molecular absorbance bands at 630, 655 and 690 nm are again conspicuous, while the ridge in the green region is less marked. The contribution of blue light did not change appreciably during the twilight periods, although a normal high level of far-red relative to orange is apparent. As the sky was uniformly overcast for the whole day except around sunrise and sunset (see Fig. 6), no special complications are introduced into the transmission surface. All these features are consistent with the parametric data illustrated in Figures 35 - 38.

The light in the oakwood was recorded for the last time on 21st January 1981, when all the trees were bare. Accordingly, during the main part of the day the relative SPFR surface (Fig. 34) is similar to that in Figure 27 for April of the previous year, as the leafless canopy was spectrally neutral. During the morning and evening twilight the contribution of blue light relative to orange was high, although in the morning there is no

1.3(ii) light environment

corresponding shoulder in the far-red. Just after dawn and before dusk a secondary increase in the relative fluence rate of blue light is apparent which is distinct from the crepuscular change, as the increase is largely at the expense of far-red light rather than of orange. The origin of this effect is obscure.

The mean values of $\overline{\mathfrak{J}}$, ϕ_c , B:R ratio and log R were calculated for $15^\circ < \alpha_s < 30^\circ$, ignoring the SPD recordings taken when the sky was clear, as sunflecks interfered with transmission (see 1.1). The results for both incident and shade light are shown in Figures 39 - 42 respectively. The B:R ratio in the woodland did not change dramatically during the canopy cycle although a significant increase was recorded on 4th July (year day 185). In contrast, $\overline{\mathfrak{J}}$ and ϕ_c were considerably lower during the leafy phase of the cycle, with significantly higher averages on 13th August and 16th September (year days 225 and 259). The variation in log R does not follow that of any of the other parameters.

The effects of the canopy upon the twilight changes in SPD were investigated statistically using a non-orthogonal ANOVAR. The result of this for each of the four parameters is shown in Table 9. Interaction between the factors was significant for the light quality parameters, indicating that the nature of the twilight effect varied. However, the effects of solar angle and date alone were significantly greater. In contrast, the log R parameter shows no interaction and a large effect of α_s relative to date.

Discussion

These findings are in close accord with those of Tasker and Smith [1977] who found that $\overline{\mathfrak{J}}$ in an oak woodland was close to unity before leaf emergence, and declined rapidly as the leafy shade developed from mid-May onwards. The minimum $\overline{\mathfrak{J}}$ recorded was about 0.4 (at the beginning of July), but thereafter the average values increased again and stabilised at about 0.7. Leaf senescence was complete by mid-November. The authors proposed three possible explanations of this behaviour. Firstly, they suggested that extensive leaf loss may have occurred in mid-summer, increasing $\overline{\mathfrak{J}}$. This is unlikely because photographic data collected simultaneously failed

to show any decline in leafy interception (Tasker, 1977) and, moreover, the data failed to show any correlation between $\bar{\epsilon}$ and mean PAR on the woodland floor during the leafy phase. Secondly, they suggested that wilting may have been responsible. Although this might not have been detected by the photographic record taken early in the morning, the explanation is also unlikely as again the PAR fluence rate would be expected to increase. Moreover, the likelihood of such severe water stress occurring in a group of mature trees over a period of weeks is very small. Their third suggestion was that changes in leaf chlorophyll content might have modified $\bar{\epsilon}$ without having dramatic effects upon PAR. Pigment content had not been measured in the course of the project because of the logistical difficulty of randomly sampling the canopy (Tasker, 1977).

A further possibility, not considered by these authors but first suggested by Gorski [1980] is that a seasonal variation in the red : far-red ratio of the incident light could be responsible for the changes observed beneath the leafy canopy. The mean value of $\bar{\epsilon}$ for incident light is 1.15 according to Holmes and Smith [1977a] and the data reported here (Table 1). The small standard error associated with this (ca. 0.02) has generally been interpreted to indicate that differences between days are negligible. This is a common fallacy. Standard error is a measure of the accuracy with which the population mean is estimated by the sample mean. Hence, given a sufficiently large sample, the standard error can tend to zero while the variability within the population is large. According to the data in Table 1, the standard deviation of the daily averages is approximately 10% of the grand mean; thus a third of recorded days would be expected to differ by more than this amount from 1.15. There is probably a seasonal change in addition to a random variation between days.

It is apparent from the twilight ANOVAR (Table 9) that significant variation in the relationships between all the light quality parameters and solar angle exists; this is, however, no greater than that found for incident light (Table 6). The modifying effects of the canopy thus act independently of solar angle, in the manner of a simple coloured filter. The analysis also implies that the effects of solar angle and date are similar, and therefore, if they are to act as zeitgebers, the plant must be able to compensate for seasonal variations.

Whether this is possible is not known, although several experiments have shown that diurnal red : far-red fluence ratios can affect flowering (see 1.1). In contrast, the log R parameter is relatively independent of leafy interception during twilight, even though there are statistically significant differences between days. Photoperiodic timing would scarcely be affected by this. In general, there is little reason for supposing that light quality zeitgebers would be of any advantage in the natural environment, and the experimental evidence for them is insubstantial.

Any change in the incident light is generally superimposed on that measured beneath a canopy. In this study data were collected simultaneously outside and beneath the oak woodland, and hence the correlation between changes at the two locations can be assessed. Equivalent data for the incident daylight are included in Figures 39 - 42, and it is apparent that the variation during the leafy phase is similar, except perhaps for ϕ_c .

This may have important repercussions in plant photoperception. According to the hypothesis that leafy shade may be assessed by comparing the fluence rates of red and far-red light (Jordan, 1969), a good correlation exists between the transmittance of the canopy at any wavelength absorbed by chlorophyll and the red : far-red fluence ratio of the transmitted light. At least two factors may interfere with this: the incident ratio may itself vary; and, as a direct relationship exists only between the ratio and the concentration of a single pigment, the correlation between the ratio and leafy interception or leaf area index may be disturbed by changes in the abundance of the various leaf pigments. Indeed, if the photoperception capacity of plants is as sophisticated as has been suggested (Smith, 1982), the latter is to be expected.

In any case, the data presented upto this point provide a poor description of the spectral properties of the canopy because it includes the effects of all the meteorological variables which modify the SPD of daylight (see 1.1). Other than nocturnal measurements using an artificial light source of suitable stability, or a mathematical approach involving an integration of the various optical features of the canopy, the only possible solution to the problem is to express the instantaneous SPFR measurements beneath the canopy as a proportion of

their counterparts outside. The principle is the same as that of the double-beam spectrophotometer. Transmittance spectra so derived can be compared directly with the spectral properties and pigment content of the leaves themselves.

The effect of the canopy

Results

Mean transmittance spectra were calculated accordingly for each day from the data recorded while $\phi > 15^\circ$ and the solar disc was obscured by cloud, as under clear skies, sunflecks introduced complications (see 1.1). The results are presented along with the corresponding spectral transmittance and reflectance values for sun and shade leaves (Figs. 43 - 56). Figure 57 shows the results of chlorophyll and carotenoid analyses performed on similar leaves.

Before and after the leafy phase (Figs. 43 and 44, respectively) the spectral transmittance of the canopy was very similar at all wavelengths except 400 nm where the sensitivity of the spectroradiometers is poor. The transmittance in the far-red is marginally higher than in the red according to the January data, but the difference is not statistically significant ($t=2.6$, $p_0 > 5\%$). The mean transmittances calculated for April and January were 58% and 48%, respectively.

Once the foliage had expanded, the canopy transmittance spectrum (Fig. 45) was radically different, showing a much lower PAR transmittance (ca. 10%), with slightly higher values in the green than in the blue and red regions. Transmittance increased abruptly at 690 - 700 nm, reaching a peak of about 20% in the far-red at 760 nm. Corresponding sun and shade leaf transmittance data (Fig. 46) are quite different, showing a pronounced peak in the green (ca. 24%) and a generally lower transmittance of blue (ca. 4%) than of red (5 - 15%) at light. Maximum transmittance of far-red was about 50% at 760 nm. The results for sun and shade leaves were similar; reflectance was not measured in this instance. The leaf pigment content was low with chlorophyll and carotenoid concentrations of ca. 0.46 and 0.1 g m^{-2} , respectively. Chlorophyll a : b ratio was approximately 3.5, being somewhat higher for sun than for shade leaves.

1.3(ii) canopy effect

The mean canopy transmittance calculated for 4th July (Fig. 47) is similar in the PAR region (ca. 11%) although a rather higher transmittance is apparent ^{between} 550 - 680 nm than 400 - 500 nm. In the far-red the maximum transmittance was higher than before (ca. 37%); there was, however, considerable variability in the data at these wavelengths. Corresponding data for the leaves ~~are~~ shown in Figure 48. Transmittance at all wavelengths had declined to about half the values recorded in May, but the data are qualitatively similar. The reflectance spectrum shows a small peak in the green (ca. 20%), and slightly higher values in the red (ca. 15%) than in the blue (ca. 12%). The far-red reflectance was very high (ca. 58%). Data for sun and shade leaves were closely similar. The chlorophyll and carotenoid content had increased by approximately one half.

The spectral transmittance forty days later (13th August) is shown in Figure 49. Blue light transmittance was about 8%, slightly lower than that in the red (ca. 9%). Maximum far-red transmittance was about 24%, and had thus declined from that recorded in July. Leaf pigment content (Fig. 57) and transmittance and reflectance (Fig. 50) were almost unchanged, except that in the far-red reflectance was somewhat lower (ca. 50%) and shade leaf transmittance was higher (ca. 30%).

On 16th September canopy transmittance (Fig. 51) was ca. 10% in the blue, increasing almost linearly to about 13% at 680 nm. Transmittance towards longer wavelengths did not increase as rapidly, nor was a peak reached at 780 nm, as had been recorded on previous days in the leafy phase. Sun leaf transmittance was generally higher than recorded in August (ca. 10% and 52% in the green and red, respectively). Leaf reflectance, shade leaf transmittance and pigment content were largely unchanged.

The canopy transmittance spectrum on the 21st October (Fig. 53) corresponds to the early stages of senescence, and indicates a decline to about 6% in the blue and 7% in the red regions. The maximum transmittance in the far-red was only about 18%. Sun leaf reflectance was higher than in September (about 30% in the green, 20% in the blue and red, and 60% in the far-red regions), while far-red transmittance was somewhat lower; the optical properties of the shade leaves were largely unchanged. Carotenoid content was a little higher,

especially in the shade leaves (ca. 0.25 g m^{-2}), while the total chlorophyll was unchanged at about $0.8 - 0.9 \text{ g m}^{-2}$; however, chlorophyll b content had increased relative to chlorophyll a (Fig. 57).

During the next three weeks the canopy became extensively senescent, and some trees had begun to shed their leaves. Figure 55 shows the transmittance spectrum at this time (11th November); this is radically different from those derived earlier in the leafy phase. Transmittance in the PAR region is much higher (ca. 25%), while the far-red maximum is about 32%. Similarly, transmittance of sun and especially shade leaves had increased dramatically, as had shade leaf reflectance in the PAR region. While the chlorophyll a : b ratio remained high, the total content, especially of the shade leaves, had declined substantially; the carotenoid levels, however, were unchanged (Fig. 57).

Considering the data collectively, Figure 58 shows the variation in the transmittance of the canopy and the individual leaves at 680 nm (the wavelength of maximum leaf absorbance in the red region) during the leafy phase. It is apparent that prior to senescence, the canopy transmittance varied about a mean of 11% with little apparent trend. This variability is predictable from the errors inherent in the data (see 1.2); hence, the statistically significant differences ($p_0 > 1\%$) do not necessarily indicate actual changes in the optical properties of the canopy. At senescence, however, the transmittance declined to about 7%, then underwent a massive increase to 27%.

These features are not shared by the transmittance of the leaves themselves. After initial expansion following bud break, the transmittance declined considerably (from 5% at the end of May to 1.7% at the beginning of July); this was associated with an increase in pigment content (Fig. 57). Thereafter, transmittance increased gradually and almost linearly until the end of October when it reached 3.4%. Chlorophyll content changed little over this period (ca. 0.9 g m^{-2}) although carotenoid levels slowly increased. The leaves senesced rapidly from the beginning of November; by the second week, sun and shade leaf transmittance had increased to 6% and 18% respectively. The large error associated with the latter estimate reflected the variability of the material, presumably indicating that senescence was not equally

1.3(ii) canopy effect

advanced in all leaves. The mean chlorophyll content of sun and shade leaves at this time was about 0.6 and 0.3 g m⁻², respectively, confirming that senescence was more advanced in the latter. Carotenoid content was unaffected. The chlorophyll a : b ratio

in October dropped to a low value in both leaf types; this was probably an early event in senescence. The particularly low canopy transmittance at this time was associated with an increase in sun leaf reflectance (from a steady 10% to 20%), and not with any change in leaf transmittance.

From the transmittance spectra of the canopy and its constituent leaves it is possible to derive an index of the effects of each upon light quality and hence the photoequilibrium of phytochrome. Such information is of significance to the hypothetical photoperception of leafy shade.

For each SPD inside and outside the wood, the relation

$$\frac{I_{t, \lambda 1}}{I_{i, \lambda 1}} \bigg/ \frac{I_{t, \lambda 2}}{I_{i, \lambda 2}} = \text{canopy transmittance ratio} \quad \dots(5)$$

(where $I_{i, \lambda}$ and $I_{t, \lambda}$ are the SPFRs at λ nm of incident and transmitted light, respectively) was calculated from the $15^\circ < \alpha < 30^\circ$ data for $\lambda_1 = 660$ nm and $\lambda_2 = 730$ nm, including only data collected when the solar disc was obscured by cloud. The equivalent ratio for the sun and shade leaves was derived. The mean values of each through the year are shown in Figure 59, from which it is apparent that the canopy transmittance ratio is close to unity before and after the leafy phase, and is remarkably constant at about 0.52 throughout the Summer and Autumn until senescence in November. For the leaves themselves the ratio remains similarly constant but much lower (ca. 0.12) during the summer and early Autumn. The initial measurement (28th June) is rather higher (ca. 0.19), associated with the low chlorophyll content (Fig. 57) at this time.

It is apparent that this relationship (Fig. 59) is more similar to the quantitative variation in transmittance at 680 nm (Fig. 58) than to the changes in

shadelight quality (Fig. 39). It was of interest, therefore, to consider what relationship exists between the measured transmittance of the canopy and shadelight quality. This is shown for λ and red light during daytime in Figure 60, along with the transmittance estimated using hemispherical photography and that calculated from light measurements beneath the bare canopy. The distribution of points is contagious for each day although, as data corresponding to times when the solar disc was "exposed" are included, deviant points are also apparent. During the leafy phase, prior to senescence, the correlation of λ and transmittance is poor.

Although not necessarily of physiological significance, covariation between transmittance and the B:R ratio was investigated. Figure 41 shows a lower proportion of blue light beneath the leafy canopy than above it, especially after the leaves had matured and even during senescence. This is associated with the initial rapid increase in carotenoid screening followed by a steady accumulation throughout the leafy phase until leaf fall (Fig. 57). Accordingly, the B:R transmittance ratio of both sun and shade leaves declined steadily (Fig. 61). The corresponding canopy transmittance ratio declined less steeply (Fig. 62). Data for the corresponding reflectance ratio for mature leaves showed a gradual decline from 0.94 (4th July) to 0.82 (21st October), and to about 0.5 on the 11th November.

Discussion

The transmittance of the bare canopy in April was significantly higher than in January of the following year ($t=11$, $p_0 < 0.1\%$); however, hemispherical photography on the later date indicated an intermediate value closer to that of the previous spring; this is likely to be similar to the true value. The 10% difference between the absolute transmittance data according to the spectroradiometers gives an indication of the accuracy of the system as a whole. The instruments are not ideally suited to this measurement, as the accuracy and stability of their calibration under field conditions leaves much to be desired. Although both instruments were carefully calibrated on either the day before or the day after each session in the field, the possibility of a significant change in sensitivity during transport was always present. It was also impossible to keep the receptor heads

perfectly clean and dry under field conditions. Such changes affect the reliability of the quantitative data, especially transmittance, while the estimation of light quality is relatively immune.

Without an independent record of canopy transmittance it is difficult to assess the significance and origin of the quantitative variation through the season. In statistical terms, the information has zero degrees of freedom, and hence significant differences cannot occur! The problem could have been partly overcome by using a second quantum meter to estimate the shadelight fluence rate independently.

Nonetheless, a pessimistic estimate of the error associated with any SPFR would be about $\pm 10\%$ for most of the spectrum, in addition to the sampling errors involved. This is in line with the variation between estimates of transmittance before and after the leafy phase, as the actual change is likely to have been very small. The decrease associated with leaf emergence is, in contrast, much greater than the likely error. Thereafter, the variation in transmittance until the end of October (Fig. 58) is again within the expected error and, hence, is unlikely to represent real changes. The estimate for October 21st, at the start of canopy senescence, is considerably lower but, thereafter, a dramatic increase is seen as the process continued.

Having taken into account changes in the incident radiation and recorded the shadelight at a fixed location (in contrast to previous work), it is a reasonable conclusion that the leaves themselves were responsible for the seasonal changes in canopy transmittance under overcast skies. Allowing for the interception of about half of the incident light by tree branches and trunks, canopy transmittance was always greater than that of the leaves themselves (Fig. 58), despite their abundance; this was a consequence of both the distribution of leaves (allowing canopy gaps to form) and multiple reflection between them.

The higher transmittance and reflectance of shade leaves relative to sun leaves reported by Eller, Gtattli and Flach [1981] in beech was not a consistent feature of the oak leaves measured here. This is probably a consequence of the much greater difference between shadelight and incident light in the beech canopy.

1.3(ii) canopy effect

Oak leaf transmittance shows an initial decline associated with maturation, a slow constant increase through the summer and autumn and a massive increase associated with advanced stages of senescence. Although canopy transmittance on October 21st had decreased, the leaf transmittance had increased. An increase in leaf area index could explain the paradox, but is most unlikely at this time of year. A more probable explanation may lie in the increased sun leaf reflectance; similarly, Sinclair, Hoffer and Schreiber [1971] found that senescence in several crops was accompanied by a higher leaf reflectance. Subsequently, both leaf reflectance and transmittance increased dramatically, while Table 8 indicates that leaf area index had begun to decline; the net effect was a large increase in canopy transmittance.

The transmittance spectra of the oak canopy do not closely resemble those of the individual leaves at any point in the cycle; generally, qualitative differences are much more pronounced in the latter. Eller et al. [1981] were unable to explain the spectrum of shadelight on the basis of simple transmission of incident light by leaves, and a similar discrepancy occurs in canopy reflectance (Colwell, 1974).

On a smaller scale still, Loomis [1965] showed that qualitative transmittance differences were more marked in chloroplast suspensions and especially chlorophyll solutions than intact leaves. The differences are related to the optical complexity of the system; for a leafy canopy, this is enormous.

When a photon is intercepted by a leaf, a number of possible fates may befall it. The refractive index of the epidermal cuticle is high relative to air and, consequently, specular reflection (that is, reflection at an angle equal and opposite to that of incidence) may occur immediately. Woolley [1971] found the probability of this to be about 0.003 for all wavelengths between 400 - 3000 nm. The simple system used to measure reflectance in the work reported here (Fig. 5) ignores this process entirely. If the photon penetrates the cell, its path is bent by refraction at the air - cell wall interface; thereafter it is likely to pass directly into a mesophyll cell where chloroplasts are abundant. If it enters one it may be absorbed by a pigment molecule such as chlorophyll, the probability depending on the pigment density and the

1.3(ii) canopy effect

wavelength of the photon; for chlorophyll, this is high for blue and red light, lower for green and insignificant for wavelengths above 710 nm. If it is not absorbed it will reach the cell wall - air interface within the leaf and may either be reflected back or move into the intercellular airspace, once more its path being bent by refraction. This "scattering" continues until either the photon is absorbed, or it emerges at any angle from the upper surface again (diffuse reflection) or from the lower surface (diffuse transmission).

The mean pathlength through the leaf is consequently much longer than its physical thickness (the detour effect) and hence the opportunity for absorption is enhanced. Conversely, the aggregation of pigment molecules in chloroplasts reduces the probability of absorption (the sieve effect). Quantitatively the system is highly complex, however, and a general solution to the problem of light propagation within leaves is not yet available. In the Kubelka-Munk theory of propagation, radiation at any depth in a homogeneously absorbing and scattering medium is considered as two fluence rates, one forwardly and the other backwardly directed; both of these decline hyperbolically as the sample thickness increases. This contrasts with non-scattering media, such as solutions, in which the decline is exponential according to Beer's Law. In a real leaf, heterogeneous scattering and pigment distribution considerably complicate matters (see Fukshanski, 1981). This is exacerbated by the directional and spectral complexity of natural daylight to which the leaf is exposed in the field.

Considering the canopy as a whole, Monsi and Saeki [1953] showed that, as a first approximation, light transmission obeys Beer's Law :

$$\text{transmittance} = \exp(-kL) \quad \dots(6)$$

where L is the leaf area index, and k is an extinction coefficient dependent on various factors including leaf distribution, orientation and pigment content, wavelength, and non-leafy structures in the canopy. Again, this is not true if the objects constituting the canopy reflect a significant amount of light and, hence, introduce a detour effect by scattering. In this case there are again two opposing vertical propagation vectors to be considered in light transmission (see Bunnik, 1978). A complete model of canopy optics is likely to be of horrendous complexity.

1.3(ii) canopy effect

Interesting predictions result from simple scattering theory, however. Using the general equation for homogeneous "canopies" derived by Bunnik [1978] for downwardly propagated light, the transmittance was calculated for a range of absorption coefficients at three different degrees of scattering using the relation :

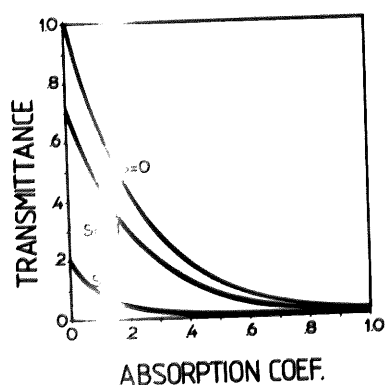
$$\text{transmittance} = \frac{(1+B)^2 - (1-B)^2}{[(1+B)^2 \cdot \exp(AL)] - [(1-B)^2 \cdot \exp(-AL)]} \dots(7)$$

$$\text{where } A = [k \cdot (k+2s)]^{0.5}$$

$$\text{and } B = [k/(k+2s)]^{0.5}$$

k and s are the statistical absorption and scattering coefficients, and L is the leaf area index.

Leaf area index was arbitrarily set at 5 and soil reflectance ignored. The results are shown in the accompanying figure. When the scattering coefficient is zero, $A = k$ and $B = 1$ and hence the equation simplifies to Monsi and Saeki's version of Beer's Law; transmittance declines exponentially with increasing absorption coefficient. As scattering is introduced, however, small differences in absorption coefficient have larger effects on transmittance, thus the medium becomes more intensely coloured. On the other hand, scattering always reduces transmittance.



While the model is far from perfect and merely illustrates the interaction between scattering and absorption, it is apparent that if the leaves were distributed homogeneously, the relatively low transmittance of blue and red would be enhanced by scattering. Conversely, the sieve effect increases overall transmittance. It is apparent from the field data that the latter has a predominant effect in the oak canopy, as the spectral variation in transmittance is much less marked than in the leaves themselves.

The data in Figure 58 provide good evidence that the canopy optics remain stable during the leafy phase. However, any effect of changes in the pigment content or detour / sieve characteristics of the leaves or canopy should be more easily detectable in the transmittance ratios (Figs. 59 and 62), as these are less affected by changes in the sensitivity of the spectroradiometers. In the case of chlorophyll, the initial increase in concentration as the young leaves matured and the subsequent fall during senescence is reflected in the 660 / 730 nm transmittance ratio of the leaves and, to some extent, of the canopy (Fig. 59). The downward trend in the B:R transmittance ratios (Figs. 61 and 62) was probably a result of the concentration of carotenoids increasing fairly uniformly throughout the season.

The recordings in a natural woodland and an approximate theoretical model suggest that, while light absorption is enhanced by scattering, it is decreased by heterogeneous pigment distribution. Consequently, while scattering accentuates spectral transmittance ratios, they are brought closer to unity by sieve effects. Thus, a leafy canopy becomes more spectrally neutral as heterogeneity increases and scattering falls. In terms of photoperception by phytochrome, Φ is likely to become less dependent upon leaf area index and chlorophyll content as the leaves of the canopy become more clumped (other factors remaining equal). On the other hand, scattering between leaves or their more uniform spatial distribution will tend to reduce canopy transmittance. If a fluence rate receptor such as cryptochrome does exist and operates alongside phytochrome, their relative importance will therefore depend not only on pigment content and leaf area index, but also on the aggregation and reflectance of the leaves.

TABLE 8

Oakwood canopy condition Autumn 1980

Tree	21st October	11th November
1	2 A	4 C
2	1 A	3-4 A
4	2 A	4 D
10	2 A	4 C-D
16	D	D
17	3 A	D
19	3 A	4 C
20	1 A	4 C
23	0 A	3 A
25	0 A	3 A
31	1 A	3 B
32	0 A	2 A
33	0 A	2 A
34	0 A	1-2 A
35	1 A	3 B

KEY:- LEAVES
 Full summer green.....0
 Yellow with green veins..2
 Brown.....4

CANOPY
 Intact.....A
 Largely intact.....B
 Partly intact.....C
 Bare.....D

TABLE 9 NON-ORTHOGONAL ANALYSIS OF VARIANCE
OAK WOODLAND : TWILIGHT ($\alpha_r < 7.5^\circ$)

<u>SOURCE</u>	<u>Df</u>	<u>Sum-of-Squares</u>	<u>Variance</u>	Error <u>V.R.</u>	D x A <u>V.R.</u>
Parameter - β					
DAYS	7	8.3	1.18	---	78
ANGLES	2	0.67	0.34	---	22
D x A	14	0.21	0.015	4	
Residue	188	0.72	3.8×10^{-3}		
Parameter - ϕ_c					
DAYS	7	0.15	0.022	---	34
ANGLES	2	0.46	0.023	---	35
D x A	14	9.1×10^{-3}	6.51×10^{-4}	7	
Residue	188	0.017	9.31×10^{-5}		
Parameter - B:R ratio					
DAYS	7	15.5	2.21	---	4
ANGLES	2	11.6	5.82	---	10
D x A	14	7.74	0.55	6	
Residue	188	16.88	0.090		
Parameter - log R					
DAYS	7	10.68	1.52	7.2	
ANGLES	2	149.7	74.9	355	
D x A	14	3.35	0.239	1.1	
Residue	188	39.67	0.211		

Figures 27 - 34

Relative SPFR surfaces of oak woodland
shadelight, 1980-81

The dashed lines correspond to sunrise and
sunset; wavelengths are in nanometers.

Figure 27: 25 April, 1980

Figure 28: 28 May, 1980

Figure 29: 4 July, 1980

Figure 30: 13 August, 1980

Figure 31: 16 September, 1980

Figure 32: 21 October, 1980

Figure 33: 11 November, 1980

Figure 34: 21 January, 1981

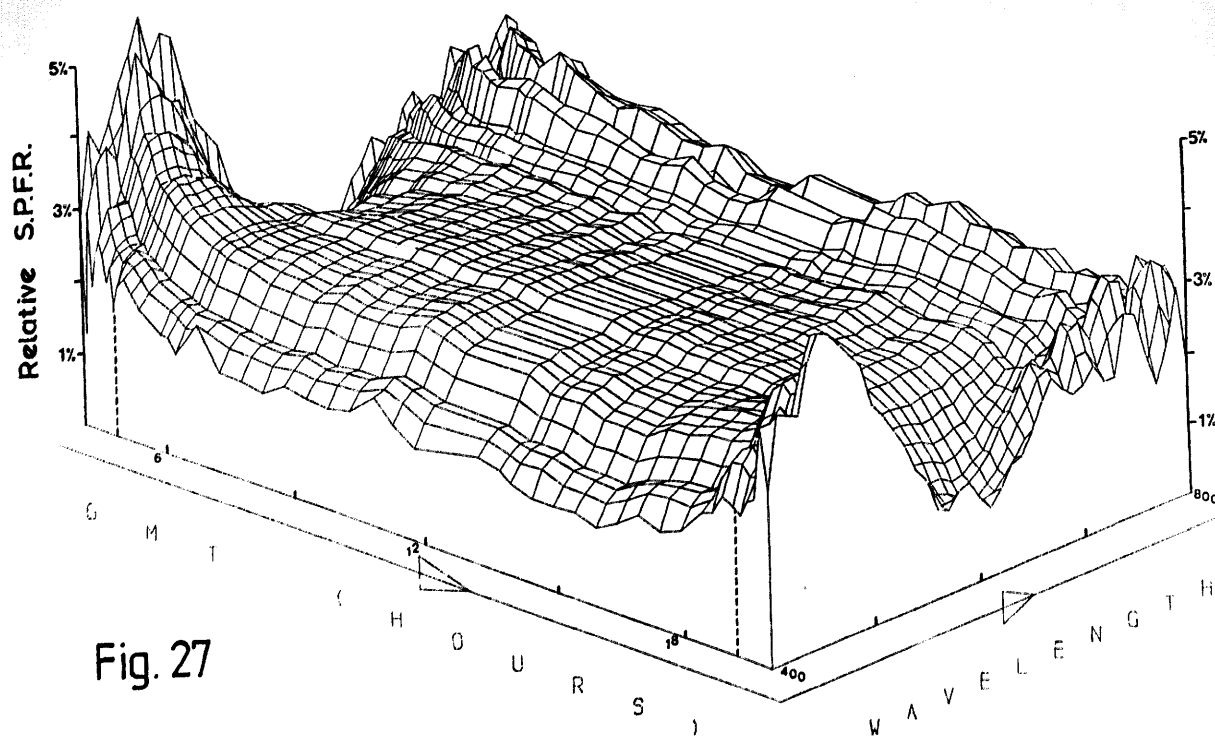


Fig. 27

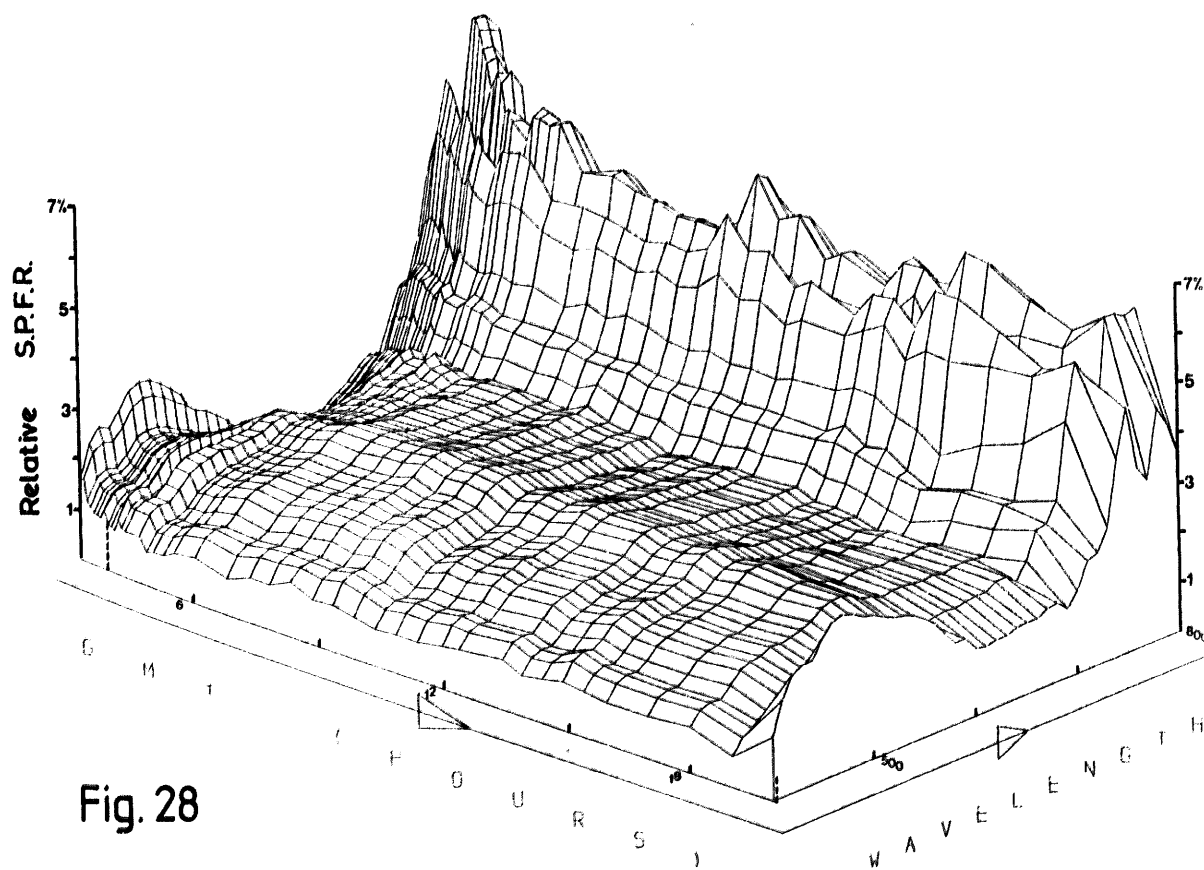


Fig. 28

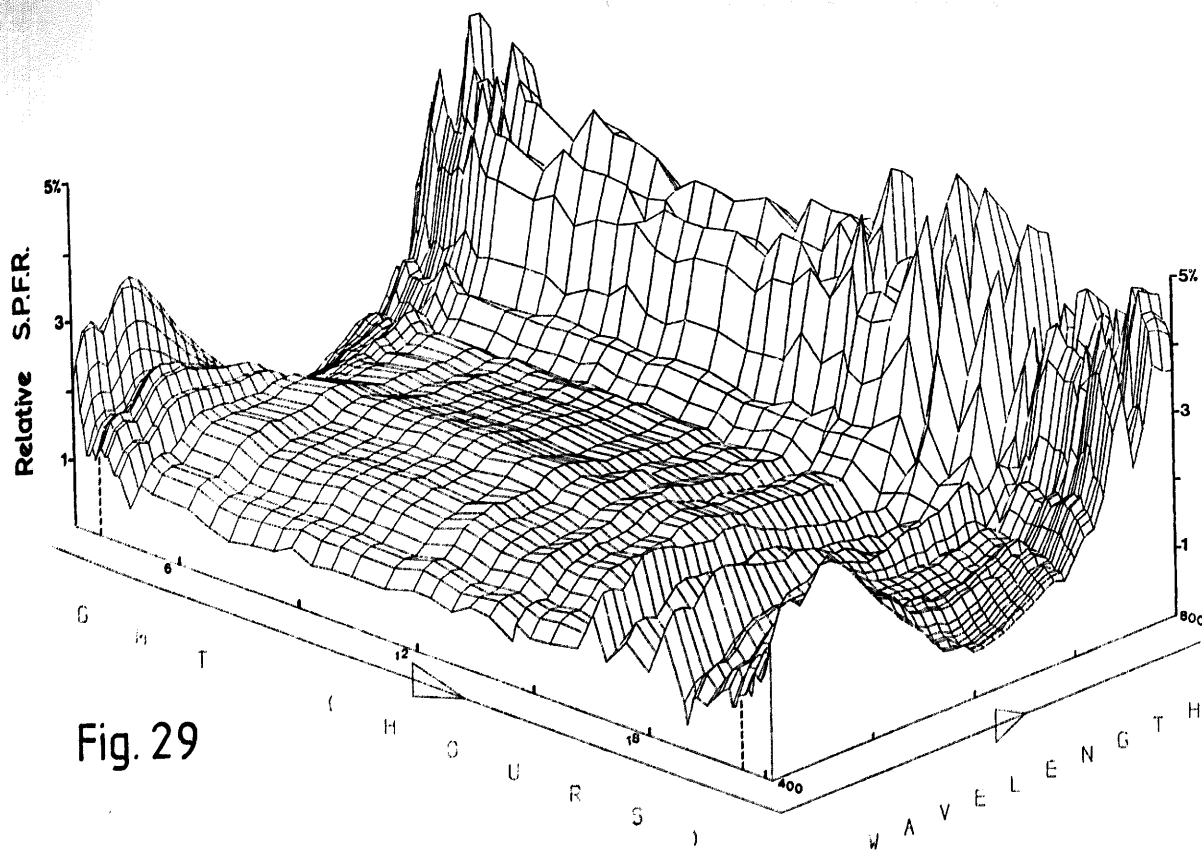


Fig. 29

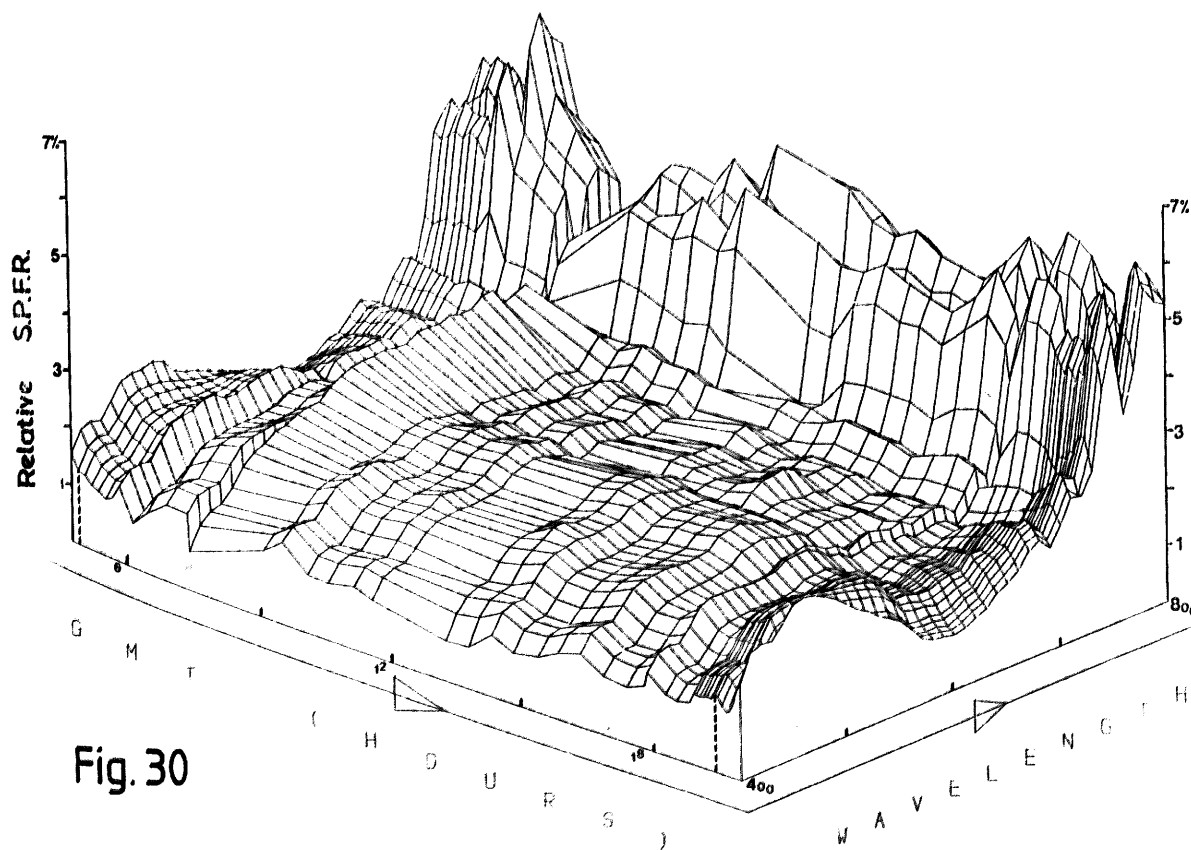


Fig. 30

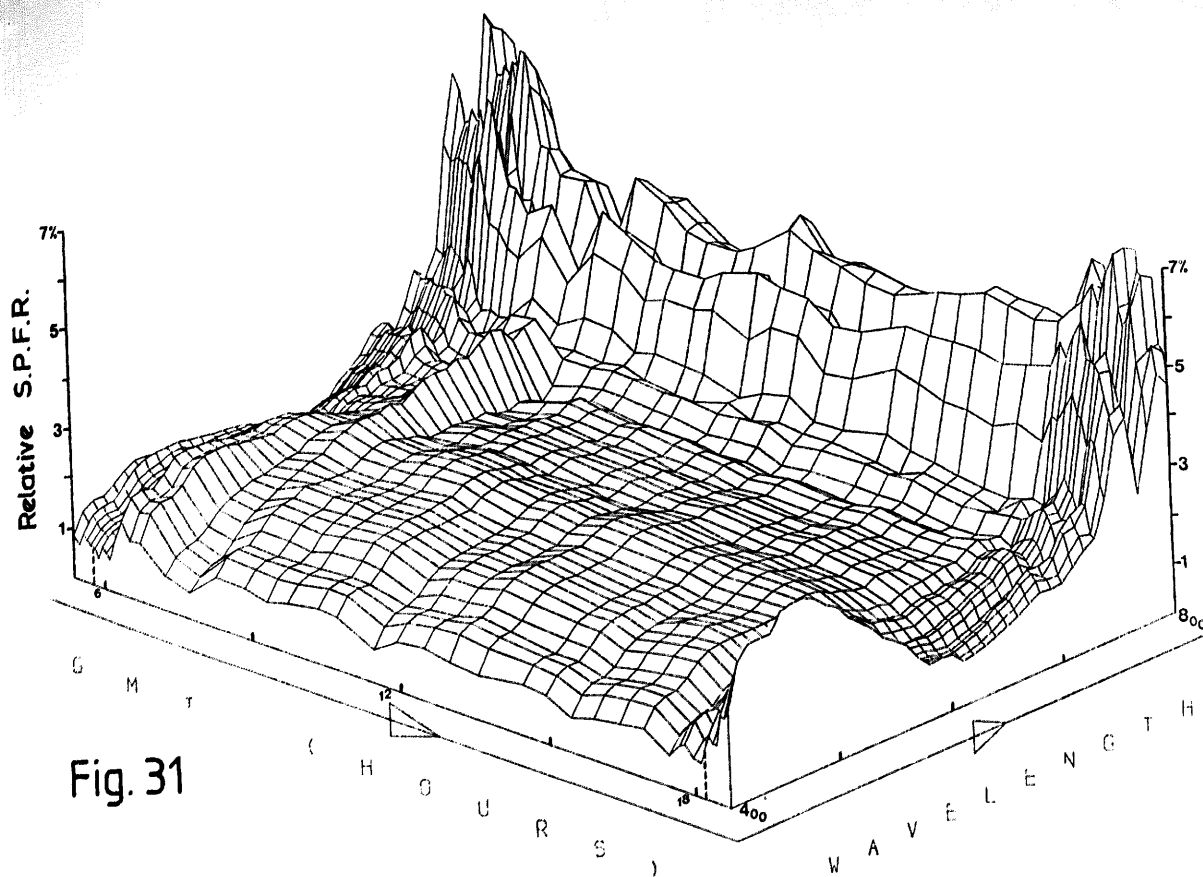


Fig. 31

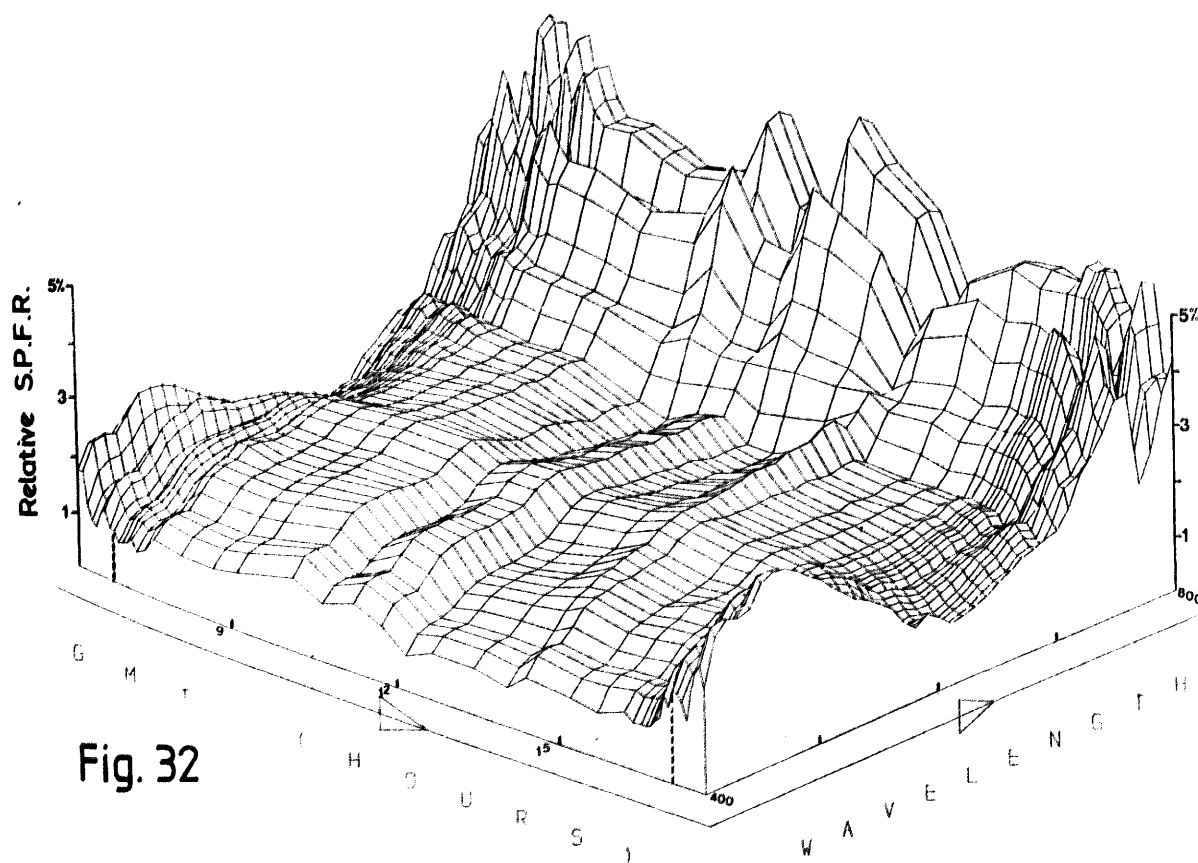


Fig. 32

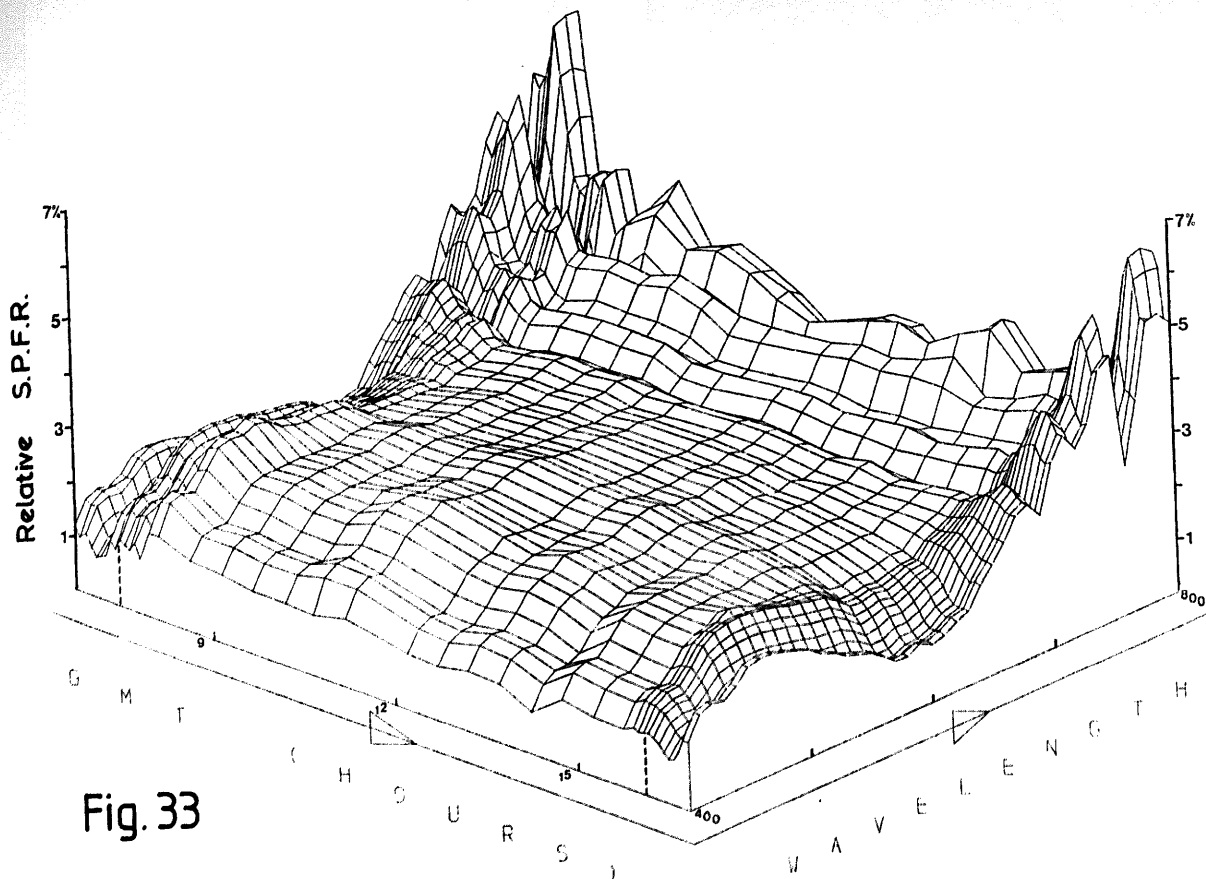


Fig. 33

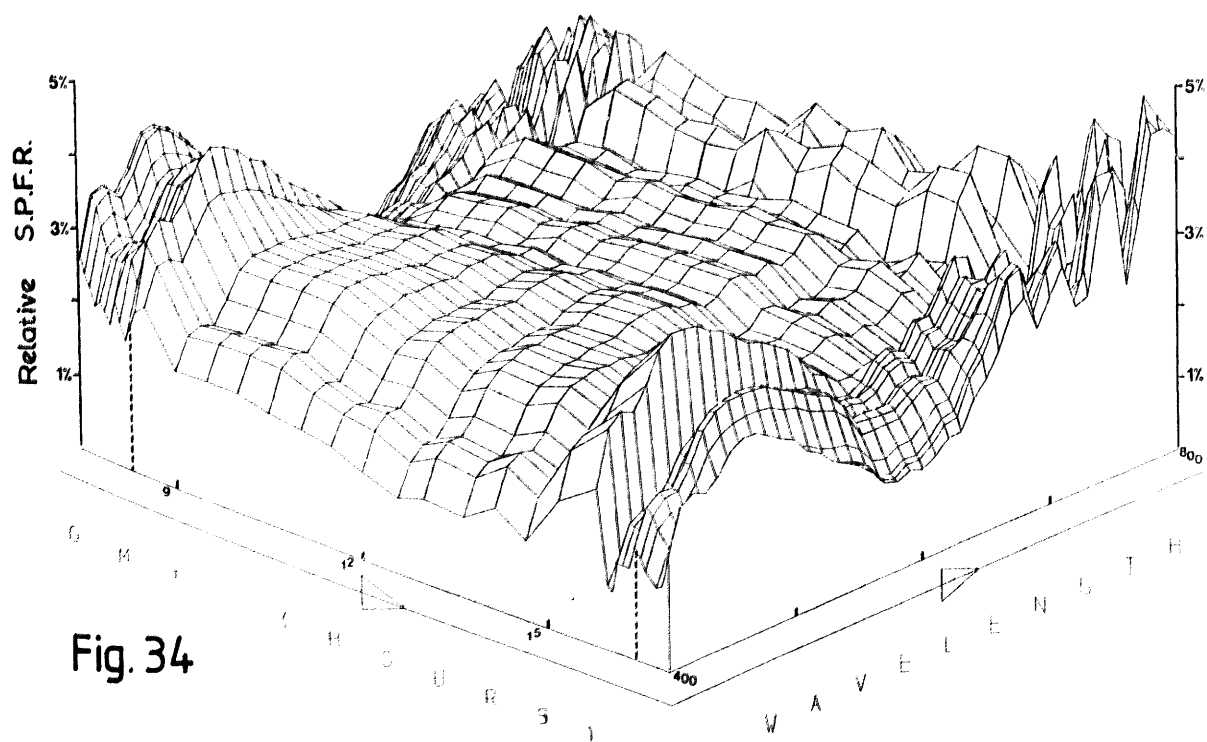


Fig. 34

Figures 35 - 38

Parameters of oak woodland shadelight vs. α_s
during canopy cycle, 1980 - 81.

Figure 35: β

Figure 36: ϕ_c

Figure 37: B:R ratio

Figure 38: $\log R$

Fig. 35

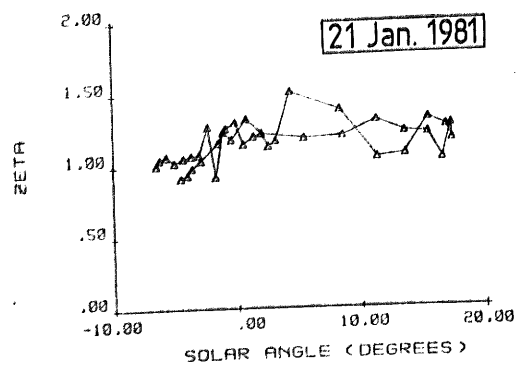
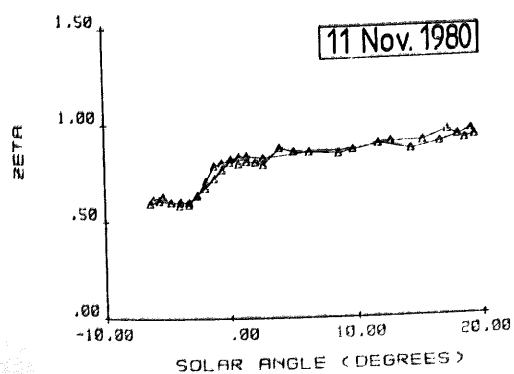
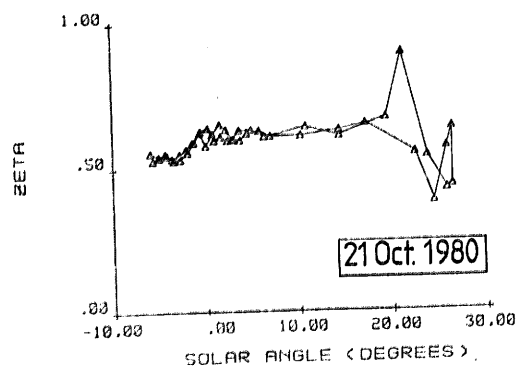
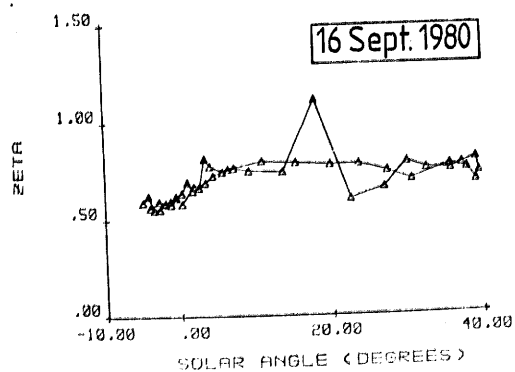
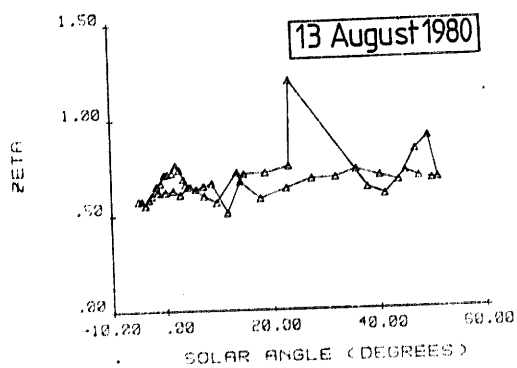
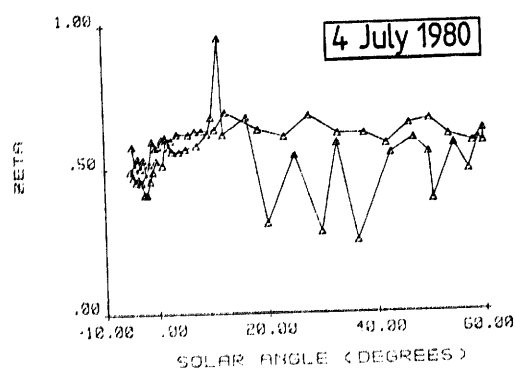
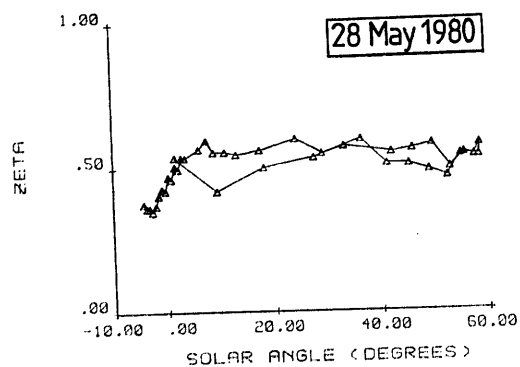
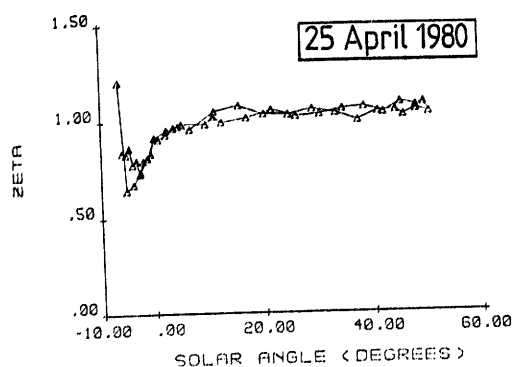


Fig. 36

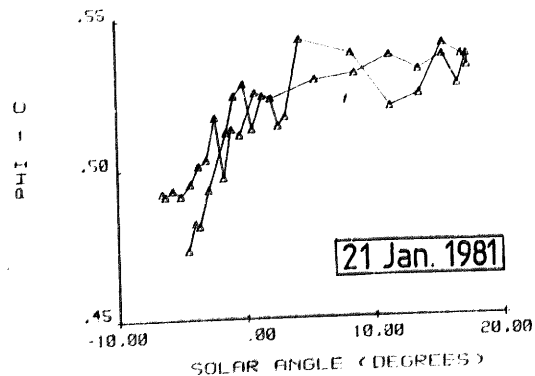
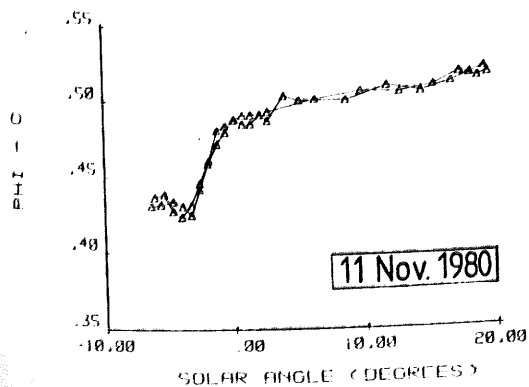
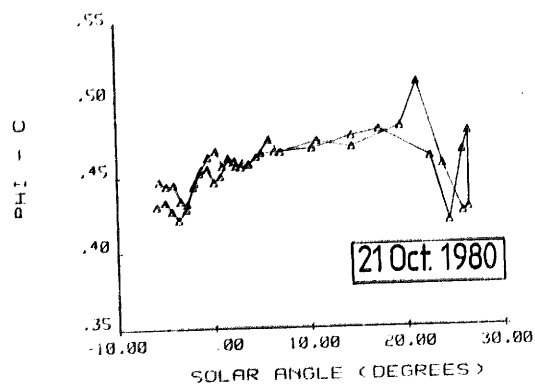
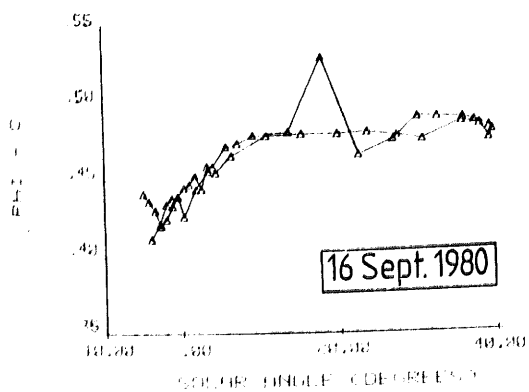
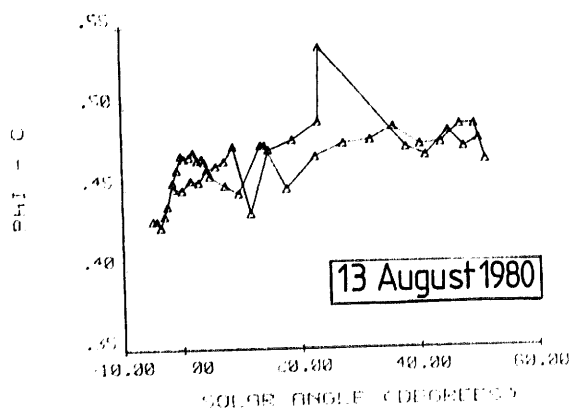
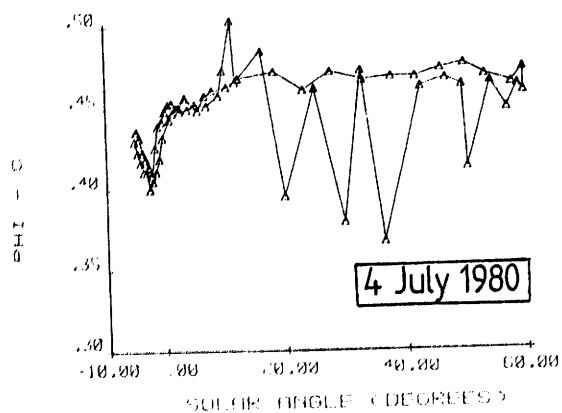
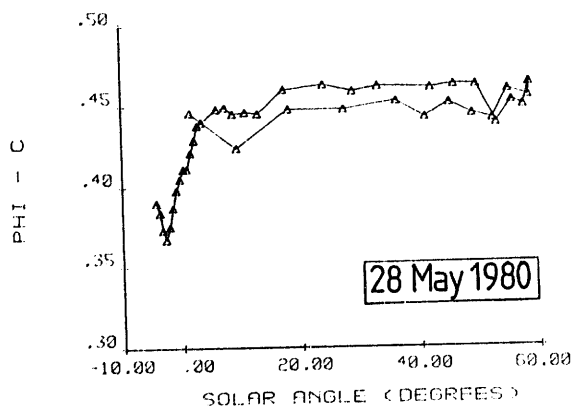
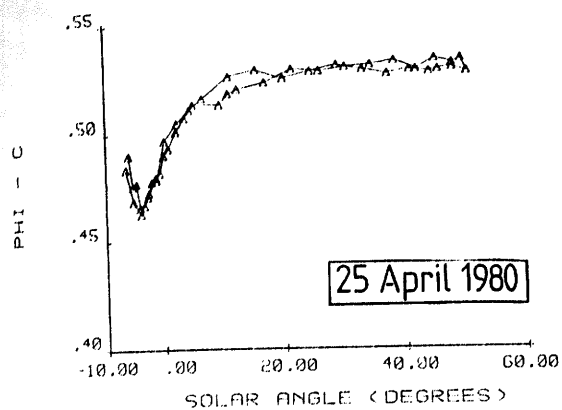


Fig. 37

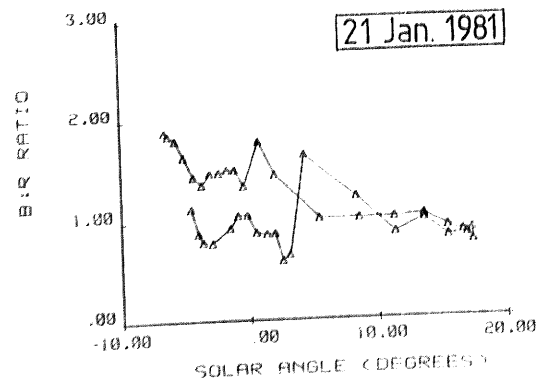
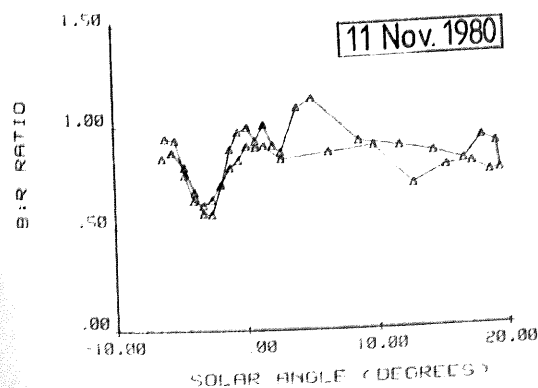
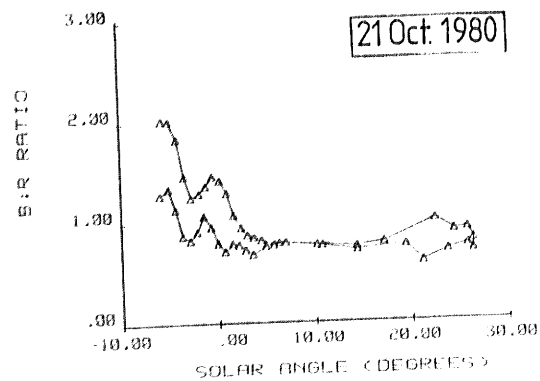
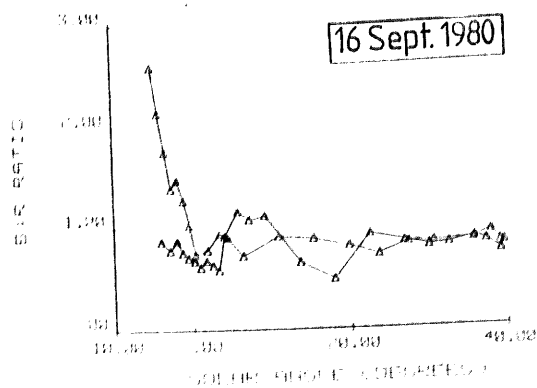
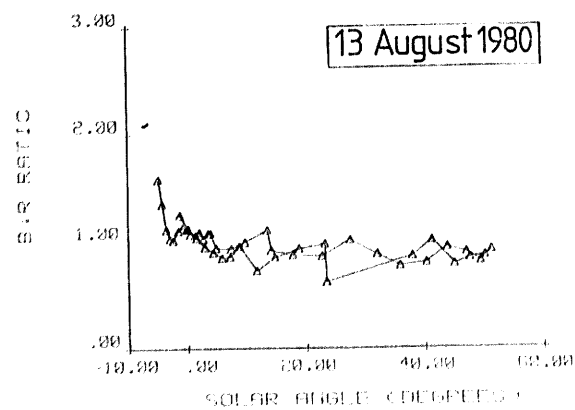
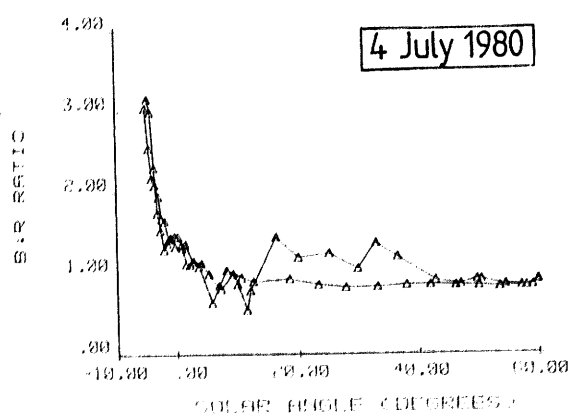
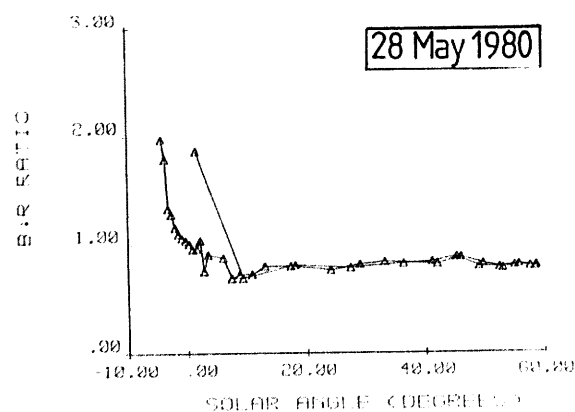
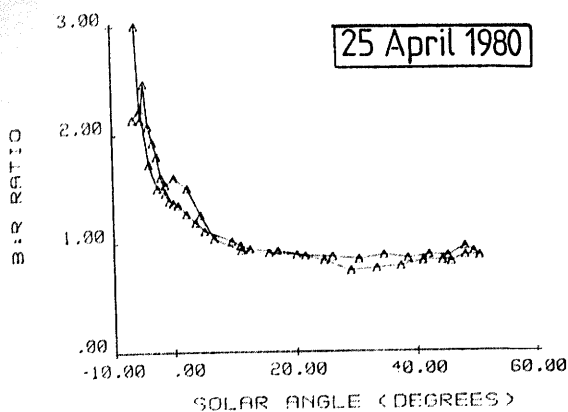
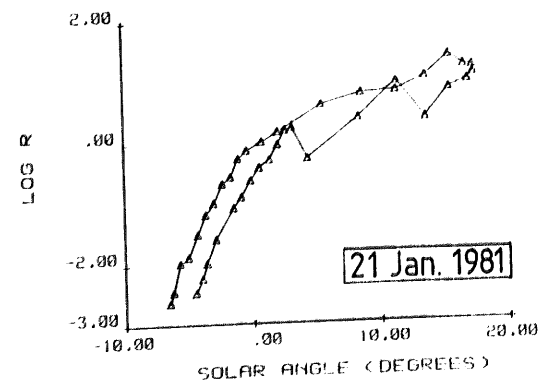
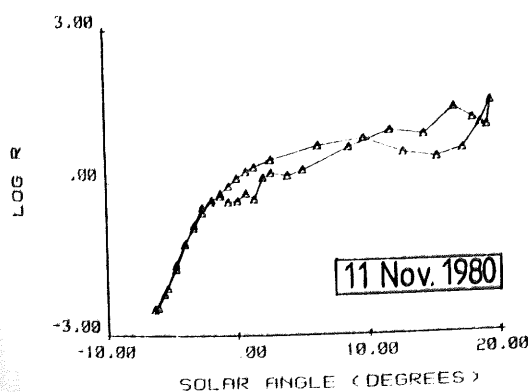
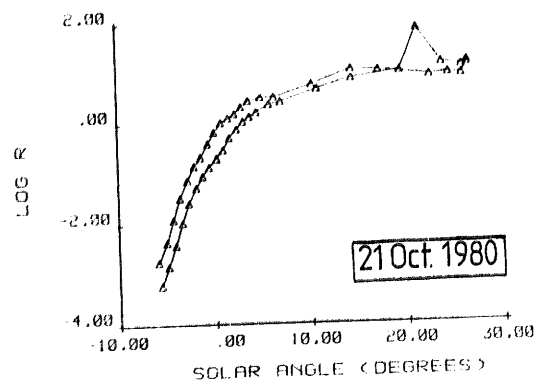
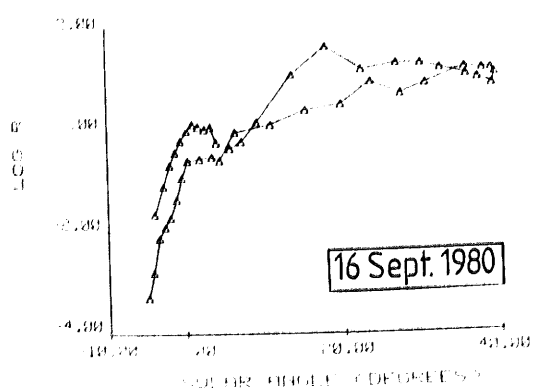
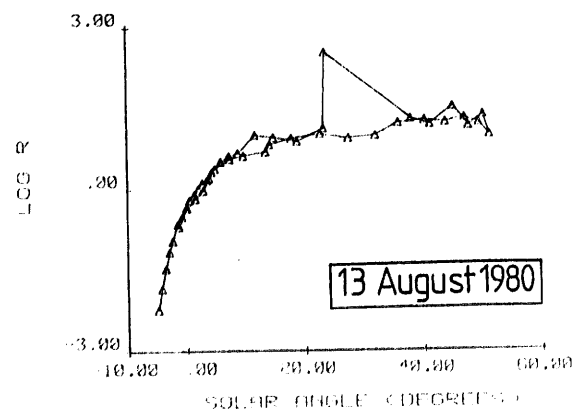
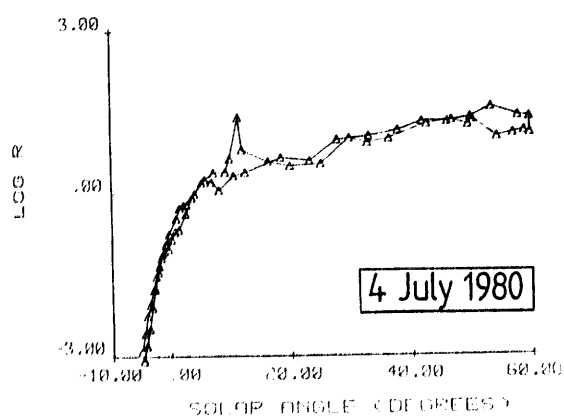
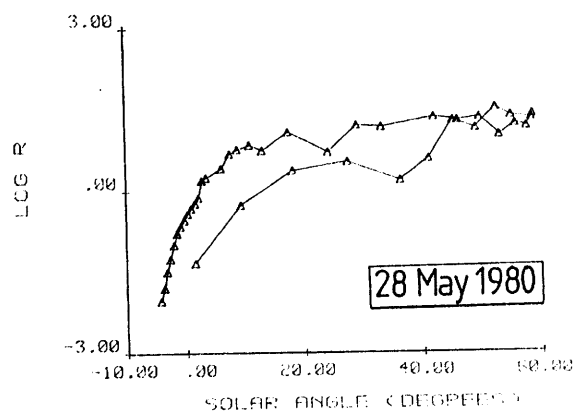
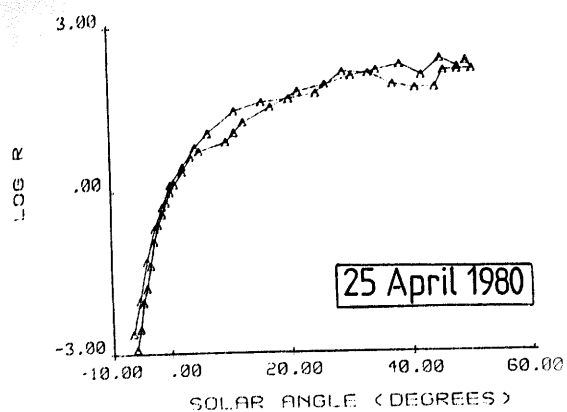


Fig. 38



Figures 39 and 40

\bar{z} and ϕ_c (means for $15^\circ < \alpha_s < 30^\circ$) vs. time
during canopy cycle in oak woodland, 1980-81

(+ 2 SE)

Fig. 39

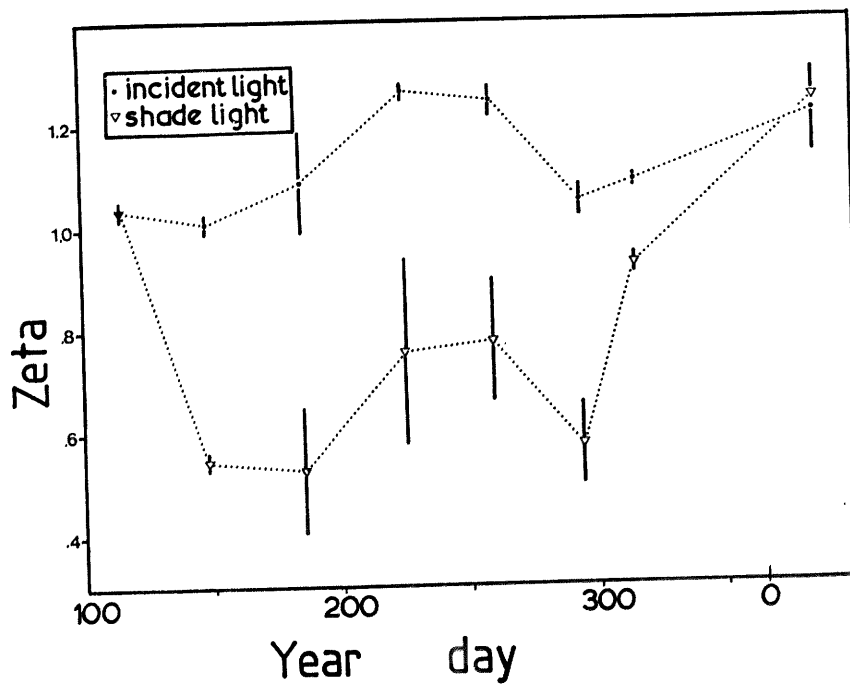
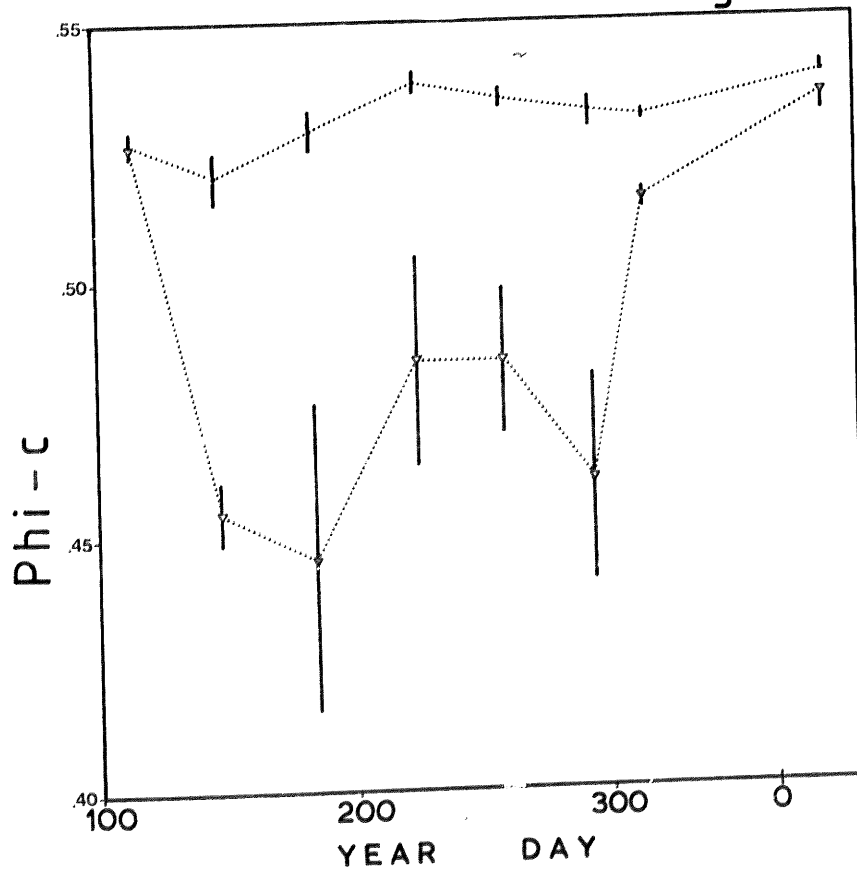


Fig. 40



Figures 41 and 42

B:R ratio and log R (means for $15^{\circ} < \alpha_s < 30^{\circ}$)
vs. time during canopy cycle in oak woodland
1980-81.

(+ 2 SE)

Fig. 41

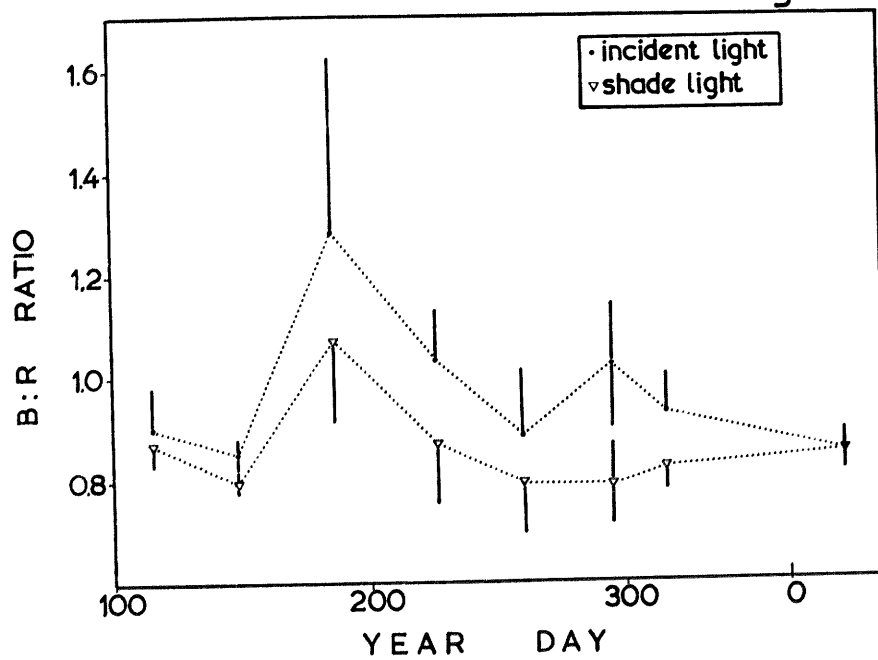
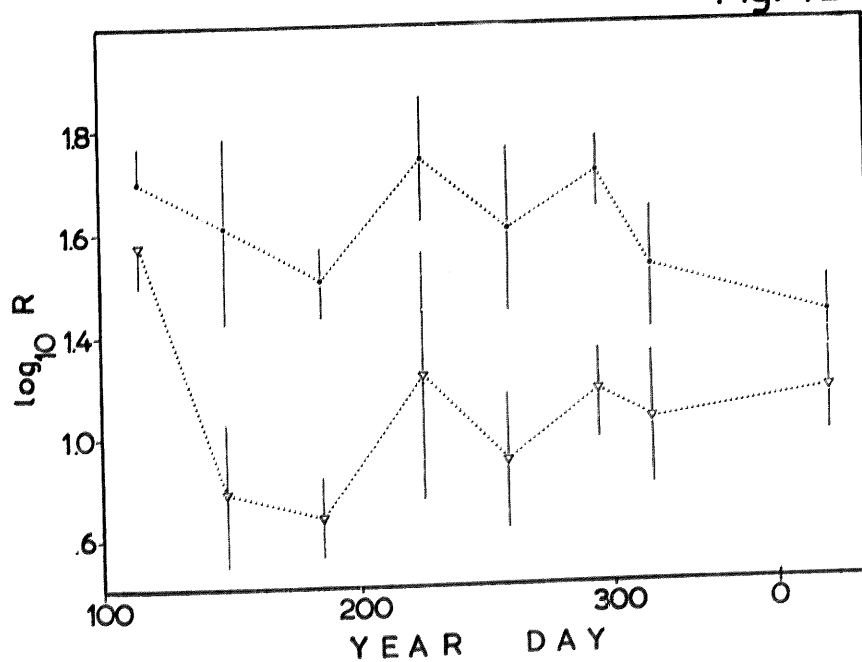


Fig. 42



Figures 43 - 56.

(\longleftrightarrow) Mean spectral transmittance of oak canopy

(—) standard error of mean

Mean spectral transmittance and reflectance of
oak leaves

(.....) shade leaves

(——) sun leaves

Figure 43: 25 April 1980, before bud break

Figure 44: 21 January 1981, after leaf fall

Figures 45 & 46: 28 May 1980

Figures 47 & 48: 4 July 1980

Figures 49 & 50: 13 August 1980

Figures 51 & 52: 16 September 1980

Figures 53 & 54: 21 October 1980

Figures 55 & 56: 11 November 1980

Fig. 43

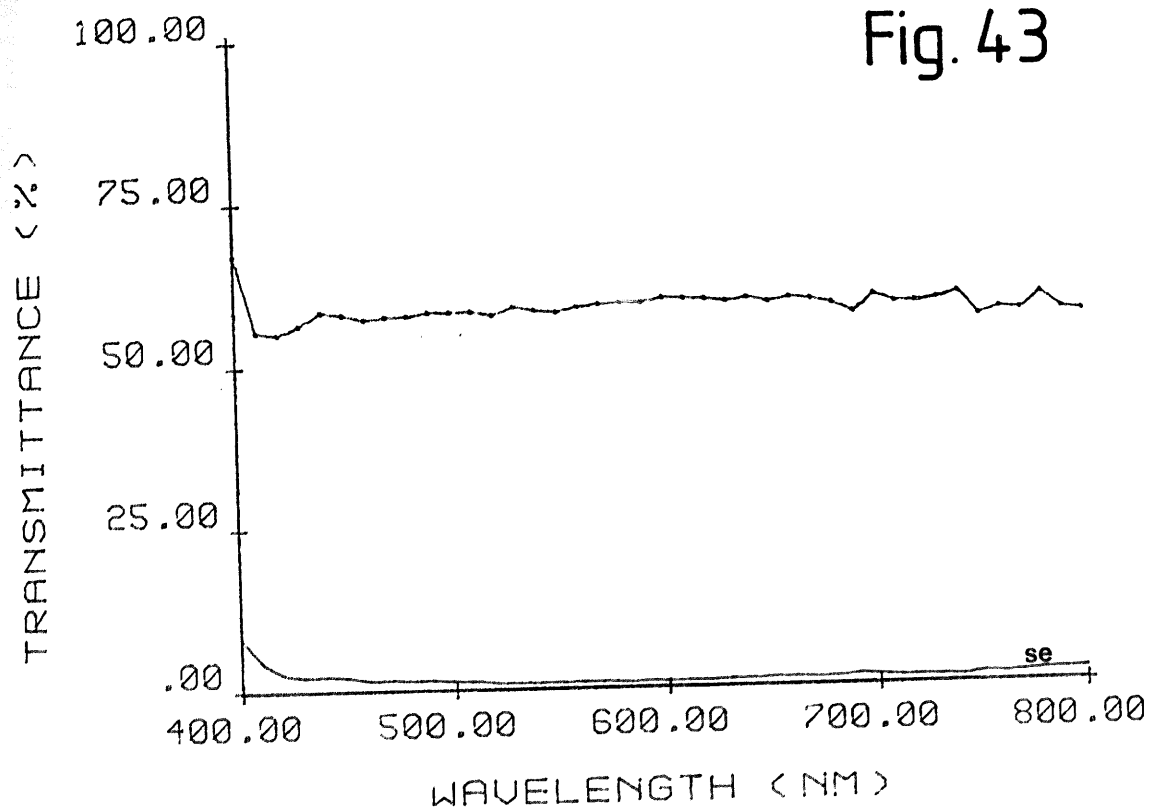


Fig. 44

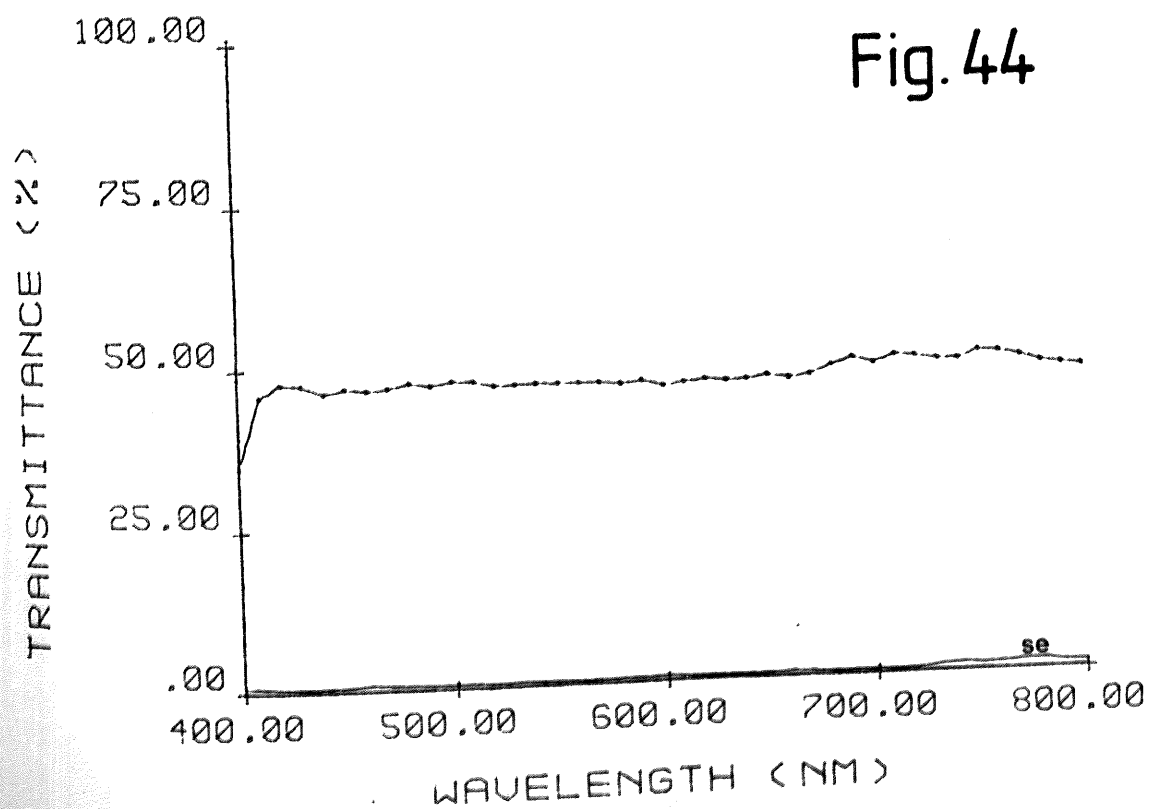


Fig. 43

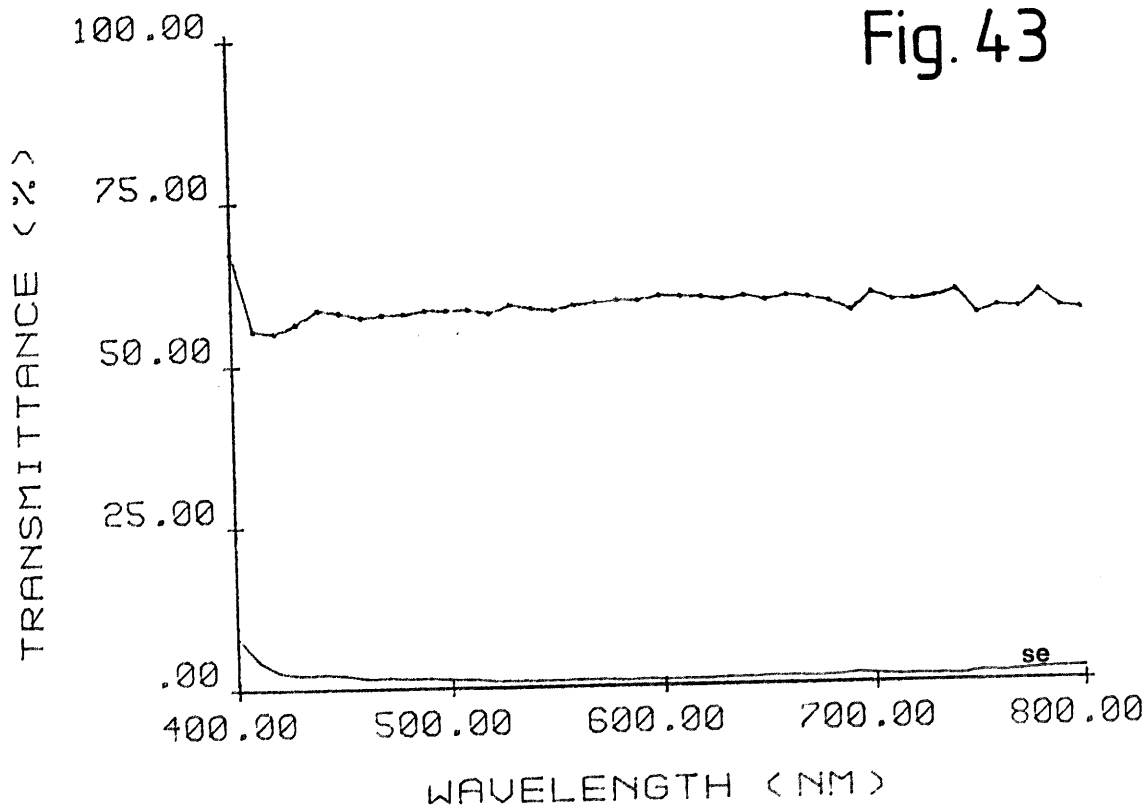
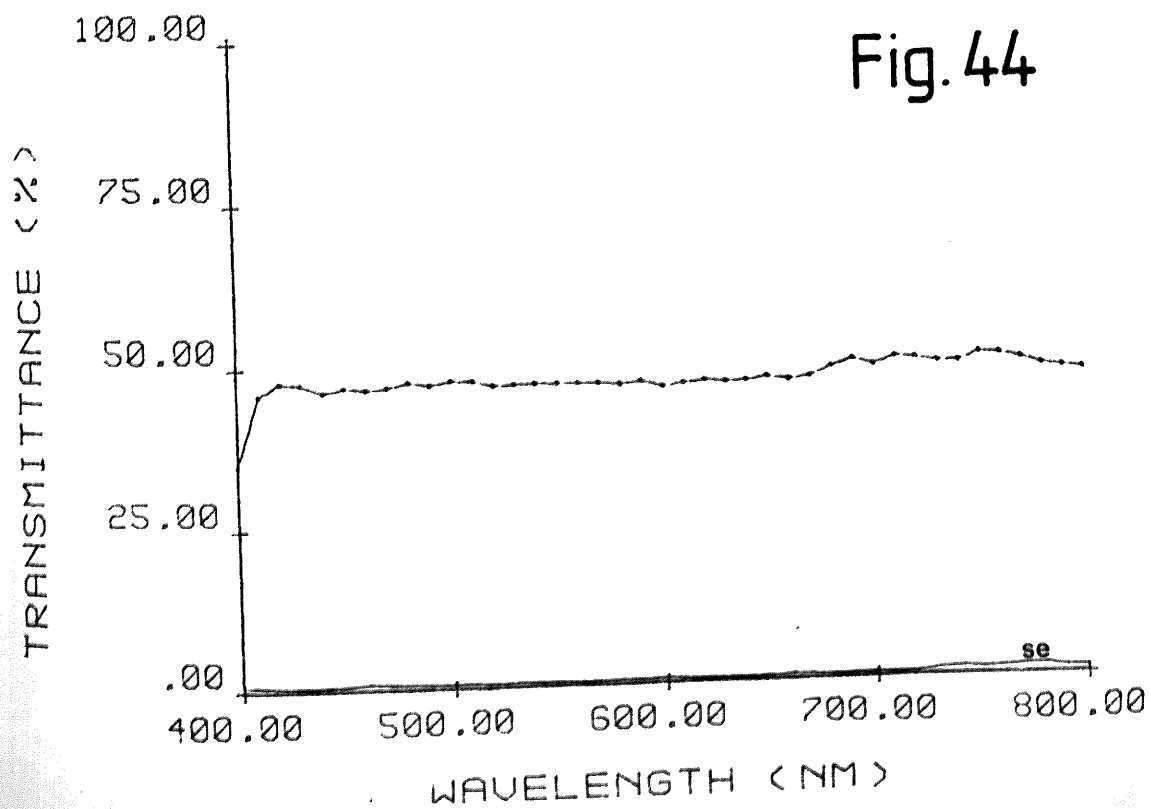
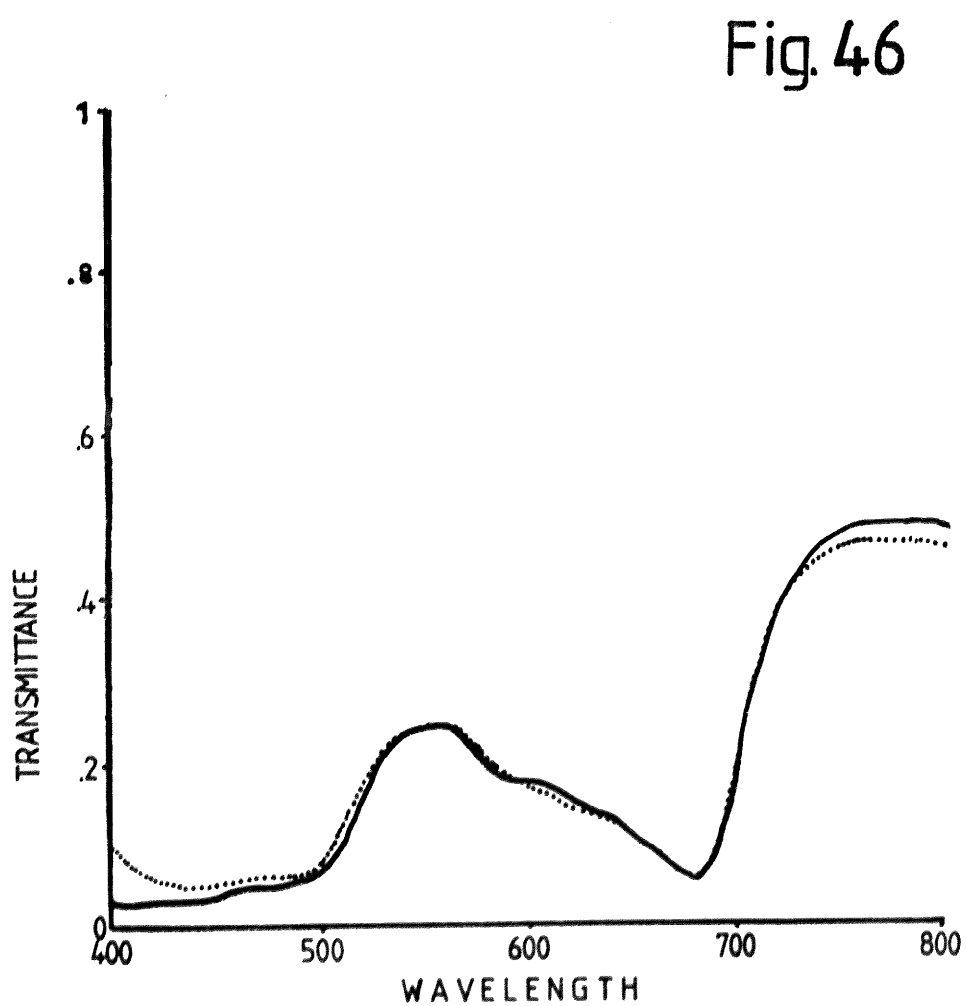
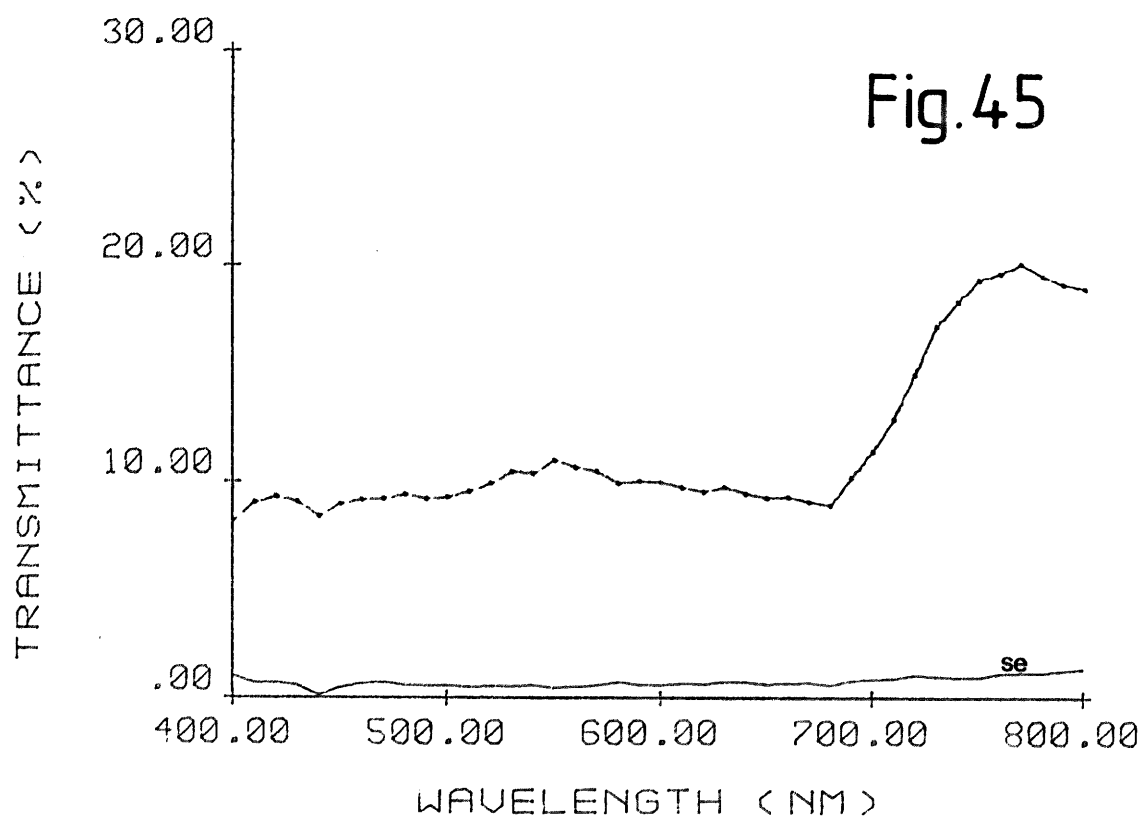
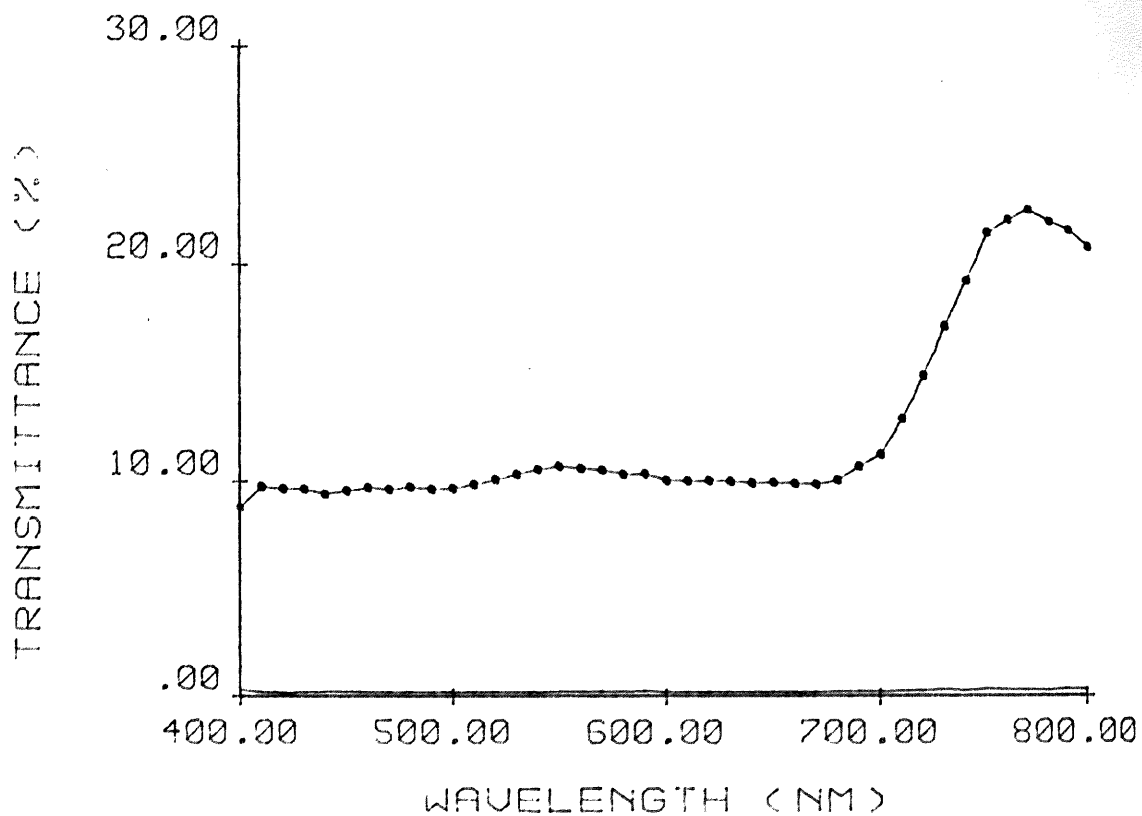


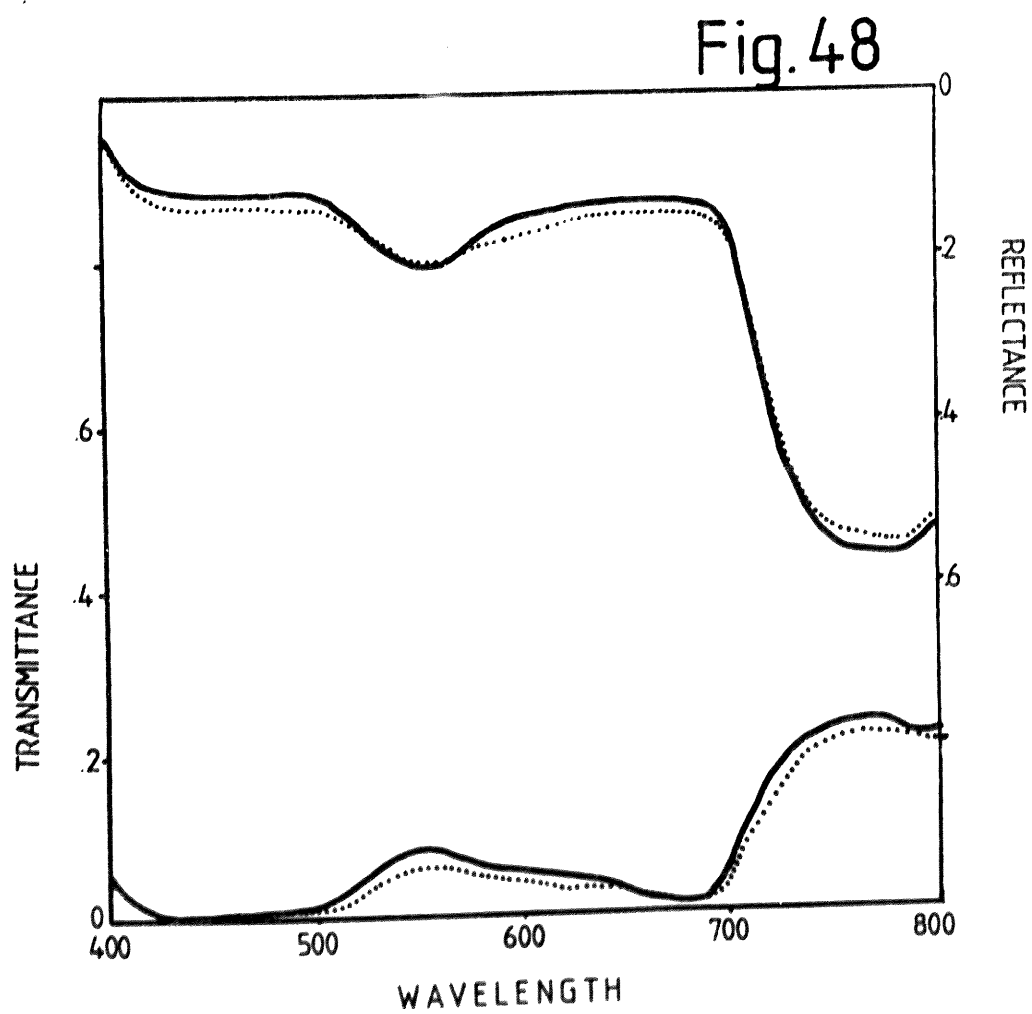
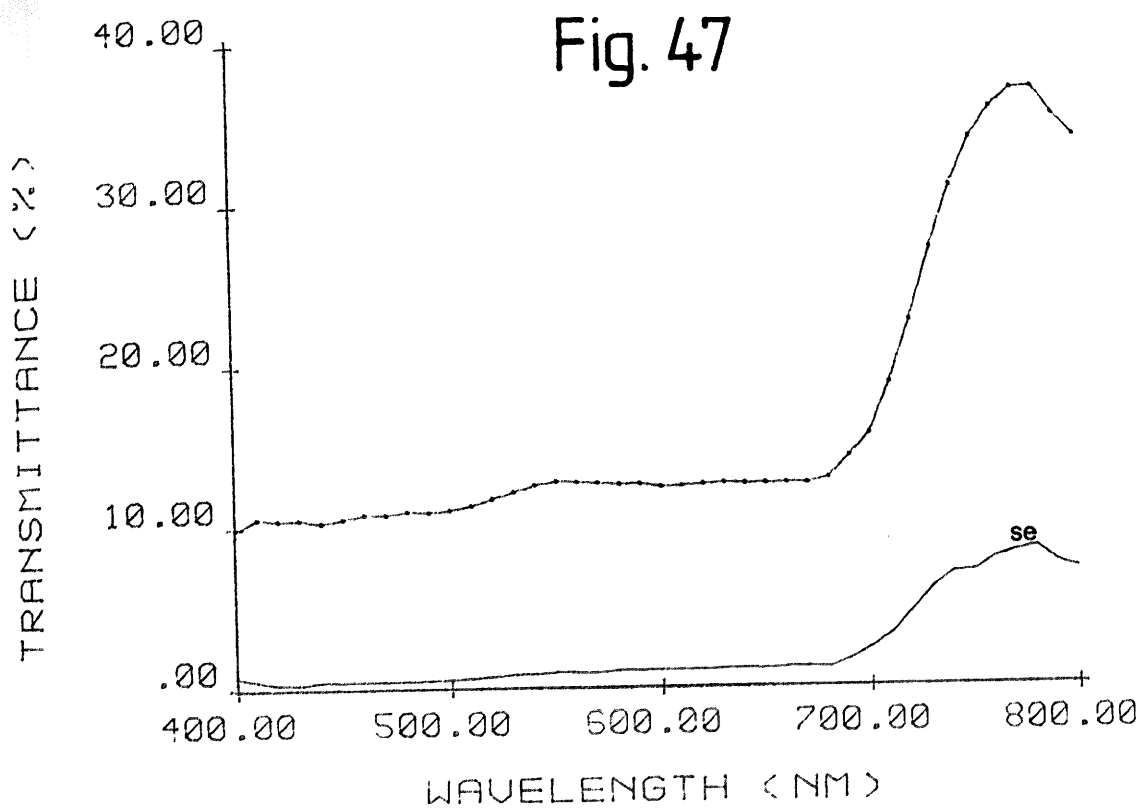
Fig. 44



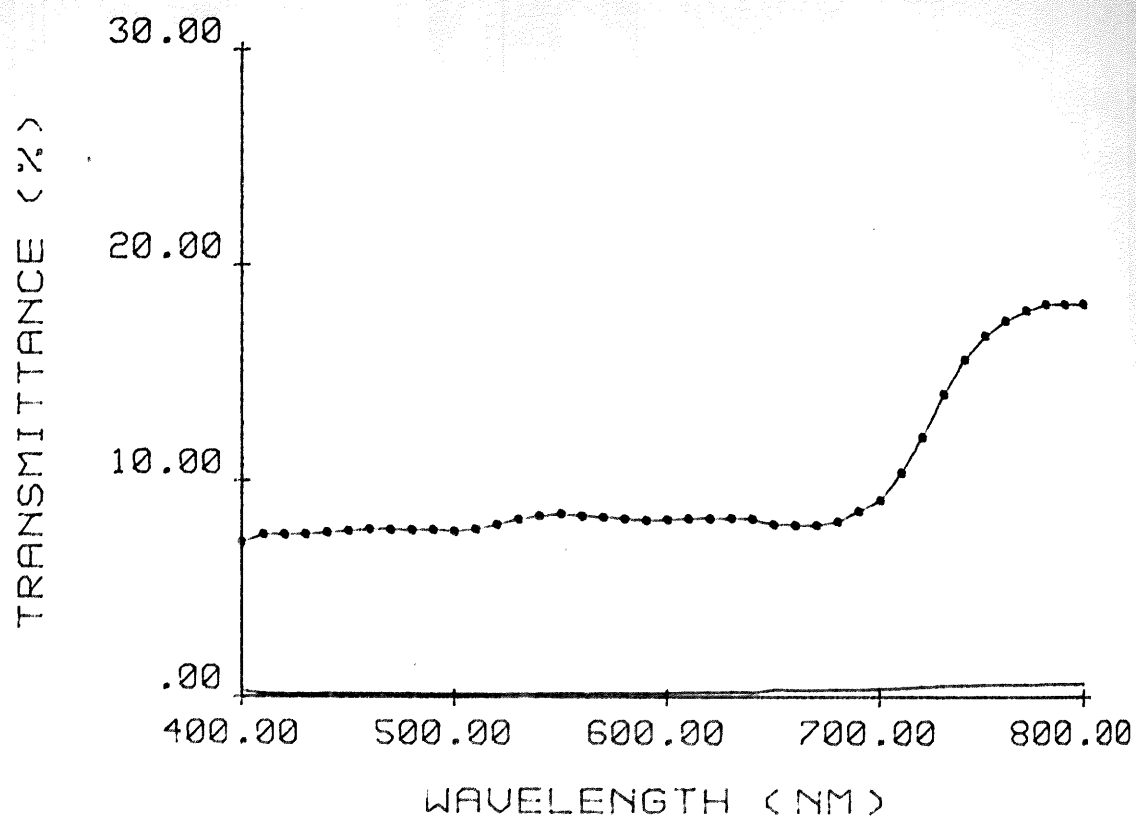


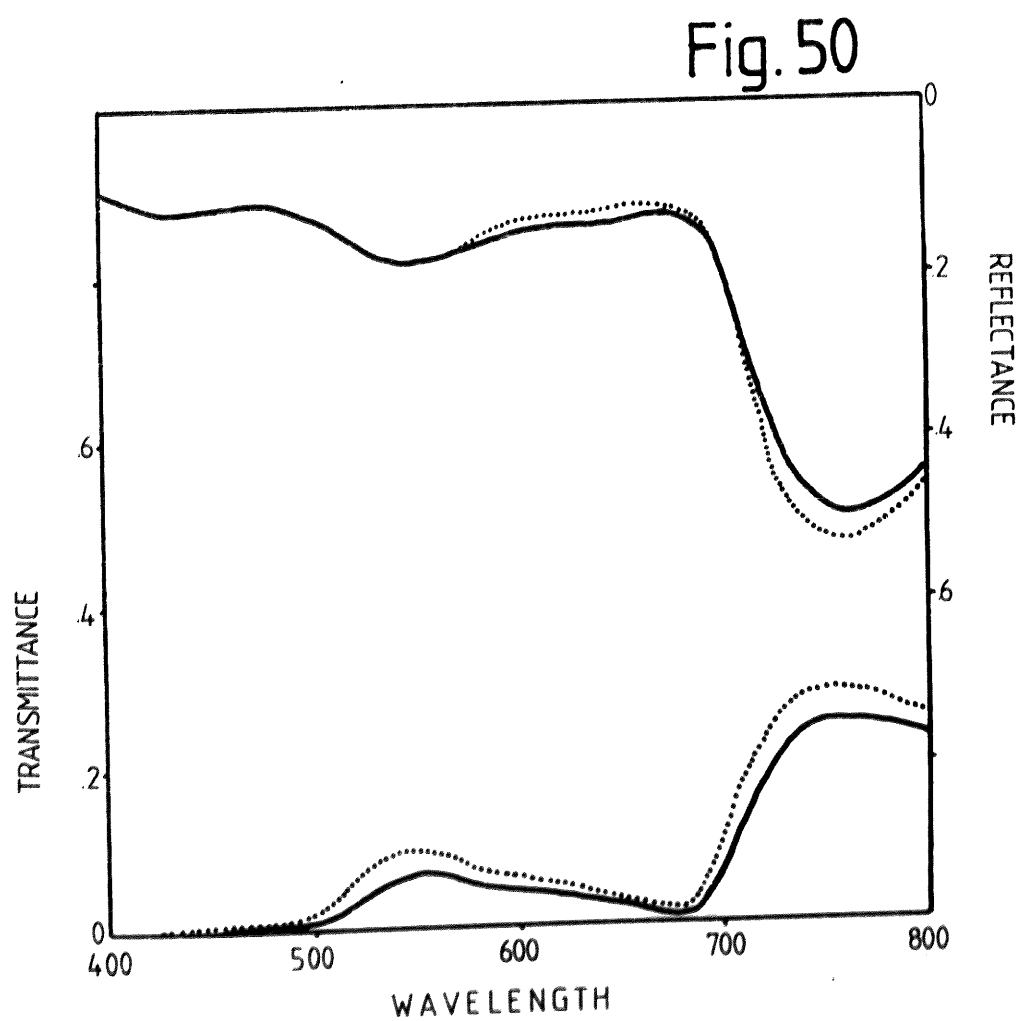
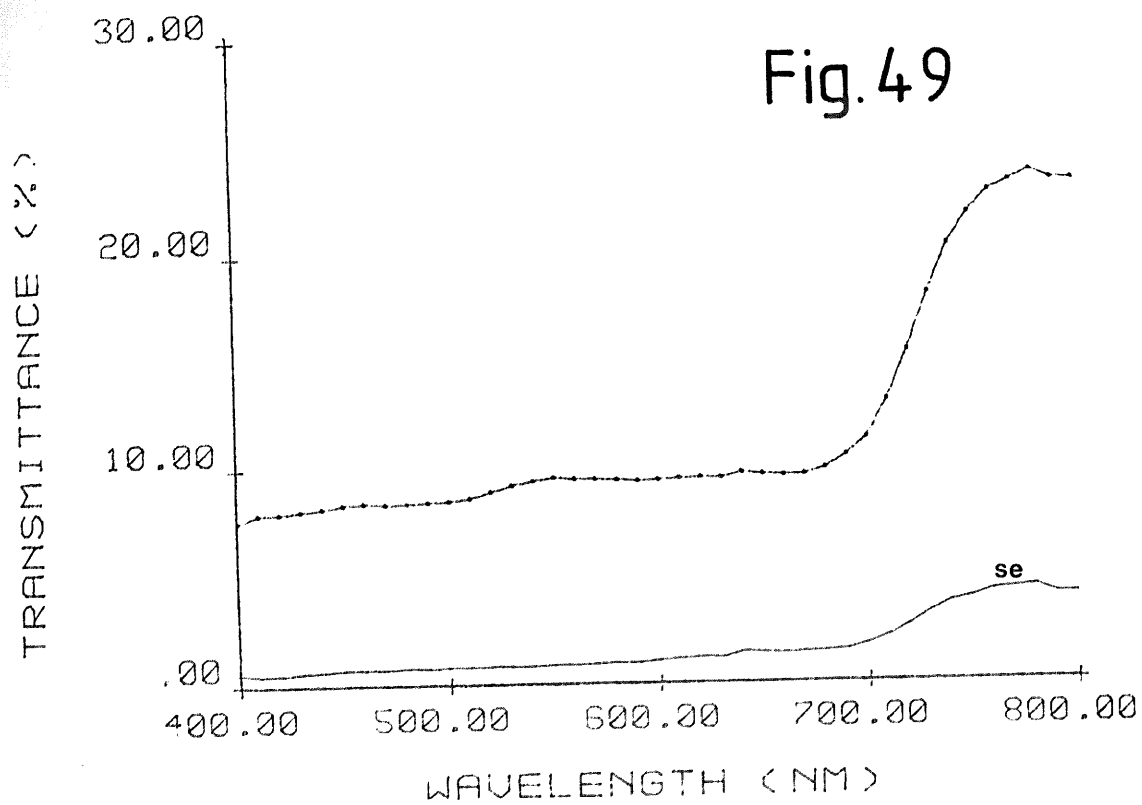
When "hazy cloud cover" data was ignored, the transmittance was as below.



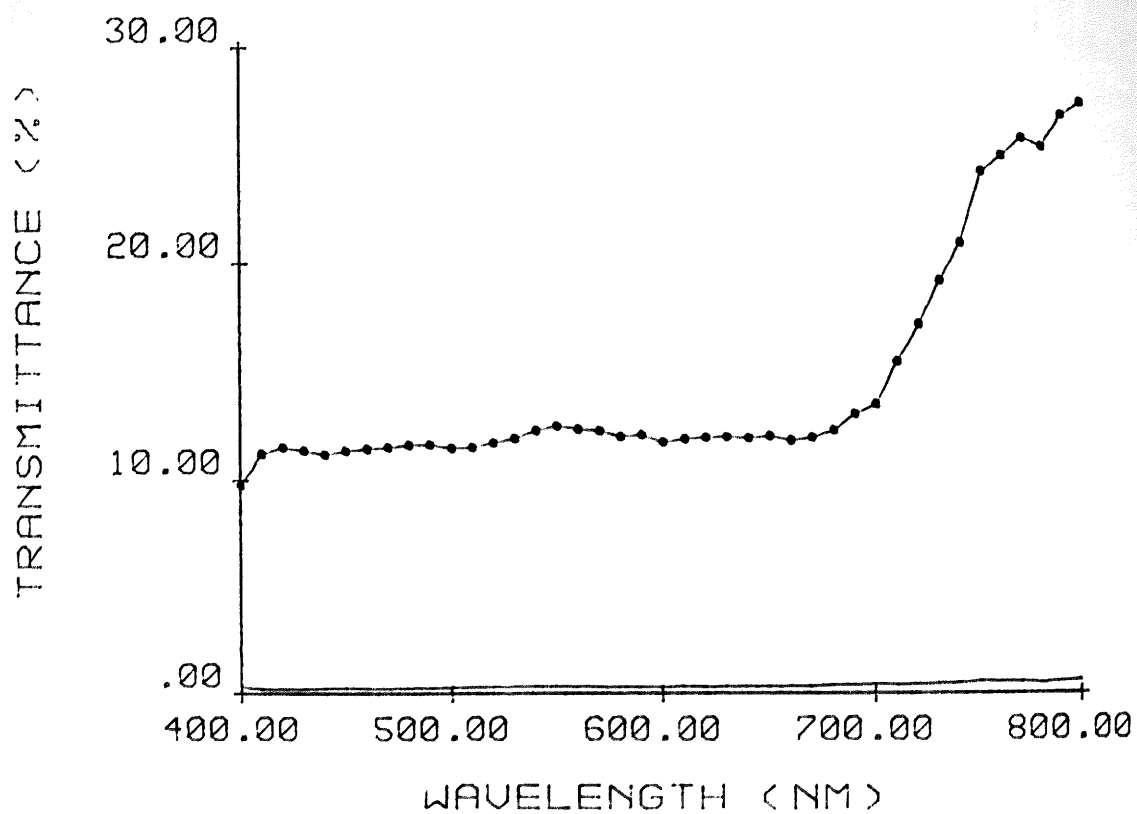


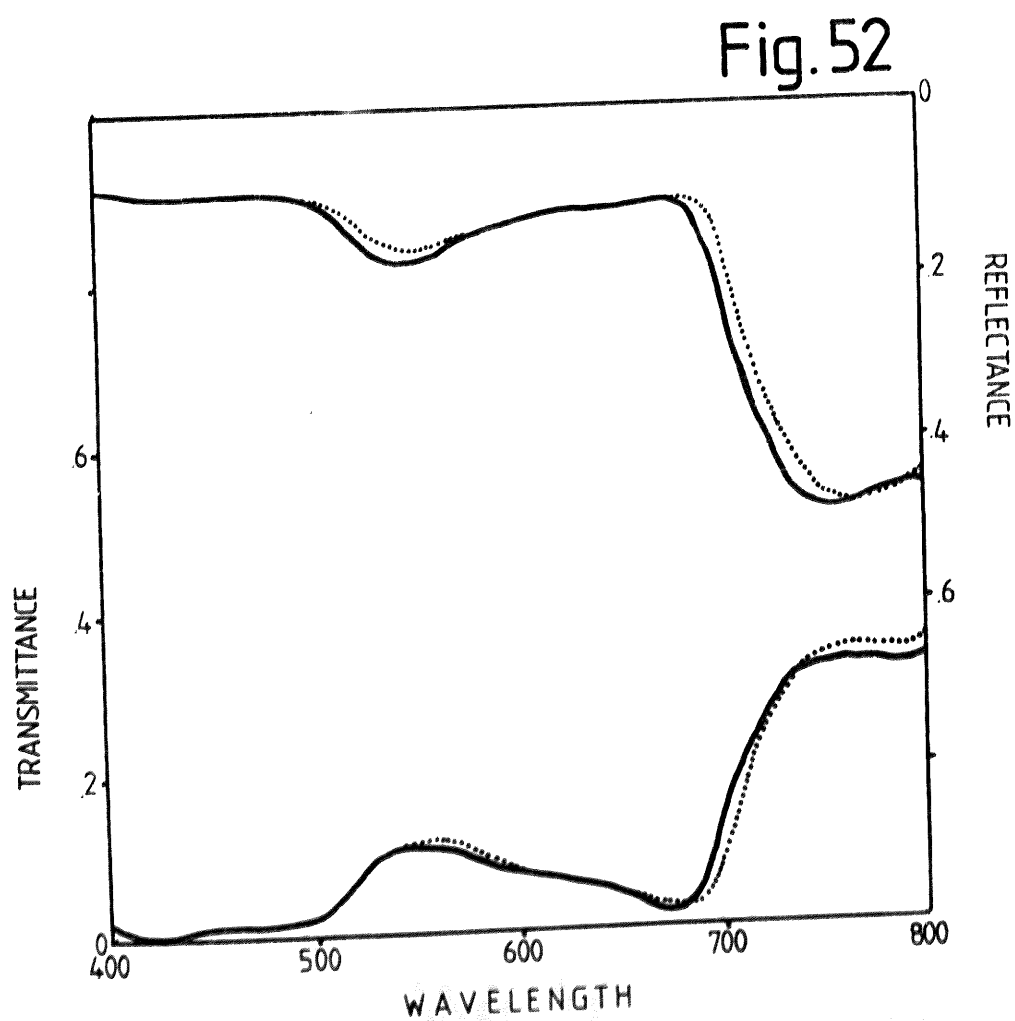
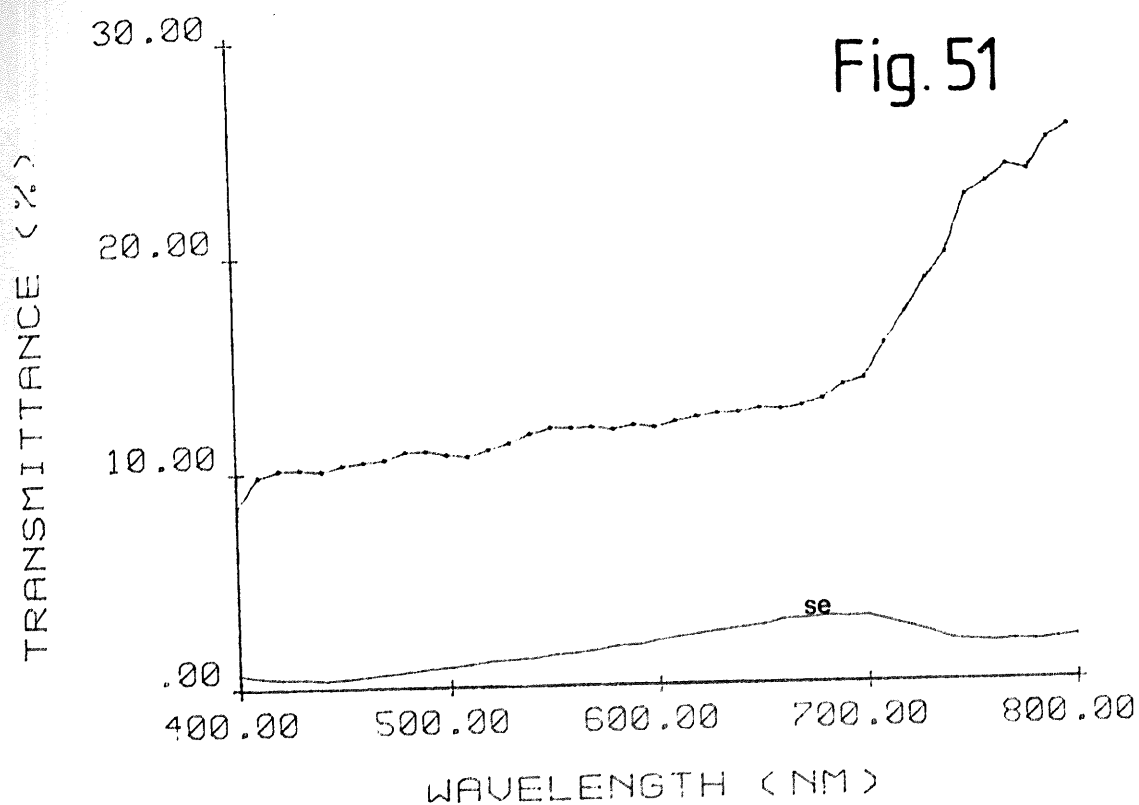
When "hazy cloud cover" data was ignored, the transmittance was as below.

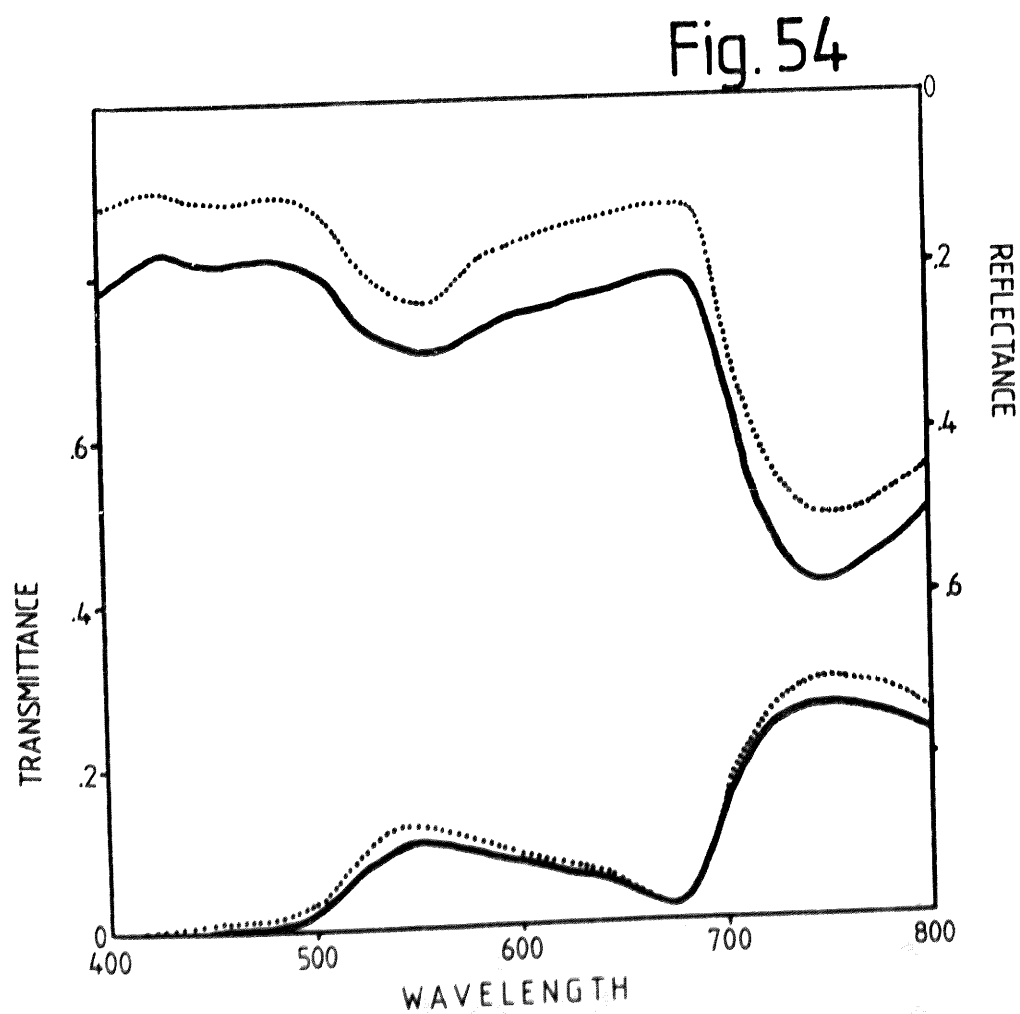
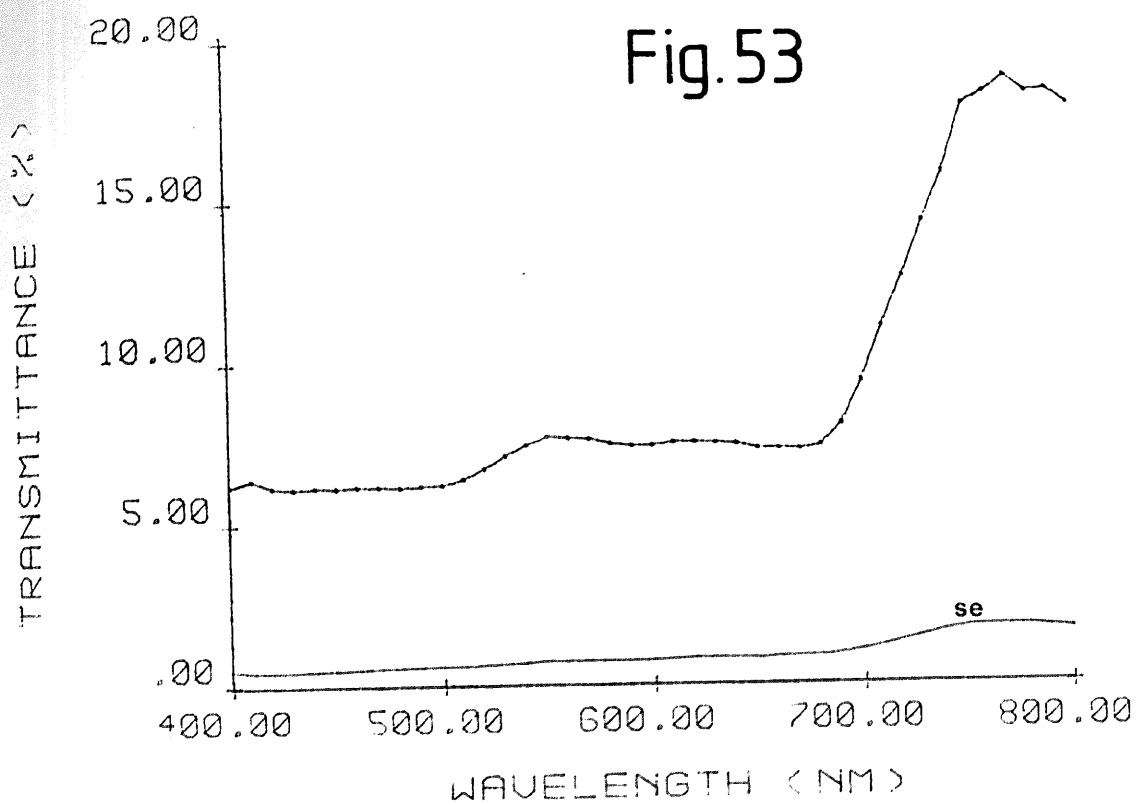


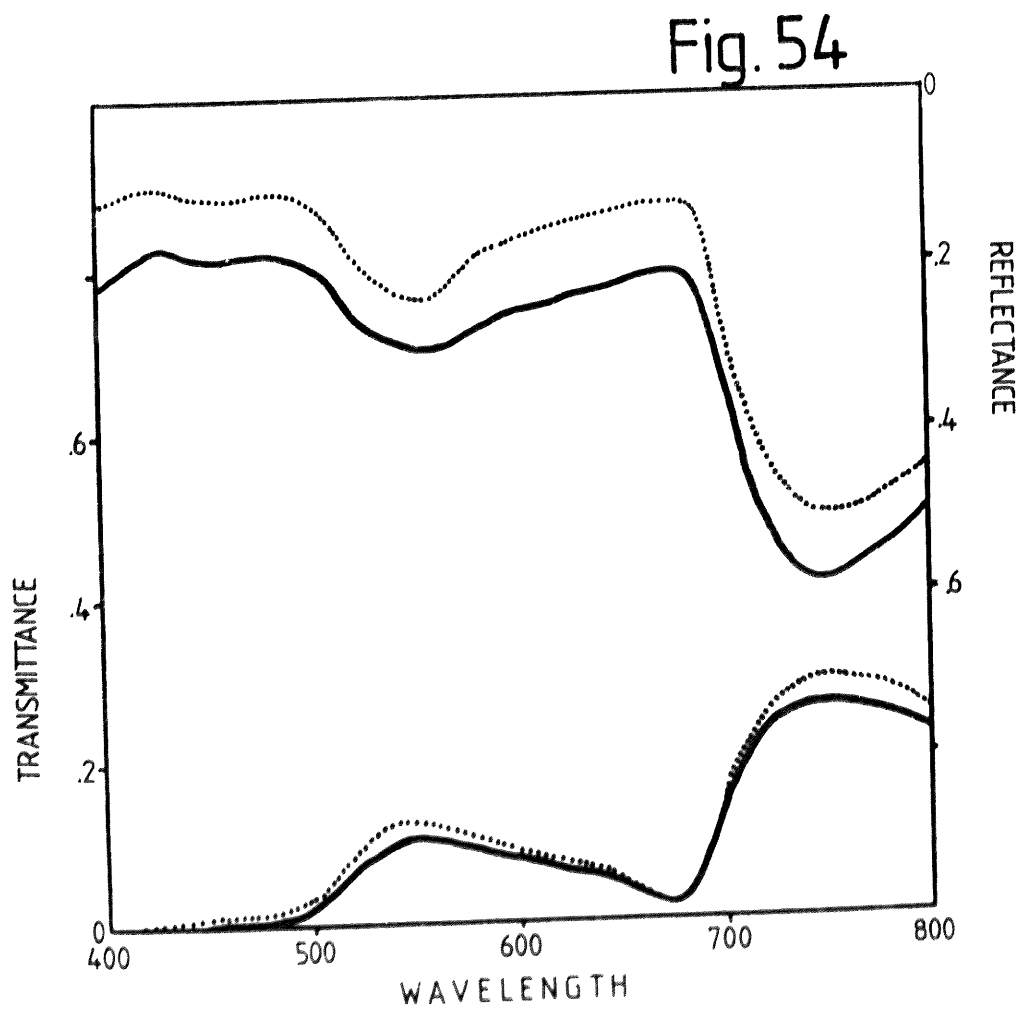
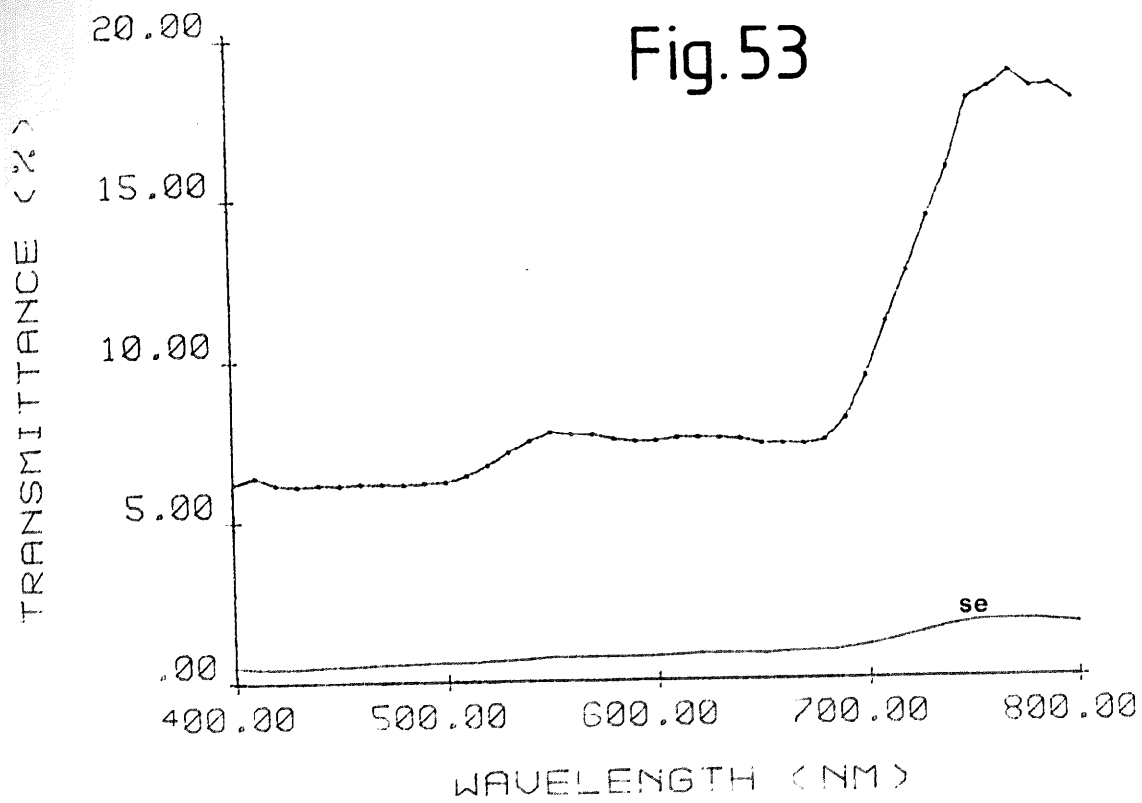


When "hazy cloud cover" data was ignored, the transmittance was as below.









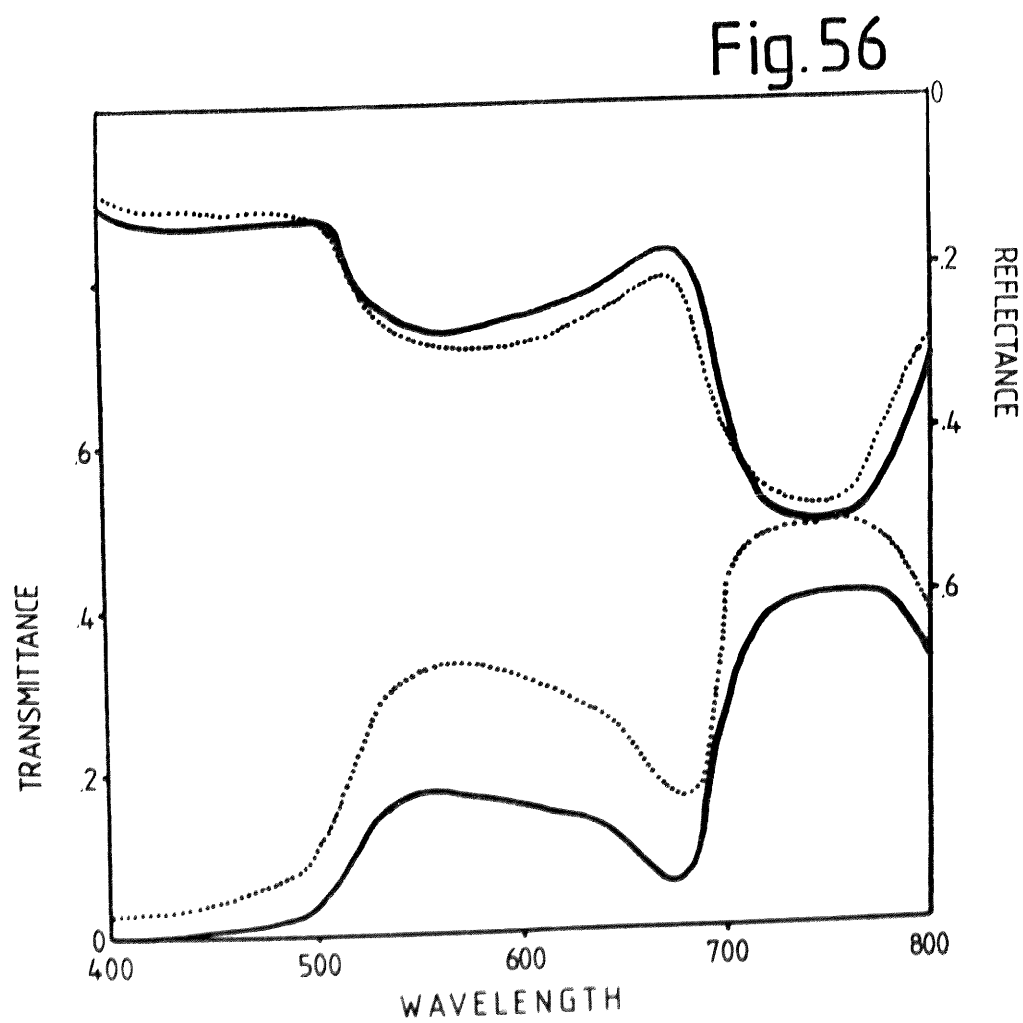
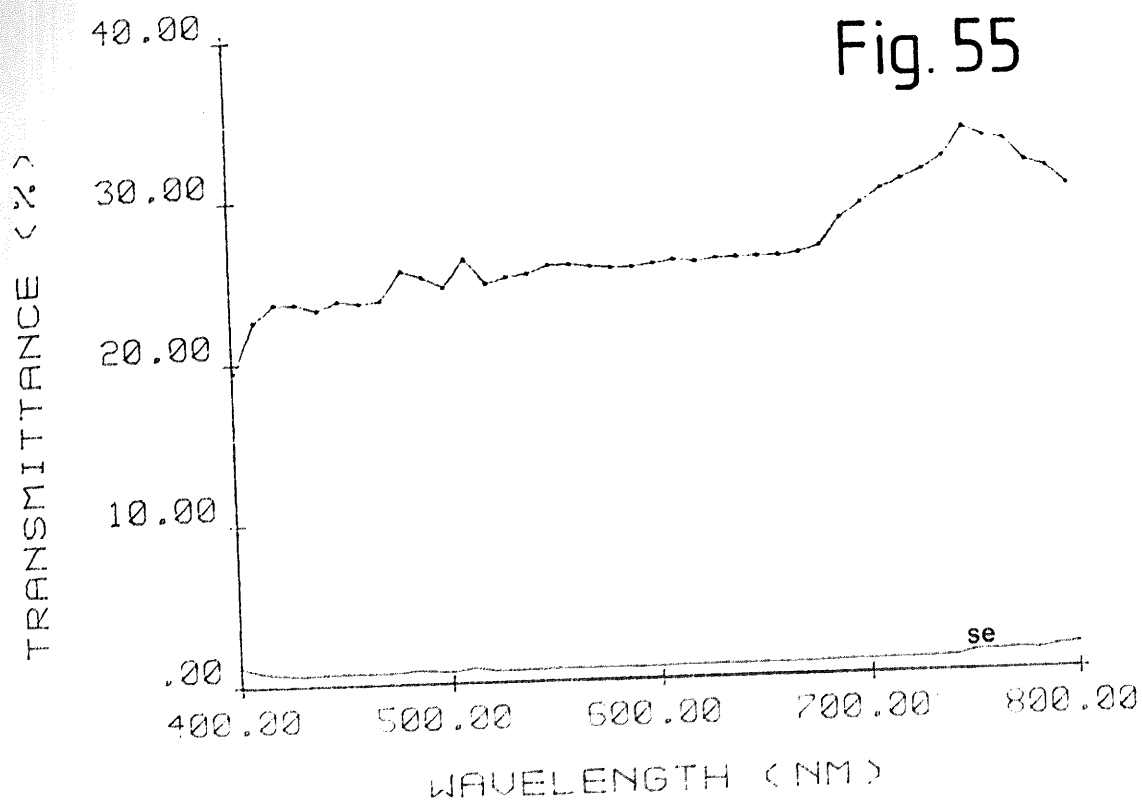


Fig. 57

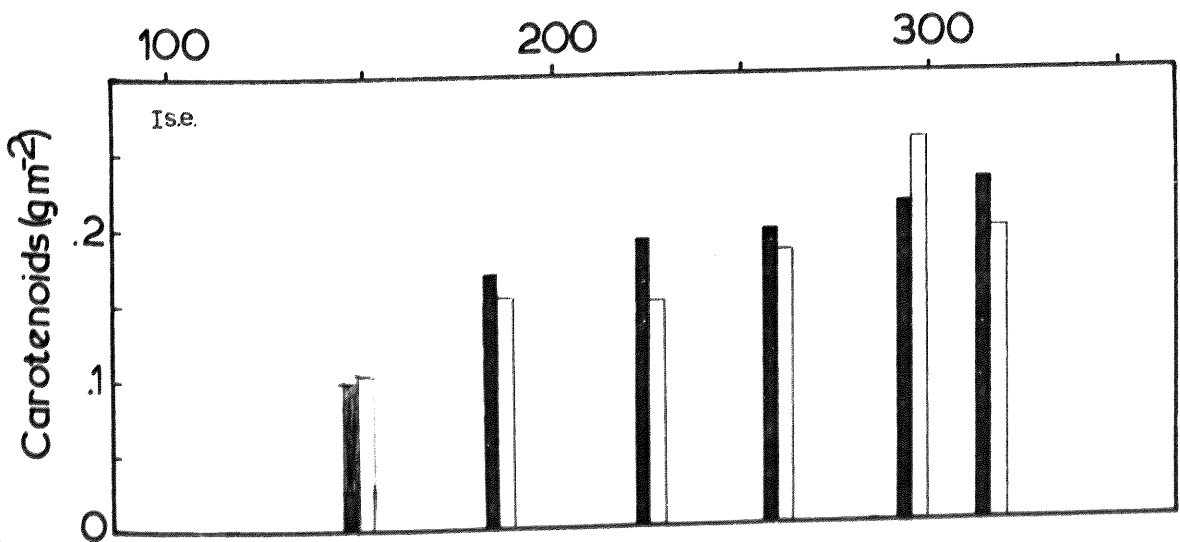
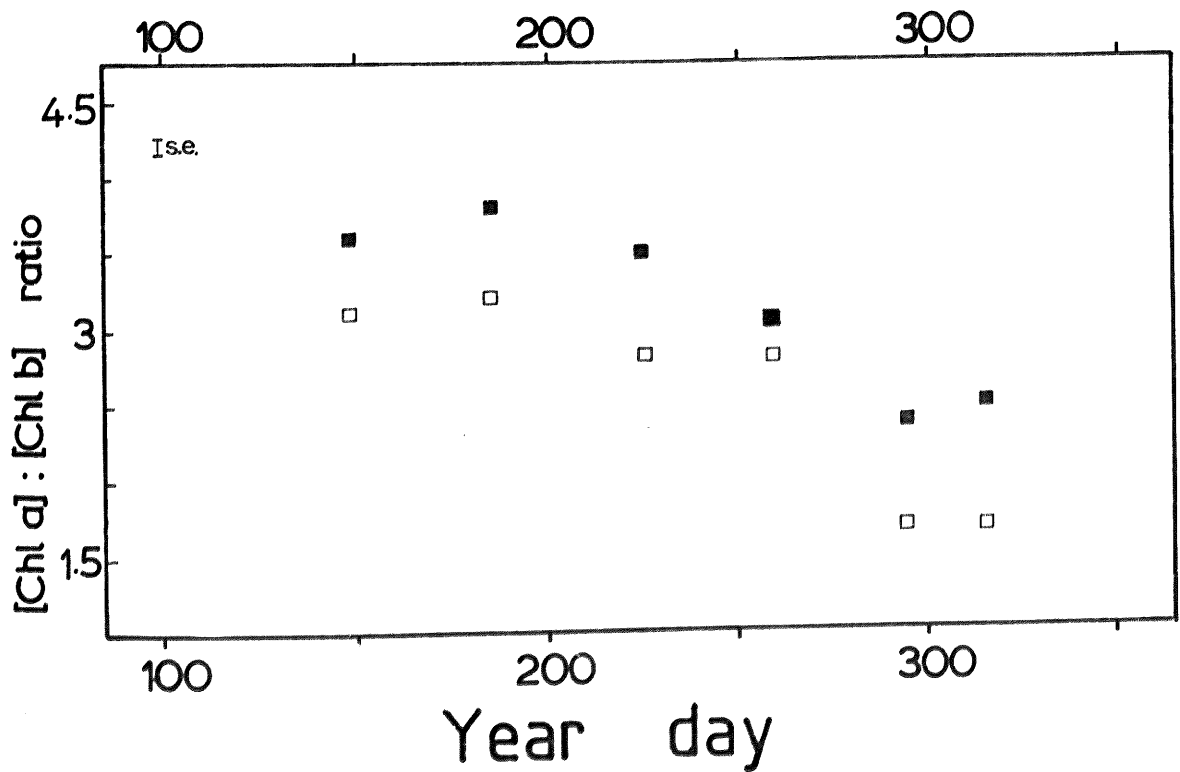
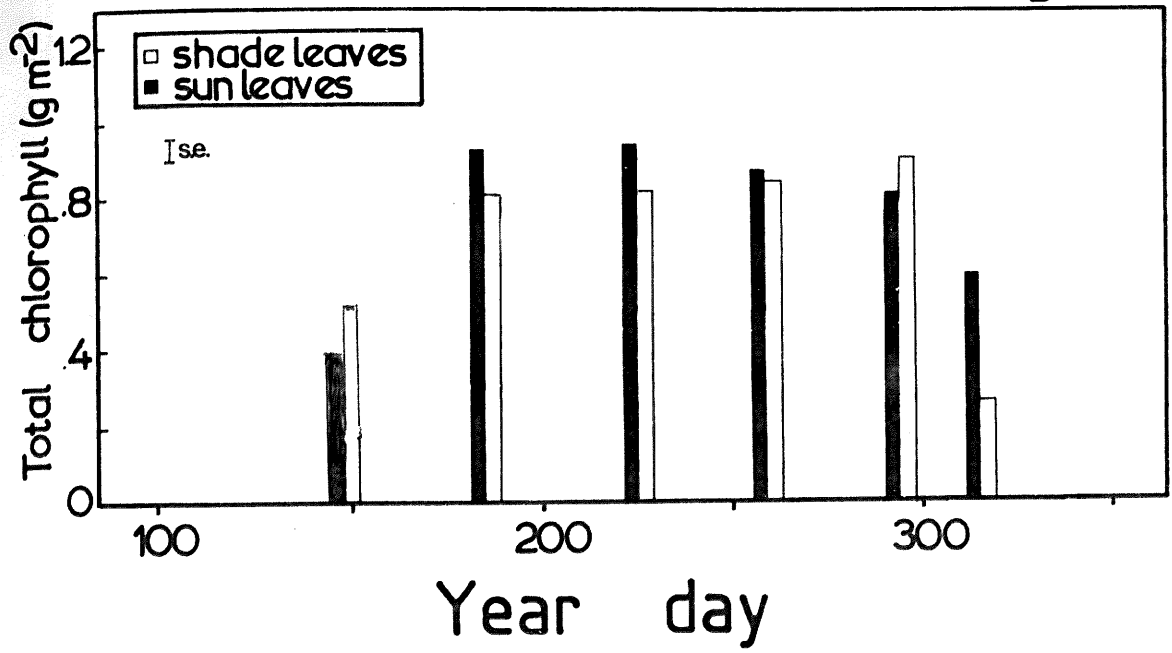


Figure 58

Seasonal changes in mean oak leaf and canopy
transmittance at 680 nm, 1980

(± 2 SE)

Figure 59

Seasonal changes in mean 660 : 730 nm
transmittance ratio of oak leaves and canopy,
1980-81.

Fig. 58

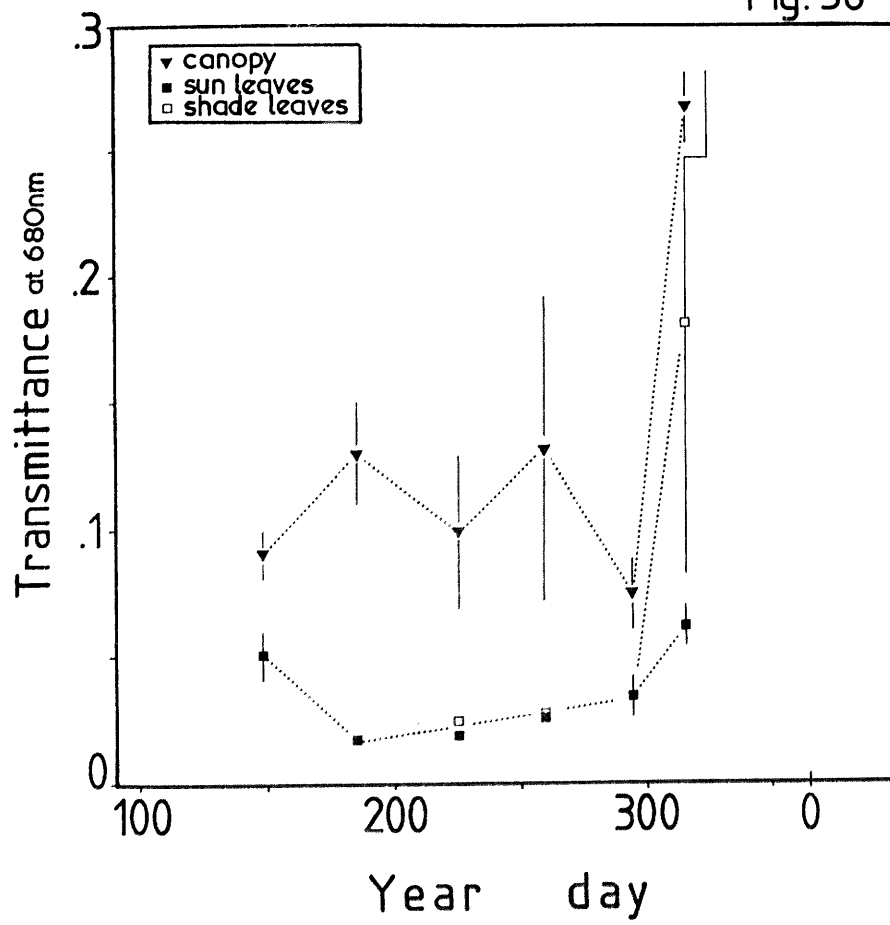


Fig. 59

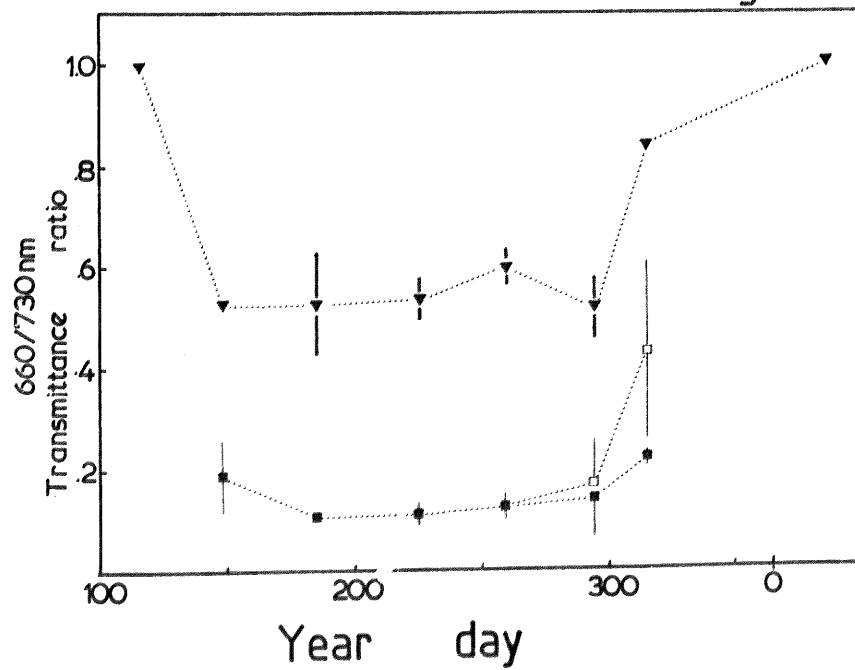


Figure 60

Oak shadelight 3' vs. canopy transmittance
to red light, 1980-81.

(•) 28 April 1980

(○) 4 July 1980

(■) 13 August 1980

(◀) 16 September 1980

(□) 21 October 1980

(◀) 11 November 1980

(a): 25 April 1980

(± 2 SE)

(b): 21 January 1981

(→): transmittance according to 21 January
photographic record.

FIG. 60

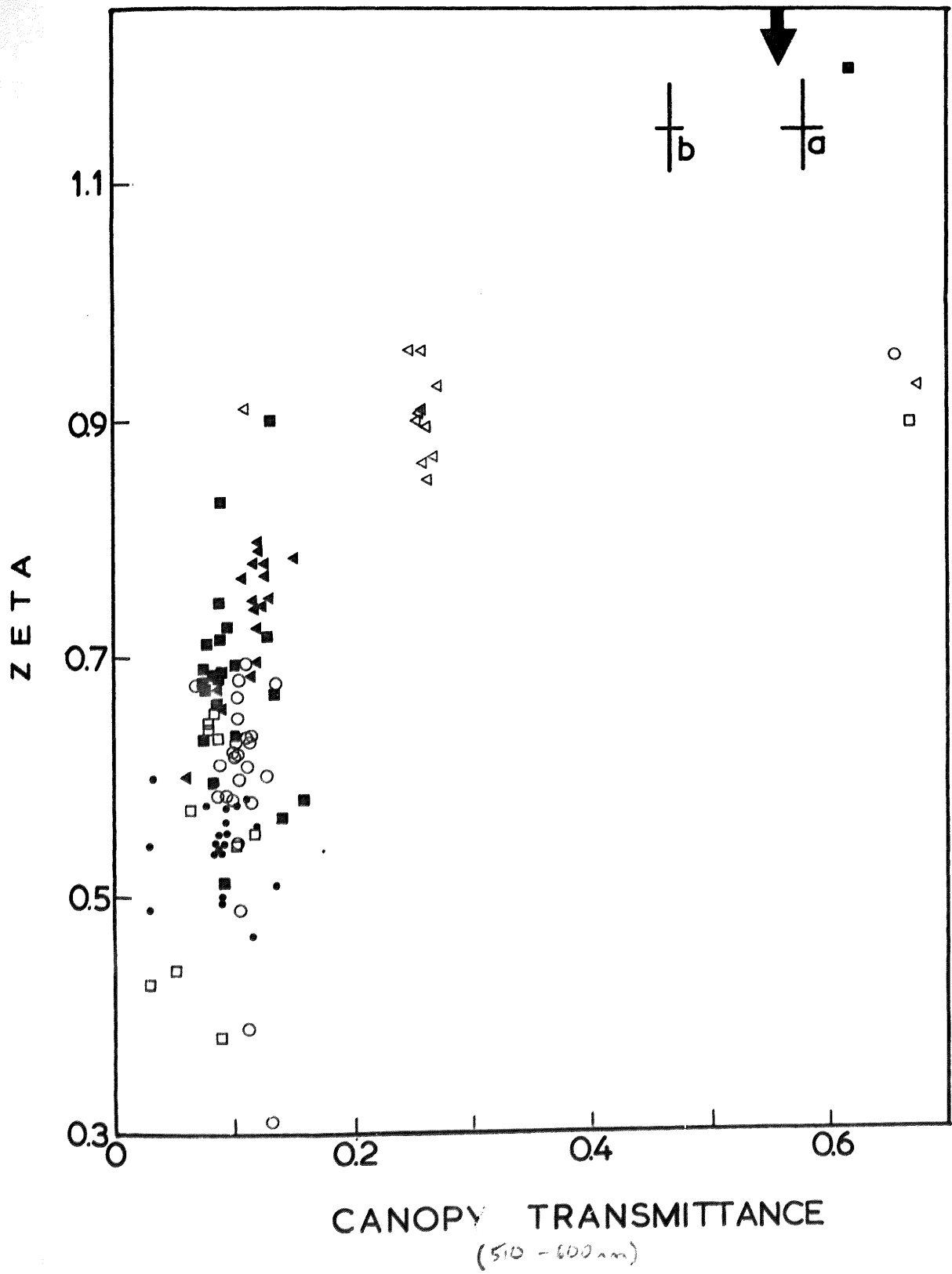


Figure 61

Seasonal changes in mean B:R transmittance ratio
of oak leaves, 1980.

(± 2 SE)

Figure 62

Seasonal changes in the mean B:R transmittance ratio
of the oak canopy, 1980-81

(± 2 SE)

Fig. 61

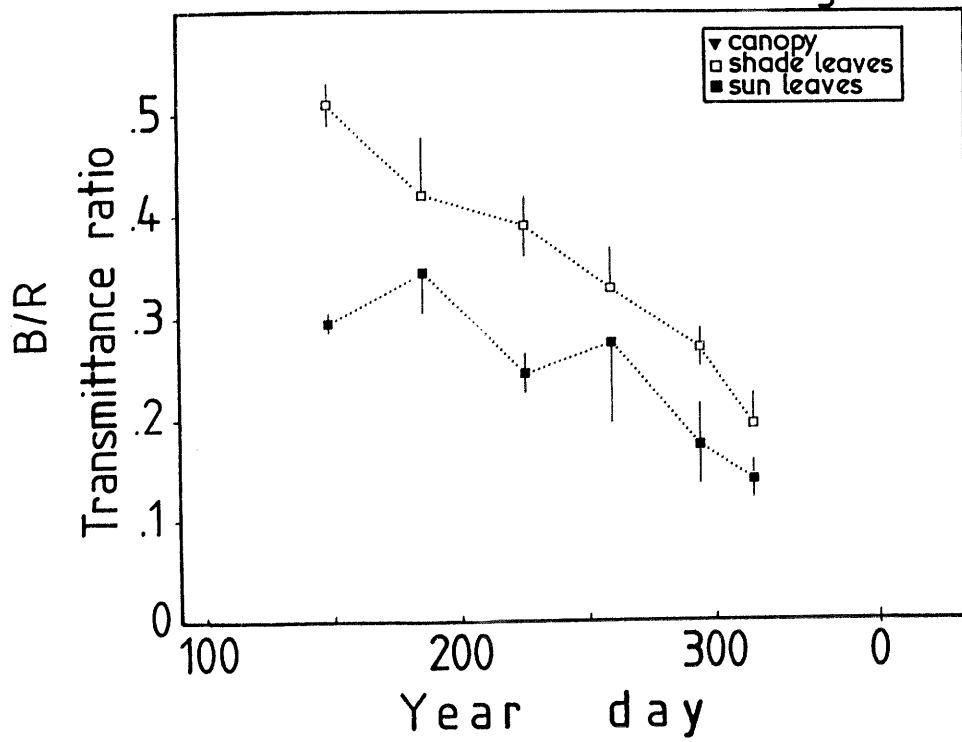
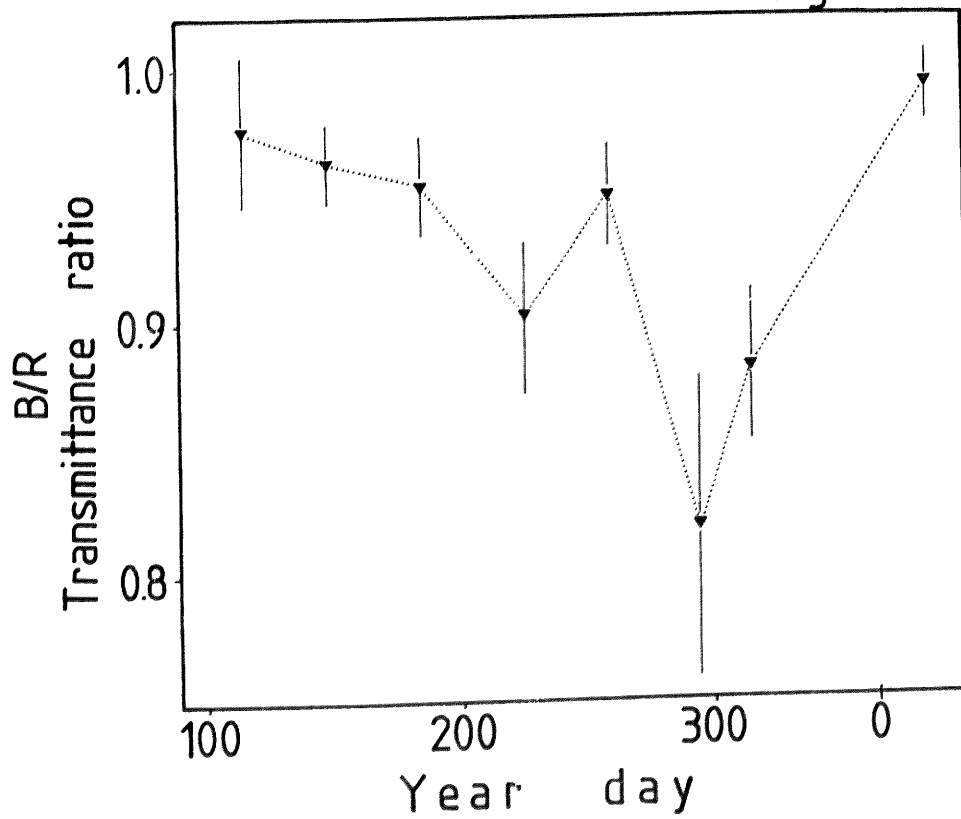


Fig. 62



iii) SHADELIGHT WITHIN THE SUGAR BEET CROP

Results

Investigations of the light environment beneath the leafy canopy of a sugar beet crop were carried out between July and December 1981. SPDs inside and outside the canopy were recorded at appropriate intervals throughout eight photoperiods approximately three weeks apart. From the shadelight data, the relative SPFR surfaces were constructed using JØ6HEF (Figs. 63 - 69; the equivalent surfaces for incident light are shown in Figs. 9 - 16), and the corresponding mean transmittance spectra were derived from both data sets, ignoring SPDs recorded when the solar disc was exposed (Figs. 71 - 77). Figures 79 - 82 show \bar{J} , ϕ_c , B:R ratio and $\log R$ versus solar angle for the shadelight data on each day. Figure 78 shows the transmittance spectrum of a typical mature sugar beet leaf.

On 7th July although still small the sugar beet plants were growing rapidly. The leaves were still only 0.1 - 0.15 m in height, and consequently, with the receptor head of the spectroradiometer 0.1 m above soil level, little shading occurred. The relative SPFR surface is not shown but is almost indistinguishable from that in Figure 9, based on data recorded simultaneously nearby. The mean daytime values of \bar{J} were 1.22 and 1.21 respectively ($t=1, p_0 > 5\%$); the B:R ratio and ϕ_c were also very similar. Therefore, the qualitative data collected by the two instruments were identical within the limits of sampling error. However, the fluence rate measured in the experimental plot was on average 7% higher than that outside at all wavelengths (Fig. 67). Such a difference is likely to be an artifact of the measuring system.

By 28th July the plants had grown to form an open canopy which substantially modified the spectral characteristics of the light beneath. This is apparent from the relative SPFR surface (Fig. 63). \bar{J} and ϕ_c (Figs. 79 and 80) were already similar to the minimum recorded beneath the oak canopy (Table 1). Both show a general increase towards higher solar angles except for three occasions in the morning around $\alpha_s = 20^\circ$ and one at $\alpha_s = 54^\circ$. The relative SPDs at the corresponding times of 6.35, 6.83, 7.41 and 11.17 h are also aberrant. All four corresponded to times when the cloud cover was incomplete and the solar disc was exposed. This is in accord with the

hypothesis advanced in Section 1.1; high values associated with sunflecks were not recorded, on account of their rarity. These apart, the cause of the general increase of \overline{J} and ϕ_c with solar angle during daytime is obscure, since no such change was recorded in the incident light. The normal rise at dawn and fall at dusk is superimposed on the canopy effect. PAR transmittance had also declined (Fig. 83), but in contrast, the B:R ratio (Fig. 81) was virtually unaffected by the presence of the canopy. This is predictable from the canopy transmittance spectrum in Figure 71, which shows similar values in the red and blue (21%) but much higher ones in the far-red (upto 57%).

By 18th August a further decline in the transmission of PAR (Fig. 83) and mean daytime \overline{J} and ϕ_c (Figs. 79 and 80) had occurred in association with the growth of the canopy. The cloud cover was uniform throughout the day, and so the data show relatively little variability, other than a typical dawn increase and dusk fall in \overline{J} and ϕ . However, although the B:R ratio (Fig. 81) was similar to that outside the canopy during daytime, little crepuscular change was detected. Because of the higher sensitivity of the instrument and the absence of the attenuating effect of the canopy, the recording of equivalent data for incident light began earlier and ended later; during these periods a typical increase in the B:R ratio occurred (Fig. 11). Again, the spectral transmittance (Fig. 72) is fairly similar in the blue and red (ca. 8%) but rather higher in the green (12% at 550 nm) and much higher in the far-red (ca. 45% at about 750 nm).

By 16th September the shade cast by the canopy was intense, the far-red transmission dominating that in the visible region (Fig. 65). Mean daytime \overline{J} and ϕ_c had fallen to 0.06 and 0.17 respectively. Although \overline{J} and ϕ both declined significantly towards low solar angles outside the crop, the corresponding trends beneath the canopy could not be followed, as the instrument used for measuring the shadelight was incapable of recording SPDs when $\alpha_s < -1.0^\circ$. The B:R ratio during daytime had fallen considerably (from ca. 1.0 to ca. 0.4); this is predictable from the transmittance spectrum (Fig. 73) in which the mean value for red light is 0.8% while that for blue is 0.5%. The peak at 550 nm was 1.8% and that in the far-red, 20%.

The density of the canopy continued to increase; although the relative SPFR surface for 29th September

(Fig. 66) is similar to its predecessor, the parametric data in Figures 79 and 80 show that a further decline in $\bar{\tau}$ and ϕ_c had occurred. The transmittance spectrum (Fig. 74) is in agreement with this. Both parameters were consistently higher in the afternoon than in the morning, even though no analogous change occurred in the incident daylight. Although cloud cover was incomplete before midday, only one SPD was recorded when the solar disc was actually exposed (at 9.57 h, $\alpha_s = 27^\circ$), and thus the "bi-modal transmittance" associated with direct solar radiation cannot be held responsible for the difference. Rather, the wilting which commonly occurs in mature water-stressed sugar beet plants may have been the cause, the change in leaf posture increasing transmittance.

In late Autumn, the shade beneath the canopy became less intense as the expansion of young leaves was retarded and the older leaves suffered wind damage. Thus, on 21st October the relative SPFR surface (Fig. 67) shows much higher transmission of visible light and, similarly, both $\bar{\tau}$ and ϕ_c had increased to ca. 0.15 and 0.25 respectively. Again the values recorded in the morning were lower than those in the afternoon. Although water stress is less likely at this time of year, frost damage and incipient leaf senescence may have lead to reduced stomatal control of transpiration (C. Black, personal communication). However, the sky was clear for most of the morning, exposing the solar disc (Fig. 7). It is therefore possible that the lower values are a consequence of the expected lower red : far-red transmittance ratio when the disc was aligned with foliage. The higher ratio at $\alpha_s = 8.6^\circ$ (7.83 h) is thus explicable as a weak sunfleck. Both before and after midday, $\bar{\tau}$ and ϕ_c tend to correlate negatively with solar angle (the opposite of the effect observed on 28th July), for some unknown reason. The B:R ratio of the shadelight was much higher than on the previous sampling date, especially in the morning. The spectral transmittance of the canopy (Fig. 75) indicates a related change, values for the blue region being higher than the red (3% and 1.7% respectively). There was no crepuscular increase in the B:R ratio.

At the beginning of winter it was apparent that the canopy had, to some extent, made good the damage caused by the high winds in the autumn. Relative SPFR surfaces for shadelight on 10th November and 2nd December (Figs. 68 and 69) appear intermediate between those of October and August (Figs. 67 and 64). The parameters of the data are

similar for the two days, but not identical. In particular, although the B:R ratio during morning and evening twilight was much higher than during daytime on 10th November, this was not apparent on the later date. The canopy was not responsible for this, as the twilight change was similarly absent from the incident spectrum (Fig. 16). On the earlier date, shadelight $\bar{\tau}$ and ϕ_c were lower in the afternoon than in the morning, a feature not apparent in the incident light; moreover, the cloud cover was uniform throughout the day. Consequently, the difference must originate from a change in the optical properties of the canopy itself. Although there was little evidence of similar changes in $\bar{\tau}$, ϕ_c fell and rose again rapidly before dawn, the opposite sequence being seen at dusk. Similar events were observed in the incident ϕ_c value. In December, the values of shadelight $\bar{\tau}$ and ϕ_c were more homogeneous during the day, and a more typical rise at dawn and fall at dusk were observed. However, $\bar{\tau}$ and especially ϕ were unusually high at 9.17 and 12.78 h; the former corresponds to a transient loss of cloud cover and therefore may represent some anomalous form of transmission; the SPD (see Fig. 69) is not that of a typical sunfleck, however, as the level of blue and green is much higher than that of red. At the latter time, cloud cover was uniform, excluding such an interpretation; the cause is, therefore, unknown. The canopy transmittance spectra in November and December are closely similar in the green (maxima of 6%), red (means of 3.6%) and far-red (maxima of 33%) spectral regions, while the transmittance of blue light was about 3.5% and 2.8% respectively.

Leaf transmittance and chlorophyll content were not measured regularly during this work, as the spectral changes during maturation and senescence would relate to individual leaves close to the sensor, rather than to the canopy as a whole. These measurements would have involved destructive sampling of the canopy at the recording site, and so were out of the question unless measurements were made at different locations in the crop on each day of recording, introducing an additional source of variation in the data. Instead, pigment assays were carried out on mature leaves in October. The mean total chlorophyll content was $460 \pm 34 \text{ mg m}^{-2}$, and the chlorophyll a : b ratio 2.3 ± 0.1 . Carotenoid content was $91 \pm 4 \text{ mg m}^{-2}$. Jaggard, Lawrence and Biscoe (1982) reported a lower value of 236 mg m^{-2} for chlorophyll in young expanded leaves of the "bush mono G" cultivar, but did not specify whether this included chlorophyll b.

Leaf transmittance was measured using a dual beam scanning spectrophotometer (model SP1800, Pye Unicam, Cambridge, U.K.) with the sample held in a purpose-built clip close to the photomultiplier in order to collect as much of the divergent scattered light as possible. However, as some was inevitably lost, the results (Fig. 78) are an underestimate. The transmittance values are closely similar to those of Smith [1974], who used a secondary scattering layer in both measuring and reference beams in order to equalise the scattering loss. This procedure will have led, however, to an overestimate of transmittance. Light incident upon the secondary layer is partly reflected back into the sample, where scattering processes can once more reverse its path and, therefore, allow it to emerge again from the side of the leaf adjacent to the photomultiplier. Hence, light transmitted by a sample has a greater chance of reaching the photomultiplier tube than light in the reference beam. The similarity of the results using both methods presumably indicates that the opposing errors were small.

Considering the data as a whole, the initial fall in canopy transmittance of PAR is illustrated in Figure 83 along with equivalent data for the whole canopy, collected using Li-Cor quantum sensors (Lincoln, U.S.A.) instead of the spectroradiometers. The rates of decline are very similar, although the transmittance values at any time are consistently lower according to the more sophisticated instruments. The quantum sensors indicated, however, that the point in the canopy occupied by the spectroradiometer probe was not exceptional. One possible explanation of the apparent difference is that the Li-Cor probe was sensitive to light above 700 nm. Another is that, as the probe was much nearer the ground than the spectroradiometer receptor head (in order to facilitate its movement between the plants), it may have been exposed to more light penetrating between the narrow leaf bases. The effect of elevating the probe was not investigated. An alternative vertical axis of leaf area index is also shown in Figure 83. The values were not measured, but calculated as an approximate function of canopy transmittance according to Equation 6. The extinction coefficient for radiation between 400 - 3000 nm was taken as 0.53 (Bremner, El Saeed and Scott, 1969), equivalent to about 0.75 for PAR assuming a conversion factor of 1.4 (M. Steven, personal communication).

Figure 84 shows that the change in shadelight \bar{J} is of a similar form. The increase during October and November is shared by the transmittance of visible light (Figs. 75 and 76) and is not affected significantly by changes in the value of incident \bar{J} (cf Fig. 39). Thus the change is likely to be caused by the canopy itself; the 660 / 730 nm transmittance ratio (Fig. 85) is in accord with this. The relationship between \bar{J} and canopy transmittance is shown in Figure 86.

Table 10 shows the results of a non-orthogonal ANOVAR of the four shadelight parameters during the twilight period. Interaction was only significant for \bar{J} . The effect of canopy development (that is, date) was large in relation to that of solar angle for both \bar{J} and ϕ_c , but log R showed the greater effect to be due to solar angle.

Discussion

During daytime, the transmittance of the sugar beet crop was very low in the PAR region from September onwards. According to a simple Beer's Law relationship, the mean PAR transmittance for 29th September (ca. 0.56%) corresponds to a leaf area index of about 7, which is high but not exceptional for sugar beet. However, several of the assumptions underlying this calculation are dubious.

The results are entirely consistent with the notion that canopy transmittance is lower under sunny conditions, as long as sunflecks are ignored. If the hypothesis outlined in 1.1 is true, when the canopy is fully closed (that is, when gaps are absent and sunflecks cannot arise) transmittance should be independent of cloud cover. The data recorded on 29th September is consistent with this, as the spectrum at 9.57 h ($\alpha_s = 27^\circ$) are similar to the rest, although the solar disc was exposed. In a winter wheat canopy, McCartney [1975] also found little difference between the correlation of \bar{J} and LAI on clear and cloudy days, although his sample size was small.

Smith [1974] derived an approximate shadelight spectral distribution based on incident spectral data for a model atmosphere and the transmittance spectrum of sugar beet leaves. The results for two leaf layers are quite similar to the shadelight measured in September (Figs. 65 and 66). However, when the transmittance of various numbers of leaves is calculated (Fig. 78) and compared with those of the canopy itself (Figs. 71 to 77), a poor

fit is apparent. The most obvious difference is the variation within the PAR region, which is generally much greater for the leaves than for the canopy. If foliage gaps are indeed responsible for this, it should be possible to eliminate their effects from the spectrum, by raising the baseline and effectively subtracting the light they admit. Considering, for example, the data for 10th November (Fig. 76); if the transmittance to blue light is negligible, the corrected transmittance at 550 nm is ca. 2.5%, which would correspond to that of ca. 2.7 leaf layers. However, the corrected canopy transmittance at 760 nm would be ca. 26%, corresponding to only 1.7 leaf layers. To obtain a solution to this paradox, the additional factors of scattering, the optical properties of leaves at different stages of development, and probably others will have to be considered.

Nonetheless, the correlation between canopy transmittance to red light and \bar{J} was close (Fig. 86), demonstrating that sensitivity to the latter would have considerable adaptive potential. McCartney [1975] also found a correlation between PAR transmittance and \bar{J} in a sugar beet crop, but considerably greater scatter was apparent, and data recorded in early autumn were aberrant from the rest, possibly as a consequence of a higher mean value of \bar{J} for incident daylight at this time (see 1.3 (i)). McCartney was able to fit a linear regression line to a selected range of the data. The data in Fig. 86 for the transmittance of red light (610 -700 nm) approximate more closely to the requirement of Beer's Law for monochromatic radiation if transmittance is wavelength dependent; the scatter is smaller and the expected curvilinear relationship is apparent.

In general, the changes in shadelight quality observed during twilight were similar to those of the incident light. This is in contrast to the results of McCartney [1975] who found that \bar{J} beneath a commercial sugar beet canopy increased on a cloudless evening. As the crop had been conventionally drilled, it is possible that the increase was due to the heterogeneity of the canopy. Indeed, according to the simple model canopy of Evans [1966], under a clear sky the red : far-red transmittance ratio of a leafy canopy should fall towards sunset, and hence the decline in \bar{J} beneath should be greater than that outside. The data provide little in support of this notion.

Similarly, the canopy seems to have little effect on the timing of the rise in logarithmic fluence rate at dawn and the fall at dusk (Figs. 23 and 82). Thus both quantitative and qualitative changes persist even under intense shade. In statistical terms, the effect of the canopy on $\bar{3}$ and ϕ_c is far greater than that of solar angle (see Table 10), and therefore a plant would have to show very effective compensation for seasonal changes in the mean daytime value if either were to act as a zeitgeber. In contrast, even beneath this dense canopy, $\log R$ was predominantly under the influence of solar angle; such a zeitgeber would be largely unaffected by leafy interception. As in the oak shadelight, the canopy has little effect on the relationship between any of the parameters and solar angle. However, the sugar beet results themselves are probably not directly relevant to photoperiodic control, as the associated low light levels are inadequate to support plant growth. Exceptions might be provided by the most shade tolerant species of tropical rainforests, but there is little evidence that these show photoperiodic control.

TABLE 10 NON-ORTHOGONAL ANALYSIS OF VARIANCE
SUGAR BEET CROP : TWILIGHT ($\alpha < 7.5^\circ$)

<u>SOURCE</u>	<u>Df</u>	<u>Sum-of-Squares</u>	<u>Variance</u>	<u>Error V.R.</u>	<u>D x A V.R.</u>
Parameter - β					
DAYS	7	23.16	3.31	----	242
ANGLES	2	0.28	0.142	----	10
D x A	11	0.15	0.014	4.4	
Residue	147	0.45	3.1×10^{-3}		
Parameter - ϕ_c					
DAYS	7	2.63	0.375	882	
ANGLES	2	0.026	0.013	28	
D x A	11	4.528	4.12×10^{-4}	0.9	
Residue	147	0.067	4.56×10^{-4}		
Parameter - B:R ratio					
DAYS	7	16.96	2.42	32	
ANGLES	2	2.78	1.39	18	
D x A	11	1.44	0.13	1.7	
Residue	147	11.00	0.075		
Parameter - log R					
DAYS	7	33.9	4.85	32	
ANGLES	2	43.6	21.80	145	
D x A	11	1.99	0.181	1.2	
Residue	147	22.1	0.150		

Fig. 63

Figures 63 - 69

Relative SPFR surfaces describing shadelight
beneath the sugar beet canopy, 1981.

The dashed lines represent the times of sunrise
and sunset; wavelengths are in nanometers

Figure 63: 28 July 1981

Figure 64: 18 August 1981

Figure 65: 16 September 1981

Figure 66: 29 September 1981

Figure 67: 21 October 1981

Figure 68: 10 November 1981

Figure 69: 2 December 1981

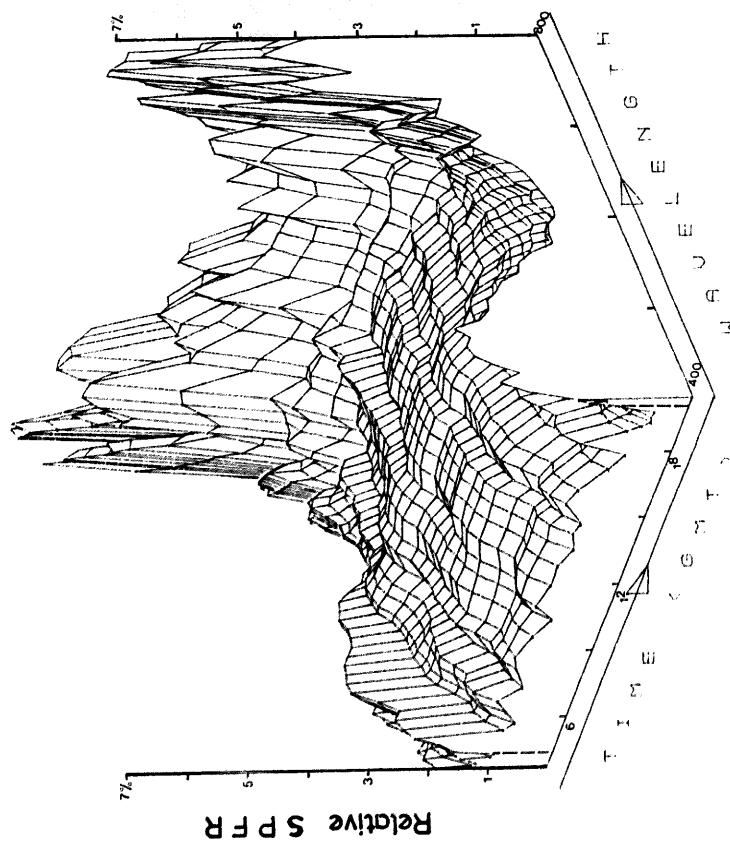


Fig. 65

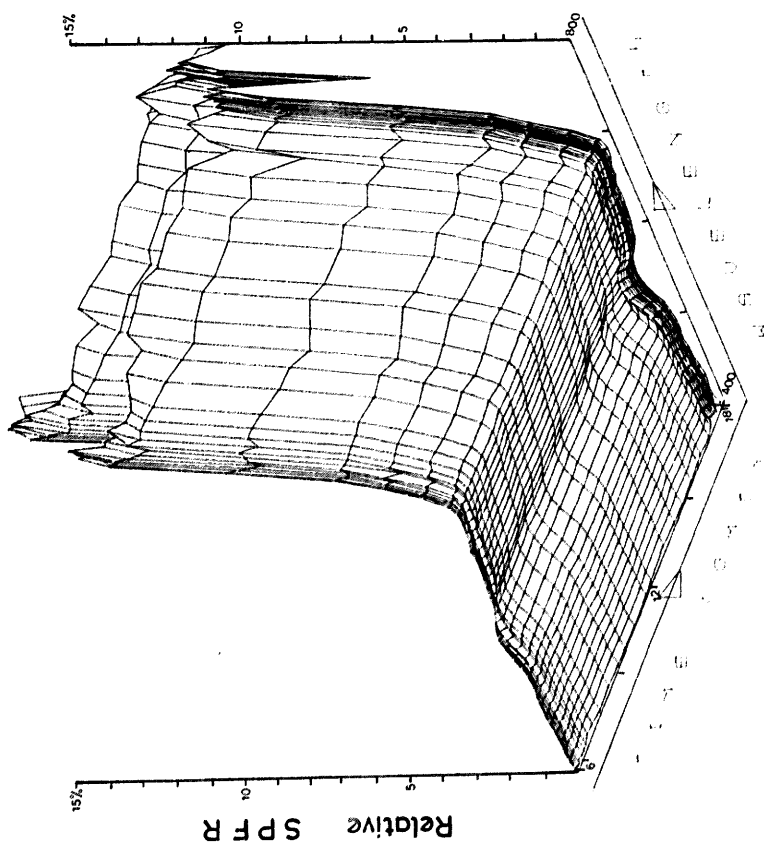


Fig. 64

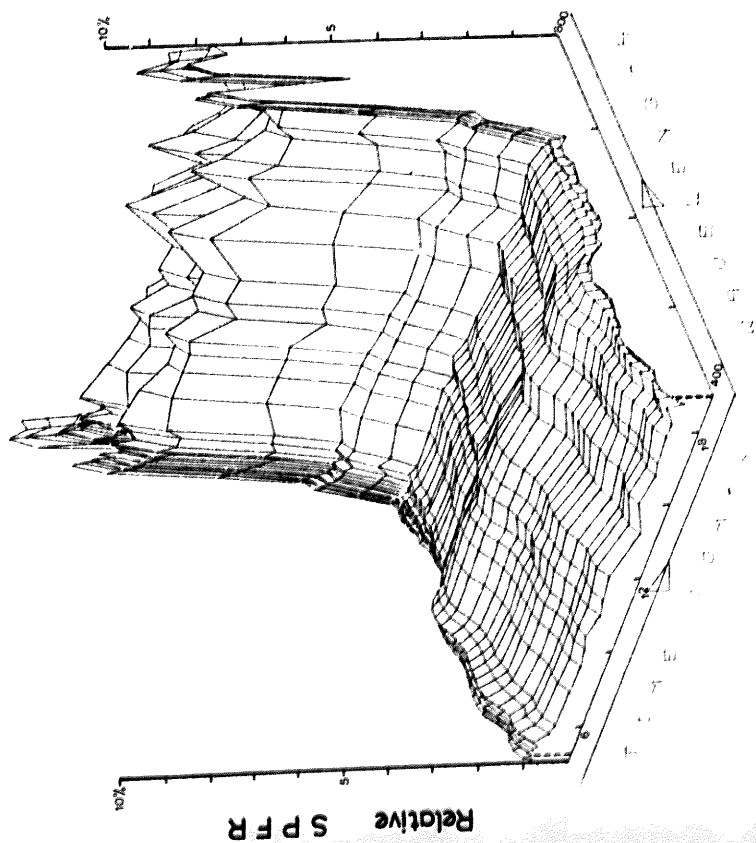


Fig. 67

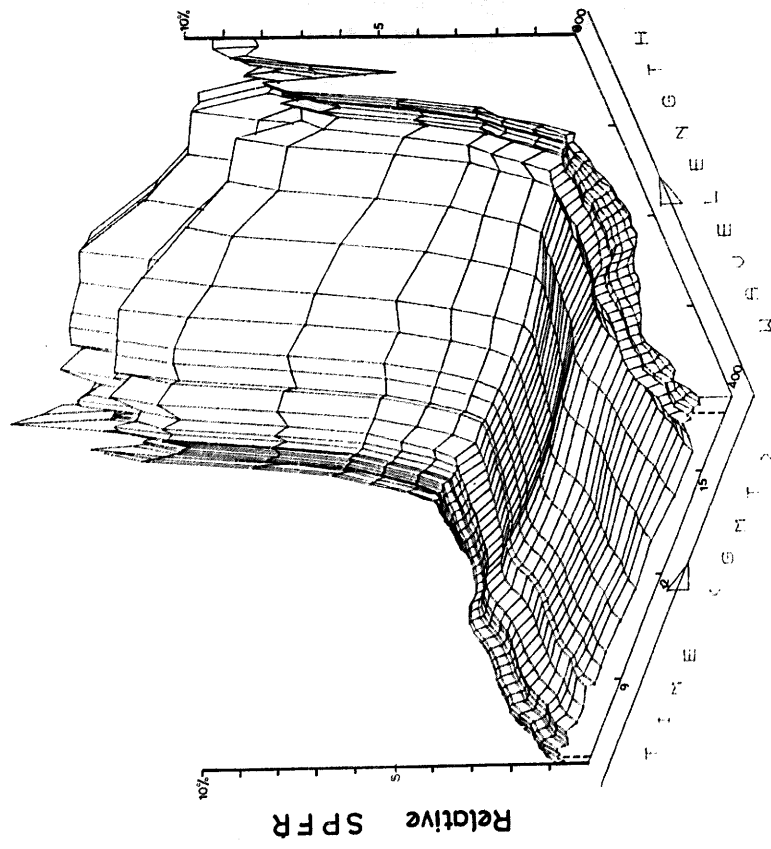


Fig. 66

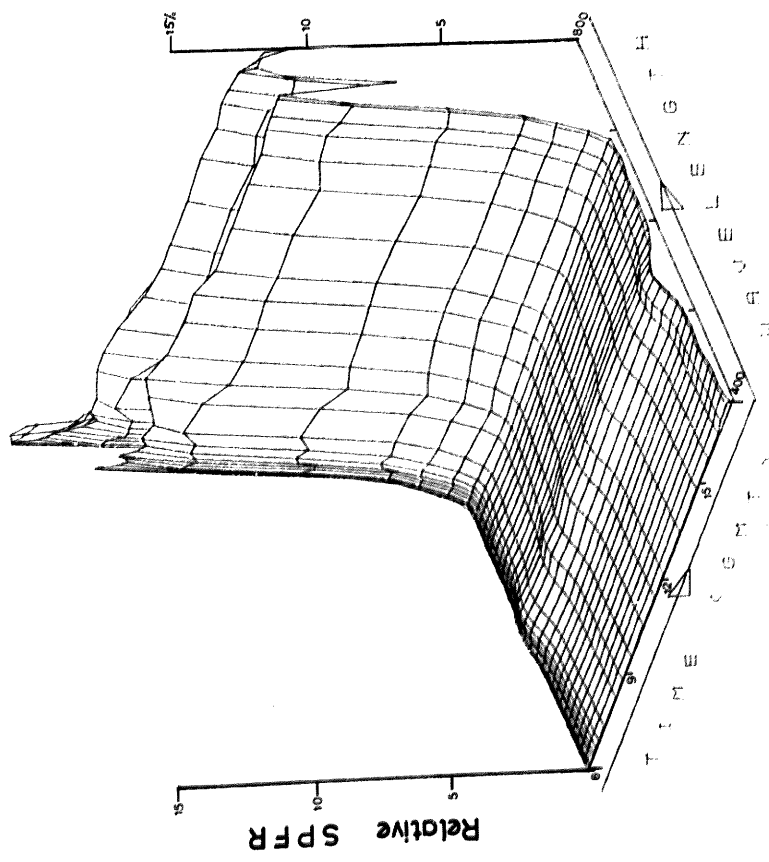


Fig. 69

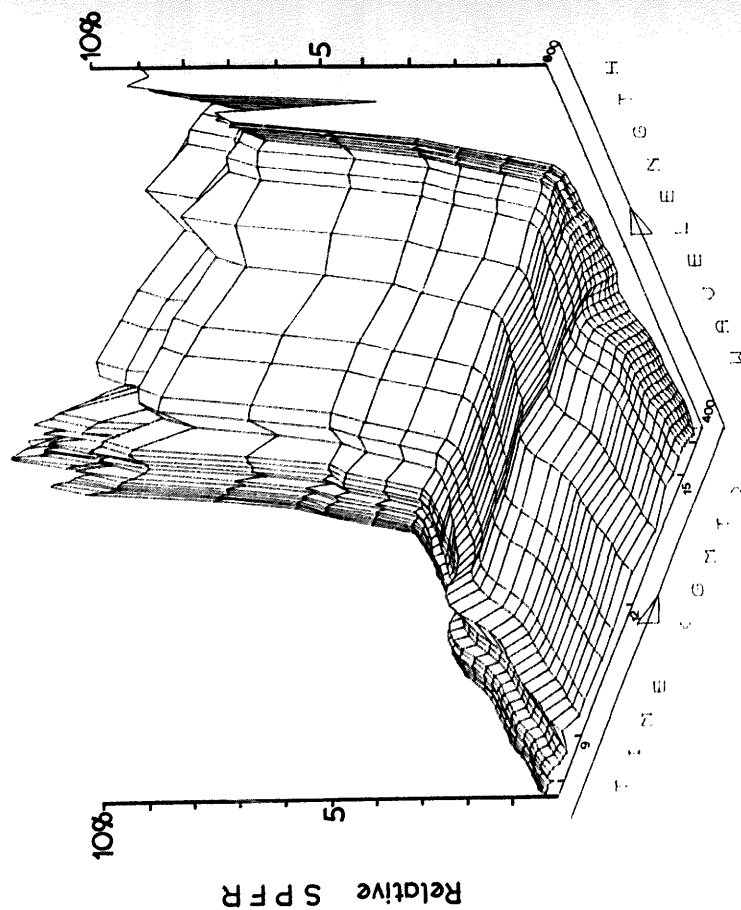


Fig. 68

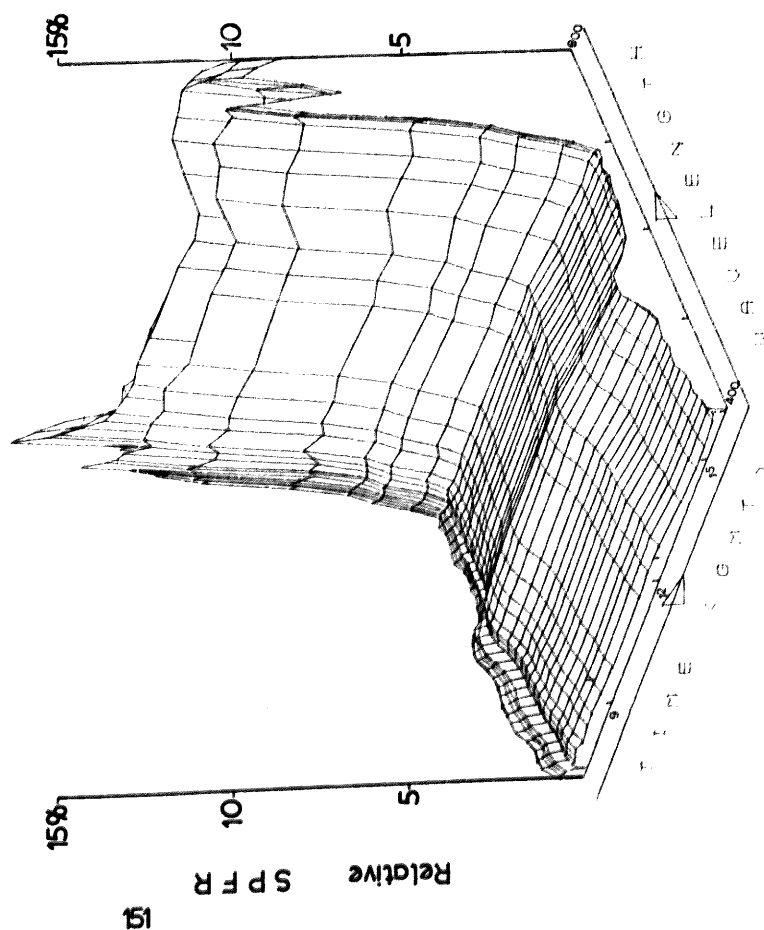


Fig. 69

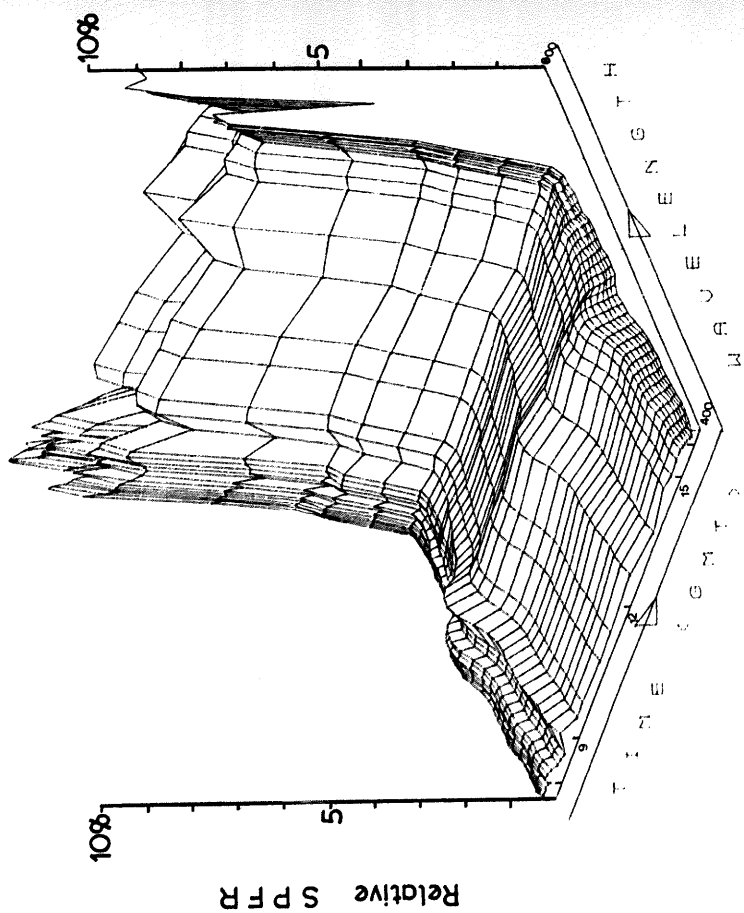
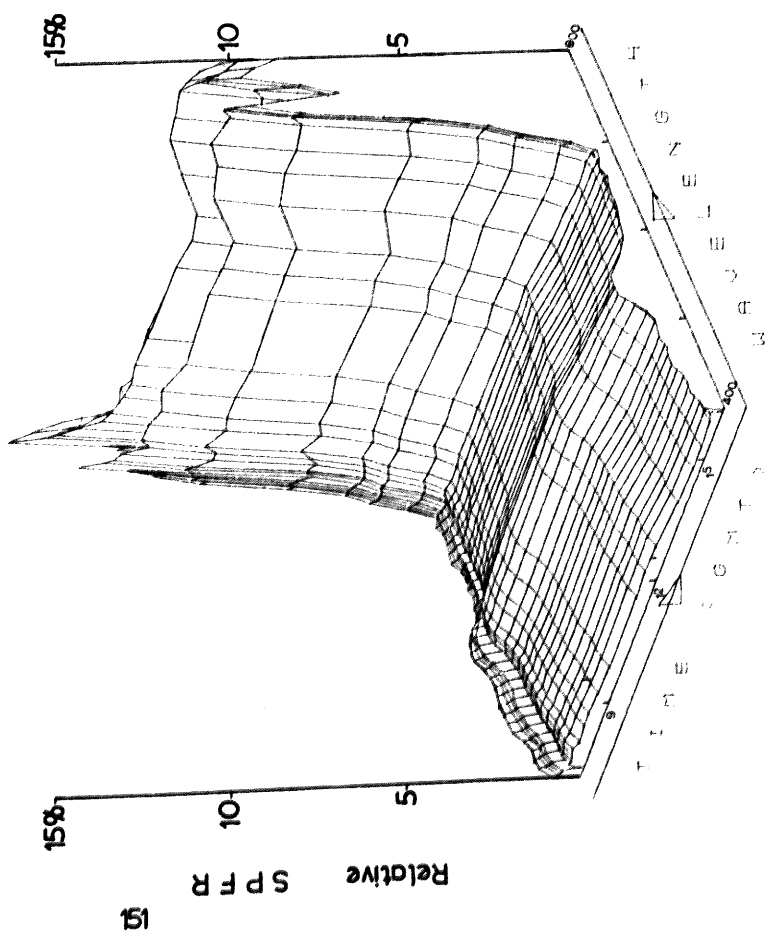


Fig. 68



Figures 70 - 77

Transmittance spectra of sugar beet canopy

1981

(\longleftrightarrow) mean for $15^\circ < \alpha_s < 30^\circ$
(——) standard error

Figure 70: 7 July 1981

Figure 71: 28 July 1981

Figure 72: 18 August 1981

Figure 73: 16 September 1981

Figure 74: 29 September 1981

Figure 75: 21 October 1981

Figure 76: 10 November 1981

Figure 77: 2 December 1981

Fig.70

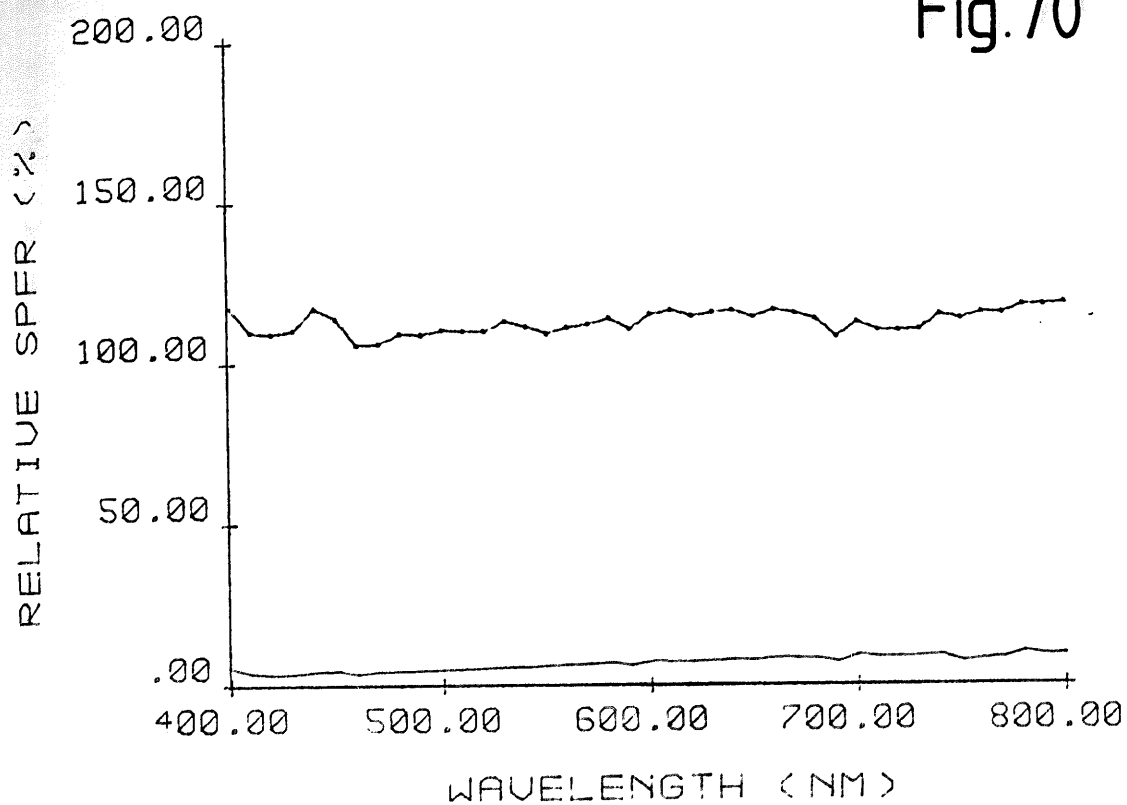
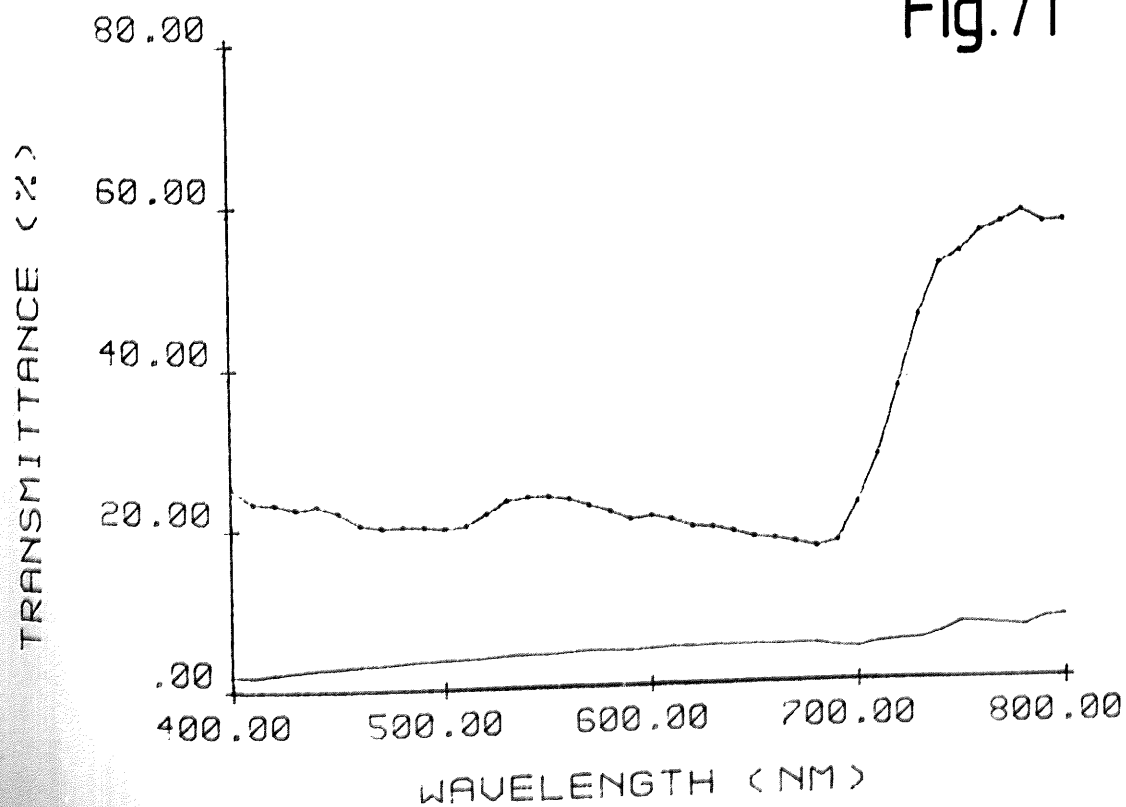


Fig.71



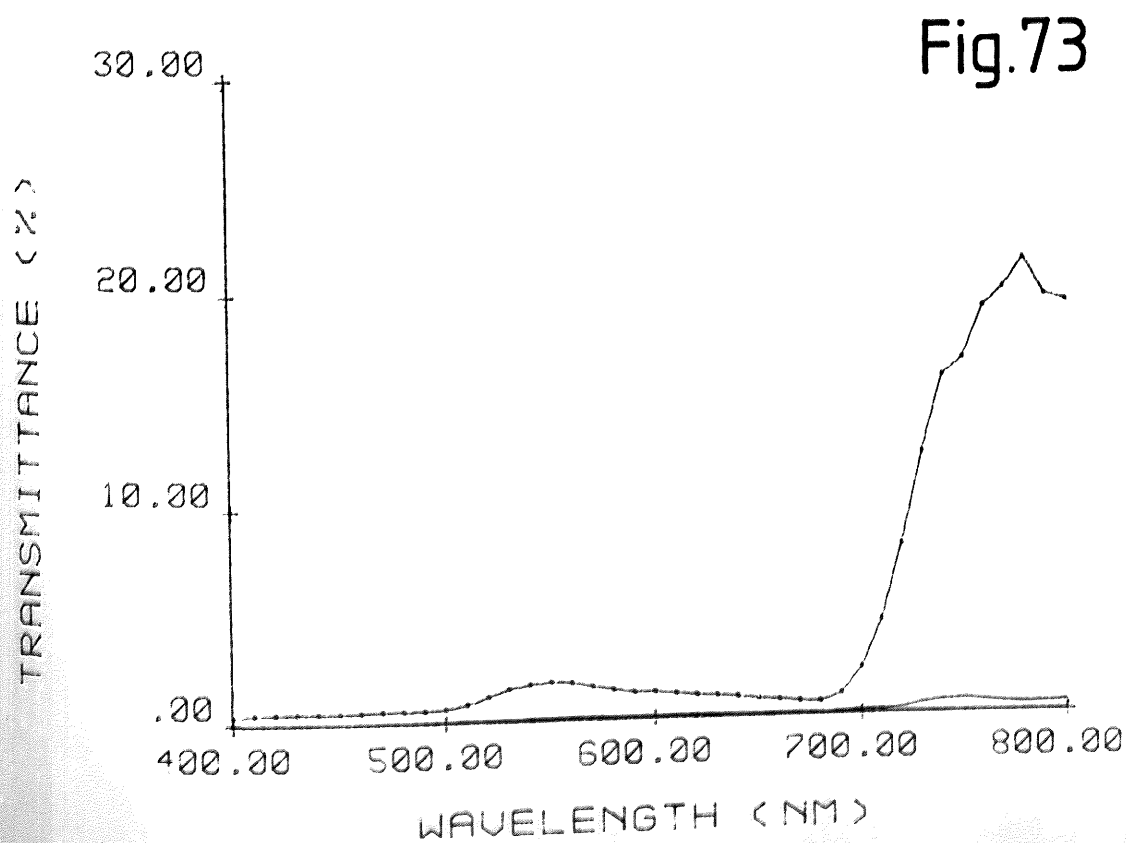
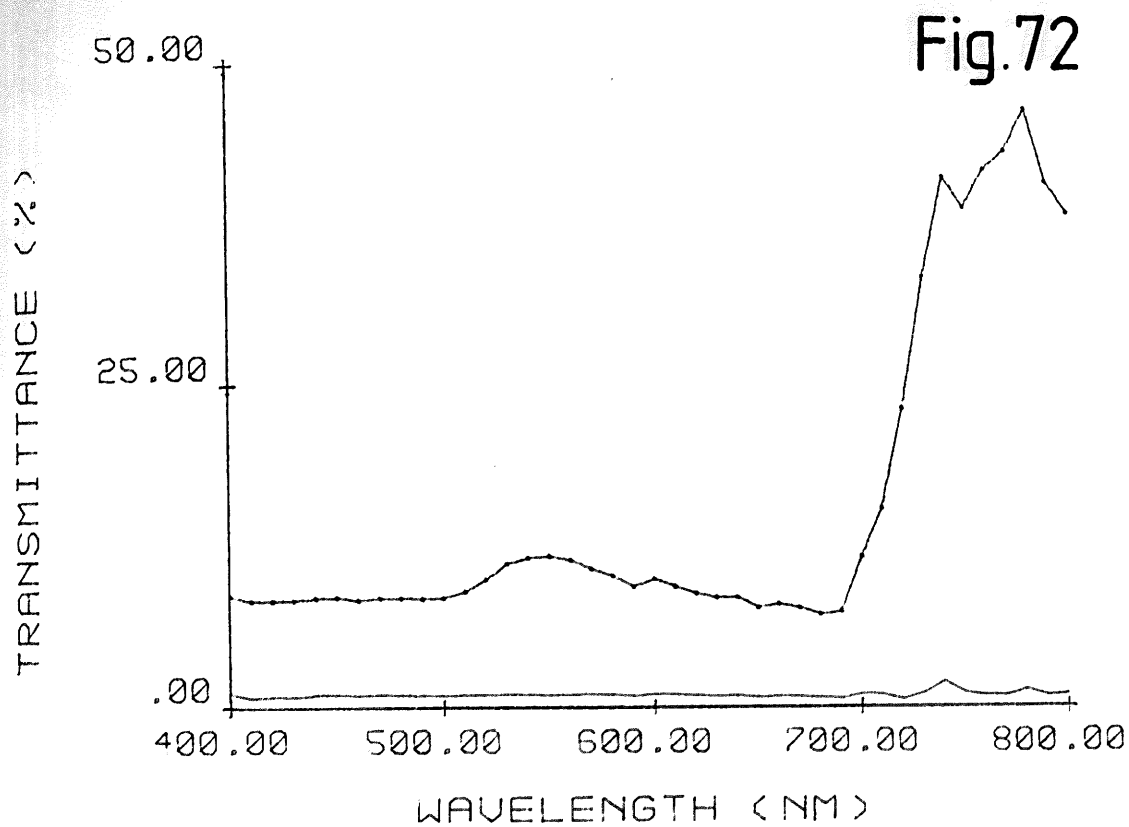


Fig.74

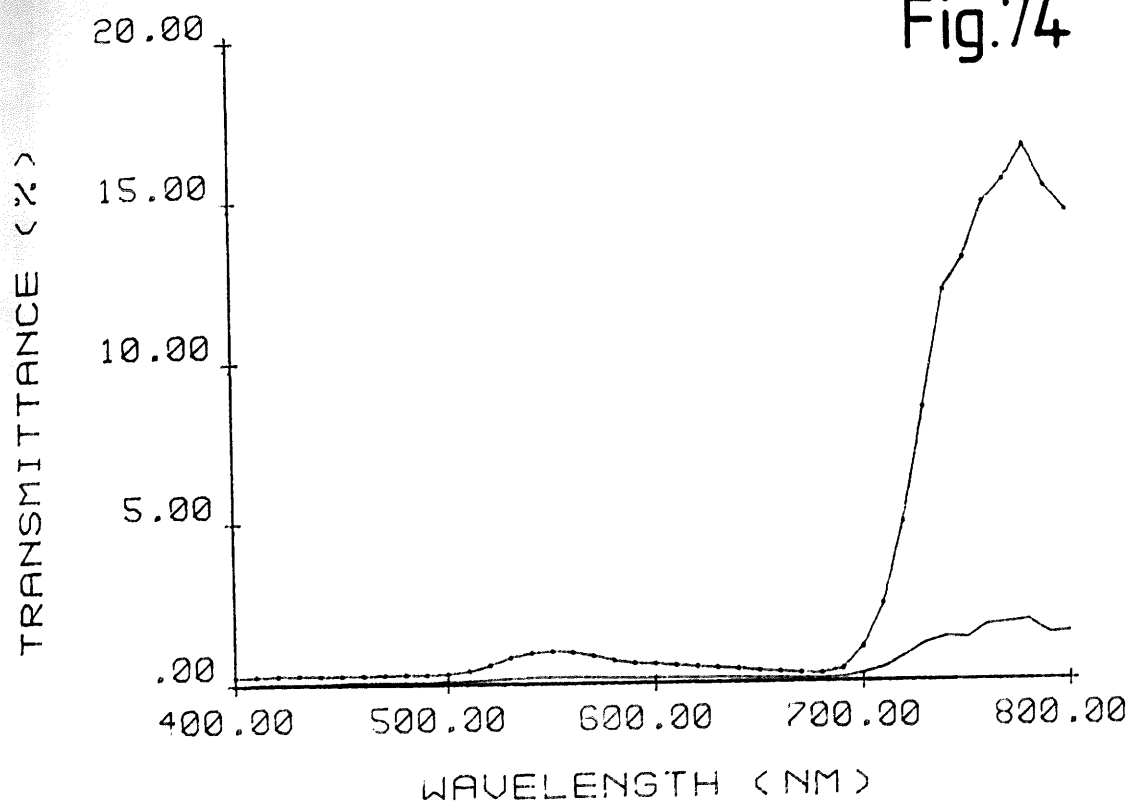


Fig.75

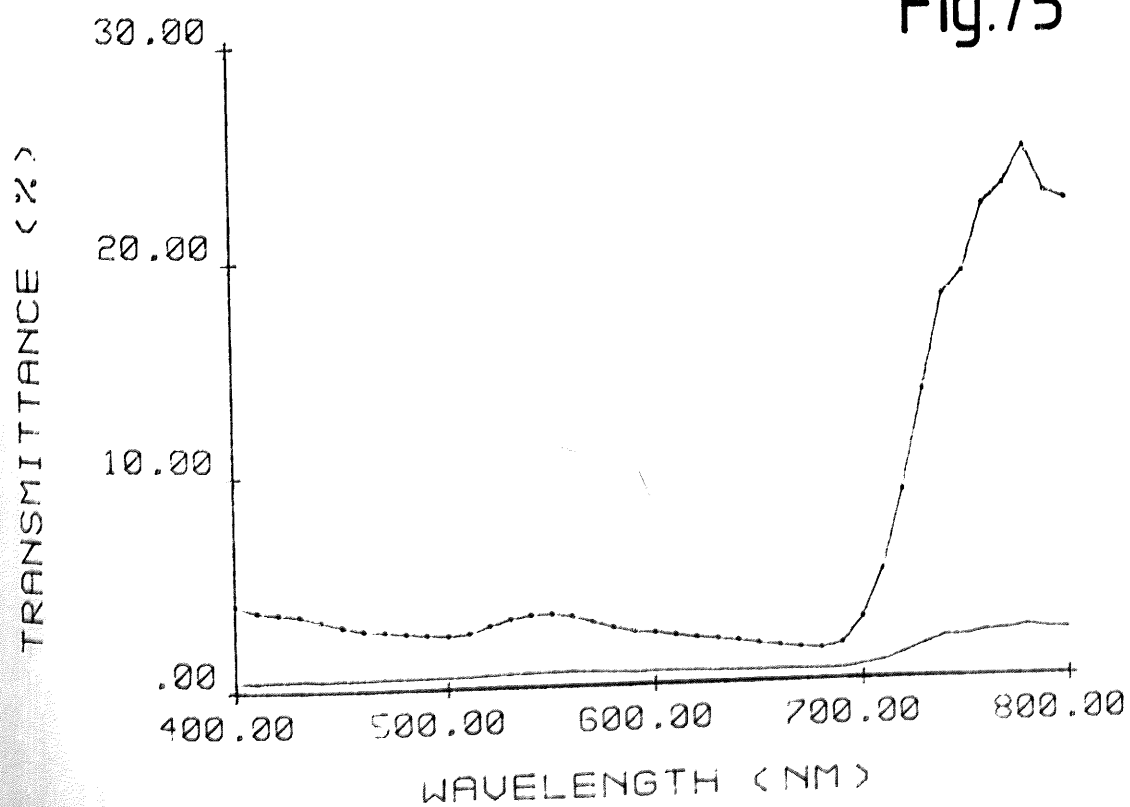


Fig.76

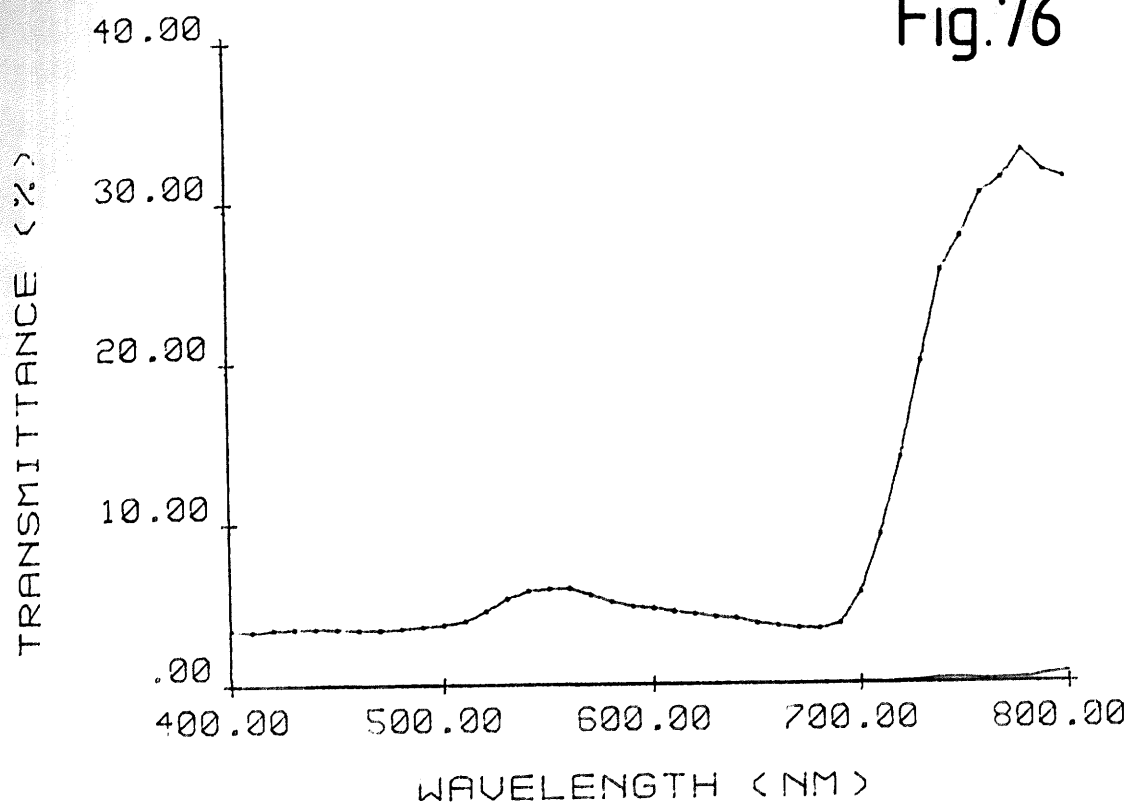


Fig.77

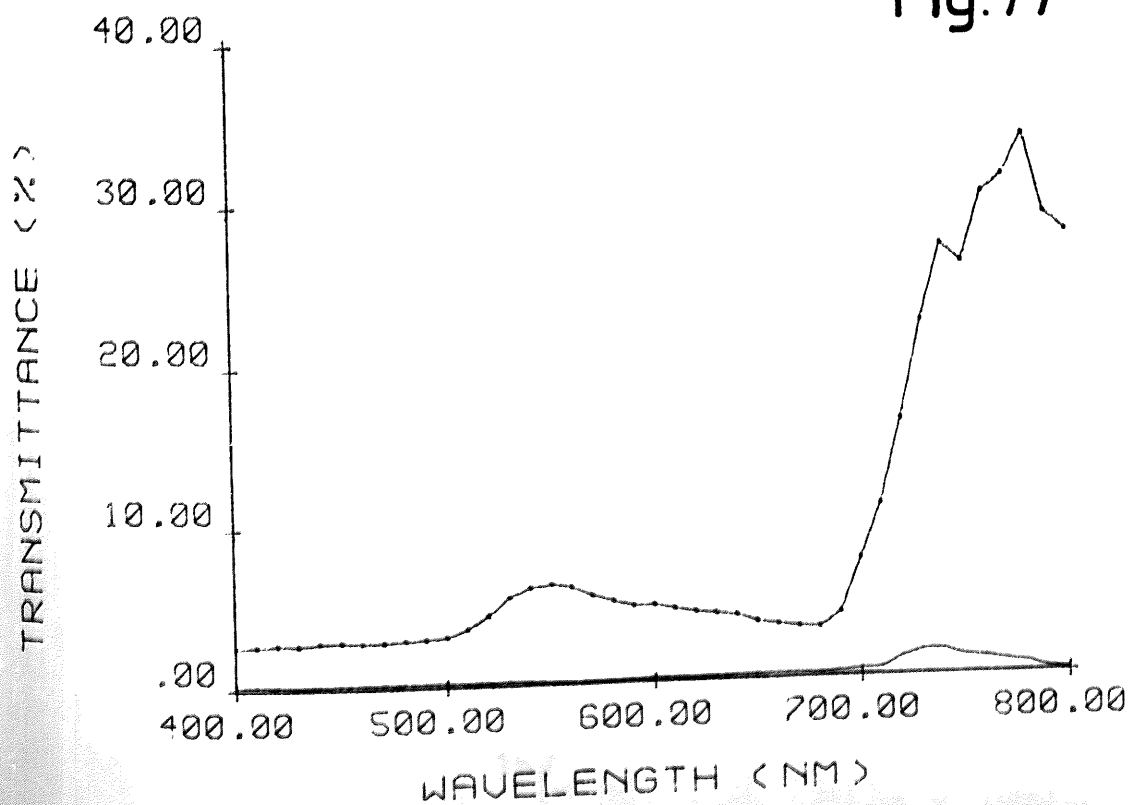
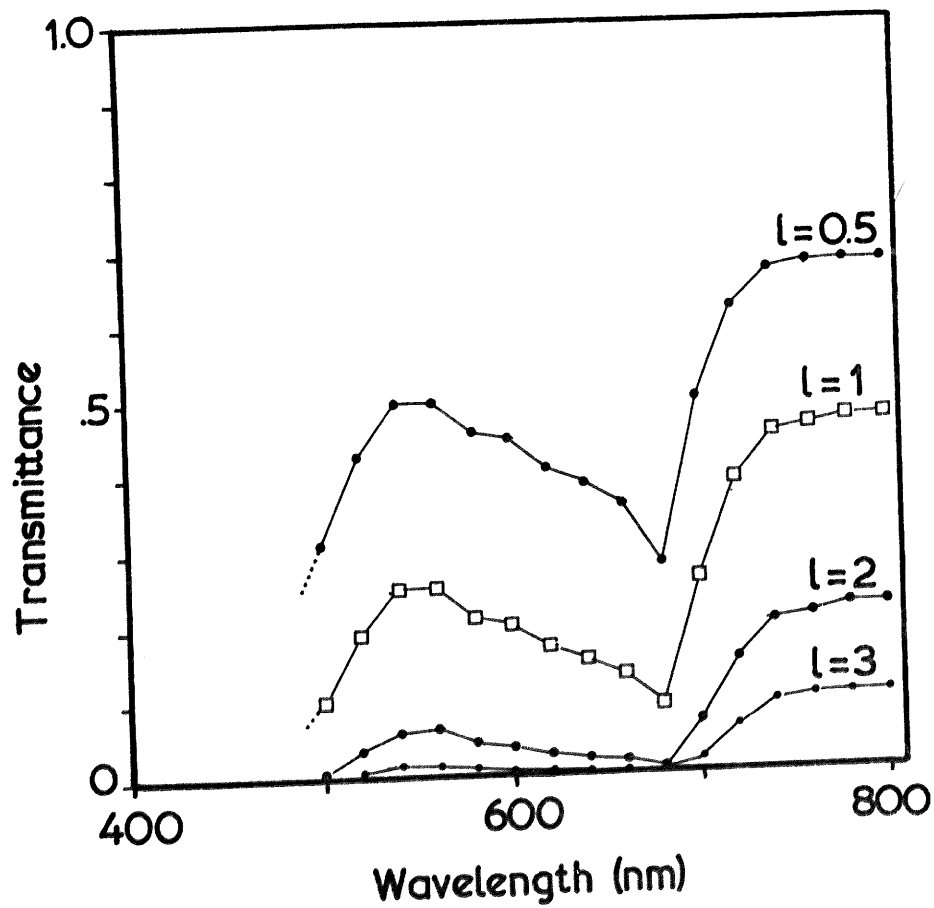


FIG. 78



Sugar beet leaf transmittance spectrum ($l=1$)
and calculated spectra for other thicknesses
($l = 0.5, 2$ and 3)

Figures 79 - 82

Parameters of shadelight beneath sugar beet canopy

vs. α_s , 1981

Figure 79: $\bar{\tau}$

Figure 80: ϕ_c

Figure 81: B:R ratio

Figure 82: $\log R$

Fig.79

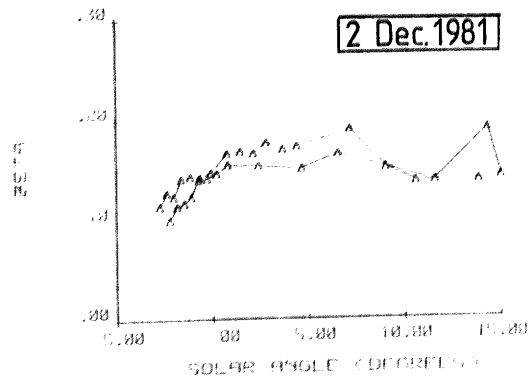
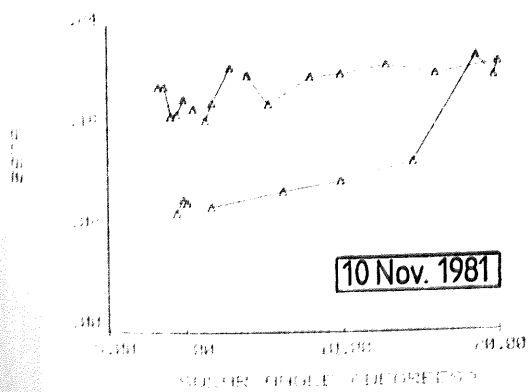
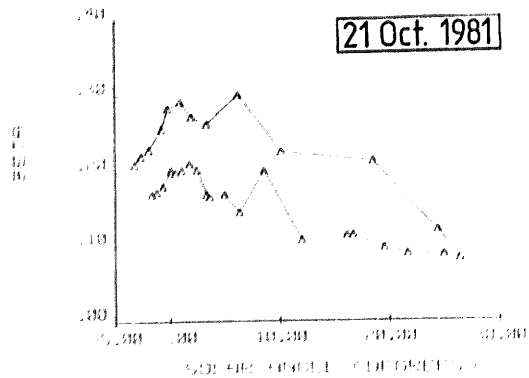
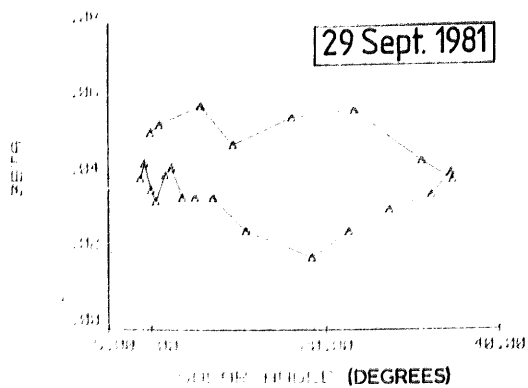
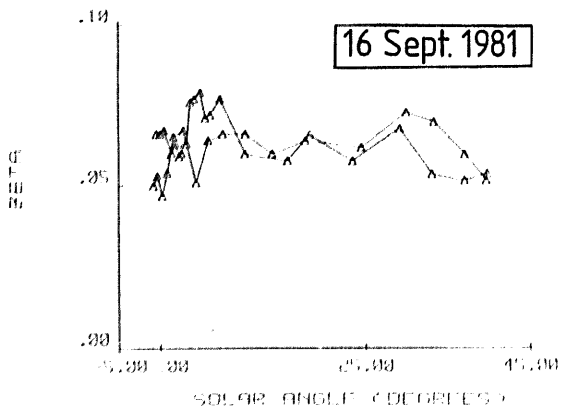
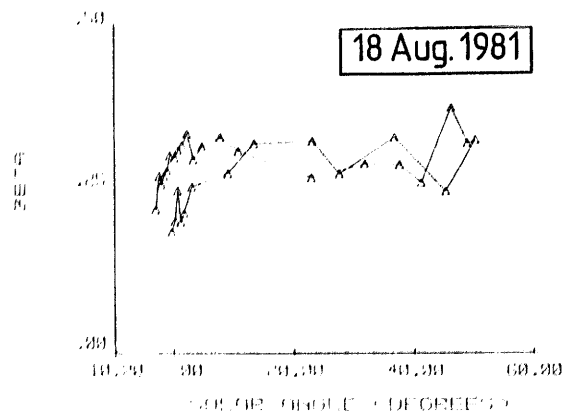
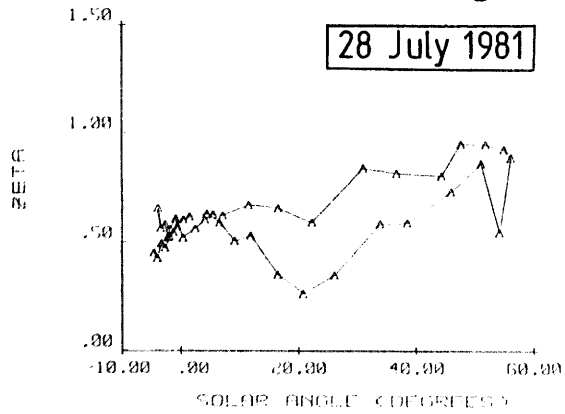
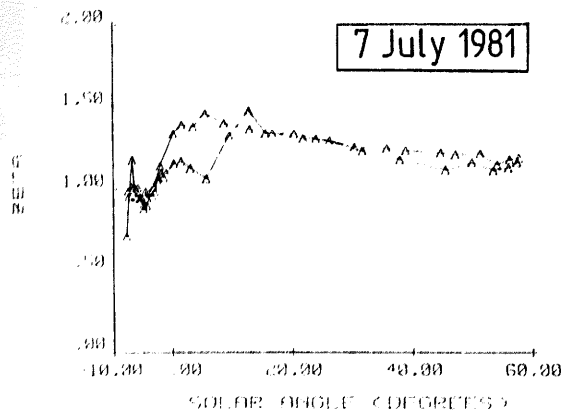


Fig. 80

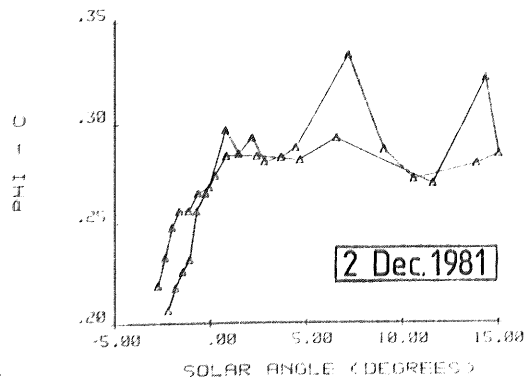
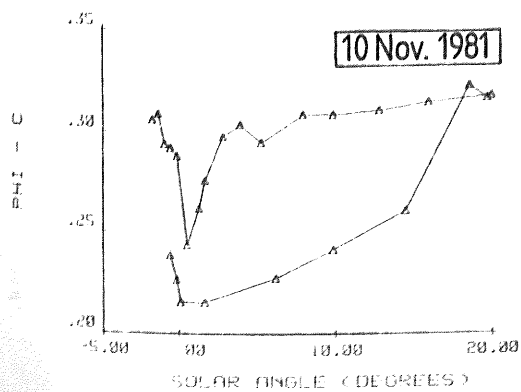
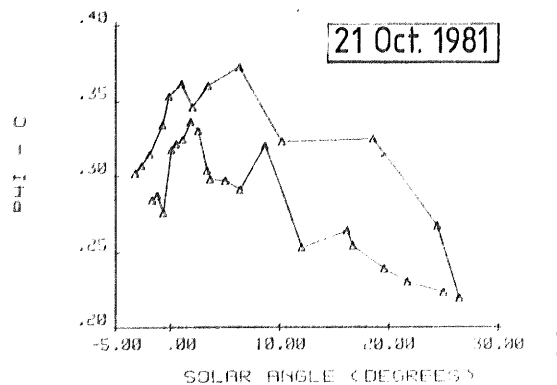
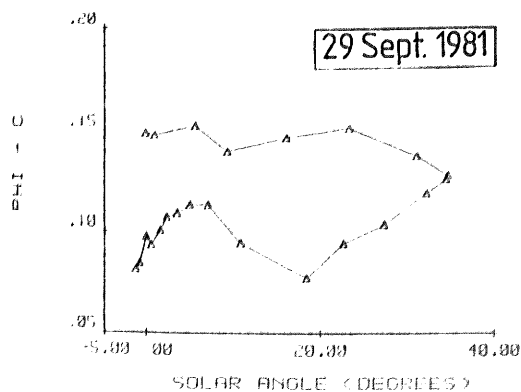
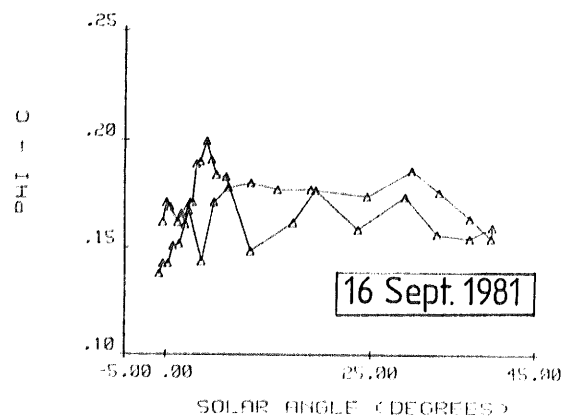
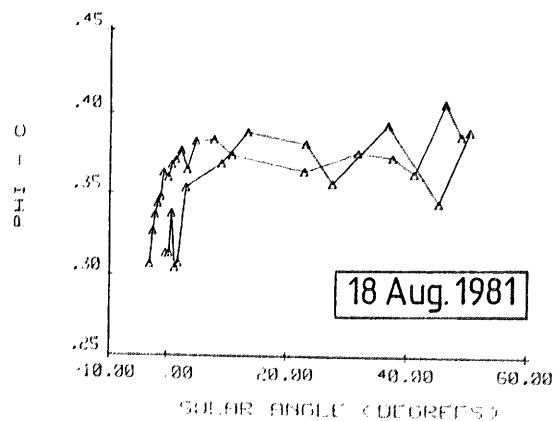
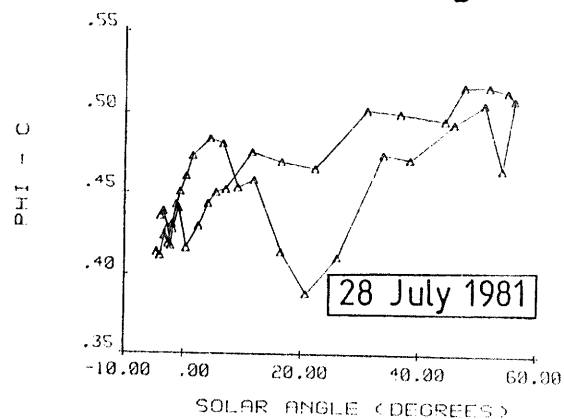
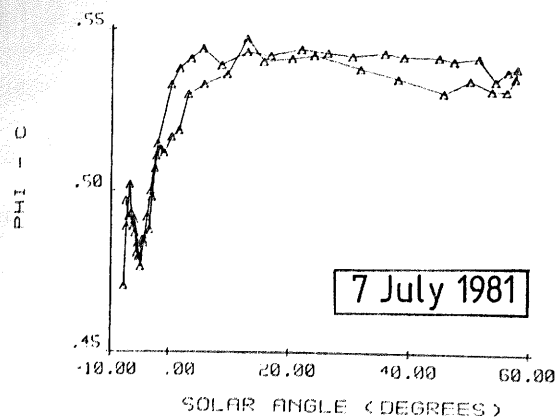


Fig. 81

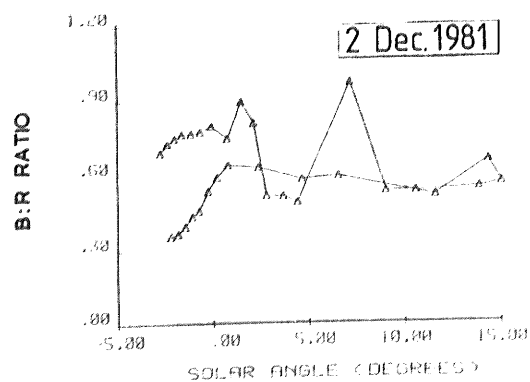
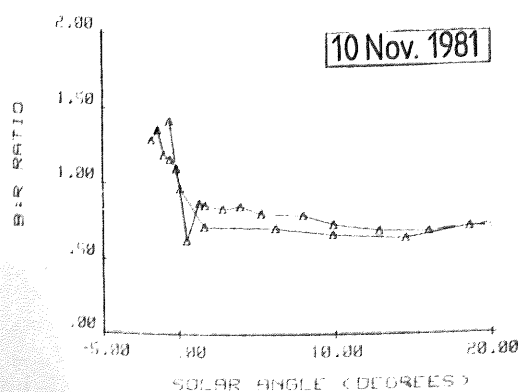
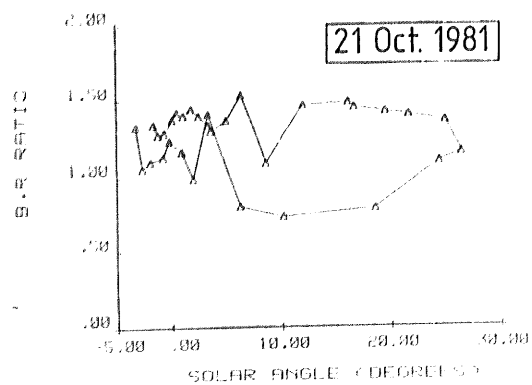
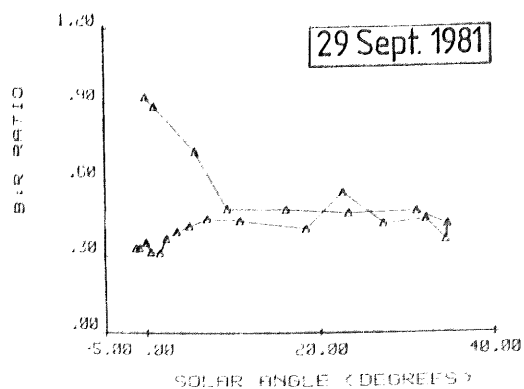
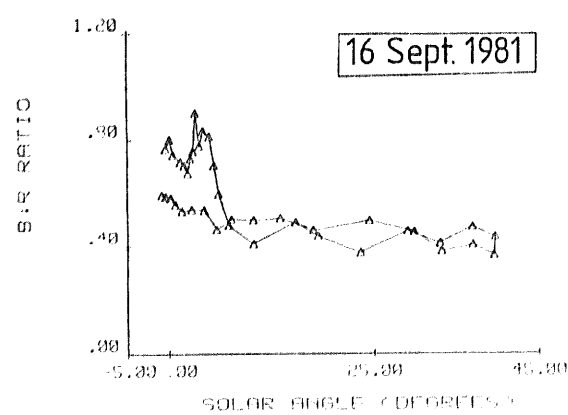
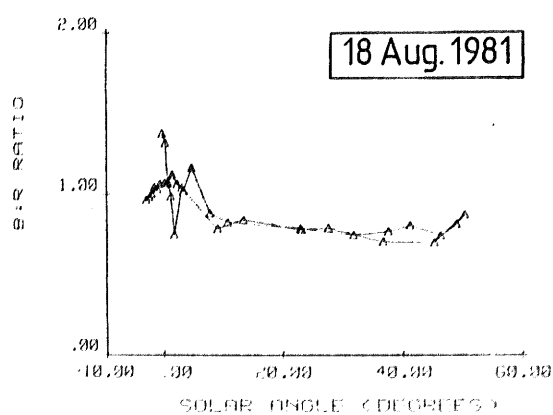
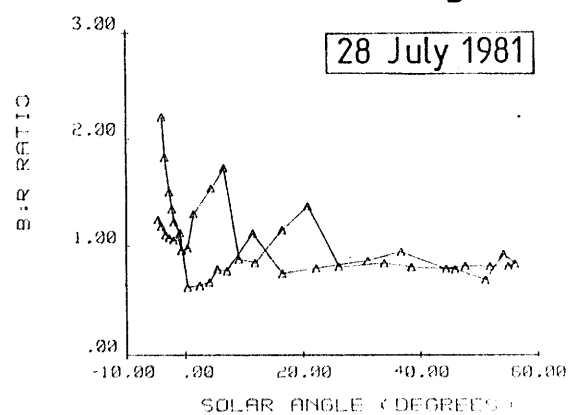
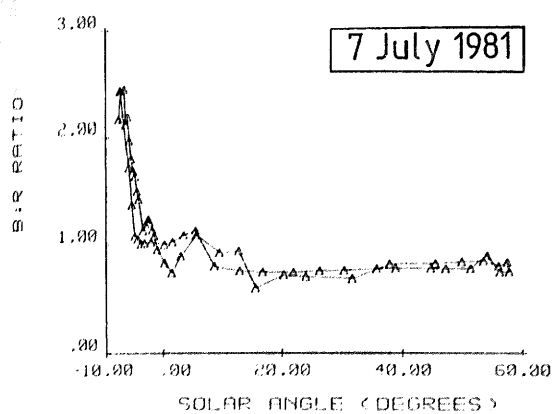


Fig. 82

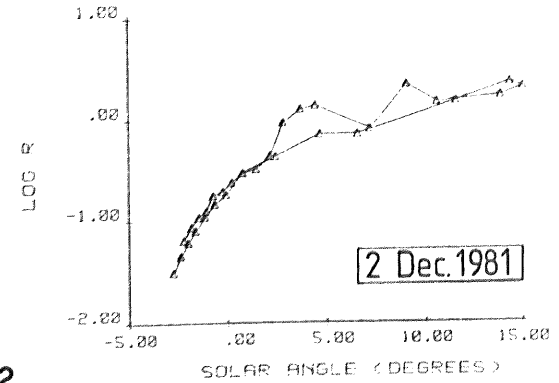
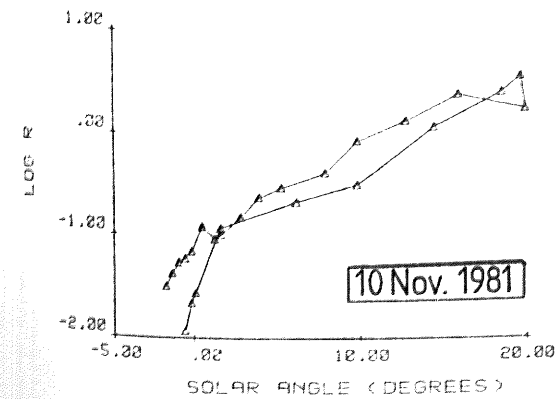
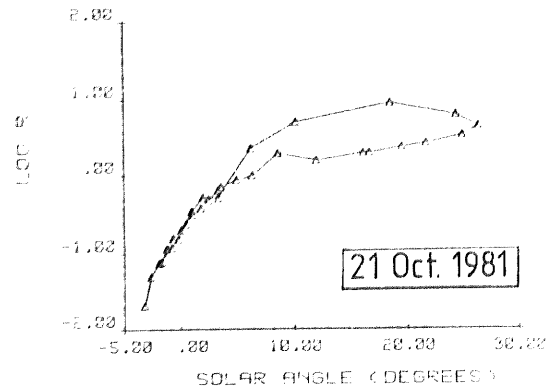
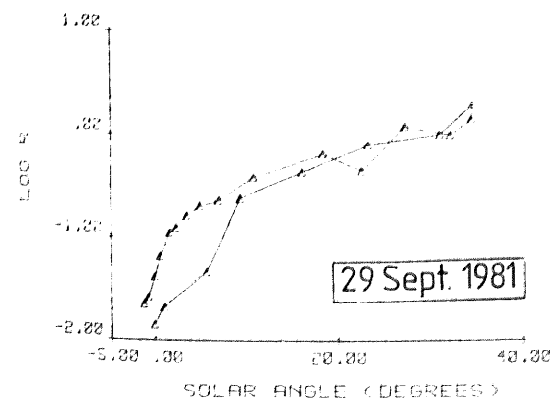
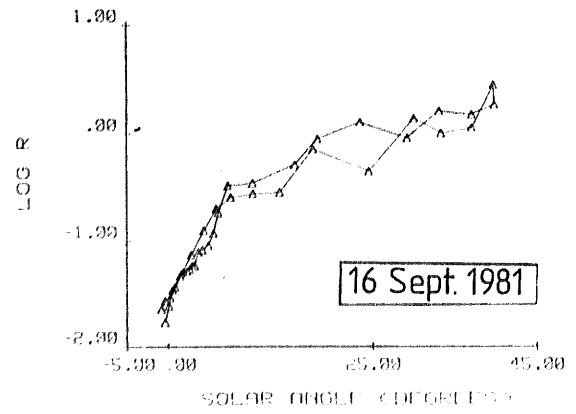
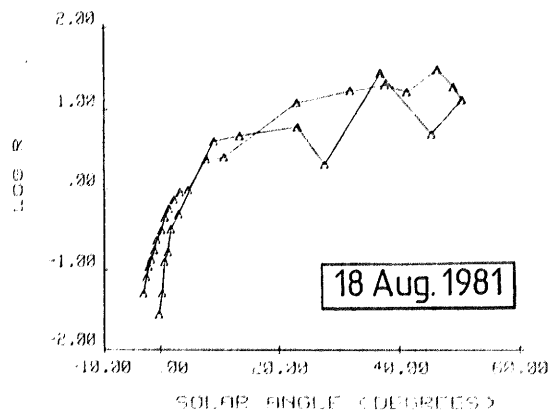
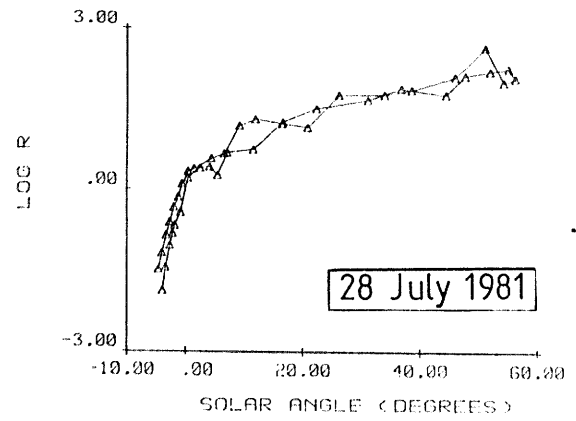
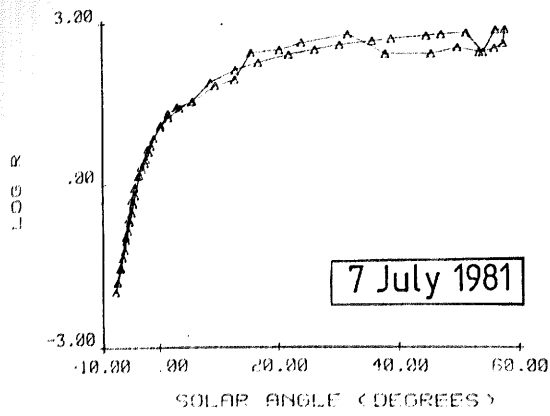


Figure 83

Mean PAR transmittance of sugar beet canopy
vs. time, Summer 1981.

Fig. 83

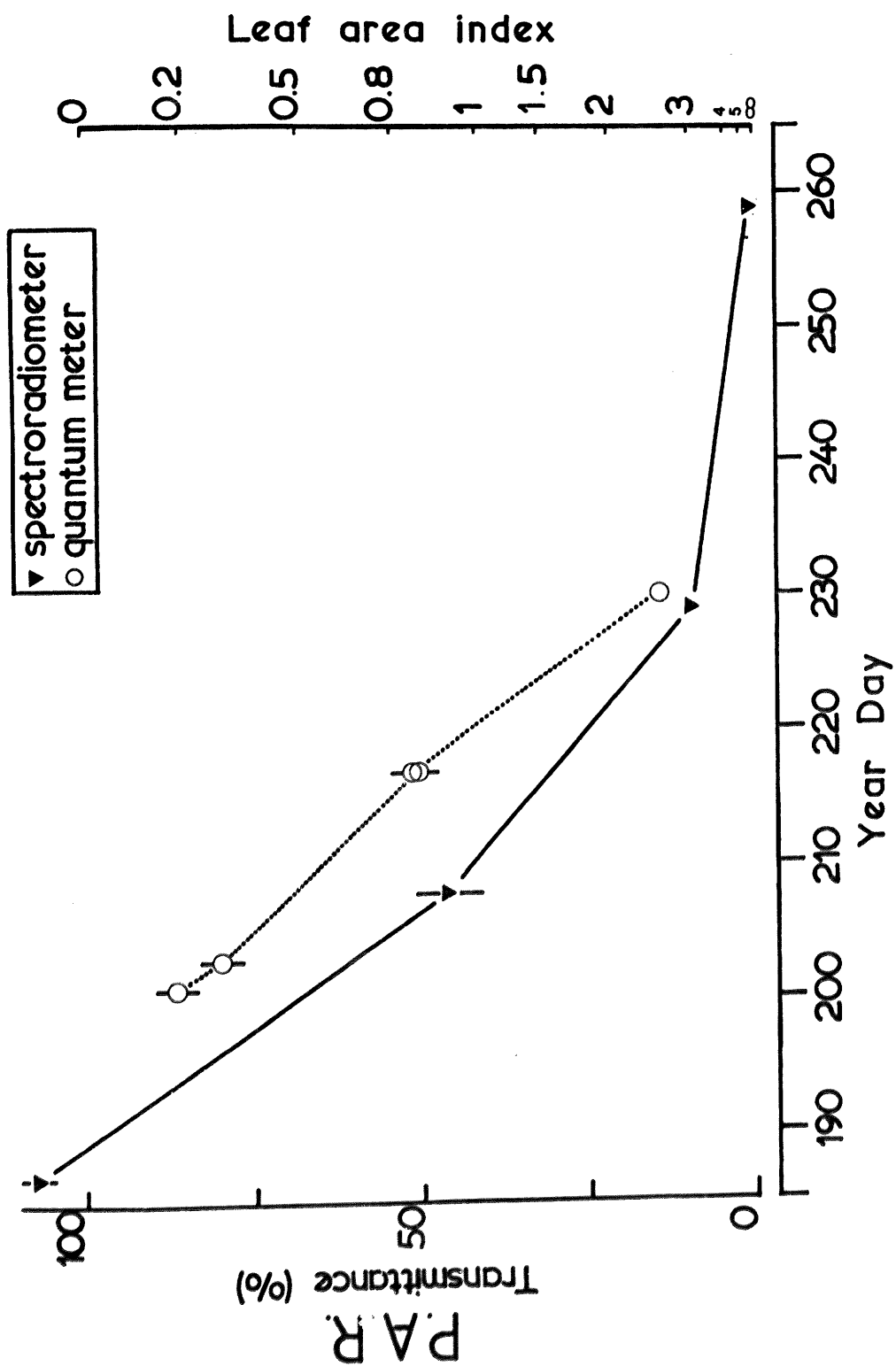


Figure 84

Seasonal changes in mean $\bar{3}$ beneath
sugar beet canopy, 1981.

(± 2 SE)

Figure 85

Seasonal changes in mean 660 : 730 nm
transmittance ratio of sugar beet canopy, 1981

(± 2 SE)

Fig.84

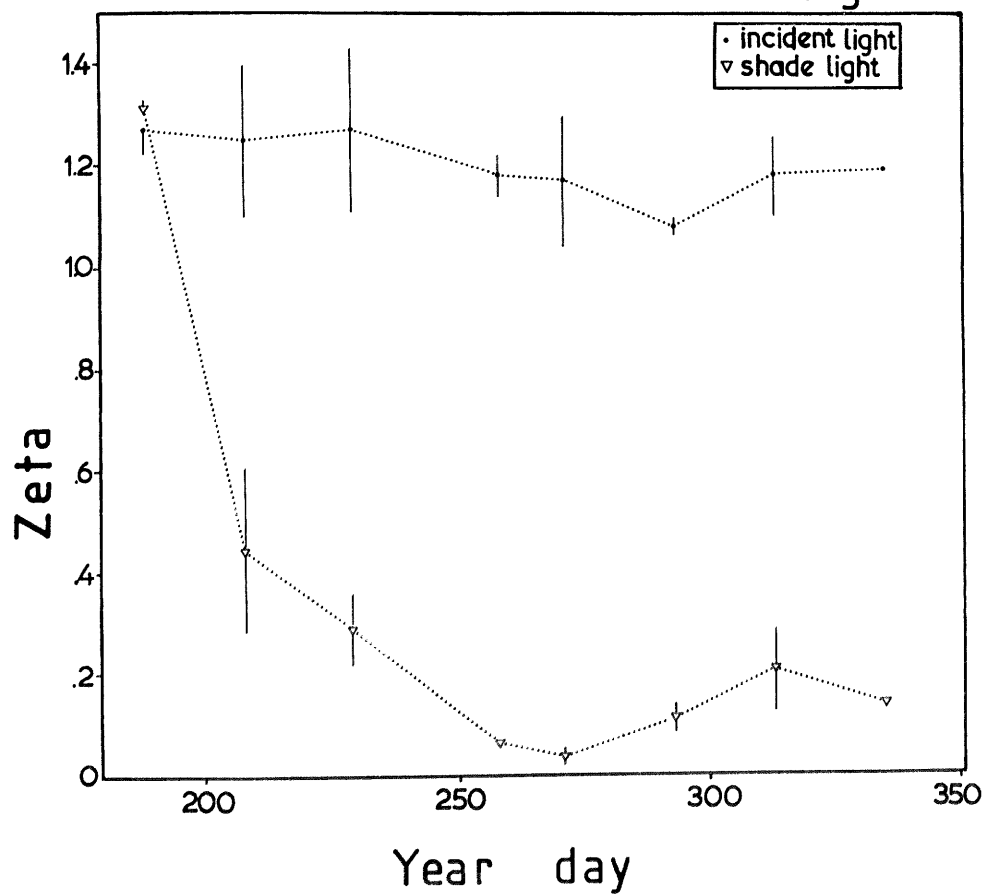


Fig.85

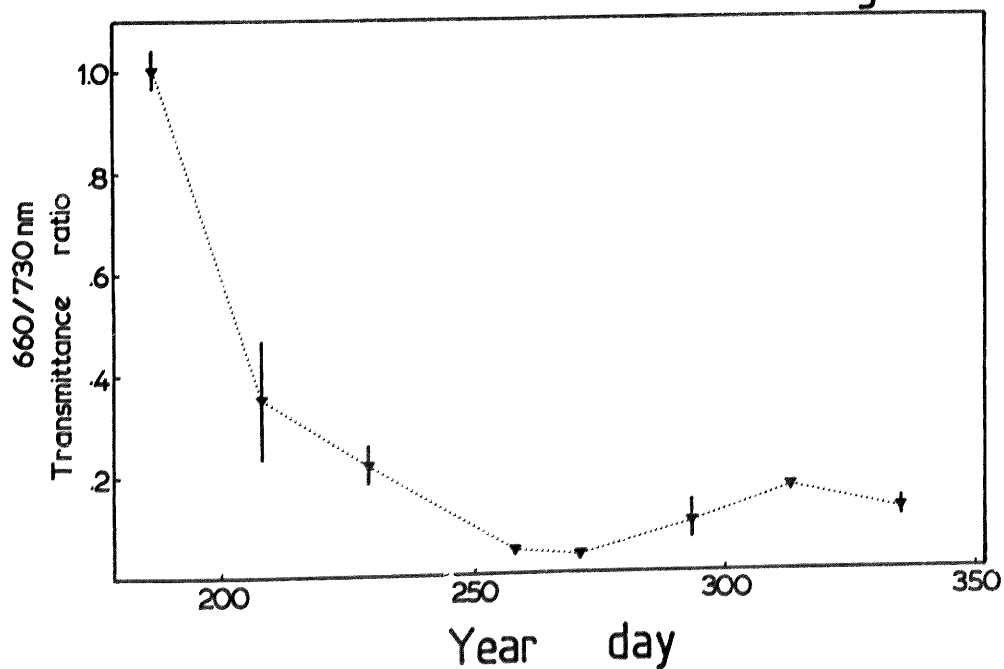
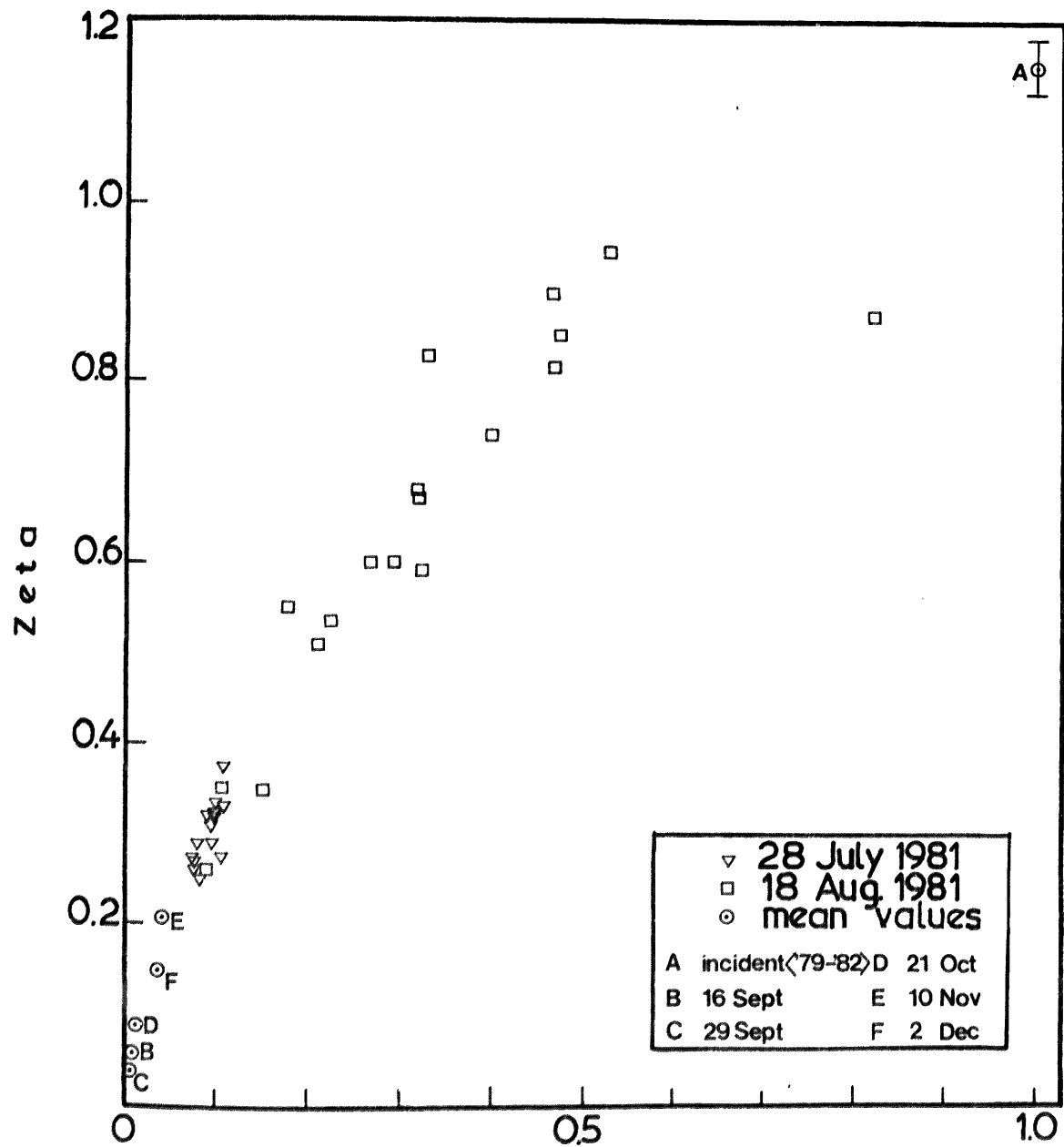


FIG. 86



CANOPY TRANSMITTANCE

(510 - 600 nm)

Sugar beet shadelight $\bar{\epsilon}$ vs. canopy transmittance to red light

CONCLUSIONS

Daylight

In most of the work reported here and elsewhere, spectral photon fluence rate is measured as that incident upon a flat horizontal surface, specially shaped to follow Lambert's Cosine Law. The principal disadvantage of this is that lateral light is underestimated relative to that from above, and upwelling light is completely ignored; there is little reason to believe this is close to the true situation in nature. Such receptors are more suited to the requirements of physics than to biology. While there is no reason to believe that plants generally absorb light equally from all directions, spherical receptors do at least take account of light from below, and have the great advantage of not requiring cosine correction.

During daytime ($\alpha_s > 7.5^\circ$), the fluence rate of incident light varied according to time and date as might be expected. The two factors acted independently. Light quality was defined principally in terms of two spectral ratios; blue : red (B:R) and red : far-red (\bar{r}). The former had a mean value of 0.86 and was significantly affected by cloud cover, being higher under overcast skies; hence, there was some variation between days of recording. Solar angle had no effect. In contrast, \bar{r} was scarcely affected by cloud cover, but significant differences are apparent between days of recording and solar angles. From the work recorded here, the mean value of \bar{r} was 1.15 ± 0.02 . There was no statistically significant seasonal trend in these data, but other sources implied that \bar{r} was lower in winter than in summer (ca. 1.0 and 1.25, respectively). Phytochrome photoequilibria, calculated on the basis of the whole spectrum and the absorbance of phytochrome in vitro, showed similar trends, with an overall mean of 0.53.

Within the oak woodland, before leaf emergence, the fluence rate was approximately half that outside, due to the interception of light by the twigs, branches and trunks of the trees. The effect was uniform at all wavelengths. Bud break at the beginning of May was accompanied by a fall in canopy transmittance and, hence, fluence rate within the wood. The selective absorbance of PAR by leaf chlorophyll lead to a large increase in the

relative proportion of far-red. Mean \bar{f} was about 0.55 (corresponding to a calculated photoequilibrium of 0.44) at the beginning of July when the transmittance of PAR had fallen to 10%. Although leaf pigment content had increased to ca 0.9 and 0.2 g m⁻² for chlorophyll and carotenoids respectively in both sun and shade leaves, leading to a fall in their transmittance, the canopy itself showed little change in its transmittance of visible light. In contrast, the average values of \bar{f} in the woodland increased significantly in August and September, before falling once more prior to senescence. This was entirely a product of changes in the red : far-red ratio of incident daylight, as the mean red : far-red transmittance ratio of the canopy was constant throughout the summer and early autumn. The correlation between canopy transmittance and \bar{f} was poor, and consequently, the capacity for phytochrome to provide information about leafy interception is probably smaller than was previously thought.

Generally, the B:R ratio beneath the canopy was lower than that outside; the equivalent transmittance ratio of the leaves themselves fell throughout the season. This was associated with a similar trend in the transmittance ratio of the canopy.

Early events in senescence were a fall in the ratio of chlorophyll a to chlorophyll b in the leaves (from ca. 3.5 to ca 2.0; the ratio in sun leaves ratio was always higher than that in shade leaves) and an increase in sunleaf reflectance. Thereafter, chlorophyll content declined rapidly, while carotenoids remained unchanged. The transmittance and reflectance of the leaves and the transmittance of the canopy increased accordingly. Similarly, \bar{f} increased and, with leaf fall, returned to the values recorded outside the canopy.

The sugar beet canopy grew rapidly during the summer months and gave rise to intense shade; during September, \bar{f} reached a minimum of 0.04 (corresponding to a calculated photoequilibrium of 0.12) and the canopy transmitted only 0.5% of the incident PAR. Thereafter, canopy transmittance increased somewhat, probably as a result of wind damage to the aging leaf population. In relation to the size of the change in the red : far-red transmittance ratio of the canopy, the variation in incident \bar{f} was small. Consequently, a close correlation between canopy transmittance and shadelight \bar{f} was observed.

Although even higher canopy densities may occur in tropical rain forest, the relationship between the LAI and the red : far-red ratio dictates that the phytochrome photoequilibrium established would be unlikely to fall below 0.1. According to Hartmann [1966], if the half life of Pfr is about 1 hour in etiolated tissue at 25°C, [Pfr] will have fallen to less than half its initial value within ten hours of exposure to such a light regime. In the oak woodland or under incident daylight, this would occur within an hour. Thus, the HIR is likely to be, at best, a transient phenomenon in the natural environment.

The transmittance spectra of the canopies never closely resembled those of the constituent leaves; generally, the spectral differences were much greater in the leaf spectra. This was probably the result of both the heterogeneous distribution of the leaves, leading to gaps in the canopy, and the scattering of light within the canopy. The same effects could explain the different transmittance properties of chlorophyll solutions and leaves.

The spectral transmittance of the canopies tended to be lower in sunny conditions than in overcast ones. The difference can be explained by the gaps in the canopy allowing a constant proportion of diffuse skylight to penetrate, but widely different proportions of the direct beam, depending on the alignment of the solar disc. Under a clear sky, canopy transmittance resembled for most of the time that which might occur when the gaps were filled. However, when the solar disc aligned with a gap, the transmittance was much higher and a sunfleck formed. The true mean transmittance spectrum (that is, one which does not discriminate against sunflecks) is likely to be closely similar under all conditions. An exception to this will occur if the solar track does not cover a representative band of the canopy. It also follows that if no gaps exist, as beneath a completely closed canopy, exposure of the solar disc should be irrelevant to the transmittance. This was found to be the case.

Twilight

The fundamental event associated with sunrise and sunset is a massive change in photon fluence rate. From sunset onwards, the rate of decline is almost exactly

logarithmic, fluence rate falling by about an order of magnitude per 2° fall in solar angle. The correlation with solar angle is very close, and in relation to this, the small day-to-day variation in fluence rate is statistically significant. The magnitude of the daily change is such that the attenuating effects of leaf development in the oak woodland, and even the growth of a dense sugar beet canopy was of small consequence. The qualitative change is similar at all wavelengths studied, and the directional sensitivity of the receptor is probably also unimportant.

Red light seems to be particularly potent in photoperiodism, and phytochrome, as well as absorbing at these wavelengths in vitro, is known at least to have the capacity to influence photoperiodic responses under certain conditions in a variety of plant species. Phytochrome may, indeed, be the only significant photoreceptor. However, the mechanism by which it could detect fluence rate remains unknown, as the present understanding of its photochromic behaviour implies that it is remarkably independent of fluence rate. Although a number of physiological responses in etiolated plants are thought to be mediated by phytochrome and yet show fluence rate dependence for some still obscure reason, this has not been observed in green plants. If phytochrome is involved in the photoperiodic detection of light and darkness in such plants, it may have at least the capacity to react to changes in light quality alone. Thus, such changes in the natural environment may be of significance in photoperiodism.

The role of blue light in photoperiodic control should be reassessed, as most experiments have been biased against this spectral region, partly because of the distortion resulting from the use of radiometric instead of quantum units, and partly because of the technical difficulty in generating high fluence rates of blue light for prolonged periods. Photoperiodic sensitivity in this region varies independently of the sensitivity to red, implying that separate photoreceptors may be involved. In addition to the possible involvement of phytochrome, cryptochrome (or some other blue light receptor) might also be active; it has often been cast in the role of a fluence rate detector. As a further complication, cryptochrome may itself be photochromic.

Thus it is possible that changes in light quality at

dawn and dusk may be relevant to, and even predominate in, natural photoperiodism; the spectral changes which occurred during twilight were considerable. Light at 550 and 710 nm tended to contribute a constant proportion of the fluence rate in the visible and far-red regions when the sun was higher than about 10° below the horizon. However, during twilight, the contribution of far-red light (above 720 nm) and blue light (particularly around 460 nm) was generally much higher with a correspondingly lower contribution of orange-red light (particularly around 600 nm). Atmospheric phenomena such as fog tended to obliterate these changes in light quality. It must be emphasised that the change was purely relative, and there was no far-red or blue "burst" at sunset. Consequently, the only likely means by which the changes could be detected is via a photochromic receptor.

The two possible light quality zeitgebers are a fall in the red : far-red ratio or an increase in the B:R ratio towards lower solar angles. The former might be mediated by phytochrome, while the latter has not been investigated physiologically. These two parameters of the incident daylight spectrum showed some variation in extent and timing in relation to solar angle on different days, but the twilight changes were sufficiently accurate to explain the capacity of plants to detect daylength in the natural environment.

The intervention of a leafy canopy had large effects upon \mathcal{J} and consequently interfered with this potential zeitgeber. However, the effect was a simple one and the actual timing and extent of the crepuscular change was not significantly affected by either the oak or the sugar beet canopy. Therefore, if this photoperiodic system were able to compensate for different levels of \mathcal{J} during the day, it might be capable of operating even below a leafy canopy. However, the wide variation of in \mathcal{J} beneath an open canopy on clear days is likely to provide the system with abundant false indications of sunset, and consequently, an efficient filtering system would be required. Even in the open, light reflected from below could have a significant effect on such a zeitgeber, and in general the spectral changes associated with twilight are directionally variable. The effect of the canopies on the B:R ratio was much smaller, but still highly significant statistically.

Thus it seems clear that fluence rate alone can act as a zeitgeber, and that the changes which occur during

Twilight would provide an accurate indication of
solar angles. In contrast, there is little
biological evidence for photoperiodic control operating
on light quality, and the changes in this during
twilight are far less reliable.

SECTION 2

Stomatal and leaf development

SECTION 2

Stomatal and leaf development

INTRODUCTION

The epidermis

The superficial cells of the plant form a specialised, relatively impermeable protective barrier against pathogenic attack, excessive water loss by evaporation and water-logging during periods of immersion. Derived from the protoderm, the primary layer consists of an almost continuous sheet of tessellated cells, the epidermis; during secondary growth woody plants replace their original epidermis with a suberised phelloderm. Because of its position at the interface between environment and organism, the epidermis is structurally and physiologically diverse (Cutter, 1979).

Whereas the epidermal cells of the root are specialised for water and mineral uptake, a primary function of the aerial epidermis is to minimise evaporative water loss, so its outer wall is usually covered by a waxy cuticle. However, the vital processes of photosynthesis and respiration require the exchange of carbon dioxide with the atmosphere via the epidermis. There is little doubt that forces of natural selection have driven plants towards reconciling these opposing necessities in various ways, but a number of physical factors hinder this; carbon dioxide diffuses more slowly than water vapour and the concentration differences driving carbon dioxide exchange are much smaller. Thus, water vapour will generally diffuse more rapidly. Furthermore, carbon dioxide molecules are larger than those of water vapour, and both molecules are quite polar and hence lipophobic. Thus, the opportunity for producing a layer differentially permeable to carbon dioxide and water vapour is very limited (Raschke, 1976), although the antitranspirant material "Mobileaf" apparently has this property (Anderson and Kreith, 1978). A further factor is that the site of evaporation is the cell wall itself, whereas carbon dioxide must dissolve and diffuse through this and the cytoplasm to reach the chloroplast.

A physiological solution to "the dilemma of opposing priorities" (Raschke, 1976) has been achieved by the development of stomatal pores in the otherwise continuous epidermis; plants are able to regulate the opening of these pores, and hence the rate of gas exchange, to best suit current conditions. Stomata are apparently absent from gametophyte thalli, but have been found in the

sporophyte structures of most mosses, the fossil psilophyte, Rhynia major, and all ferns and higher plants. They are most abundant on leaves, especially their lower surfaces (Meidner and Mansfield, 1968).

The structure and ontogeny of stomata has been discussed by Cutter [1978] and Palevitz [1981]. The apparatus consists of a pair of guard cells, often surrounded by a number of somewhat specialised subsidiary cells. The guard cells are kidney-shaped in most families, but in grasses and sedges they are elongated and dumbbell-shaped. They are joined at their ends, enclosing the stomatal pore between them. Guard cells are rich in mitochondria and chloroplasts are usually present too. Although these apparently cannot synthesise sugars from fixed carbon dioxide, cyclic photophosphorylation does occur (Outlaw, Manchester, Dicamelli, Randall, Rapp and Veith, 1979; Outlaw, Mayne, Zenger and Manchester, 1981; Zeiger, Armond and Melis, 1981).

Gaseous diffusion

The theory of gaseous diffusion into and out of leaves has been discussed by Meidner and Mansfield [1968] and Cowan and Milthorpe [1968]. Essentially, this is governed by Fick's Law (the rate of diffusion is proportional directly to the concentration gradient and the cross-sectional area of the path, and inversely to the path length). Under natural conditions the rate of water loss from a leaf by evaporation (transpiration) is seldom significantly inhibited by the presence of the epidermis when the stomata are open; on the other hand, closed stomata usually reduce transpiration to a very low level.

Following the pioneering work of Brown and Escombe at Kew, it has become traditional to consider the various constraints upon transpiration as a network of diffusive resistances and to apply Ohm's Law for the flow of current in an electrical circuit (current is proportional to the voltage applied) to the system, substituting differential vapour concentrations for voltage, and deriving an analogous proportionality constant, G , for a unit area of leaf surface. Hence

$$E = G \cdot (C_i - C_a) \quad \dots(8)$$

2.1 gaseous diffusion

where E is the rate of transpiration ($\text{mg m}^{-2} \text{s}^{-1}$)
 G is the diffusive conductance (mm s^{-1})
 C_a is the ambient water vapour concentration (g m^{-3})
 C_i is the saturation water vapour concentration at the site of evaporation (g m^{-3}).

The concept has proved very useful in analysing plant-water relations although, as in electrical theory, it is only a crude approximation to the known situation. Including capacitive elements improves the dynamic behaviour of the model (see Meidner and Sheriff, 1976), but unfortunately the extent of our understanding of electrical current flow has sometimes resulted in a teleological approach to the study of transpiration. While sophisticated electrical analogues often "prompt novel experiments", these will generally be fruitless. Negative results do not invalidate the model as the experimental technique may have been inadequate, and conversely, positive results indicate only that the analogy is potentially correct. Thus, neither possible result is helpful. Only models constructed to mimic experimental results can be useful; if the model fails, the analogy is inadequate.

Nonetheless, the concept of diffusive conductance in leaves is usually reasonable. The gaseous diffusion pathway for water vapour begins at the principal evaporation sites in the mesophyll of the leaf (cf. Meidner, 1975, 1976); diffusion from there to the stomata is a function of the mesophyll conductance. The rate of diffusion through the stomatal pore can be calculated for model pore shapes (see Cowan and Milthorpe, 1968), but no means of measuring the true stomatal conductance has been devised. Consequently, estimates of "stomatal conductance", g_s , always include mesophyll conductance. Diffusion via the cuticle bypasses both of these pathways, offering a conductance, g_c . The values of g_s and g_c are both affected by the surface structure of the epidermis (for example, by the presence of hairs). Diffusion away from the surface of the leaf offers an aerodynamic conductance, g_a , a complex function of windspeed and other factors (Sestak, Catsky and Jarvis, 1971; Monteith, 1973).

The diffusion of carbon dioxide into the leaf during photosynthesis follows a similar path in the opposite direction. However, diffusive conductances to carbon dioxide are only 60 - 70 % of those to water vapour and, additionally, the diffusion path to the chloroplasts

2.1 gaseous diffusion

includes a liquid-phase with an associated conductance, g_l' .

An estimate of g_a can be obtained by measuring the evaporation rate from a wet surface of similar size and shape to the leaf under similar conditions. g_a is then equal to G from Eq. 8; the water vapour concentration at the surface of the model leaf is a function of its temperature, while that in the surrounding air can be measured.

If a real leaf is substituted, G can be found for this and $(g_s + g_c)$ calculated from

$$1/(g_s + g_c) = 1/G - 1/g_a \quad \dots(9)$$

g_c cannot be measured directly (except when stomata are absent) but only from a minimum value of G when the stomata have been "closed" by some treatment (see below), when g_s is assumed to be zero.

Assuming such estimates to be accurate, when the stomata are open, G can again be derived from Eq.8 and

$$g_s = \frac{G \cdot g_a}{g_a - G} - g_c \quad \dots(10)$$

Conductances to carbon dioxide, G' (mm s^{-1}), in still air can be calculated from

$$G' = 0.62 G \quad \dots(11)$$

while for a turbulent boundary layer

$$G' = 0.73 G \quad \dots(12)$$

(see Sestak et al. 1971)

If the ambient and intercellular CO_2 concentrations, C_a' and C_i' (mg m^{-3}), and the net assimilation rate, A ($\mu\text{g m}^{-2} \text{s}^{-1}$), are known, it follows from Ohm's Law that

$$C_i' = C_a' - (A / G') \quad \dots(13)$$

2.1 gaseous diffusion

although mass flow of water vapour out of the leaf may reduce the true value of C_i' slightly. The concentration of carbonate ions in the chloroplasts themselves, C_p' , is controversial; although previously assumed to be negligible (Gaastra, 1959), this is now thought to be unlikely, at least in C3 species. If so, many published values of the diffusive conductance to carbon dioxide in the liquid phase, estimated from the relation

$$g_l' = A / (C_i' - C_p') \quad \dots(14)$$

are massive underestimates (Farquhar and Sharkey, 1982).

A range of typical published values for diffusive conductances to water vapour are given in the following table; figures in parentheses refer to xerophytes.

CONDUCTANCE PATH	VALUES (mm s^{-1})		MODIFYING FACTORS	
	minima	maxima	short term	long term
g_a	3	30	wind speed	leaf size
g_c	(0.03) 0.1	5	hydration	water stress
g_s	0	20	numerous	numerous
g_l'	? 1	? 5	? light	? light

The factors which influence g_s are of the utmost importance to the plant. The nastic responses of stomata regulate gas exchange in the short term (that is, over periods of less than one day) by hydraulic opening and closing of the stomatal pores; water stress can also induce a persistent hydraulic closing, often lowering the mean conductance for several days even if the stress is removed. These phenomena, have been extensively studied and are reviewed below, but long term effects on g_s have received relatively little attention, although they are possibly of great importance. These responses are morphogenic and irreversible, occurring during the growth and differentiation of the leaf.

Stomatal morphogenesis and gas exchange

In most species, as the primary divisions of the protoderm cells covering the young leaf cease, stomatal differentiation begins. Each stoma is derived from a meristemoid cell in the epidermis which divides asymmetrically to form a small "guard cell mother cell". These first meristemoids are followed by others, but similar divisions are inhibited in a zone around each. Consequently, stomata are more or less evenly spaced in the epidermis as the leaf begins to expand. In the grasses and sedges, however, stomata are formed initially at the tip of the leaf and are produced in longitudinal rows towards the base as the leaf elongates. The density and size of the stomatal pores may both be of great significance to the subsequent productivity and water use economy of the leaf.

The work of Salisbury [1927] on the ecological significance of stomatal density in the English woodland flora dwarfs that of others before and since. He recognised that one of the factors important in controlling stomatal density (stomata mm^{-2}) was the induction of meristemoids in the expanding leaf. He introduced the concept of stomatal index to define "the proportions of the ultimate divisions of the dermatogen of the leaf which have been converted into stomata."

$$\text{stomatal index (\%)} = \frac{100 S}{S + E} \quad \dots(15)$$

where, in a given area, S is number of stomata and E is the number of other epidermal cells. He also recognised that leaf expansion would affect the final stomatal density. A further factor is the primary mitotic activity of the protoderm prior to stomatal initiation.

Salisbury (*ibid.*) found that stomatal density was approximately inversely proportional to leaf area within a species, while the stomatal index was remarkably constant within each plant. In herbaceous species, since leaves tend to become smaller towards the apex, it follows that stomatal density increased towards the apex. However, the trend was also apparent in grasses, where no such change in leaf area occurs. Stomatal density generally increased towards the tips and edges of leaves. Moreover, on average, shade tolerant herbaceous species had the lowest

total stomatal density (that is, the sum of those of upper and lower epidermes), followed by marginal herbs, shrubs and finally trees (means of 90, 170, 300 and 450 mm^{-2} , respectively). Thus stomatal density tended to increase with the degree of "exposure" of the leaf. In various simple experiments, increased stomatal density was found to be correlated with water stress, probably largely because of the reduced leaf area, as stomatal index was scarcely affected. Also, in the bluebell (Endymion non-scriptus), the density change closely correlated with the ratio of total maximum pore area : leaf area (relative pore area, RPA), implying that the epidermal cells were smaller too.

Thus Salisbury refuted the idea that low stomatal density, and hence low values of the maximum attainable stomatal conductance ($g_{s\text{max}}$), lead to reduced water loss in the face of water stress. Surprisingly, the paradox that potentially high values of g_s might be associated with water stress has not been considered in the light of current views on water use efficiency. The more "exposed" leaves receive a higher photon fluence rate, and thus the potential maximum rate of carbon fixation in photosynthesis is higher. These leaves are also subject to greater wind speeds so the boundary layer conductance, g_a , would be much larger. Thus, in order to maximise the potential rate of photosynthesis, $g_{s\text{max}}$ should also increase with exposure. Lleras [1977] pointed out that very high values of $g_{s\text{max}}$ in exposed habitats would allow rapid gas exchange on the rare occasions when conditions favoured photosynthesis. Of course, increasing stomatal density is not the only factor affecting RPA; for instance maximum pore size is often correlated with leaf area (Salisbury, 1927; Meidner and Mansfield, 1968). Bjorkman et al. [1972] found that, in the sun plant Atriplex patula, stomatal density declined with fluence rate while the pores were of similar length (no leaf area data were provided).

There are few other published data on the effect of fluence rate on RPA itself, but the conflicting reports of its effect upon leaf area merit consideration here. Negative correlations between leaf area and fluence rate have been reported on many occasions, usually in shade tolerant species (for example, Blackman and Wilson, 1951; Jarvis, 1964; Lichtentalle et al. 1981; Lee and Cavers, 1981; Patterson, 1982). In contrast, positive correlations have been found in many sun plants, including Chenopodium album (Child, Morgan and Smith, 1981), Helianthus annuus

(Penfound, 1931; Dengler, 1980) and Rumex obtusifolius (McLaren and Smith, 1979). When an element of shade tolerance is present, leaf area increases as fluence rate decreases from full daylight; increased area for light absorption thus partly compensates for reduced availability and buffers the rate of biomass accumulation (see Bjorkman, 1981; data of Warrington and Mitchell [1976]). Depending on the species, there comes a point where the response cannot compensate adequately; thereafter, increased shading drastically reduces leaf area and promotes stem extension. Morgan and Smith's [1981] data for Ch. album indicate that this change occurs between 45 and 100 $\mu\text{mol m}^{-2}\text{s}^{-1}$. This has been considered a shade-avoidance reaction as the effort of the plant is reorganised in an attempt to raise the leaves above the presumed obstacle; leaf growth is reduced as an austerity measure. It is hardly surprising that obligate sun plants are the first to resort to this response. Most crops are derived from sun plants and have generally been selected for maximum yield. Consequently, they have little capacity for further leaf area increase, and reduced fluence rates can reduce yield enormously.

Blackman and Wilson's [1951] approach was more complex, involving an analysis of the ratio of leaf area : total biomass (LAR) and net assimilation rate at different levels of shading. They concluded that shade species were characteristically able to increase LAR, while it was already close to maximal in sun species. They considered that the maximal rate of biomass accumulation per unit standing biomass (relative growth rate) indicated the physiologically optimal fluence rate for the species. Although well correlated with ecological distribution, some of their results were peculiar, implying that optimal growth in some species was achieved only at fluence rates double those of summer daylight. Furthermore, Jarvis [1964] found that LAR showed only a small response to shading in Quercus petraea seedlings, despite their common occurrence in deep woodland shade. He suggested that account should be taken of the LAR values in full daylight when assessing the shade response. In any case, relative growth rate is not related to fluence rate in many stressful habitats.

Bjorkman and co-workers pioneered work on the effects of shade on the photosynthesis of ecotypes from different habitats. It has been found that "exposed" types can respond to higher fluence rates during growth by

increasing their saturated rate of photosynthesis. The apparent liquid phase conductance, g_l' , increases (Holmgren, Jarvis and Jarvis, 1965), probably because of the much higher ribulose biphosphate carboxylase activity in the mesophyll, and consequently lower C_p' (Eq.14) but this was not appreciated. Electron transport capacity may also increase. These responses are absent in most shade types but, conversely, these acclimate better to utilise low fluence rates and show lower dark respiration rates (Boardman, 1977; Bjorkman, 1981).

Such physiological diversity is in close accord with concepts of ecological strategy in ruderal and stress tolerant species (McArthur and Wilson, 1967; Grime, 1979). According to Bjorkman's scheme, the photosynthetic capacity of the leaf is reduced to "cut the running costs" and maintain a permanently low relative growth rate. Shade habitats do, however, provide occasions when light becomes abundant, and some plants may be able to acclimate physiologically to exploit these, but there are few published data in this area. According to strategy theory, such plants might be expected to show a particularly low competitive ability.

If leaf area is affected by fluence rate, stomatal densities would be expected to change, but in the simplest case where only cell expansion is affected, RPA and $g_{s_{max}}$ would remain fairly constant. However, as the capacity for carbon fixation per unit area increases with fluence rate, $g_{s_{max}}$ might usefully follow suit. While Salisbury [1927] found that changes in leaf area rather than stomatal index usually were responsible for variation in stomatal density in most woodland species, Penfound [1931] reported the reverse in the sun species, Helianthus annuus. Leaf area was unaffected by fluence rate but stomatal density was 50% lower in plants grown at about 18% of full daylight than unshaded controls. Correlation between stomatal index and fluence rate has subsequently been confirmed in other species (Schurmann, 1959; Schouch, Zinsou and Sibi, 1980). In tomato, Lycopersicon esculentum, stomatal density was inversely correlated with leaf area in expanding leaves but was constant in mature leaves irrespective of their size (Gay and Hurd, 1975).

It is therefore unsafe to assume that stomatal density is inversely proportional to leaf area in a given species and, moreover, it is doubtful whether the numerous published studies of stomatal densities or indices alone

2.1 morphogenesis

actually provide useful information about variation in $g_{s\max}$. For example, in Solidago virgaurea, although the photosynthetic capacities of the sun and shade ecotypes varied, all showed a similar increase in stomatal density and decrease in pore length at higher fluence rates (Bjorkman and Holmgren, 1963). Holmgren [1968] used the same clones and showed that although $g_{s\max}$ increased in the "exposed" ecotypes when grown at high fluence rates, this was not apparent in the shade types. Thus, while relative pore area apparently changed in both cases, $g_{s\max}$ did not necessarily reflect this. Conversely, Bjorkman et al. [1972b] showed that, in the sun plant Atriplex patula, pore length was unaffected by fluence rate during growth. Nonetheless, $g_{s\max}$ did increase with fluence rate, owing to an increase in stomatal density. Stomatal density, cell size and g_s were all strongly reduced in leaves of Sinapis alba grown at reduced fluence rates (Wild, 1979). Thus, the correlation between epidermal morphology and gas exchange physiology is poor.

Most reports of shading effects on leaf development have ignored any role of light quality. In 1974, Fitter and Ashmore showed that the shade intolerant arable weed Veronica persica responded in numerous ways to an "artificial canopy" consisting of an overhead screen of red and blue gelatin filters transmitting only far-red. Relative to control plants grown at a similar PAR fluence rate (ca. 10% of full daylight) beneath a neutral filter, leaf area was massively reduced along with LAR and the area : biomass ratio of the leaf (specific leaf area, SLA). Total chlorophyll content per leaf was unaffected. Phytochrome was thought to mediate this shade avoidance reaction (see 1.1).

Similar responses were reported for Chenopodium album and Tripleurospermum maritimum grown under incandescent lamps and fluorescent tubes (fairly low and very high Φ values, respectively) at similar levels of PAR. Here, however, the chlorophyll content declined and internode extension was massively stimulated at low Φ (Holmes and Smith, 1975). Although interpreted as a phytochrome mediated response, other factors could have been at work; in particular, the relative levels of blue light in the treatments were very different. Subsequent work therefore involved adding supplementary far-red light to a constant background of visible light from other sources. This is technically difficult to achieve as there

2.1 morphogenesis

is no efficient means of producing far-red light at an intensity comparable with that of daylight. Deitzer et al. [1979] used special discharge tubes with a far-red emitting phosphor, but high fluence rates were difficult to attain. Filters similar to those used by Fitter and Ashmore [1974], which form an effective barrier to PAR while transmitting most far-red light, have been used in conjunction with incandescent lamps to produce intense far-red light, albeit at very low thermal efficiency (Morgan, 1977; Heathcote, Bambridge and McLaren, 1979). Work using such facilities has tended to confirm that supplementary far-red light reduces leaf area, chlorophyll content and axillary growth, but increases hypocotyl, internode and petiole extension (Frankland and Letandre, 1978; McLaren and Smith, 1978; Morgan and Smith, 1978a).

The effects of fluence rate and the red : far-red ratio on each of the characters are diverse. Morgan and Smith [1981b] found little correlation between leaf area and Φ (0.15 - 4.26) or fluence rate (25 - 100 $\mu\text{mol m}^{-2}\text{s}^{-1}$); SLA increased slightly at low fluence rates, but Φ had little effect. On the other hand, while stem extension was always stimulated by far-red light, the effect was much more pronounced at higher fluence rates, indicating interaction between the two factors.

The uppermost leaves of tall plants growing in typical controlled environment cabinets are significantly closer to the light sources than those lower on the stem and hence receive higher fluence rates. Precautions against this are as essential as they are presently rare. Working on Chenopodium album, Child et al. [1981] found that leaf areas were positively correlated with plant height, and hence negatively correlated with Φ , when the plants were allowed to grow up from a fixed position. However, when the plants were lowered to keep the apex at a constant distance from the lamps, leaf areas were similar in both treatments.

Child et al. (ibid.) provided the first published data on the effects of light quality on stomatal development. One month old plants (grown at 160 $\mu\text{mol m}^{-2}\text{s}^{-1}$ PAR; 16 h photoperiod) were transferred to a growth cabinet (Heathcote et al., 1979) as the sixth leaf was expanding. Contrasting Φ levels of 0.26 and 3.43 at PAR fluence rates of 100 $\mu\text{mol m}^{-2}\text{s}^{-1}$ were maintained for a further 15 days prior to harvest. Stomatal indices, epidermal cell densities and leaf areas were unaffected in

leaves 6 and 7, as these had reached a late developmental stage before the treatment was imposed. Leaves 10 and 11 were of similar area in both treatments, but the stomatal index was much lower for both epidermes in the lower \mathfrak{J} treatment; the cell density of the lower epidermis was slightly increased, but there was no such increase on the upper epidermis. When the leaves were inverted, the morphologically upper epidermis responded even more strongly, while the other was now unaffected by the far-red treatment.

As the mean epidermal cell size was scarcely affected by the treatment, stomatal density must have declined along with the stomatal index at low \mathfrak{J} . Thus RPA was presumably much smaller, although this was not measured. Assuming that the maximum pore size on upper and lower epidermes was similar and unaffected by the treatment, $g_{s\max}$ at $\mathfrak{J} = 4.3$ would have been 80 - 90% greater than that at $\mathfrak{J} = 0.26$. However, g_s was not measured by these authors. In the same species and in Rumex obtusifolius, gas exchange techniques failed to reveal any correlation between \mathfrak{J} and assimilation rates (J.S. McLaren, unpublished data). However, in nature, Chenopodium album seldom occurs where the mean daytime fluence rate is less than $500 \mu\text{mol m}^{-2} \text{s}^{-1}$ PAR, and consequently the irradiation conditions of the experiments were quite different from those to which the species is adapted. Experimental data indicate that the interaction between the effects of fluence rate and \mathfrak{J} can be substantial (Morgan and Smith, 1981b). Clearly, while an eco-physiological interpretation of these data is premature, the possibility exists that light quality may substantially modify the rates of gas exchange. An integrated assessment of these and related problems was considered an important research area.

Nastic responses of stomata

Their ability to vary g_s rapidly over a wide range is one of the factors which have allowed plants to colonise remarkably diverse terrestrial habitats. It permits the entry of carbon dioxide into the leaf when conditions favour photosynthesis, or the conservation of water when necessary.

g_s is controlled by hydraulically closing and opening the stomatal pores. The guard cells are

2.1 nastic responses

constructed so that the vacuolar swelling associated with increased turgor causes the cells to move apart, enlarging the pore between them. The increase in turgor results partly from an active transfer of potassium ions from the neighbouring cells across the cell membranes into the guard cell vacuole. Chloride ions accompany potassium in many cases, but malate is often synthesised within the guard cells (via the carboxylation of phosphoenol pyruvate produced by starch hydrolysis) during opening, and this at least partly substitutes for Cl^- in many species (Hsiao, 1976; Allaway, 1981; McRobbie, 1981). Several lines of evidence suggest, however, that "proton" extrusion may drive potassium accumulation and the antiport of other ions, possibly by chemiosmosis (Zeiger, Bloom and Hepler, 1978). "Passive" turgor changes also occur; they result from a net gain or loss of water from the guard and subsidiary cells caused either by variations in the peristomatal transpiration rate or by the availability of water to the stomatal complex. The important mechanism by which guard cell turgor falls during stomatal closure has received scant attention.

Changes in guard cell turgor, and hence g_s , are effected by a number of external stimuli, including light, carbon dioxide concentration, humidity, water stress and temperature. These are considered below.

Light

Stomata generally are closed in darkness but open in light. Most studies of the opening reaction have shown that blue is the most potent spectral region (Mouravieff, 1958; Karve, 1961; Mansfield and Meidner, 1966; Hsiao, 1973; Zeiger and Hepler, 1977; Jarvis and Morrison, 1981; Sharkey and Raschke, 1981a). Zeiger, Field and Mooney [1981] showed that blue light is predominant in stimulating stomatal opening at dawn under field conditions and suggested that this was of adaptive significance since the high relative fluence rates of blue light before dawn might cause the stomata to open sooner and thus allow the early morning light to be utilised for photosynthesis. However, linear regression of the data in Figure 23 (1.3(ii)) shows that for red light before dawn

$$\log (\text{fluence rate}) = 0.4\alpha_s + 0.6 \quad \dots(16)$$

2.1 nastic responses

Ignoring seasonal effects, the rate of change of α_s (degrees min^{-1}) during twilight is

$$d\alpha_s/dt \approx 0.25 \cos(\text{latitude}) \quad \dots(17)$$

According to Zeiger et al., g_s starts to increase about 40 min before sunrise. Eq.17 indicates that α_s is then about -8° at that latitude. From Eq.16, even with a very high B:R ratio of 3, a given fluence rate of blue light would occur not more than five minutes earlier than the same fluence rate of red light. This would probably be of little importance; in any case, as the fluence rate of PAR is always greater than that of blue light alone, sensitivity to the latter is inherently disadvantageous. The cryptochrome system may of course have physiological advantages over the photosynthetic system here, and moreover, the stomatal response could be to the B:R ratio itself; indeed Ogawa, Ishikawa, Shimada and Shibata [1978] found that blue and red light acted synergistically in stimulating malate synthesis in Vicia faba.

Once stomata are open, similar fluence rates of either red or blue light are equally effective (Kuiper, 1964). Apart from its wavelength dependence, the "opening" response differs from the "maintenance" response in its sensitivity to carbon dioxide and inhibitors of photosynthetic electron transport, and, at least in grasses, its kinetics. Stomatal closure has seldom been studied; Roth-Bejerano and Itai [1981] suggested that phytochrome may have a role in this, but Evans and Allaway [1972] found no phytochrome-like responses in Vicia faba.

Carbon dioxide

Even in light, stomata generally close as carbon dioxide concentrations increase, whereas in darkness they can be induced to open if CO_2 is depleted. The similarity between action spectra for the maintenance of opening and for photosynthesis (McCree, 1972a) has been considered a simple reflection of this phenomenon. However, photon fluence rate and Ca^{++} act largely independently in controlling g_s (see Meidner and Mansfield, 1968) and it has recently been shown that the action of light on stomatal opening may persist when photosynthesis is inhibited (Sharkey and Raschke, 1981b). In Zea mays at least, the sensitivity and speed of the response to CO_2 is remarkably high owing to the existence of a negative

2.1 nastic responses

feedback loop which attempts to maintain a constant value of C_i' (Raschke, 1972). Why increasing $[CO_2]$ tends to reduce stomatal aperture when CO_2 is also required in malate synthesis is unknown; reduced pH may inhibit carboxylase activity, or CO_2 may act at another point in the system (Raschke, 1975a; Travis and Mansfield, 1979). C_3 plants tend to be more sensitive to carbon dioxide concentration than C_4 species, especially at elevated temperatures (see below); this is reasonable, because at any given g_s their water use efficiency is lower.

Humidity

Ambient water vapour concentration is an environmental factor to which the stomata of most species also respond. This action seems to be largely independent of water stress in the leaf as a whole. In desert-grown apricot (Prunus armenica) g_s was correlated with ambient relative humidity and was independent of leaf water potential (Schulze, Lange, Buschbom, Kappen and Evenari, 1972). This is in harmony with work on epidermal strips mounted above a small chamber of humid air, which showed that tiny jets of dry air played on the outer surface could lead to local stomatal closure; this was probably a result of rapid transpiration from the walls of the guard and nearby epidermal cells causing a loss of turgor (Lange, Lössch, Schulze, and Kappen, 1971). These initial changes occur too quickly to involve an effect on ion exchange, although later this may become significant in stabilising the altered value of g_s (Lössch and Schenk, 1978). The effects of reduced humidity often decline gradually in the long term (Hall, Camacho-B and Kaufmann, 1975).

There is some debate over the site of peristomatal transpiration. The most logical site is the outer wall of the guard or adjacent cells; areas apparently specialised for rapid evaporation have been reported (Jarvis and Morrison, 1981; Appleby and Davies, in press). Meidner [1975, 1976] has challenged this, however, suggesting that peristomatal transpiration (and most of the total leaf transpiration) occurs from the inner walls of the guard and subsidiary cells. However, ambient humidity detection via this route becomes impossible once the stomata have closed, while Lange et al. [1971] demonstrated that low ambient humidity is capable of maintaining closure for prolonged periods.

Temperature

Studies of the effects of temperature on stomata have often been confounded by indirect effects on water vapour concentration gradients. When these have been held constant, conductance generally increased with temperature up to a critical point (which is dependent on species and ambient conditions during leaf development); this is probably a means of increasing evaporative cooling. Above the critical temperature, conductance falls rapidly, possibly as a result of water stress (Hall, Schulze and Lange, 1977). Another possible factor, in C3 species at least, is the thermal stimulation of photorespiration (see Berry and Bjorkman, 1980), which increases C_p' and presumably C_i' , thereby promoting stomatal closure.

Water stress

This longer term effect on g_s generally results from the synthesis (or release) of abscissic acid in the mesophyll chloroplasts. Exogenous ABA usually induces stomatal closure within a few minutes, and it is thought that similar events follow the arrival of endogenous ABA at the guard cells. At low concentrations, recovery from the effects of exogenous ABA can occur within hours, but at higher levels the process may take weeks.

The role of ABA in controlling g_s is a matter of contention. In a factorial experiment, Mansfield [1976] showed that CO_2 and ABA acted independently in inducing closure, but other experiments have shown that ABA increases stomatal sensitivity to C_i' (Raschke, 1975b; Dubbe, Farquhar and Raschke, 1978). If this is so, ABA may act to shift the balance between the opposing priorities of maximising assimilation and minimising transpiration or, in other words, the ratio of $A:E$. This work was carried out under steady-state conditions, however, and it has been questioned whether such sophisticated control is ever achieved in a rapidly varying environment (Jarvis and Morrison, 1981). Nonetheless, control over the mean level of C_i' would still be perfectly feasible, and moreover, while very rapidly varying fluence rates do occur under cyclonic conditions and beneath leafy canopies, most plants seldom experience such events. Woods and Turner [1971] found that the speed of stomatal opening was correlated with shade tolerance in a number of tree species. The existence of feedback systems in stomatal

2.1 nastic responses

control is also apparent from their responses to transient environmental changes. If the response is slow in relation to the transient, oscillation will occur in any such system as it overshoots stable equilibrium. Such events are well known in stomatal physiology (see Barrs, 1971).

Endogenous rhythms

The final important nastic response of stomata involves the circadian variation in g_s under constant conditions following daily light-dark cycles. Such rhythms seem to persist longer under continuous light than under continuous darkness (Martin and Meidner, 1971). Circadian rhythms of sensitivity to light also occur; in plants entrained to a light - dark cycle, stomatal opening in response to light was most rapid around the usual time of "light on" (Mansfield and Heath, 1963; Mansfield 1965). Little is known of the the physiology of these phenomena.

* * *

In the second part of this work, a number of experiments were carried out in the growth cabinet described in 2.2 to elucidate:-

- 1) Which photoreceptors are active in controlling stomatal morphogenesis?
- 2) Which of the variable factors affecting stomatal density (namely, leaf area, stomatal index and protodermal cell population) are affected?
- 3) How do the morphological changes affect gas exchange?

MATERIALS AND METHODS

Growth cabinet

In order to investigate the effect of light upon stomatal morphogenesis, a "controlled environment" growth cabinet was designed and built, but to justify the considerable capital cost, the facility was intended to fulfill a number of additional requirements.

1) General features

Air temperatures should be maintained to within $\pm 0.5^{\circ}\text{C}$ despite changes in ambient temperature or fluence rate in the growth chamber. A nocturnal temperature offset should be available. Relative humidity should be maintained at a fairly high level as it is known to affect stomatal conductance, and possibly morphogenesis too. Windspeed should be sufficient to give a high leaf boundary layer conductance and to prevent large time delays in the air temperature control system. As it was intended to measure leaf gas exchange in situ, access to the growth chamber should cause little disturbance to the plants. Finally, the cabinet should be capable of operating safely and reliably for prolonged periods with minimal maintenance; it should be constructed durably with possible future adaptations in mind.

2) Special features

Many controlled environment facilities provide PAR fluence rates less than 5% of full daylight; the new cabinet should provide light levels much closer to those occurring in natural habitats. High fluence rates should be available throughout the 400 - 800 nm region, but the infra-red component above 1 μm should be minimal to reduce the heating effect. The wavebands of specific interest were PAR (400 - 700 nm), blue (410 - 500 nm), red (610 - 700 nm) and far-red (700 - 800 nm); the fluence rates of each of these should be independently variable. The growth chamber should be divided into optically isolated quarters to allow four light treatments to be maintained simultaneously. In each of these, the fluence rates in any waveband should be controllable both manually and via time switches, and should be substantially uniform both horizontally and vertically. It should be possible to lower the plants to keep their apices at a constant fluence rate throughout the growth period.

3) Constraints

Capital outlay, maintenance and running costs should be minimised, and the cabinet should be completed within 18 months of the start of the project.

The cabinet was constructed of timber and hardboard with expanded polystyrene insulation, along similar lines to the prototype "Zeta" cabinet described by Heathcote et al. (1979). In this, air at constant temperature was circulated through two optically isolated growth areas, each of which was normally divided by a light-proof but porous aluminium partition. All surfaces in the growth chamber were covered with silvered polypropylene film (Melinex, Superfine Tapes Ltd., Watford, U.K.). Lamps, filters and associated air-cooling equipment were mounted in lighting modules about 1.2 m above the floor of the cabinet. Fluorescent tubes provided PAR and incandescent filament lamps (with acrylic sheet and water filters) provided supplementary far-red light in order to depress the phytochrome photoequilibrium. Φ depends on the fluence rates of both PAR and far-red light and could not be depressed much below 0.2 at $100 \mu\text{mol m}^{-2}\text{s}^{-1}$ in the cabinet (P. ffoukes, personal communication). The Zeta cabinet was intended solely for phytochrome research, and therefore offered no control over the SPD within the 400 - 700 nm region. In order to accomplish this, the lighting modules were substantially modified in the new design.

Light Sources

Xenon arc lamps constitute an ideal source of light for plant growth, as they provide an almost uniform SPD from 350 to 800 nm at fluence rates well above those of full daylight. Unfortunately, however, few substances cause more attenuation of red than of far-red light (see below), and so Φ values greater than unity would be difficult to attain in light from a xenon arc; furthermore, the lamps and their sophisticated control equipment are prohibitively expensive. Discharge lamps or tubes are generally cheaper and produce minimal quantities of far-red light, so the Φ value of the native spectrum is already high. An independent source of far-red light can be used to depress Φ .

3) Constraints

Capital outlay, maintenance and running costs should be minimised, and the cabinet should be completed within 18 months of the start of the project.

The cabinet was constructed of timber and hardboard with expanded polystyrene insulation, along similar lines to the prototype "Zeta" cabinet described by Heathcote et al. (1979). In this, air at constant temperature was circulated through two optically isolated growth areas, each of which was normally divided by a light-proof but porous aluminium partition. All surfaces in the growth chamber were covered with silvered polypropylene film (Melinex, Superfine Tapes Ltd., Watford, U.K.). Lamps, filters and associated air-cooling equipment were mounted in lighting modules about 1.2 m above the floor of the cabinet. Fluorescent tubes provided PAR and incandescent filament lamps (with acrylic sheet and water filters) provided supplementary far-red light in order to depress the phytochrome photoequilibrium. Φ depends on the fluence rates of both PAR and far-red light and could not be depressed much below 0.2 at $100 \mu\text{mol m}^{-2}\text{s}^{-1}$ in the cabinet (P. ffoukes, personal communication). The Zeta cabinet was intended solely for phytochrome research, and therefore offered no control over the SPD within the 400 - 700 nm region. In order to accomplish this, the lighting modules were substantially modified in the new design.

Light Sources

Xenon arc lamps constitute an ideal source of light for plant growth, as they provide an almost uniform SPD from 350 to 800 nm at fluence rates well above those of full daylight. Unfortunately, however, few substances cause more attenuation of red than of far-red light (see below), and so Φ values greater than unity would be difficult to attain in light from a xenon arc; furthermore, the lamps and their sophisticated control equipment are prohibitively expensive. Discharge lamps or tubes are generally cheaper and produce minimal quantities of far-red light, so the Φ value of the native spectrum is already high. An independent source of far-red light can be used to depress Φ .

Fluorescent tubes were rejected as possible sources of PAR because of their low radiance (light output per unit area of the source); adequate fluence rates could only have been achieved using numerous closely spaced tubes, leaving little space for the other light sources. The radiance of high pressure discharge lamps is much higher, but conventional types have a very restricted spectral output. More sophisticated mercury vapour lamps incorporating traces of various metal halides have a more uniform output in the visible region. The SPDs of two types are shown in Figure 87. The spectral output of the "Kolorarc" lamps (Thorn-EMI) was much more uniform and, despite their cost (ca. £50 control equipment; £50 per lamp) these were adopted as the principal sources of PAR. Subsequently, however, dysprosium-based metal halide lamps have become available and show a further improvement in radiance and SPD.

Using appropriate filters, the proportions of different wavelengths in the visible region could be altered. In common with fluorescent tubes, Kolorarcs are well suited to work on phytochrome mediated responses, as the native SPD has a \bar{y} value between 2 and 3, giving a ϕ_r (Smith and Holmes, 1977) close to 70%, which is somewhat higher than that of daylight. This could be depressed through the daylight range down to leafy canopy levels simply by increasing the far-red supplement; there would rarely be a need to filter out far-red to increase \bar{y} .

Fluorescent lamps with an enhanced far-red output, as used by Deltzer et al. (1979), operate at low radiance and are not available in the U.K. The only alternative sources for this waveband were incandescent filament lamps. These have a very high far-red radiance and are therefore well suited to producing high fluence rates. The tungsten halogen type are particularly suitable as they are long-lived, inexpensive (ca. £5 per lamp, and no special control equipment is required), and give a relatively high output. The SPD of light from an incandescent object is dependent upon its temperature; at about 4000 K the SPFR peak lies in the far-red, but output declines gradually towards longer wavelengths, and therefore most of the energy produced would be useless. Unfortunately, 4000 K is above the melting point of all known substances, and tungsten filaments are operated nearer 3000 K (ca. 500 K below melting point) to prolong their life, giving an SPFR maximum at about 1 μ m, and leading to an even lower efficiency. Moreover, when this

2.2 growth cabinet

radiation is absorbed by a leaf, the heat produced can have considerable physiological effects; hence infra-red stop filters were used to reduce the "heat load" on the plants. The native SPD of a 117 mm 500 W tungsten halogen lamp (Phillips Ltd.) is shown in Figure 87.

The filament and Kolorarc lamps were mounted in specially built moveable aluminium lamphouses which concentrated the light downwards into the growth chamber. These and their associated filters fitted into the lamp tray in the lighting module (Fig. 88). In this, forced air-cooling was provided by a 375 W centrifugal blower producing an air flow of $1 \text{ m}^3 \text{ s}^{-1}$.

The Kolorarc lamphouses were designed to give an even, high fluence rate on the floor of the growth chamber. Within the limitations imposed by the rest of the design, the angles of the reflecting surfaces were optimised on a test rig, and the dimensions of the lamphouse were calculated accordingly. Melinex film on the inside of the lamphouses increased reflectivity and improved the efficiency of light capture. However, because the lamp was large in relation to its housing, a substantial proportion of the emitted light was reflected back to the the phosphor of the bulb and was "self-absorbed". Dysprosium lamps do not require a phosphor and hence show little self-absorption.

The filament of a tungsten lamp is relatively small, so that self-absorption need not be a problem. Commercially available chromium-plated reflectors (Sun 500, Phillips Ltd.) were used in conjunction with simple pre-fabricated aluminium housings. The light output from such a lamphouse was found to be spatially heterogeneous, however, so the reflecting surfaces were slightly deformed, using a ball-pein hammer. This radically improved the angular distribution of the light output; preliminary experiments showed, however, that close attention to the design of these surfaces could substantially improve the efficiency of light capture.

The Kolorarc lamphouses were twice as long as those for the filament lamps and upto four Kolorarcs or eight filament lamps could be accommodated above each quarter of the cabinet.

2.2 growth cabinet

Filters

The Kolorarc lamps were primarily envisaged as sources of broadband PAR but, despite the low level of far-red, their total infra-red output was significant. The filament lamps provided a powerful source of both far-red and infra-red light. Various filters were used to isolate specific spectral regions and to remove infra-red from each source.

The spectral transmittance of a wide variety of commercially available gelatin and acrylic filters was determined using a scanning spectrophotometer. The desirable features were high transmittance in the "pass" band and low transmittance in the "stop" band, with a sharp transition between them. A summary of the spectral transmittances (T) of the most potentially useful filters for photomorphogenic work is tabulated below.

MATERIAL	T < 13% at λ	T > 82% at λ	Notes
Yellow (200) "Perspex"	$\lambda < 460 \text{ nm}$ $\lambda > 2.5 \mu\text{m}$	475 nm - 2.5 μm	
Amber (300) "Perspex"	$\lambda < 520 \text{ nm}$ $\lambda > 2.5 \mu\text{m}$	560 nm - 2.5 μm	
Red (400) "Perspex"	$\lambda < 590 \text{ nm}$ $\lambda > 2.5 \mu\text{m}$	620 nm - 2.5 μm	T = 33% at 380 nm
Black PRF700 "Plexiglass"	$\lambda < 700 \text{ nm}$ $\lambda > 2.5 \mu\text{m}$	730 nm - 2.5 μm	
Deep Blue (20) "Cinemoil"	$\lambda < 390 \text{ nm}$ 520 - 700 nm $\lambda > 2.5 \mu\text{m}$	810 nm - 2.5 μm	
Blue (703) "Perspex"	$\lambda < 350 \text{ nm}$ 570 - 630 nm $\lambda > 2.5 \mu\text{m}$	690 nm - 2.5 μm	
Green (600) "Perspex"	$\lambda < 470 \text{ nm}$ $\lambda > 2.5 \mu\text{m}$	710 nm - 2.5 μm	T = 16% at 620 nm
Neutral (914) "Perspex"	$\lambda > 2.5 \mu\text{m}$		T = 55% 400 - 800 nm

2.2 growth cabinet

The only substances which absorb far-red selectively are solutions of ferrous sulphate, which are unstable, and a few cupric salts; of these, even the best (CuCl_2) absorbs strongly in the red region too (see Fig. 89). All other transparent substances absorb very little far-red light. Consequently, for work on phytochrome, the Kolorarc has an advantage over a xenon arc, in that its far-red content is small and there would rarely be any need to reduce it further.

The filters used were cut from acrylic sheet (Perspex; I.C.I. Ltd.) and small diamond-shaped separators cemented to each corner, allowing air to be passed between a number of stacked filters. In order to establish a particular SPD, appropriate filters were selected and stacked in the lamp tray, and the appropriate lamphouse was slid into place above them. Thin aluminium sheets were used to separate neighbouring light sources and filter stacks.

The transmittance of 3 mm acrylic sheet is negligible in the infra-red region above 2.4 μm , but is about 75% between 1 - 2 μm , irrespective of dye content (J.A. Keitch (I.C.I. Ltd.), personal communication). Water absorbs strongly in this region, but is almost transparent to visible and far-red light; certain special glasses also have such properties, but are very expensive. Perspex cavity windows were successfully incorporated into the prototype Zeta cabinet, water being pumped through them transversely and recirculated via a series of air-cooled copper radiators. The minimum aqueous pathlength necessary was estimated by measuring the infra-red transmittance of various depths of water in a clear Perspex tank. A tungsten halogen lamphouse was set up 150 mm above the tank, itself 1 m above a glass-domed thermopile radiometer shielded by a Wratten 88A gelatin filter (giving a spectral sensitivity range of about 1 - 2.5 μm). The transmittance of the empty tank was about 80% (close to that quoted by the manufacturer). Water was run into the tank to give a range of aqueous pathlengths upto 125 mm. The measured transmittance is shown in Figure 90. Beer's Law is not obeyed as the extinction coefficient varies through the wavelength range; in fact, the data are closely described ($r=0.997$) by the regression

$$\text{transmittance (\%)} = 64 - 25 (\log \text{depth}) \quad \dots(18)$$

Half the infra-red radiation is lost at pathlengths of

2.2 growth cabinet

only 5 nm, but 13% remains even at 125 nm. According to a Li-cor quantum meter, PAR transmittance was ca. 95% at all depths. Hence the pathlength for the cavity windows was somewhat arbitrarily set at 30 nm (25% transmittance) and they were constructed accordingly.

Growth chamber and air-conditioning system (Fig. 91)

This part of the design generally followed that of the Zeta cabinet (Heathcote *et al.*, 1979), but a number of refinements were included. A thin inner wall with an inspection window at eye-level and an access hatch were fitted inside the conventional insulated door. Plants could be manipulated even without opening the hatch door, as two large holes, guarded by flexible foam plastic flaps, formed self-sealing access routes through the door. The growth chamber was divided into four quarters (labelled NE, NW, SE and SW according to their compass bearing).

Plant pots were seldom placed on the chamber floor as the fluence rates experienced by the apex of the plant increased with height; to overcome this, pots were placed on movable shelves so that they could be lowered as the internodes extended. Figure 92 represents a surface describing the spatial variation in fluence rate in one of the cabinet quarters when illuminated by two Kolorarc lamps. These data were recorded 300 nm above the floor of the cabinet, the height at which the plant apices were maintained; the mean fluence rate 150 nm from the floor was about 6% lower, and similarly distributed.

The variation in temperature (ca. $\pm 1.5^{\circ}\text{C}$ with a 5 minute periodicity) was considered too large for gas exchange work, so the existing set-up was modified to reduce the amplitude of the oscillation. The heaters were rewired to allow 500 W to be switched in continuously, the thermistor sensor was moved from the air-conditioning inlet duct into the the growth chamber itself, and a decoupling capacitor was connected across the thermistor terminals of the temperature controller (allowing it to be operated at a higher gain without becoming unstable). Subsequently, the air temperature within the growth chamber was maintained to $\pm 0.5^{\circ}\text{C}$.

Despite considerable exchange between growth chamber and ambient air, transpiring plants tended to keep the relative humidity of the growth chamber quite high

2.2 growth cabinet

(ca. 75%) except when the total leaf area was small, during periods of darkness (when the stomata were closed), or when the ambient temperature was very low. To avoid the expense of a humidity controller, a shallow water tray was placed in the air duct, offering a surface area for evaporation of about 500 cm^2 ; this maintained adequate humidity levels.

Control and safety systems

Electricity for the cabinet was provided by a single-phase 60 A, 240 V spur. The power was distributed to the air-conditioning system and lighting modules by the switching system shown in Figure 93. The cut-out loop (13-14-15) made the lighting module "fail safe" when any of the cooling systems ceased to function properly.

Gas exchange

General

Methods for measuring leaf gas exchange were comprehensively reviewed by Sestak, Catsky and Jarvis (1971). The technique adopted here (see Fig. 94) utilised an "open" leaf cuvette into which air at constant temperature and humidity was injected. Water vapour and carbon dioxide exchange between the enclosed leaf and the cuvette atmosphere were measured by comparing the concentrations of inlet and exhaust air using appropriate gas analysers. Boundary layer conductance within the cuvette was determined (according to Eq.8) for different gas flow rates using a moist leaf replica cut out of green blotting paper.

Cuvette

The cuvette was designed to allow the "goosefoot" leaf of Chenopodium album to be accommodated with sufficient space around it to allow efficient mixing, while not introducing an undue time delay into the analysis system. Dimensions of $35 \times 70 \times 80 \text{ mm}$ (ca. 200 cm^3) were found satisfactory, and a frame was built using 1.5 mm diameter stainless steel rod. This supported an envelope of polypropylene film (Propafilm C, I.C.I. Ltd.) which has a high transmittance to both visible and infra-red radiation and thus allowed heat generated by absorbed light to be dissipated by radiative cooling at long wavelengths ($5 - 50 \text{ }\mu\text{m}$), minimising the temperature rise in the

2.2 gas exchange

cuvette. One end of the frame was left open to allow the leaf to be inserted, and the other carried a short exhaust gas pipe. Air was forced into the cuvette through four hypodermic needles (size 40-8) attached to the corners of the frame at the exhaust end, pointing towards the centre of the cuvette. Air escaped from these at high velocity, causing turbulence and efficient mixing of air in the cuvette ($ga > 14 \text{ mm s}^{-1}$); no additional stirring was necessary.

To measure gas exchange, the cuvette was set up to allow the leaf to enter the open end. The leaf was held in a horizontal position at the centre of the cuvette between a pair of trapezoidal support frames of 32 SWG stainless steel wire, attached to the cuvette frame by fine nylon threads under tension. These supports were held apart with forceps as the leaf was carefully slid into place between them; when the forceps were removed, the leaf was gently clamped in position. Taking great care not to disturb the leaf, the open end of the cuvette was then sealed with strips of "Sellotape" and a silicone rubber formulation (Silflo, Flexico Developments Ltd., London) was used to achieve a seal around the petiole.

Leaf temperature was monitored using a small ($< 0.2 \text{ mm}$) copper-constantan thermocouple junction attached to the lower support and pressed onto the leaf surface. Cuvette air temperature was measured by a similar junction 5 mm below the leaf. Reference junctions were maintained at 0°C in a vacuum flask filled with melting ice. Electrolysis at the junctions was avoided by dipping them in electronic-grade insulating lacquer (RS Components Ltd., London, U.K.) after soldering; moisture was thus excluded. Reference junctions were also protected by a layer of PVC sleeving. According to an electronic microvoltmeter (Comark Ltd., Littlehampton, U.K.) the thermocouples had a sensitivity of $24.4^\circ\text{C mV}^{-1}$; however, the need for this conventional calibration factor was avoided by altering the sensitivity of the internal amplifier to give a direct temperature read-off on the meter scale.

Air supply

Initial experiments indicated that the rate of photosynthesis typical of an expanded Chenopodium album leaf under growth cabinet conditions required a flow rate of about $1 \text{ dm}^3 \text{ min}^{-1}$ to give a CO_2 depletion of about

2.2 gas exchange

20 ppm at $300 \mu\text{mol m}^{-2} \text{s}^{-1}$ PAR. Gas exchange measurements over a period of many hours thus required large volumes of air at constant temperature, humidity and CO_2 concentration.

To this end, air was drawn from outside the building via a 50 dm^3 buffer chamber into a humidification system. In this, a pump (model P65; Charles Austin Ltd.) was used to circulate air rapidly between a copper heat exchanger situated in the air-conditioning duct of the growth cabinet and a large humidity-buffering column. This contained a saturated solution of magnesium nitrate, giving a relative humidity of about 50%, and was constructed from a 1 m length of 110 mm domestic polythene drain-piping and various gland connectors (Osma Ltd.). These materials were inert to the concentrated salt solution, gas tight, inexpensive and robust. The surface area for equilibration between the air bubbles and the solution was increased by loosely filling the base of the column with expanded polystyrene chips. Air bubbles carried these up the column as far as the funnel of the reflux pipe; the solution trickled over the edge of this and was returned to the bottom of the column. A number of baffles and a glass-wool filter prevented droplets of solution leaving the column. Changes in column temperature were reduced by placing it in an insulated enclosure maintained at 28°C ; the return pipe from the heat exchanger was well lagged. It was important to maintain the column close to atmospheric pressure, as departures from this affected humidity and encouraged air leaks. The arrangement adopted fulfilled this requirement and ensured that the air outlet was slightly above atmospheric pressure and delivered air close to equilibrium with the salt solution. This outlet supplied air to the reference line of the gas analysis equipment and to the cuvette via a $0 - 1000 \text{ cm}^3 \text{ min}^{-1}$ flow gauge (Cap Ltd., Basingstoke, U.K.). In order to overcome the resistance imposed by the injection needles, the air was pressurised by a small pump; the flow rate into the cuvette was controlled by a bypass needle valve.

Gas analysis

Air was drawn from the cuvette exhaust by a small pump and fed through a dew-point hygrometer (Type 1100AP, General Eastern Corp., Watertown, U.S.A.) and an infra-red CO_2 gas analyser (IRGA; Mk.II, A.D.C. Ltd., Hoddesdon, U.K.) set up in differential mode. As the humidity of the

2.2 gas exchange

reference air tended to vary slowly, this was measured hourly; a time-switch controlled two solenoid valves, which alternated the analysis air line between the sample and reference air lines. This also allowed any zero drift in the IRGA to be detected.

The hygrometer and IRGA readings were generally recorded on a single-pen Servoscribe chart recorder, as a twin pen instrument was not always available. Each "channel" was recorded alternately using an electronic astable switch, the circuitry of which is shown in Figure 95; all components were supplied by RS Components Ltd. A conventional mains power pack supplied 18 V.D.C. to a "555" integrated circuit timer, the cycling rate being determined by the charging rate of the two 10 μ F low-leakage capacitors. The hygrometer or IRGA input channel was connected to the output (and hence the chart recorder) by a change-over relay which also lit the gallium arsenide light-emitting diode corresponding to that channel. The relay was controlled via a function switch, allowing either manual switching between the channels or automatic cycling by direct connection to the output of the timer. Since the output signal from the hygrometer was approximately 30 dB higher than that from the IRGA and the range of recorded values was quite different (10 - 25°C and -10 to +30 ppm, respectively), attenuation and offset controls were built into the switch circuit.

Water vapour concentrations (g m^{-3}) were calculated from the saturation vapour pressures (mbars; from Smithsonian Tables) at leaf or dewpoint temperatures (K) according to

$$[\text{H}_2\text{O}] = (217 \cdot \text{vapour pressure}) / \text{temperature} \dots (19)$$

(Monteith, 1973).

The water vapour content of the sample and reference air lines could be measured within $\pm 2\%$ and CO_2 depletion estimates were accurate to about $\pm 2 \text{ mg m}^{-3}$. The ventilation rate of the cuvette was accurate to only $\pm 10\%$, however, because of the pressure variation produced by the pump.

2.2 experimental techniques

Experimental techniques

A series of experiments were carried out to investigate the effects of light on leaf morphogenesis and gas exchange in the ruderal weed species Chenopodium album L. Preliminary experiments with the shade tolerant species Circaea lutetiana L. indicated that, although the stem extension response to far-red light was small, leaf development was massively affected. However, seed collected locally showed low viability, and mortality amongst young seedlings was high; consequently, the intended comparative study of the photoresponses shown by the contrasting species was unsuccessful.

Seed was collected from mature Ch. album plants growing locally on arable land. Dormancy was removed by freezing at -5°C for several weeks. When required, seed was sown in small trays containing Levington Universal compost and covered with ca. 2 mm of fine sand. The compost was kept moist and the seedlings grown up in the cabinet under Kolorarc lamps (16 h photoperiod; constant 20°C in all experiments). Precocious individuals from immature seed appeared within a few days, but these were pricked out and only seedlings from the main phase of germination were used. After ca. 25 days, 20 - 30 uniform seedlings were carefully selected and transferred to individual 7 cm pots containing John Innes No.1 compost. After two days, when the seedlings had recovered from this disturbance, non-uniform individuals were discarded and 3 - 7 of the rest randomly placed in each quarter of the cabinet.

The experimental light treatments were designed to investigate the role of PAR, blue and far-red fluence rates in stomatal development and physiology. Although phytochrome photoequilibria in etiolated tissue are closely related to the red : far-red fluence ratio, current spectrophotometric techniques are unable to detect phytochrome in green plants (see 1.1), and so the actual values of ϕ established within the tissue of the experimental plants were unknown. The effective value of ϕ in green tissue is thought to be simply related to that in etiolated material (Morgan and Smith, 1978a) and it is possible to predict this value for any light source from either \bar{S} (Smith and Holmes, 1977) or the SPD as a whole (Tasker, 1977), yielding ϕ_e and ϕ_c respectively. As ϕ_e is unreliable in the presence of high fluence rates in the 680 - 710 region, ϕ_c was preferred.

2.2 experimental techniques

The values of ϕ_c for several of the growth treatments were checked by a direct spectrophotometric assay of crude phytochrome extracts. 4 day old etiolated oat coleoptiles were harvested and homogenised in cold tris/HCl buffer (pH 7.7; equal weights of tissue and buffer). The bris was passed through several layers of muslin, made 10 mM with respect to CaCl_2 and stirred slowly for 20 min. The extract was then spun at 20,000 g for a further 20 min. The supernatant was made up to 20% NH_4SO_4 by slowly adding the powdered salt while stirring. After this, the extract was spun at 16,000 g for 10 min and the supernatant discarded. The pellet was stored at -15°C until required. All operations were performed at 5°C under a dim green safelight at the Department of Botany, University of Leicester. Pellets were resuspended in 5 cm³ of 50 mM tris/HCl buffer at pH 7.5, decanted into cuvettes and exposed to the light environment of the growth chamber for 1 min in order to photo-equilibrate. After this, they were wrapped in situ in aluminium foil, placed on ice and rapidly transported to the Leicester laboratory where ϕ was measured using a Perkin Elmer 156 dual wavelength spectrophotometer set at 660 and 730 nm (see Smith, 1975). The rate of Pfr loss at 0°C was estimated by measuring the decline in ϕ following a saturating red pulse. After this was taken into account, the measured value of ϕ was generally very close to ϕ_c .

The plants were watered when the surface of the compost became dry to the touch and always before any signs of wilting were apparent. The shelves were lowered 2 cm at a time in order to maintain a constant fluence rate at the apices and the plant positions were randomised every other day. Most morphological and gasometric measurements were made after about 3 weeks growth in the various treatments.

Morphology

Routinely, internode length, total height and leaf areas were measured. Chlorophyll was determined according to McKinney's method (see 1.2). Stomatal counts were made using one of two methods. Usually, leaves were placed in vials containing a concentrated solution of chloral hydrate which destroyed the chlorophyll and slowly loosened the attachment between mesophyll and epidermis, allowing considerable areas to be peeled off easily. These epidermal strips were then stained in aqueous Ruthenium

2.2 experimental techniques

Red, which binds to the pectins of the epidermal cell middle lamellae and the guard cell walls, and mounted in 20% glycerol. Alternatively, Silflo was painted onto the intact leaf to form a cast of the surface structure; microrelief replicas were made in clear nail varnish.

A projection microscope was used to count the numbers of unspecialised epidermal cells and stomata in 10 to 20 randomly selected 0.132 mm^2 fields. An edge correction was always applied and the preparations were assayed at random. The stomatal population on each epidermis was calculated from leaf area and stomatal density (SD); epidermal cell population was derived similarly using the total cell density (CD, stomata being counted as one cell). Stomatal index (SI) was calculated for each field rather than from mean densities. To give some indication of changes in maximum stomatal pore size, the axial dimensions of 20 guard cell pairs were measured and their area calculated assuming an elliptical shape.

Initial counts showed that the stomatal density was most homogeneous between the midrib and the principle lateral vein of the lamina; all subsequent counts were confined to this area. Figure 96 shows the variation in stomatal index and density along transects of a typical leaf surface. Although the upper epidermis shows little general trend, there is a pronounced decline in SD towards the tip and edge on the lower epidermis.

Gas exchange

Preliminary experiments indicated that good resolution of g_s required a difference in dewpoint between the inlet and exhaust air lines for the cuvette of at least 1°C , corresponding to flow rates of $500 - 1000 \text{ cm}^3 \text{ min}^{-1}$ for the fairly low transpiration rates found to be typical of Chenopodium. In any case, a flow rate of at least $400 \text{ cm}^3 \text{ min}^{-1}$ was required along the sample line, as slower rates led to very slow hygrometer response times ($> 10 \text{ min}$). Accurate measurements of g_s using moist leaf replicas were difficult at such low flow rates because the water vapour content of the exhaust air approached saturation. This problem could be largely eliminated by supplying the cuvette with dry air for g_s estimates, but the consequent high evaporation rates caused substantial cooling of the "leaf" (ca. 2°C below ambient). Such a temperature difference modifies the assumptions on which Eq.8 is based, and thus unknown

2.2 experimental techniques

errors were associated with the estimates of g_a , which ranged between 14 and 20 mm s^{-1} . In any case, the derivation of g_a was based on an assumed value of C_a halfway between cuvette inlet and outlet water vapour concentrations; this may have been only a crude approximation to the actual effective value, especially at high transpiration rates.

Cuvette air and leaf temperatures were $20 \pm 2^\circ\text{C}$ and did not differ by more than 1°C . At this temperature, C_a generally corresponded to a relative humidity of about 50% at average transpiration rates. A mean CO_2 concentration of 340 ppm (670 mg m^{-3}) was assumed (A. Buckenham, personal communication). Prolonged darkness following water-stress produced transpiration rates below the sensitivity threshold of the system (ca. $3 \text{ mg m}^{-2} \text{ s}^{-1}$), so g_c was assumed to be zero. C_a in Eq.8 was calculated as the mean of the inlet and outlet concentrations. Photosynthesis was estimated to ca. $\pm 30 \mu\text{g m}^{-2} \text{ s}^{-1}$, transpiration to ca. $\pm 15\%$, g_s to ca. $\pm 20\%$ and C_i' to ca. $\pm 30 \text{ mg m}^{-3}$.

Figure 87

Relative SPDs of light sources
(arbitrary vertical scale)

(A) Incandescent tungsten-halogen filament lamp

(B) Phillips metal halide lamp

(C) Thorn metal halide ("Kolorarc") lamp

Fig.87

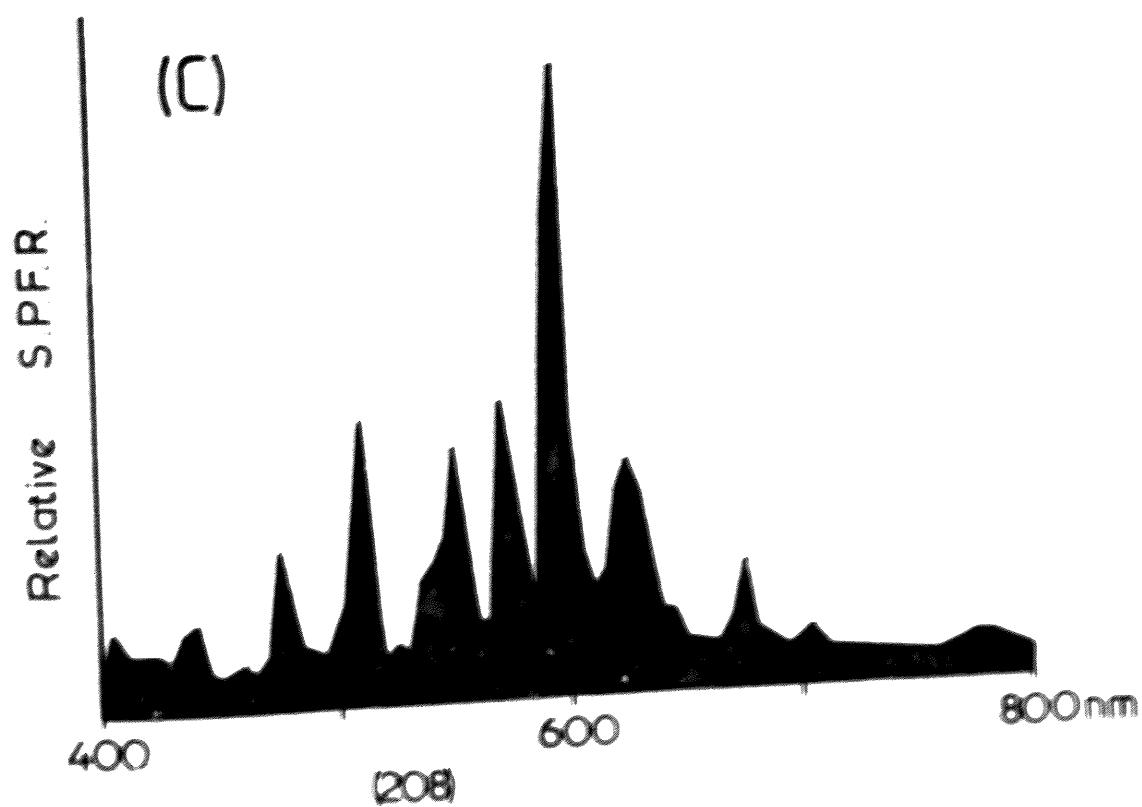
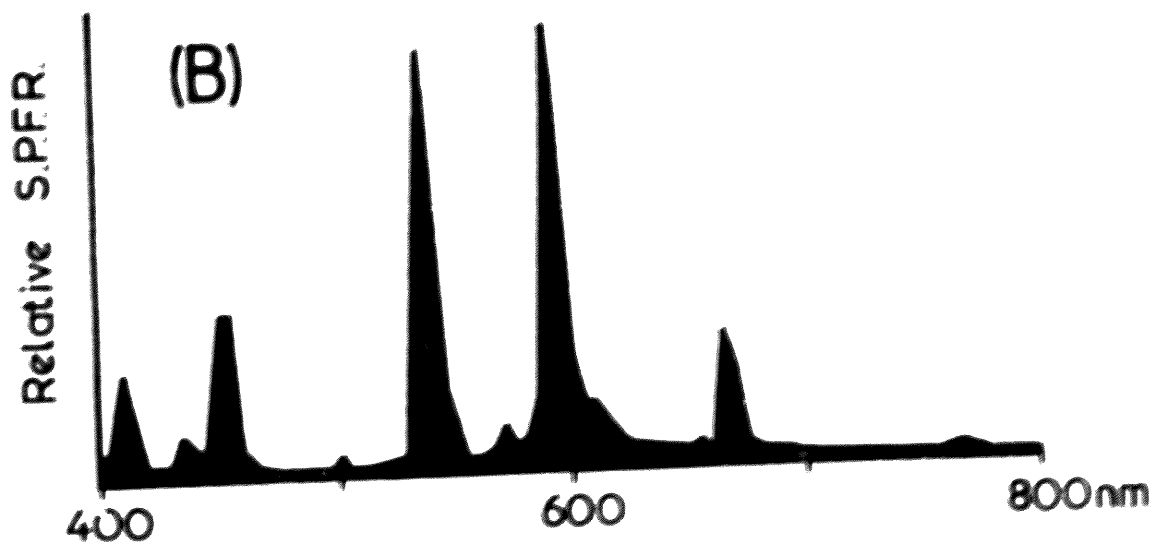
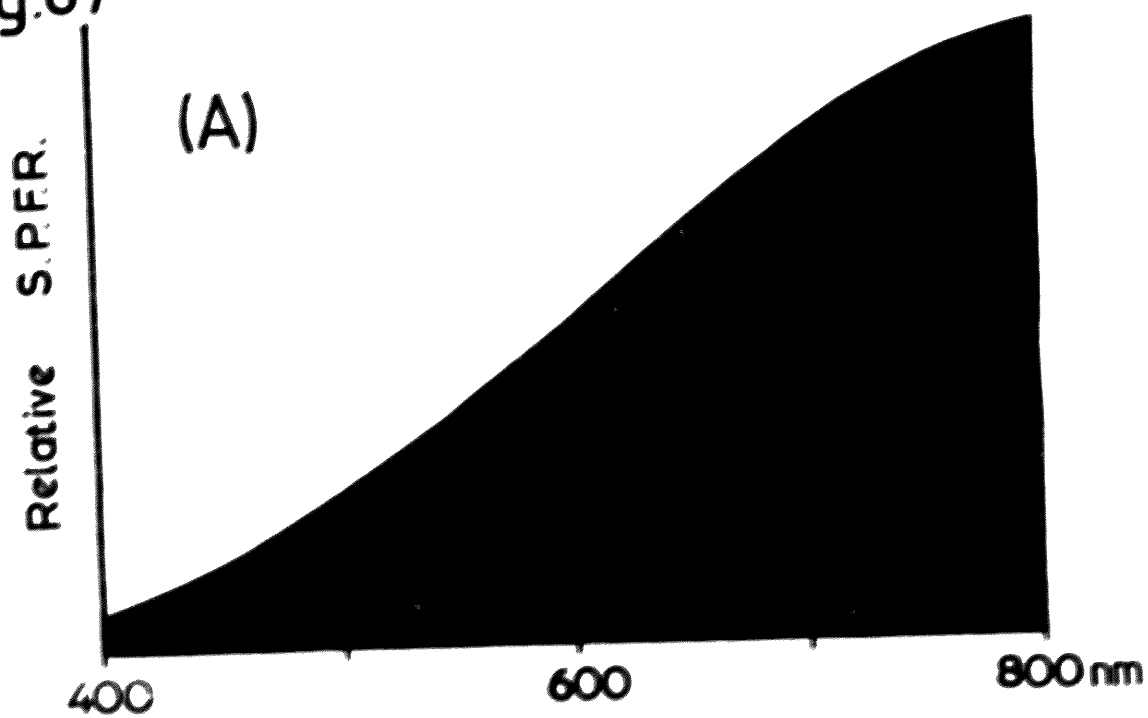
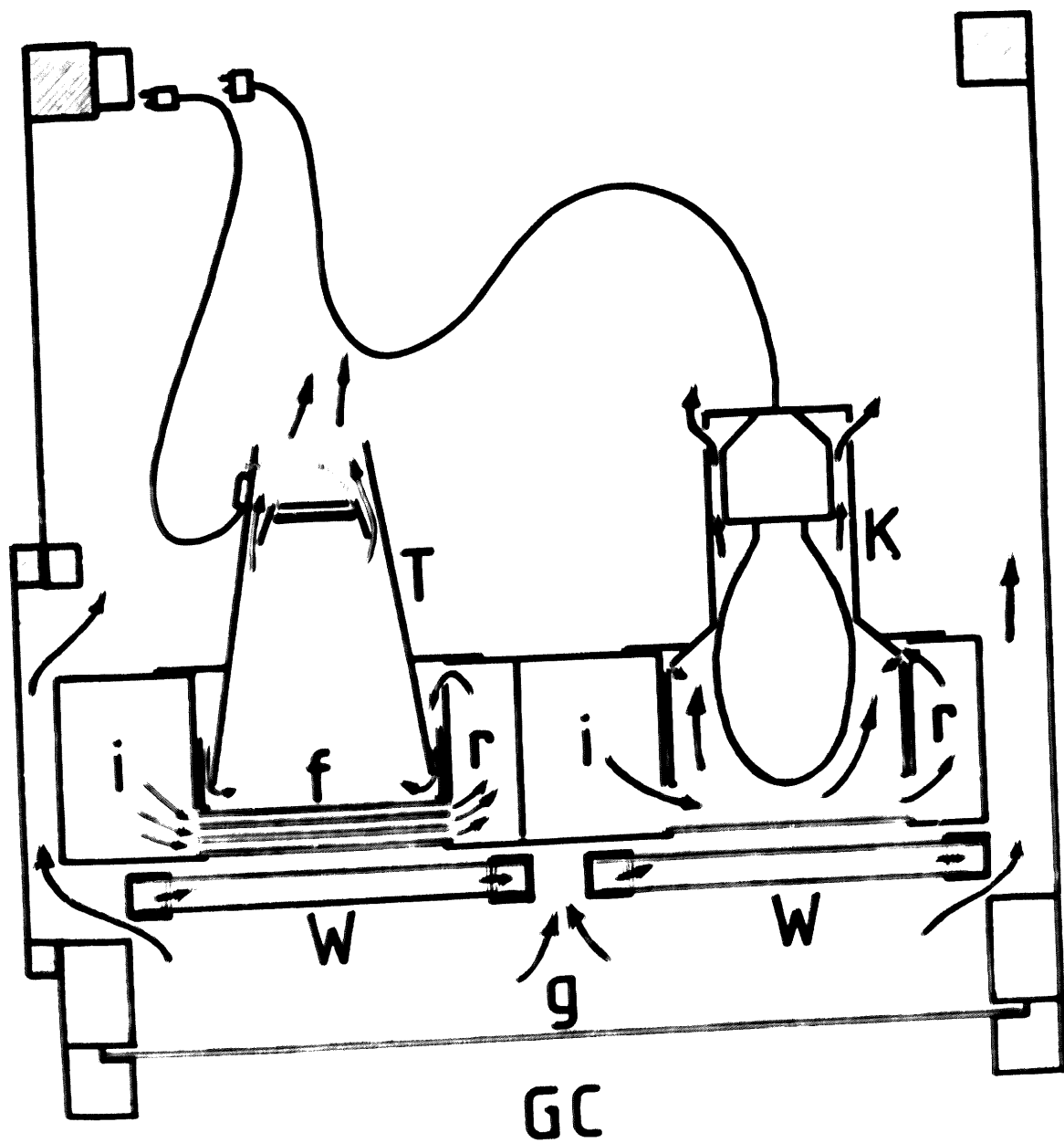


Figure 88

Diagram of lighting module (to scale)

- i** inlet air duct
- r** return air duct
- f** filter stack
- g** glass sheet (3 mm window glass)
- GC** growth chamber
- T** tungsten-halogen lamp house
- K** Kolorarc lamp house
- W** water cavity window
- direction of air or water flow

Fig. 88



0.1m

Fig.89

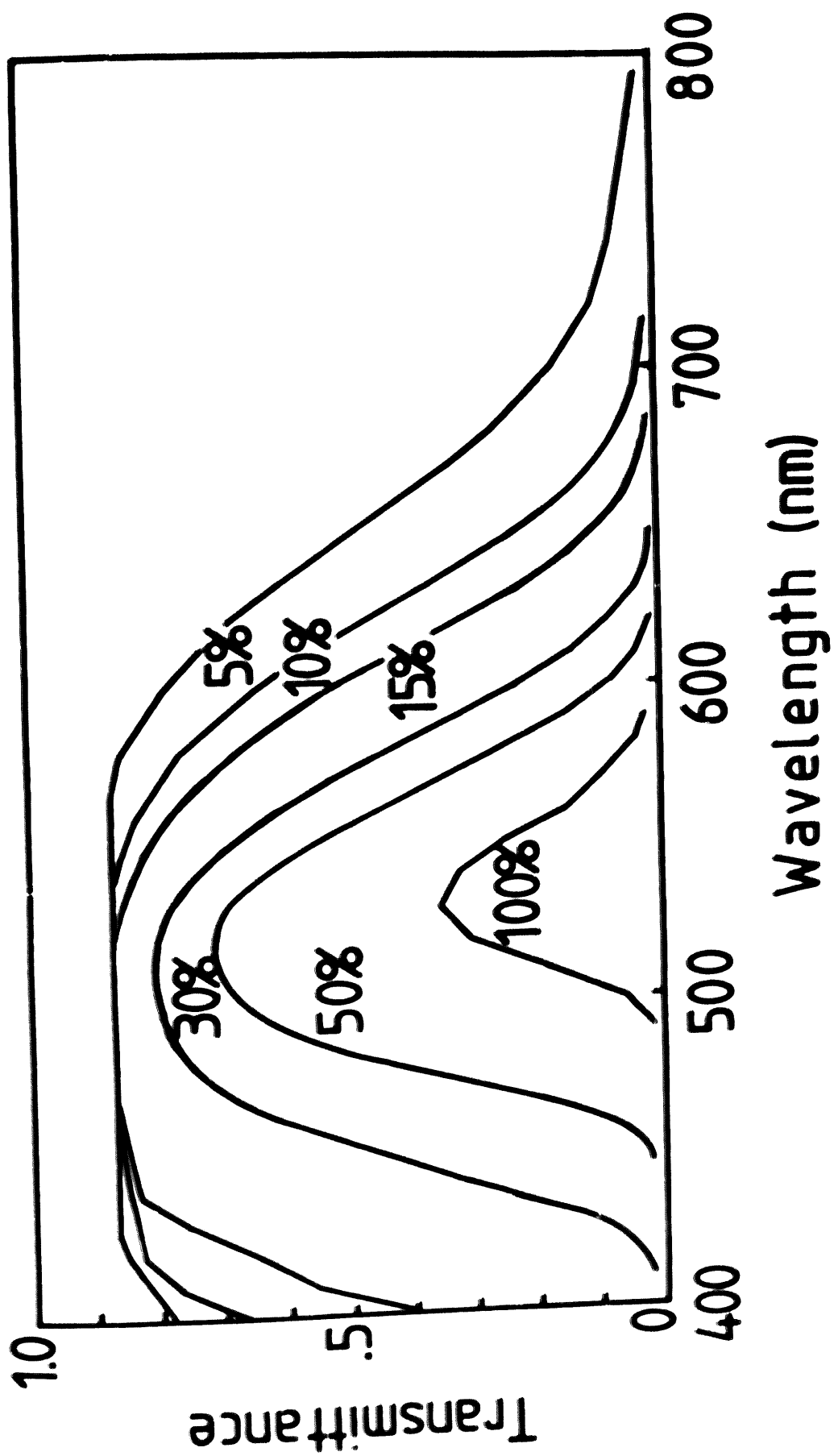


Figure 89

Spectral transmittance of CuCl_2 solutions

in perspex cell

(aqueous pathlength = 4 mm)

100% = saturated solution at 20°C.

Fig.89

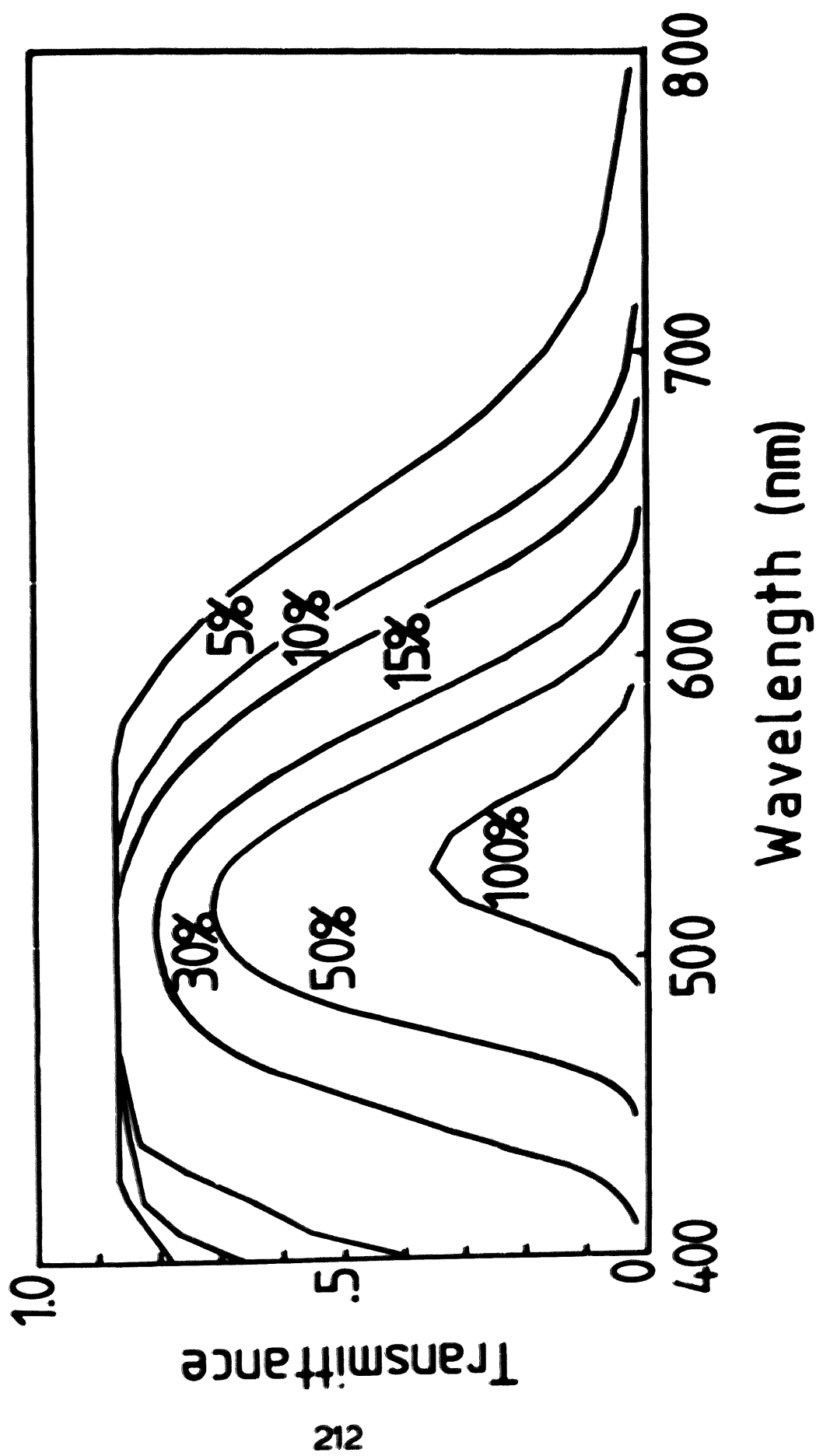


Fig.90

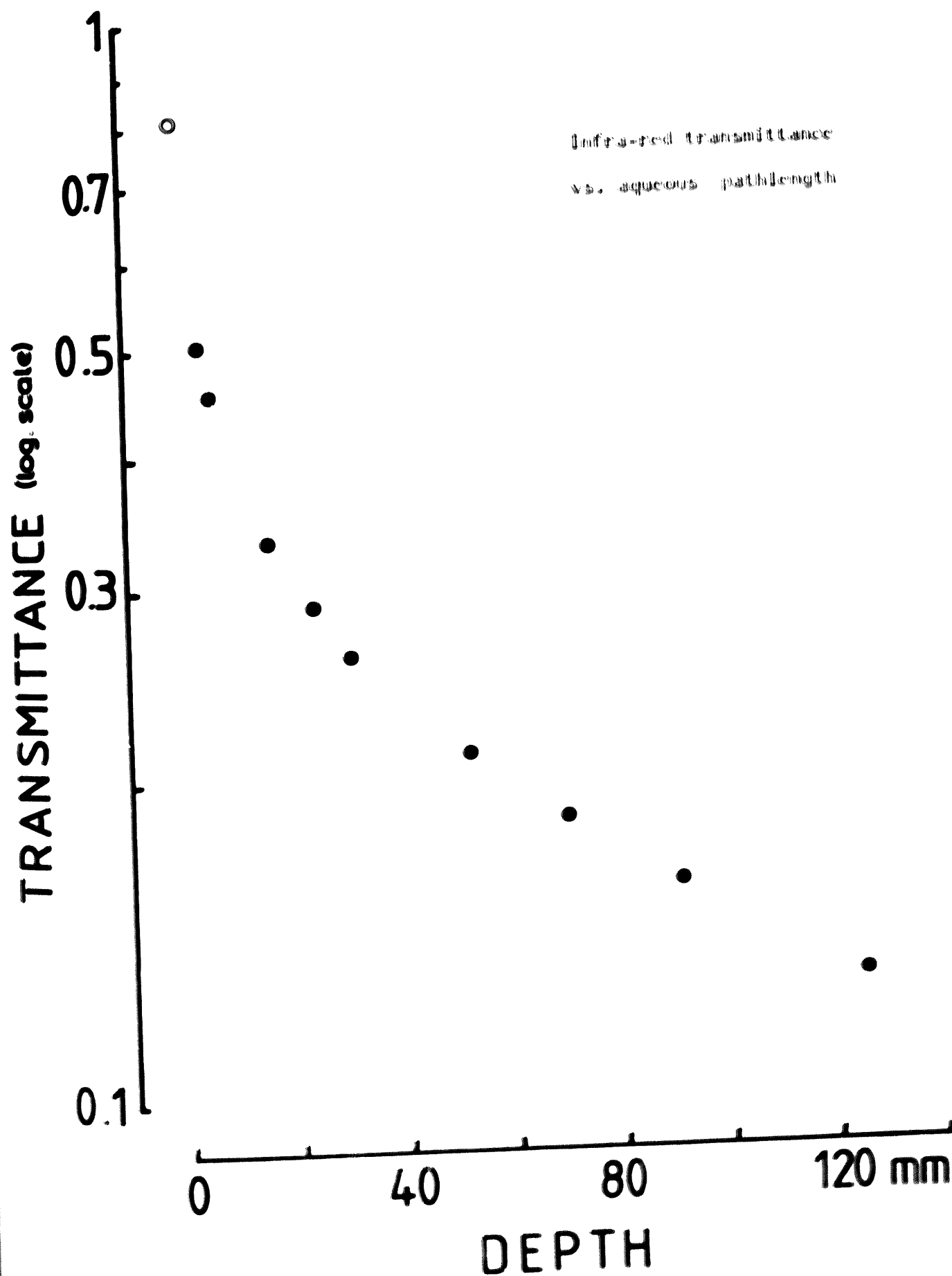


Figure 91

Diagram of growth cabinet (to scale)

- A access hatch
- D ducts for cooling air
- CC growth chamber
- I insulation door
- L lamps
- O observation window
- W water reservoir for humidifier
- H heaters
- S moveable shelf
- T drip-tray
- R refrigeration

Fig. 91

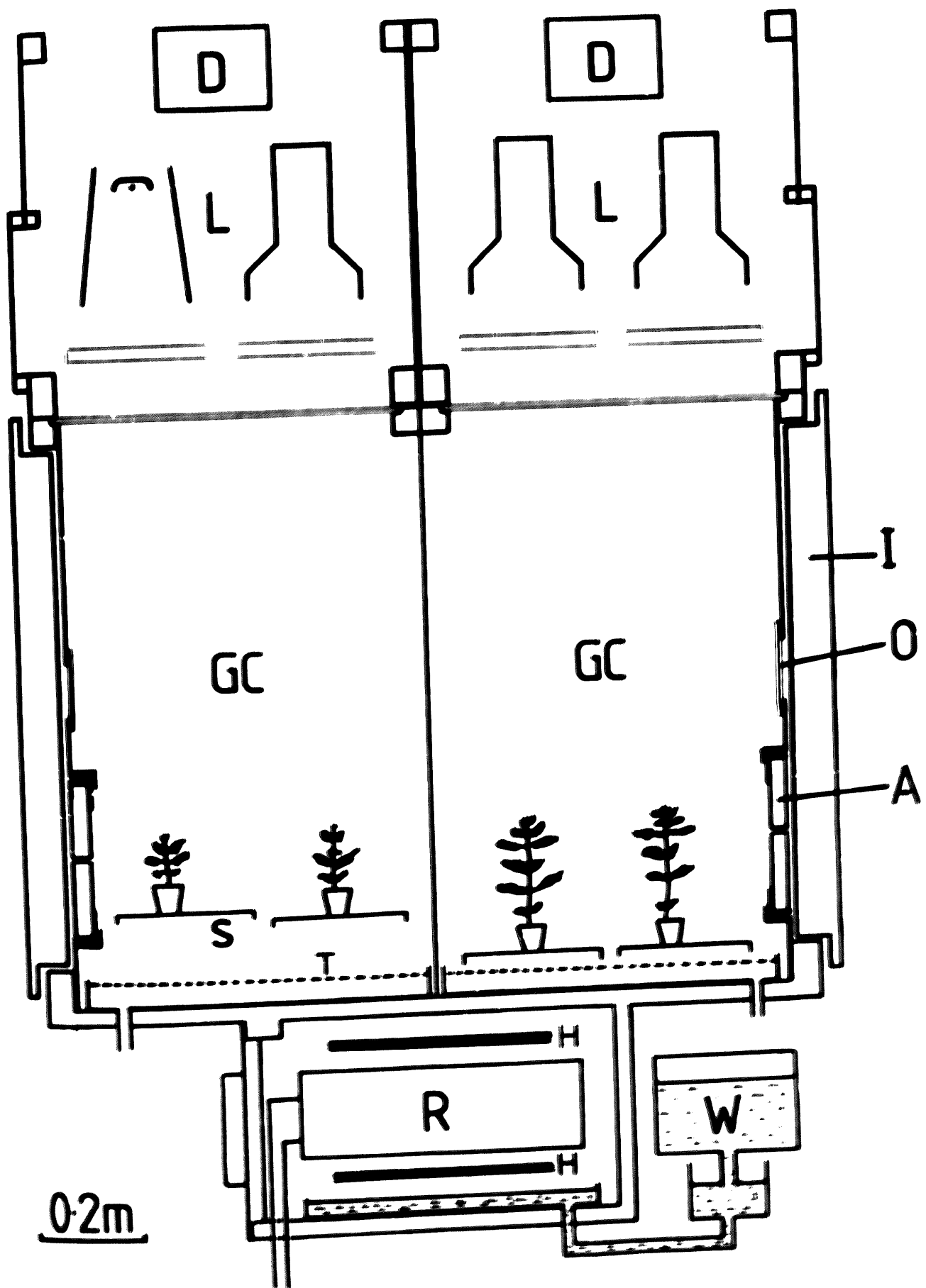


Fig. 92

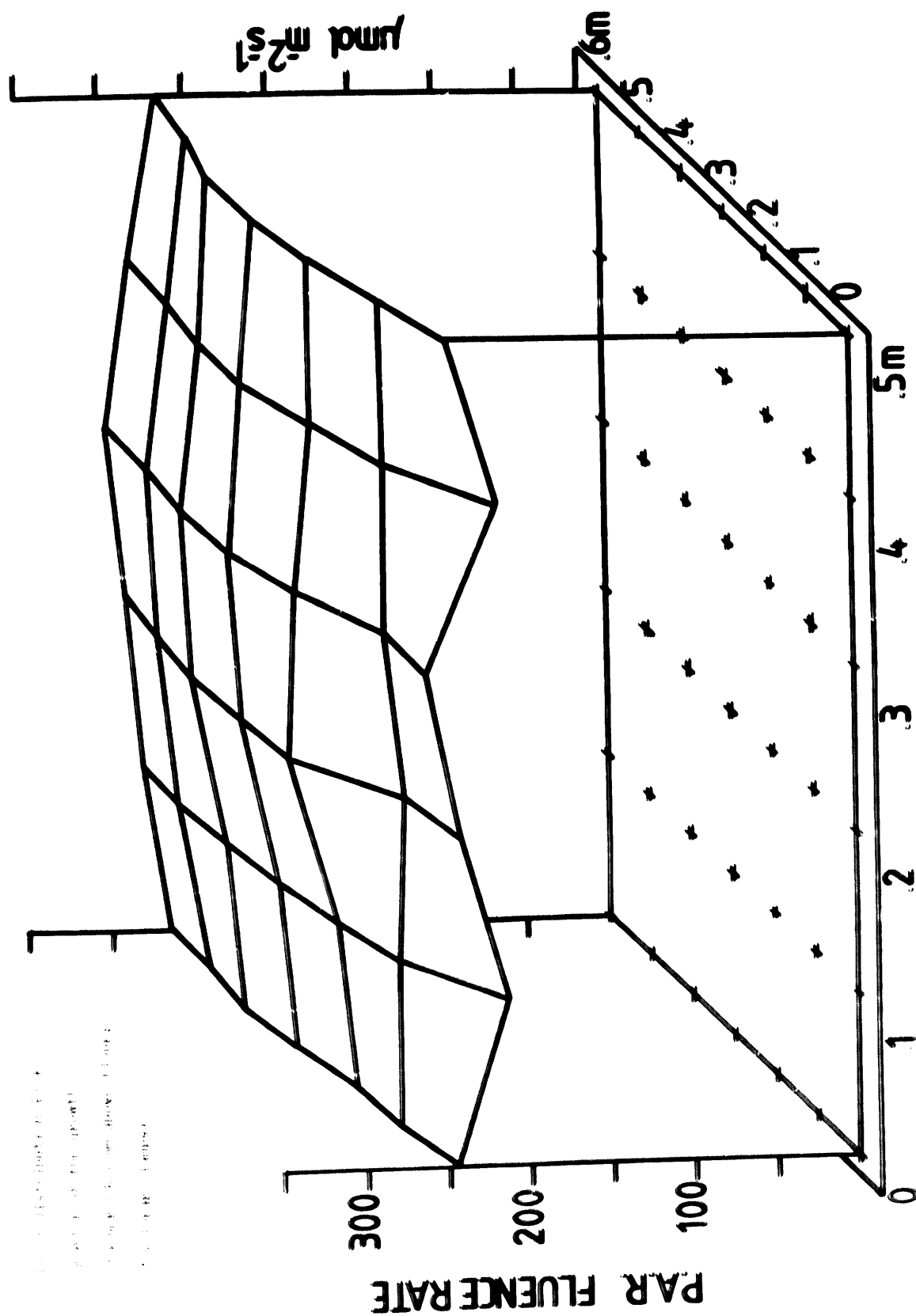





Figure 93

Circuit diagram of growth cabinet (east side)

- A** Main module power line
B Air cooling and air conditioning "night offset" control line
-  relay
 relay winding
-  relay to main module power line
- 1 Main isolating switch
 - 2 (East) module switch
 - 3 "START" button
 - 4 Isolating relay
 - 5 Time switch No. 1
 - 6 " " " No. 2
 - 7 Night temp. offset and cooling fan switch-over
 - 8 Time switch - lamp control board; either timer can control any lamp relay
 - 9 Tungsten-halogen relays (one with time delay to reduce "switch-on" current surge)
 - 10 Kolorarc relays
 - 11 Tungsten-halogen lamps and switching bank
 - 12 Kolorarc lamps and switching bank
 - 13 Thermal cut-out
 - 14 Wind " "
 - 15 Water " "
 - 16 Air conditioning thermal cut-out
 - 17 Heaters
 - 18 Heater power switches (no heat; 1 Kw switched via (24)); 1 Kw switched via (24) only at night; 500 w continuous supplement)
 - 19 Heater relay
 - 20 Refrigeration solenoid
 - 21 Day temperature control
 - 22 Night temperature offset control
 - 23 Temperature sensor (thermistor)
 - 24 "Sunvic" temperature controller
 - 25 Power to west module
 - 26 Air cooling blower (with delay switch)
 - 27 Cavity window water pump
 - 28 Air conditioning fan

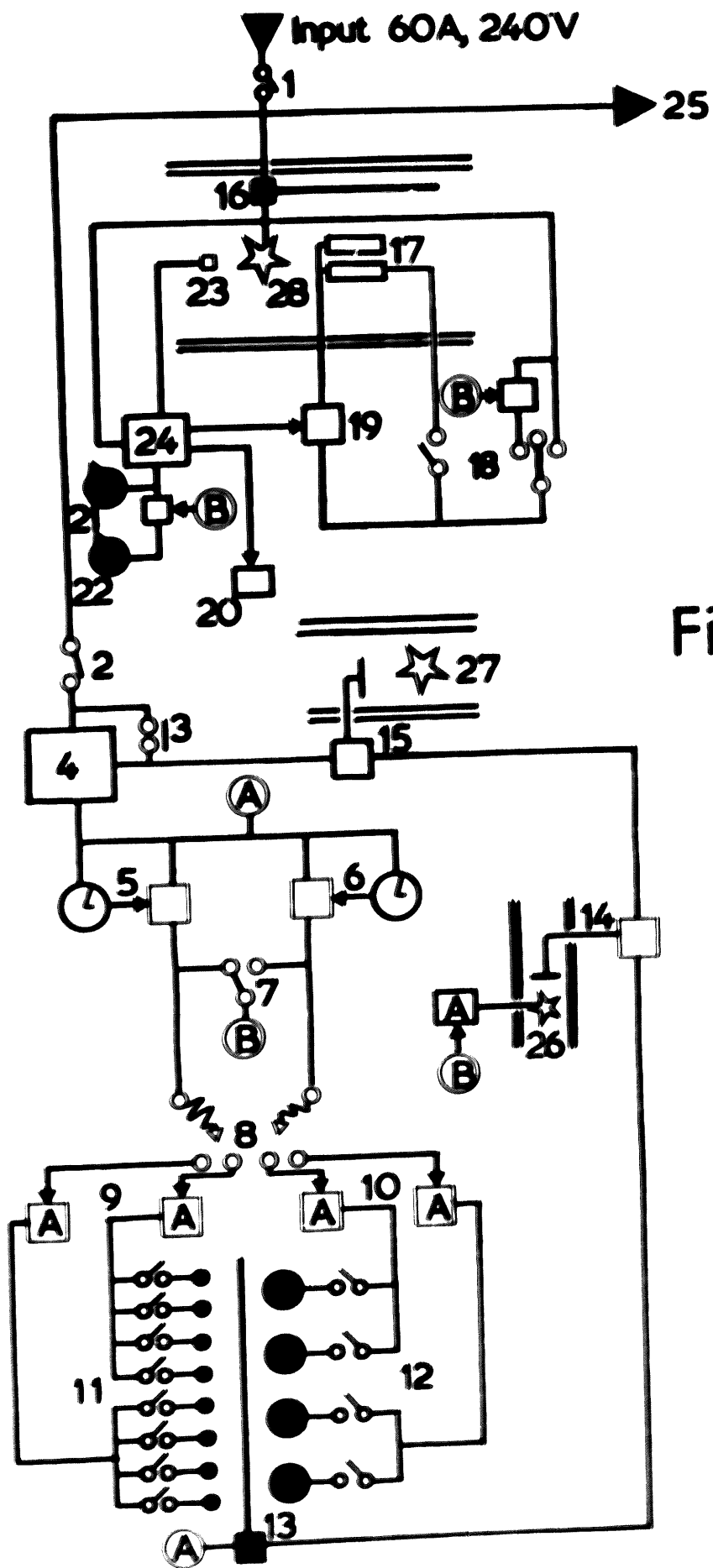


Figure 94

**System used to study leaf gas exchange
(not to scale)**

- 1 Air inlet
- 2 Primary buffer chamber (50 dm³)
- 3 Secondary buffer chamber (20 dm³)
- 4 Circulation pump
- 5 Copper heat-exchanger in duct
- 6 Humidification column
- 7 Reflux pipe
- 8 Baffles
- 9 Air outlet
- 10 Cuvette air valve
- 11 " " flow gauge
- 12 " " pressurising pump
- 13 " " pressure valve
- 14 Cuvette
- 15 Hypodermic needle air jet
- 16 Cuvette air exhaust
- 17 Reference air valve (for baseline checks)
- 18 " " " (for IRGA)
- 19 Sample line
- 20 Sampling pump
- 21 Sampling rate valve
- 22 Reference / sample line switch-over
- 23 Dew-point hygrometer
- 24 IRGA (in differential mode)
- 25 Chart recorder interface
- 26 Chart recorders
- 27 Thermocouples
- 28 Reference junction ice flask
- 29 "Comark" microvoltmeter
- 30 Thermostat and 100 w heater
- 31 Insulated enclosure

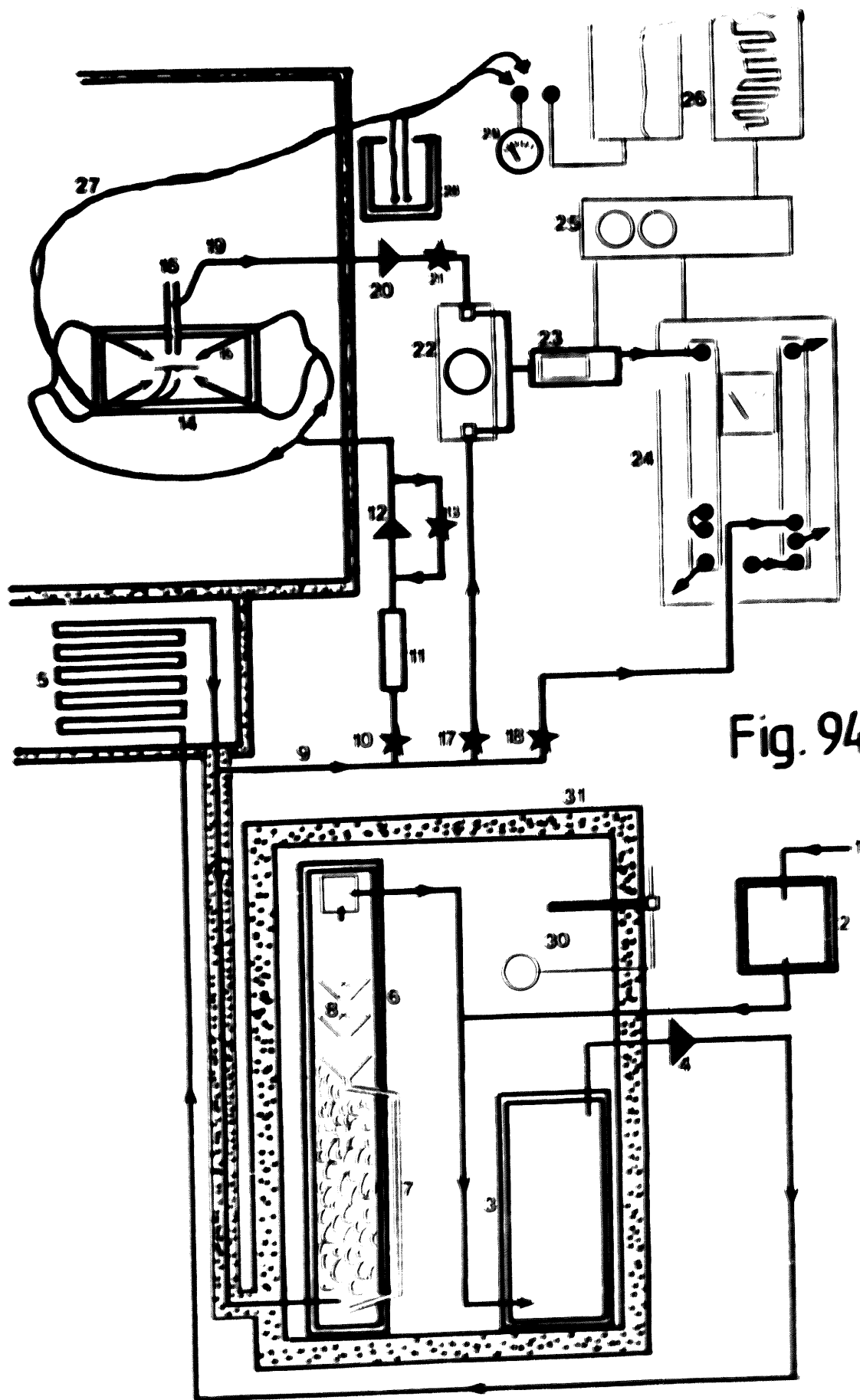


Fig. 94

CIRCUIT DIAGRAM OF ELECTRONIC SWITCH

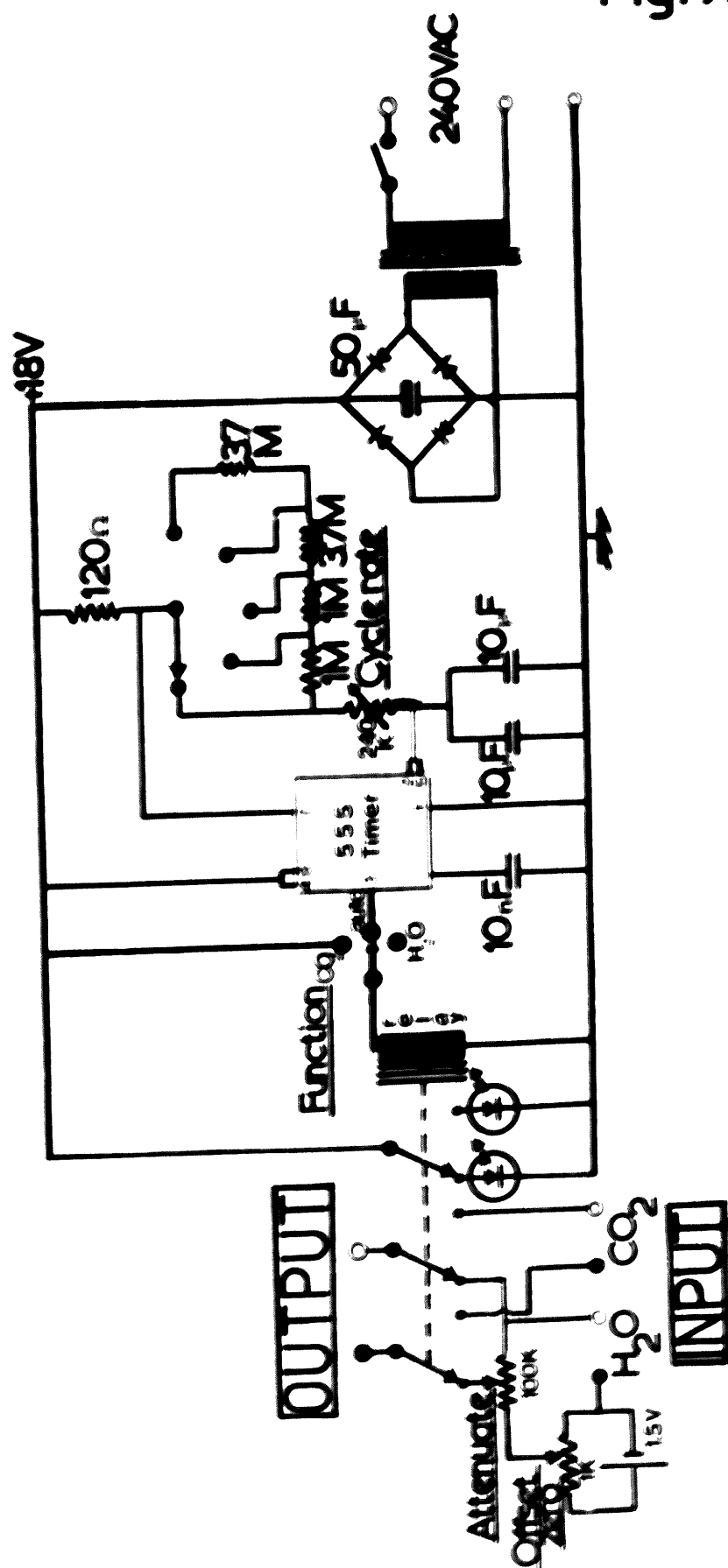


Fig. 95

Figure 96

Transects of Chenopodium album leaf
(arrows indicate position of lateral vein)

Upper epidermis:

(▲) SD (▲) SI

(a) transverse

(b) longitudinal

Lower epidermis:

(●) SD (□) SI

(c) transverse

(d) longitudinal

Fig. 96

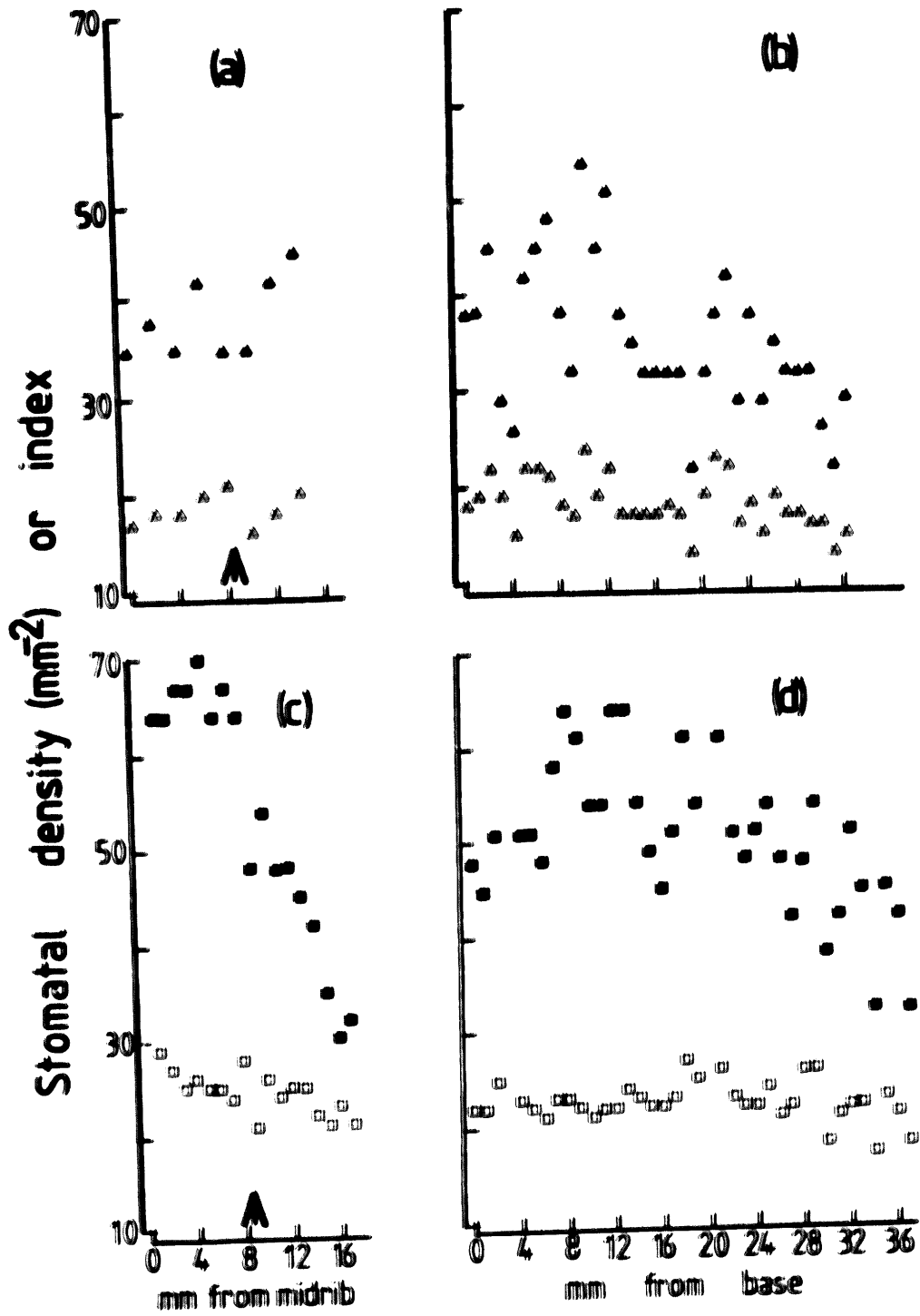
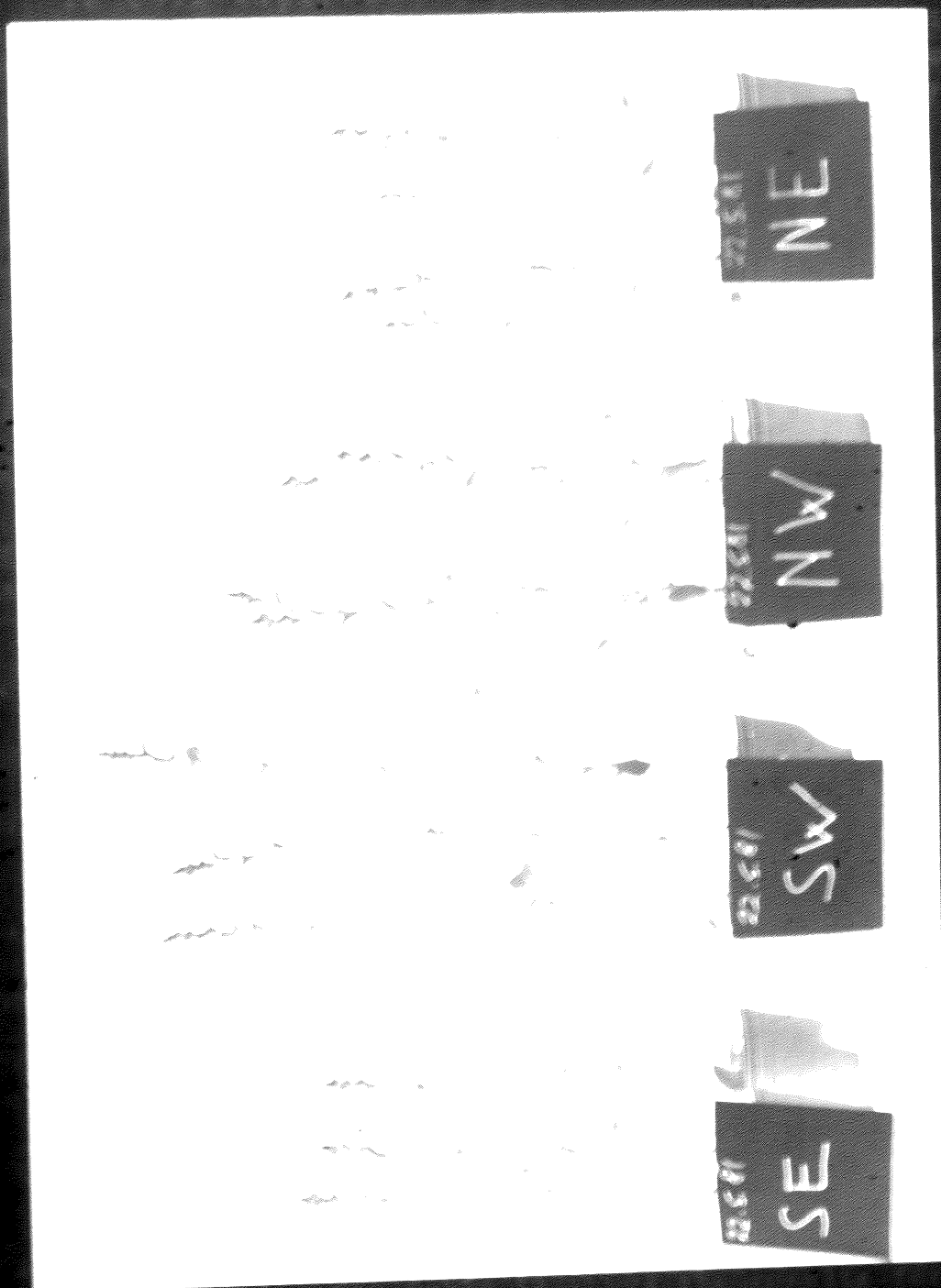


Fig. 97



NE $\bar{y} = 2.6$

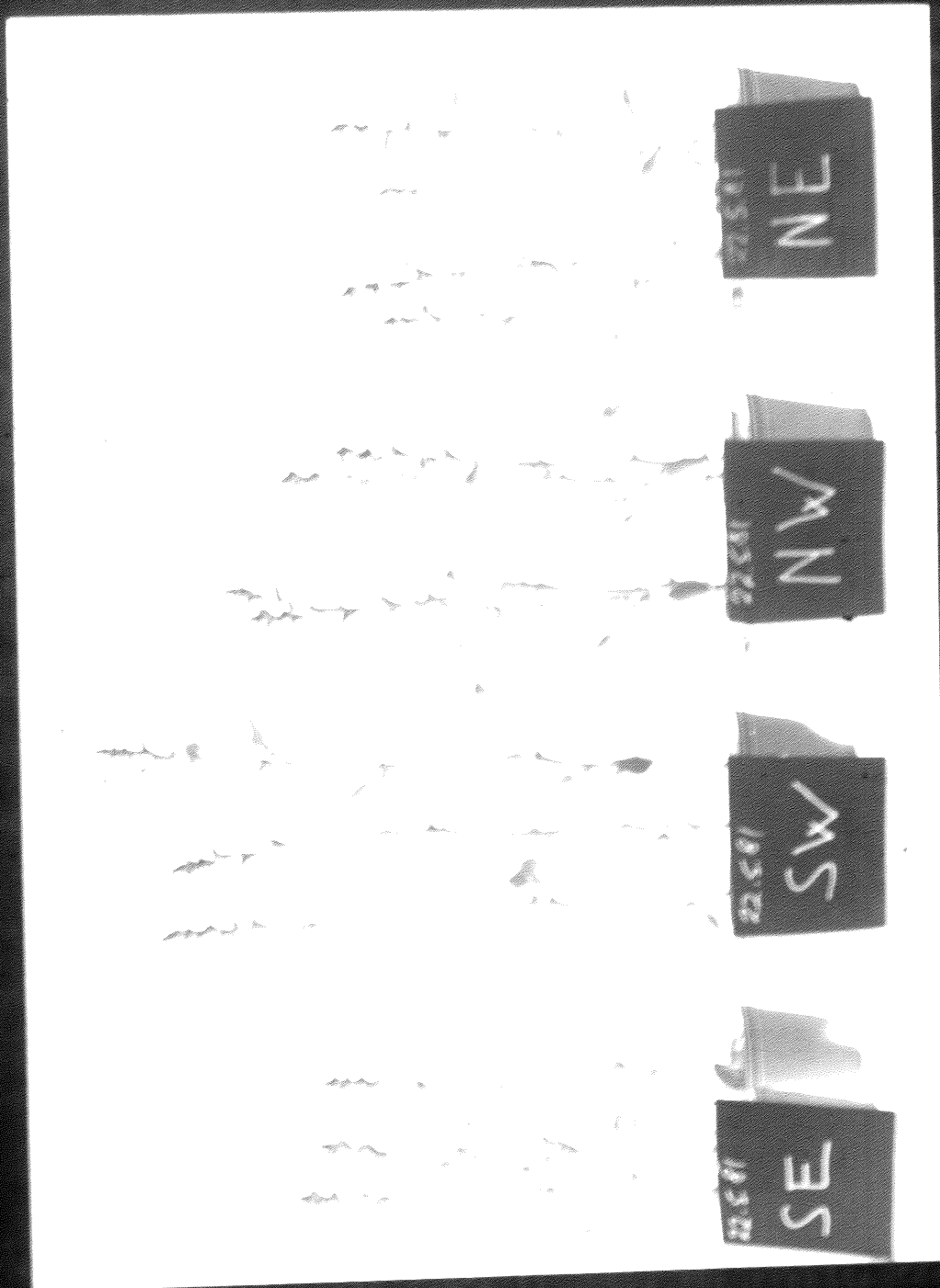
NW $\bar{y} = 0.63$

SW $\bar{y} = 0.29$

SE $\bar{y} = 0.5$

Experiment III Chenopodium album at time of harvest

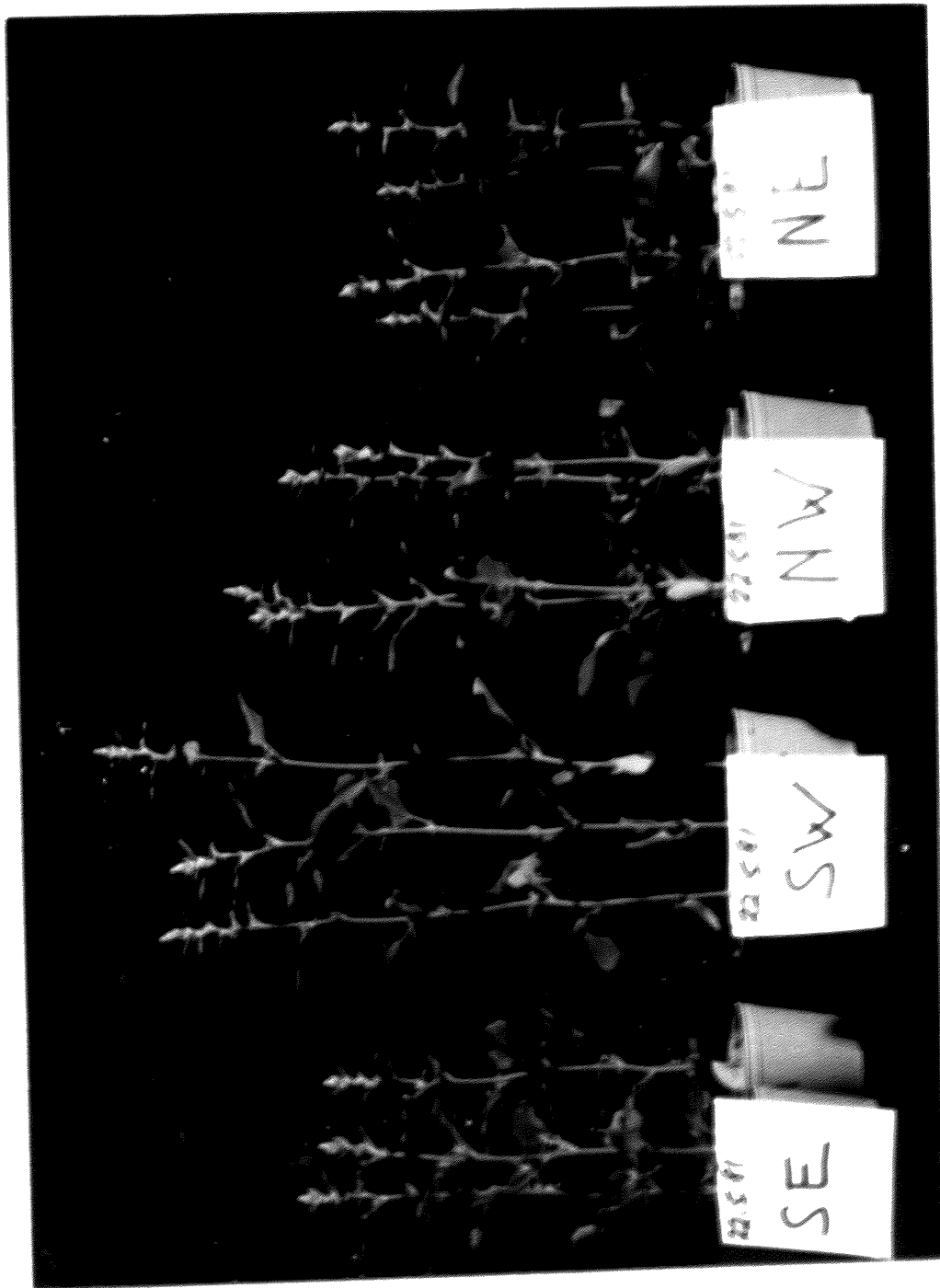
Fig. 97



SE $\bar{y} = 0.5$ SW $\bar{y} = 0.29$ NW $\bar{y} = 0.63$ NE $\bar{y} = 2.6$

Experiment III Chenopodium album at time of harvest

Fig. 97



NE 2.6

NW 0.53

SW 0.29

SE 0.25

Experiment III: A comparison of the effect of time of harvest

RESULTS

Morphology

EXPERIMENT 1: The effects of reduced PAR fluence rate and supplementary far-red on leaf development.

In this experiment, the effect of reduced PAR fluence rate with and without supplementary far-red light on stomatal and leaf development was investigated in order to establish the relative importance of light quantity and quality.

Seeds were germinated and grown for 18 days at $150 \mu\text{mol m}^{-2} \text{s}^{-1}$ in the growth cabinet (16 hour photoperiod, constant 20°C in this and other experiments). Seedlings in which the second true leaf was emerging were potted and four transferred to each of three quarters of the growth chamber where the treatment conditions shown below were maintained using tungsten halogen lamps filtered by red and green perspex and unfiltered Kolorarc lamps.

Qtr.	Treatment	\bar{f}	δ_c	B:R	PAR $\mu\text{mol m}^{-2} \text{s}^{-1}$
---	-----	---	---	---	-----
SE	High PAR : high \bar{f}	2.88	0.64	0.75	276
NW	Low PAR : high \bar{f}	2.82	0.63	0.77	137
SW	Low PAR : low \bar{f}	0.21	0.41	0.47	140

The plants were harvested when they began to flower, 34 days later. Leaves from plants in the SE quarter were noticeably narrower than the others, while in the SW quarter the plants were much taller. Stained epidermal strips from two of the largest leaves (5th and 7th true leaves) were scored using the projection microscope.

Results

The treatment means and standard errors ($n=4$) for the epidermes of leaves 5 and 7 are given in Tables 11 and 12 respectively, while Table 13 shows the results for leaf area and pigment content. The significance level of the results according to t-tests between treatment pairs are

2.3 morphology

also shown (***, $p_0 < 0.1\%$; **, $p_0 < 1\%$; *, $p_0 < 5\%$; ns, $p_0 > 5\%$).

PAR fluence rate differences had no significant effects on the SI of any of the epidermes studied, whereas supplementary far-red light reduced the indices substantially, especially on the upper epidermis. However, the total stomatal population on each epidermis (calculated as leaf area \times SD) did not always reflect this and both epidermes of leaf 7 showed a significant effect of fluence rate on this population. These effects might have been caused by a simultaneous increase in the total cell population (via an effect on mitosis in the protoderm), but the data indicate that, if anything, the opposite generally occurred. Reduced PAR fluence rate led to a large increase in the area of leaf 7, but the effect was not statistically significant for leaf 5. CD mirrored this effect and, as the cell population was much less affected, it is likely that the increase in area was associated with increased cell expansion rather than mitosis. SLA showed highly significant differences; low PAR increased SLA but the effect was smaller in the presence of supplementary far-red light.

SD was strongly reduced both by the low PAR fluence rate and by supplementary far-red light. Although changes in SI would have had large effects on SD, the increase in the area of leaf 7 associated with low PAR and supplementary far-red would contribute substantially.

On both fresh weight and area bases, the chlorophyll a content of the leaves was apparently greater in the low PAR treatments, but the effect was reduced by supplementary far-red. The relative carotenoid content showed a similar pattern, but the chlorophyll a:b ratio was largely unaffected.

EXPERIMENT II: The effect of different levels of supplementary far-red light at high PAR fluence rates.

In this experiment, the developmental effect of a range of levels of supplementary far-red light against a constant, relatively high PAR fluence rate was investigated. The PAR fluence rates used were typical of daylight under an overcast sky.

The four quarters of the growth chamber provided the following irradiation conditions (6 values were measured

2.3 morphology

in crude phytochrome extracts and corrected for the rate of Pfr loss; see 2.2);

Qtr.	Far-red content	\bar{S}	δ_c	δ	B:R	PAR $\mu\text{mol m}^{-2}\text{s}^{-1}$
----	-----	----	----	----	----	-----
NE	none	2.8	0.64	0.64 0.60	0.73	359
NW	low	1.04	0.60	0.58	0.73	360
SE	mid	0.47	0.55	0.54 0.52	0.70	364
SW	high	0.35	0.52	0.53 0.49	0.60	358

In each treatment, PAR was supplied by 2 unfiltered Kolorarc lamps, and the far-red by 2 or 4 tungsten halogen lamps fitted with red and green Perspex filters; intermediate levels of far-red were provided by including an additional sheet of neutral perspex in the filter stack.

Seeds were germinated and grown in the NE quarter for three weeks before uniform seedlings in which the 6th leaf was emerging were potted and three or four transferred to the different treatments. The 9th leaf became visible 6 days after the treatments were imposed and had completed its expansion by the 16th day. The plants were harvested after 30 days in each treatment. Stained epidermal strips were used to score stomata and undifferentiated epidermal cells. Leaf area, SLA and pigment contents were assayed as before.

Results

The results are given in Tables 14 and 15 as mean values for each treatment followed by an ANOVA summary showing the number of degrees of freedom, sum-of-squares, variance, variance ratio, and significance level. Cell counts were not obtained for the SE quarter as the samples were inadvertently destroyed during storage.

On the upper epidermis, SI was significantly reduced by far-red light, implying an effect on stomatal induction; however, the estimated total stomatal

2.3 morphology

population on that surface was not significantly affected. SD and CD were significantly reduced on the upper surface and also on the lower epidermis where SI was apparently unchanged. SD and CD might have been affected by differential leaf expansion or meristematic activity within the protoderm caused by the various treatments. However, neither hypothesis is adequately supported by the data as there were no significant effects on leaf size or the calculated total cell population of each epidermis. Stomatal size was similar in all treatments and on both upper and lower epidermes. Pigment content and SLA were not significantly affected.

EXPERIMENT III: The effect of different levels of supplementary far-red light at low PAR fluence rate.

A third growth experiment was carried out with a range of far-red fluence rates provided against a background of PAR approximately half that in Experiment II. The treatments were as follows:

Qtr.	Far-red content	\bar{S}	δ_c	B:R	PAR $\mu\text{mol m}^{-2}\text{s}^{-1}$
----	-----	----	----	----	-----
NE	None	2.8	0.64	0.54	191
NW	Low	0.83	0.58	0.51	178
SE	Mid	0.50	0.55	0.54	179
SW	High	0.29	0.47	0.46	171

The seedlings were grown for 3 weeks in the NE quarter, and then uniform individuals in which the 4th leaf was emerging were selected, potted and transferred to each of the treatments. 22 days later the plants (see Figure 97) were harvested and stained epidermes of leaves 3, 5 and 7 scored as before.

Results

The results obtained from this work are given in Tables 16, 17 and 18 (for leaves 3, 5 and 7 respectively) as treatment means followed by an ANOVAR.

2.3 morphology

A significant effect of far-red light on SI and SD was found on both epidermes of leaf 3, but although a similar trend is apparent in the stomatal population data, statistical analysis indicates that this is not significant. Stomatal size was not significantly affected. Leaf area differed significantly between treatments, but was poorly correlated with the level of far-red light. Significantly larger leaves were produced in the high far-red treatment than in the others; the leaves in this treatment probably received the lowest PAR fluence rate, both because the fluence rate at the height of the apex was slightly lower in that quarter, and because the older leaves were considerable further from the lamps because of the enhanced stem elongation. However, some quite different causal factor may have been involved.

The upper and lower epidermes of the 5th leaf both showed significant differences in SI and SD between treatments, which were apparently related to the level of supplementary far-red light. Although significant differences between treatments are apparent in CD, stomatal and total cell populations on the lower epidermis and in stomatal population on the upper epidermis, these do not appear to be associated with the level of far-red light. A similar trend is evident in the leaf area data, but the origin of the effect is obscure.

In marked contrast, most of the data for the 7th leaf show insignificant differences between treatments. The significant effects on CD on the upper surface were unrelated to the level of far-red light. A possible explanation is that the effect of the light treatments had not become apparent because leaf 7 had not fully expanded at the time of harvest. Gay and Murd [1975] found that SD was closely related to the degree of expansion of young tomato leaves. However, SI would probably be immune to these late events.

Some 100,000 cells were scored in this experiment and, unfortunately, time did not allow it to be repeated to test the generality of the paradoxical findings mentioned above.

2.3 morphology

EXPERIMENT IV: The effects of different fluence rates of blue light.

In this experiment, the relatively sophisticated control over light quality offered by the cabinet was exploited in order to investigate the effects of different levels of blue light on leaf and stomatal development of the plant, while PAR and phytochrome photoequilibrium were held constant.

Ch. album seeds were germinated and raised for 20 days in the cabinet under light from a single Kolorarc lamp (ca. $150 \mu\text{mol m}^{-2}\text{s}^{-1}$ PAR). Seedlings in which the third leaf was beginning to expand were potted and 5 - 6 transferred to each of the three treatments shown below (again, ϕ was estimated spectrophotometrically and corrected for Pfr loss):

Qtr.	Blue content	\bar{f}	ϕ_c	ϕ	B:R	$(\mu\text{mol m}^{-2}\text{s}^{-1})$ Blue PAR	
----	-----	----	----	----	----	----	-----
NW	High	0.89	0.57	0.60	1.80	42	130
SW	Mid	1.48	0.59	0.57 0.57	0.77	26	135
SE	Low	0.68	0.58	0.58	0.29	12	128

The high blue treatment was derived from 3 Kolorarc lamps. Beneath one of these, a 1 cm pathlength cavity filter containing a 5% saturated CuCl_2 solution served to reduce the red and especially the far-red light input to the chamber, leaving predominantly green and blue light (with a very high \bar{f} value). Light from the other two lamps was filtered through blue Perspex, effectively removing green and red light while allowing most of the blue and far-red to enter the chamber. Thus not only was the level of blue light increased, but ϕ_c was brought closer to that of daylight (0.53; Table 2). An intermediate level of blue light was provided in the SW quarter using a single Kolorarc lamp and, in order to depress ϕ_c to the level in the high blue treatment, far-red light free of red contamination was supplied by 4 tungsten halogen lamps filtered through red Perspex and blue Cinemoid. The plants in the SE quarter received light from a single Kolorarc filtered through yellow Perspex to remove wavelengths

below 470 nm and thus strongly reduce the level of blue light. Photoequilibrium was reduced to the level in the NW quarter using 2 tungsten halogen lamps filtered through red, green and neutral Perspex sheets.

The plants were harvested after 28 days of exposure to the treatments. Epidermal cell counts were made from micro-relief replicas of the 6th leaf of four plants from each quarter. Pigment analyses were carried out on the 8th leaf.

Results and Discussion

The data collected are summarised in Tables 19 and 20 as treatment means followed by an ANOVAR. The low blue treatment significantly increased the leaf area, biomass and petiole lengths, and reduced the chlorophyll a content (fresh weight basis) and chlorophyll a:b ratio. The plants grown in this quarter were also much taller. The mean values for the high and mid-blue treatments (NW and SW) were similar, however. Both leaf area and cell population were greater in the low blue treatment, partly explaining the insignificant effects on CD. Although implying that low levels of blue light stimulate mitosis in the protoderm, the fall in cell density toward leaf edges and tip may have confounded this interpretation. Moreover, the effect is the opposite of that to reduced PAR (Experiment I).

These results are consistent with the idea of blue light acting in a threshold manner. However, although SI and SD of the upper epidermis of leaf 6 also showed significant differences between treatments, both characters appear to have been more linearly related to the level of blue light; a similar trend may have existed on the lower epidermis, but this was without statistical significance here. Further experiments are required if these observations are to be properly established and characterised.

Although the effects observed do not seem to be associated with the level of supplementary far-red light used in each of the treatments, perhaps the most important objection to the above interpretation is whether the ϕ value (or level of Pfr) in the experimental plants was actually constant in the different treatments. The true value of ϕ must be lower than that calculated and measured in vitro because of screening by leaf pigments. Although

Fukshansky [1981] showed that ϕ can (at least in theory) be estimated quantitatively at any point in the leaf, the actual sites of light detection are unknown at present. However, Morgan and Smith [1978a] showed that a correlation between stem extension rate and ϕ would persist even if ϕ was perceived beneath the leaf. The effective value of ϕ in the green plant is not important here as long as it is related to ϕ_c in a simple way; however, if the treatments themselves altered the screening effects, the relationship will become very complex. The chlorophyll content per unit leaf area was unaffected by the different treatments, so it was assumed that the screening properties were approximately constant. However, the SLA data imply that leaf structure, and hence scattering, may have been affected. There may also be differences between the light absorbing properties of phytochrome in green and etiolated tissue.

Gas exchange

EXPERIMENT V: Time course of stomatal opening induced by dim blue and red light.

The effects of spectral quality on the kinetics of stomatal opening and closing were investigated. Seedlings were raised in the SE quarter of the cabinet, exactly as in Experiment III (that is, $\phi_c = 0.55$, PAR = $180 \mu\text{mol m}^{-2}\text{s}^{-1}$). In the NE quarter of the chamber, Kolorarc lamps were set up with appropriate filters to provide either $30 \mu\text{mol m}^{-2}\text{s}^{-1}$ of red or $17 - 20 \mu\text{mol m}^{-2}\text{s}^{-1}$ of blue light. A preliminary experiment using a porometer had indicated that these fluence rates would produce similar conductance values at equilibrium.

About 3 weeks after they had been potted and placed in the growth treatments, representative plants were transferred to the NE quarter and their 5th or 6th leaves (the largest on the plants) sealed inside the cuvette. Although the conductance of each epidermis could have been measured separately with a diffusion porometer, such a procedure disturbs the light environment of the leaf and so could not be used for continuous measurements; the cuvette, on the other hand, was well-suited to continuous gas analysis. It was only possible to record a complete series of replicated time-courses for a single plant, so the results must be considered preliminary, but dew point data for other plants showed a similar kinetic behaviour to this.

Results

Red or blue light was supplied for periods of several hours separated by dark periods of similar length. Stomatal conductance (g_s) and transpiration rate (E) began to increase within minutes of the light being switched on, and reached a peak after about 25 min followed by a trough about 25 min later in all cases. A damped sinusoidal oscillation generally persisted for at least one further cycle, but recordings were not always continued after the second peak.

The data in Table 21 correspond to the maxima, minima and stable values achieved after t min of irradiation. E closely followed the changes in g_s in all cases. Under blue light, photosynthesis (A) was close to the compensation point and since the net CO_2 exchange was very slow, neither A nor the internal CO_2 concentration (C_i') was much affected by g_s . A was greater under the higher fluence rate and more photosynthetically effective red light but, despite the fluence rate difference and the generally lower C_i' , conductances were substantially smaller. For these reasons both A and C_i' were far more susceptible to changes in conductance. The origins of the differences in A between similar time-courses is obscure, however.

The results indicate that stomatal opening in response to blue and red light is essentially similar in its kinetics under these conditions, as the periodicity of the oscillations was unaffected. In contrast, the equilibrium conductance level was greater under blue light despite the substantially lower fluence rate. A consistent difference between the effects of the two wavelengths was also noted during stomatal closure. Following the blue photoperiods g_s fell over a 30 min period to 1.0, 1.6 and 1.9 $mm\ s^{-1}$ respectively, and then increased again to a transient peak (9, 10.6 and 7.5 $mm\ s^{-1}$) about 30 min later. Over the following hour, g_s fell to $<0.2\ mm\ s^{-1}$. In contrast, after a red photoperiod g_s fell directly to $<0.2\ mm\ s^{-1}$ within 20 minutes, and showed no tendency to increase again in either leaf 6 or leaf 5. Further investigation of this interesting difference was not attempted due to constraints of time.

EXPERIMENT VI: The effect of different light regimes during development on leaf gas exchange characteristics.

This experiment was intended to examine the effects of differences in PAR fluence rate and spectral composition during leaf ontogeny on the gas exchange characteristics of Ch. album leaves. Preliminary experiments using a diffusion porometer (Delta-T Instruments Ltd., Newmarket, U.K.) indicated that gs varied considerably during the photoperiod in cabinet-grown plants and this seemed to be aggravated by the measurement procedure. This may have been due to stomatal sensitivity to the darkness temporarily imposed by the porometer clip, or to mechanical damage; as the variation was reduced when the cuvette was used, this technique was preferred.

Plants were germinated and grown for about three weeks in the cabinet under Kolorarc lamps providing approximately $150 \mu\text{mol m}^{-2}\text{s}^{-1}$ PAR before being potted when the 1st true leaf was emerging. Various batches of 4-6 plants were grown for a further three weeks at 85, 110, 200, or $230 \mu\text{mol m}^{-2}\text{s}^{-1}$ ($\phi_c = 0.64$, $\mathcal{J} = 2.8$). Other batches of plants were grown with a background of white light supplemented by far-red (PAR = $110 \mu\text{mol m}^{-2}\text{s}^{-1}$, $\phi_c = 0.38$, $\mathcal{J} = 0.19$). In the final experiment, the plants used were from Experiment IV in which PAR and ϕ_c were held constant while the level of blue light was varied. Typical plants from each treatment were selected and the gas exchange characteristics of the 6th leaf investigated under white light supplied by Kolorarc lamps.

Results

Transpiration, net photosynthetic rate, stomatal conductance and internal CO_2 concentration were calculated from the gas exchange data. The stable values reached after the transpiration rate had stabilised are given in Table 22.

The transpiration rate followed changes in the stomatal conductance, although variation in the ambient humidity prevented exact consistency. Considering the data as a whole, there was good correlation between photosynthesis and PAR fluence rate in the cuvette ($r=0.86$) despite the widely differing growth conditions. The calculated photosynthetic rates are similar to those of Bjorkman et al. [1972b] for Atriplex triangularis

(Chenopodiaceae). At $150 \mu\text{mol m}^{-2}\text{s}^{-1}$, there was no consistent difference in g_s between leaves B and C and leaves E and F although their growth conditions were substantially different; C_i' was also largely unaffected. Indeed, considering leaves A - F, there was no correlation between g_s and either the cuvette or the growth PAR fluence rates ($r=-0.08$ and 0.01 , respectively). In leaf G where the cuvette fluence rates were lower, the correlation between g_s and cuvette fluence rate was also poor ($r=0.41$).

As there was no reason to believe that the growth or cuvette treatments had specific effects on g_s , the grand mean (the mean of the mean values for each leaf) was calculated as 6.6 ± 0.7 for leaves A - F; this was similar to the mean of 6.7 for leaves I, J and K, but rather lower than that for leaves G and H (8.0), despite the lower PAR fluence rate in the cuvette and the lower stomatal index resulting from the far-red treatment. However, this difference is not statistically significant, as the value is within the 95% confidence range of the grand mean. Unfortunately, time did not permit this possible effect to be studied more fully.

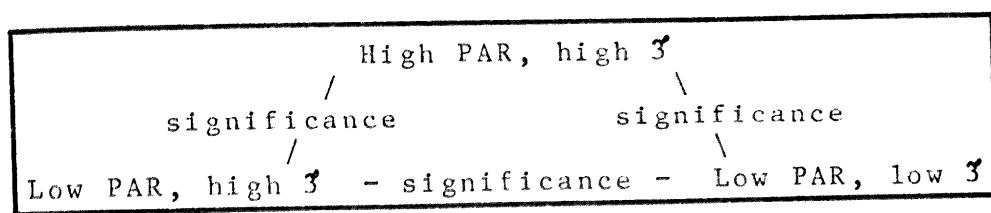
There were several possible sources of the considerable variability within the data. Effects of gradual acclimation to the cuvette environment are unlikely to have been involved; the results for each leaf are presented in the order they were recorded and there is no consistent trend in the g_s values during the enclosure period of 12 - 48 hours. An endogenous rhythmical factor may have been at work, as no special precautions were taken to provide uniform pre-treatments in the NE quarter other than to give at least two hours of darkness prior to the photoperiod. The most significant source of variation was likely to have been measurement error, however. The coefficient of variation for the grand mean of g_s for leaves A - F was 26%, only slightly greater than the expected error of $\pm 20\%$. It was therefore reasonable to conclude that any effects of the treatments were below the detection limit of the system.

(Chenopodiaceae). At $150 \mu\text{mol m}^{-2}\text{s}^{-1}$, there was no consistent difference in g_s between leaves B and C and leaves E and F although their growth conditions were substantially different; C_i' was also largely unaffected. Indeed, considering leaves A - F, there was no correlation between g_s and either the cuvette or the growth PAR fluence rates ($r=-0.08$ and 0.01 , respectively). In leaf G where the cuvette fluence rates were lower, the correlation between g_s and cuvette fluence rate was also poor ($r=0.41$).

As there was no reason to believe that the growth or cuvette treatments had specific effects on g_s , the grand mean (the mean of the mean values for each leaf) was calculated as 6.6 ± 0.7 for leaves A - F; this was similar to the mean of 6.7 for leaves I, J and K, but rather lower than that for leaves G and H (8.0), despite the lower PAR fluence rate in the cuvette and the lower stomatal index resulting from the far-red treatment. However, this difference is not statistically significant, as the value is within the 95% confidence range of the grand mean. Unfortunately, time did not permit this possible effect to be studied more fully.

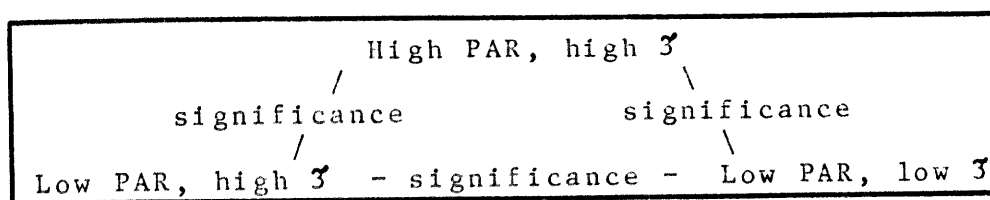
There were several possible sources of the considerable variability within the data. Effects of gradual acclimation to the cuvette environment are unlikely to have been involved; the results for each leaf are presented in the order they were recorded and there is no consistent trend in the g_s values during the enclosure period of 12 - 48 hours. An endogenous rhythmical factor may have been at work, as no special precautions were taken to provide uniform pre-treatments in the NE quarter other than to give at least two hours of darkness prior to the photoperiod. The most significant source of variation was likely to have been measurement error, however. The coefficient of variation for the grand mean of g_s for leaves A - F was 26%, only slightly greater than the expected error of $\pm 20\%$. It was therefore reasonable to conclude that any effects of the treatments were below the detection limit of the system.

TABLE 11
EXPERIMENT I: Effects of reduced PAR fluence rate and supplementary far-red light on upper and lower epidermes of leaf 5



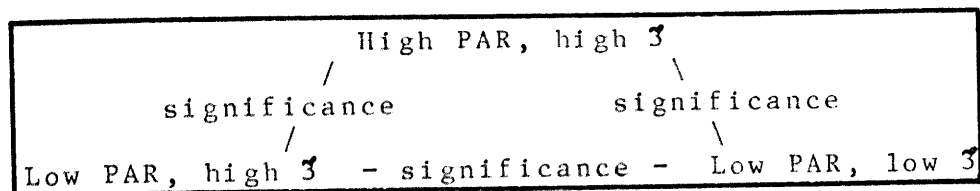
Upper epidermis		Lower epidermis
16.8 (1.8) ns * 14.9 (0.9) —*— 11.0 (0.8)	SI	22.4 (1.0) ns ns 22.4 (0.13) —*— 20.0 (0.9)
126 (15) * ** 74 (2) —**— 50 (5)	SD stomata mm ⁻²	180 (18) ** ** 95 (7) —ns— 97 (7)
818 (63) ** ** 499 (20) —ns— 433 (25)	CD cells mm ⁻²	799 (55) *** ** 425 (31) —ns— 484 (33)
111 (67) ns * 75 (4) —ns— 57 (12)	Stomatal population (x 1000)	159 (22) ns ns 99 (13) —ns— 113 (18)
708 (67) ns ns 515 (56) —ns— 498 (74)	Cell population (x 1000)	704 (71) * ns 441 (60) —ns— 568 (100)

TABLE 12
EXPERIMENT I: Effects of reduced PAR fluence rate and supplementary far-red light on upper and lower epidermes of leaf 7



Upper epidermis		Lower epidermis
16.1 (0.2) ns *** 16.0 (0.1) —***— 11.6 (0.6)	SI	20.7 (0.4) ns * 21.6 (0.6) —*— 19.6 (0.2)
232 (10) *** *** 112 (3) —**— 83 (5)	SD stomata mm ⁻²	331 (15) *** *** 153 (2) —ns— 163 (10)
1440 (167) *** *** 703 (24) —ns— 728 (56)	CD cells mm ⁻²	1592 (48) *** *** 707 (17) —ns— 834 (60)
140 (4) * *** 121 (6) —**— 80.5 (6)	Stomatal population (x1000)	199 (5) * ** 165 (9) —ns— 156 (7)
866 (23) ns ** 759 (43) —ns— 698 (36)	Cell population (x1000)	958 (8) * ** 768 (57) —ns— 799 (34)

TABLE 13
EXPERIMENT I: Effects of reduced PAR fluence rate and
supplementary far-red light on area and pigment
content of Leaves 5 and 7



Leaf 5		Leaf 7
8.7 (0.4) ns ns 10.2 (0.7) — ns — 11.5 (1.5)	Leaf area (cm ²)	6.0 (0.1) *** *** 10.8 (0.6) — ns — 9.7 (0.5)
171 (3) *** *** 446 (24) — *** — 287 (10)	SLA (cm ² g ⁻¹)	172 (6) *** *** 440 (28) — ** — 292 (9)
1.37 (.07) *** * 2.25 (.12) — ** — 1.56 (.03)	Chlorophyll a (mg g ⁻¹)	1.43 (.05) *** ** 2.40 (.11) — ** — 1.76 (.8)
3.28 (.16) ns ns 3.36 (.9) — ns — 3.07 (.9)	Chlorophyll a : b ratio	3.82 (.3) ns ns 3.12 (.1) — ns — 3.13 (.3)
5.98 (.17) ns ns 6.31 (.03) — *** — 5.95 (.03)	Chlorophyll : Carotenoid ratio	5.65 (.15) ** * 6.26 (.03) — * — 5.97 (.09)

Table 14
EXPERIMENT II: Effect of different levels of supplementary far-red light at high PAR fluence rate on upper and lower epidermes of leaf 9

means No far-red : Low far-red : High far-red

Upper Epidermis

SI	<u>means</u>	19.3	17.7	17.4			
	treatment	2	8.85	4.42	6.2	*	
	error	9	6.44	7.15			
	total	11	15.3				
SD (mm ⁻²)	<u>means</u>	243	184	178			
	treatment	2	10201	5100	8.8	**	
	error	9	5200	578			
	total	11	15400				
CD (mm ⁻²)	<u>means</u>	1256	1037	1023			
	treatment	2	1.37x10 ⁵	6.58x10 ⁴	5.3	*	
	error	9	1.17x10 ⁵	1.30x10 ⁵			
	total	11	2.54x10 ⁵				
Stomatal popln.	<u>means</u>	9.6x10 ⁴	8.2x10 ⁴	8.8x10 ⁴			
	treatment	2	3.98x10 ⁸	1.99x10 ⁸	0.93	ns	
	error	9	1.92x10 ⁹	2.13x10 ⁸			
	total	11	2.32x10 ⁹				
Cell popln.	<u>means</u>	5.0x10 ⁵	4.6x10 ⁵	3.8x10 ⁵			
	treatment	2	2.82x10 ¹⁰	1.41x10 ¹⁰	0.5	ns	
	error	9	2.49x10 ¹¹	2.77x10 ¹⁰			
	total	11	2.78x10 ¹¹				

Table 14 (contd.)

EXPERIMENT II: Effect of different levels of supplementary far-red light at high PAR fluence rate on upper and lower epidermes of leaf 9

means No far-red : Low far-red : High far-red

Lower epidermis

SI	<u>means</u>	21.6	20.5	22.0			
	treatment	2	4.59	2.29	3.2	ns	
	error	9	6.41	7.12			
	total	11	11.0				
SD (mm ⁻²)	<u>means</u>	324	257	254			
	treatment	2	12532	6266	5.6	*	
	error	9	9978	1108			
	total	11	22510				
CD (mm ⁻²)	<u>means</u>	1501	1250	1182			
	treatment	2	2.26x10 ⁵	1.13x10 ⁵	4.7	*	
	error	9	2.15x10 ⁵	2.39x10 ⁴			
	total	11	4.41x10 ⁵				
Stomatal popln.	<u>means</u>	1.30x10 ⁵	1.14x10 ⁵	1.25x10 ⁵			
	treatment	2	4.63x10 ⁸	2.31x10 ⁸	0.36	ns	
	error	9	5.77x10 ⁹	6.41x10 ⁸			
	total	11	6.24x10 ⁹				
Cell popln.	<u>means</u>	5.97x10 ⁵	5.56x10 ⁵	5.79x10 ⁵			
	treatment	2	3.28x10 ⁹	1.64x10 ⁹	0.16	ns	
	error	9	9.17x10 ¹⁰	1.01x10 ¹⁰			
	total	11	9.50x10 ¹⁰				

Table 15
EXPERIMENT II: Effect of different levels of supplementary far-red light at high PAR fluence rate on leaf area, stomatal size and pigment content of leaf 9

means No far-red : Low far-red : Mid far-red : High far-red

Leaf area (cm ²)	<u>means</u>	4.0	4.8	4.9	4.9		
	treatment	3	2.26		0.75	1.2	ns
	error	11	6.71		0.61		
	total	14	8.97				

SLA (cm ² g ⁻¹)	<u>means</u>	153	143	140	127		
	treatment	3	1.14x10 ³		381	2.8	ns
	error	10	1.36x10 ³		136		
	total	13	2.50x10 ³				

Stomatal size (um ²)	grand mean	410					
	treatment	2	4300		2150	2.3	ns
	surface	1	1121		1121	1.2	ns
	error	2	1842		921		
	total	5	7263				

Chl. a ₁ (mg g ⁻¹ fresh weight)	<u>means</u>	1.56	1.47	1.54	1.27		
	treatment	3	0.17		0.057	1.8	ns
	error	11	0.35		0.032		
	total	14	0.52				

Chl. a ₂ (mg m ⁻² leaf area)	<u>means</u>	211	189	204	176		
	treatment	3	2673		891	2.4	ns
	error	11	3992		363		
	total	14	6665				

Chl. a:b ratio	<u>means</u>	3.00	3.22	3.67	3.47		
	treatment	3	0.98		0.33	3.0	ns
	error	11	1.22		0.11		
	total	14	2.20				

Chl.: Carot. ratio	<u>means</u>	5.47	5.42	5.62	5.40		
	treatment	3	0.12		0.041	1.7	ns
	error	11	0.26		0.024		
	total	14	0.38				

Table 16
EXPERIMENT III: Effects of different levels of supplementary far-red light at low PAK fluence rate on upper and lower epidermes, leaf area and stomatal size of leaf 3

menas No far-red : Low far-red : Mid far-red : High far-red

Leaf area (cm ²)	<u>means</u>	5.87	5.68	5.91	6.99		
	treatment	3	3.38		1.13	10.2	**
	error	10	1.10		0.11		
	total	13	4.48				

Upper epidermis

SI	<u>means</u>	18.3	17.7	17.0	13.8		
	treatment	3	37.9		12.6	13	***
	error	10	9.55		0.955		
	total	13	47.5				

SD (mm ⁻²)	<u>means</u>	75.4	67.0	59.1	46.7		
	treatment	3	1.52x10 ³		506	8.5	**
	error	10	592		59.2		
	total	13	2.11x10 ³				

CD (mm ⁻²)	<u>means</u>	411	378	347	338		
	treatment	3	1.14x10 ⁴		3.81x10 ³	3.3	ns
	error	10	1.14x10 ⁴		1.14x10 ³		
	total	13	2.28x10 ⁴				

Stomatal popln.	<u>means</u>	4.46x10 ⁴	3.79x10 ⁴	3.49x10 ⁴	3.26x10 ⁴		
	treatment	3	2.93x10 ⁸		9.76x10 ⁷	2.4	ns
	error	10	4.04x10 ⁸		4.04x10 ⁷		
	total	13	6.97x10 ⁸				

Cell popln.	<u>means</u>	2.43x10 ⁵	2.15x10 ⁵	2.05x10 ⁵	2.37x10 ⁵		
	treatment	3	3.34x10 ⁹		1.11x10 ⁹	1.0	ns
	error	10	1.06x10 ¹⁰		1.06x10 ⁹		
	total	13	1.39x10 ¹⁰				

Table 16 (contd.)

EXPERIMENT III: Effects of different levels of supplementary far-red light at low PAR fluence rate on upper and lower epidermes, leaf area and stomatal size of leaf 3

means No far-red : Low far-red : Mid far-red : High far-red

Stomatal grand mean = 700

size (μm^{-2})	treatment	3	6843	2281	2.1	ns
	surface	1	2112	2112	2.0	ns
	error	3	3214	1071		
	total	7	12170			

Lower epidermis

SI means 22.8 22.7 21.9 20.4

treatment	3	12.8	4.26	8.5	**
error	10	5.03	0.503		
total	13	17.8			

SD
(mm^{-2})

means 92 86 77 67

treatment	3	1.17×10^3	390	5.3	**
error	10	735	735		
total	13	1.91×10^3			

CD
(mm^{-2})

means 401 377 349 331

treatment	3	9.84×10^3	3.28×10^3	2.8	ns
error	10	1.19×10^4	1.19×10^3		
total	13	2.17×10^4			

Stomatal
popln.

<u>means</u>		5.42×10^4	4.86×10^4	4.52×10^4	4.73×10^4	
treatment	3	1.60×10^8	5.34×10^7	0.9	ns	
error	10	5.89×10^8	5.89×10^7			
total	13	7.49×10^8				

Cell
popln.

<u>means</u>		2.36×10^5	2.14×10^5	2.06×10^5	2.32×10^5	
treatment	3	2.18×10^9	7.28×10^8	0.7	ns	
error	10	1.09×10^{10}	1.09×10^9			
total	13	1.31×10^{10}				

Table 17
EXPERIMENT III: Effects of different levels of supplementary far-red light at low PAR fluence rate on upper and lower epidermes and leaf area of leaf 5

means No far-red : Low far-red : Mid far-red : High far-red

Leaf area (cm ²)	<u>means</u>	8.23	7.38	7.75	8.51		
	treatment	3	2.66		0.886	4.3	*
	error	10	2.04		0.204		
	total	13	4.70				

Upper epidermis

SI	<u>means</u>	17.8	16.5	15.9	14.8		
	treatment	3	15.9		5.29	5.5	*
	error	10	9.52		0.952		
	total	13	25.4				

SD (mm ⁻²)	<u>means</u>	140	117	111	105		
	treatment	3	2.50x10 ³		835	6.2	*
	error	10	1.35x10 ³		135		
	total	13	3.85x10 ³				

CD (mm ⁻²)	<u>means</u>	789	707	698	710		
	treatment	3	1.91x10 ⁴		6.38x10 ³	2.5	ns
	error	10	2.55x10 ⁴		2.55x10 ⁴		
	total	13	4.46x10 ⁴				

Stomatal popln.	<u>means</u>	1.15x10 ⁵	8.63x10 ⁴	8.64x10 ⁴	8.93x10 ⁴		
	treatment	3	2.30x10 ⁹		7.65x10 ⁸	4.7	ns
	error	10	1.62x10 ⁹		1.62x10 ⁸		
	total	13	3.92x10 ⁹				

Cell popln.	<u>means</u>	6.46x10 ⁵	5.22x10 ⁵	5.42x10 ⁵	5.98x10 ⁵		
	treatment	3	3.62x10 ¹⁰		1.21x10 ¹⁰	3.7	ns
	error	10	3.25x10 ¹⁰		3.25x10 ⁹		
	total	13	6.87x10 ¹⁰				

Table 17 (contd.)

EXPERIMENT III: Effects of different levels of supplementary far-red light at low PAR fluence rate on upper and lower epidermes and leaf area of leaf 5

means No far-red : Low far-red : Mid far-red : High far-red

Lower epidermis

SI	<u>means</u>	22.6	22.1	21.4	20.2		
	treatment	3	10.9	3.65	8.1	**	
	error	10	4.46	0.446			
	total	13	15.4				
SD	<u>means</u>	198	163	153	150		
	treatment	3	5.29×10^3	1.76×10^3	8.9	**	
	error	10	1.99×10^3	199			
	total	13	7.27×10^3				
CD (mm ⁻²)	<u>means</u>	875	737	711	744		
	treatment	3	6.10×10^4	2.03×10^4	7.1	**	
	error	10	2.84×10^4	2.84×10^3			
	total	13	8.93×10^4				
Stomatal popln.	<u>means</u>	1.63×10^5	1.20×10^5	1.19×10^5	1.28×10^5		
	treatment	3	4.97×10^9	1.66×10^9	6.4	*	
	error	10	2.59×10^9	2.59×10^8			
	total	13	7.56×10^9				
Cell popln.	<u>means</u>	7.21×10^5	5.44×10^5	5.53×10^5	6.33×10^5		
	treatment	3	7.77×10^{10}	2.59×10^{10}	6.9	**	
	error	10	3.73×10^{10}	3.73×10^9			
	total	13	1.15×10^{11}				

Table 18
EXPERIMENT III: Effects of different levels of supplementary far-red light at low PAR fluence rate on upper and lower epidermes and leaf area of leaf 7

means No far-red : Low far-red : Mid far-red : High far-red

Leaf area (cm ²)	<u>means</u>	5.87	5.44	5.86	5.59		
	treatment	3	0.49		0.163	0.5	ns
	error	10	3.27		0.327		
	total	13	3.76				

Upper epidermis

SI	<u>means</u>	17.9	16.9	17.5	17.0		
	treatment	3	2.34		0.780	0.27	ns
	error	10	28.6		2.86		
	total	13	30.9				

SD (mm ⁻²)	<u>means</u>	179	192	176	165		
	treatment	3	1.21x10 ³		405	0.8	ns
	error	10	5.13x10 ³		513		
	total	13	6.35x10 ³				

CD (mm ⁻²)	<u>means</u>	996	1128	1013	974		
	treatment	3	5.27x10 ⁴		1.76x10 ⁴	4.8	*
	error	10	3.64x10 ⁴		3.64x10 ³		
	total	13	8.91x10 ⁴				

Stomatal popln.	<u>means</u>	1.05x10 ⁵	1.04x10 ⁵	1.03x10 ⁵	9.29x10 ⁴		
	treatment	3	3.14x10 ⁸		1.05x10 ⁸	0.37	ns
	error	10	2.82x10 ⁹		2.82x10 ⁸		
	total	13	3.13x10 ⁹				

Cell popln.	<u>means</u>	5.83x10 ⁵	6.14x10 ⁵	5.91x10 ⁵	5.45x10 ⁵		
	treatment	3	8.28x10 ⁹		2.76x10 ⁹	0.76	ns
	error	10	3.65x10 ¹⁰		3.65x10 ⁹		
	total	13	4.48x10 ¹⁰				

Table 18 (contd.)
 EXPERIMENT III: Effects of different levels of supplementary
 far-red light at low PAR fluence rate on upper and lower
 epidermes and leaf area of leaf 7

means No far-red : Low far-red : Mid far-red : High far-red

Lower epidermis

SI	<u>means</u>	22.6	21.9	23.4	22.1		
	treatment	3	4.11		1.37	1.2	ns
	error	10	10.8		1.09		
	total	13	14.9				

SD (mm ⁻²)	<u>means</u>	306	286	292	276		
	treatment	3	1.63x10 ³		543	0.7	ns
	error	10	8.19x10 ³		819		
	total	13	9.82x10 ³				

CD (mm ⁻²)	<u>means</u>	1350	1305	1249	1250		
	treatment	3	2.47x10 ⁴		8.22x10 ³	0.9	ns
	error	10	9.14x10 ⁴		9.14x10 ³		
	total	13	1.16x10 ⁵				

Stomatal popln.	<u>means</u>	1.78x10 ⁵	1.57x10 ⁵	1.70x10 ⁵	1.54x10 ⁵		
	treatment	3	1.39x10 ⁹		4.62x10 ⁸	2.3	ns
	error	10	2.00x10 ⁹		2.00x10 ⁸		
	total	13	3.38x10 ⁹				

Cell popln.	<u>means</u>	7.89x10 ⁵	7.17x10 ⁵	7.28x10 ⁵	6.97x10 ⁵		
	treatment	3	1.76x10 ¹⁰		5.87x10 ⁹	1.8	ns
	error	10	3.30x10 ¹⁰		3.30x10 ⁹		
	total	13	5.06x10 ¹⁰				

Table 19
EXPERIMENT IV: Effects of different fluence rates of
blue light on upper and lower epidermes of leaf 6.

means High blue : Mid blue : Low blue

Upper epidermis

SI	<u>means</u>	16.8	14.9	13.3		
	treatment	2	25.2	12.6	8.0	**
	error	9	14.1	1.57		
	total	11	39.3			
SD (mm ⁻²)	<u>means</u>	67.2	56.4	48.3		
	treatment	2	722	361	4.0	*
	error	9	801	89.0		
	total	11	1523			
CD (mm ⁻²)	<u>means</u>	399	374	360		
	treatment	2	3.25x10 ³	1.62x10 ³	1.1	ns
	error	9	1.35x10 ⁴	1.50x10 ³		
	total	11	1.68x10 ⁴			
Stomatal popln.	<u>means</u>	5.3x10 ⁴	5.1x10 ⁴	5.5x10 ⁴		
	treatment	2	4.1x10 ⁷	2.0x10 ⁷	0.3	ns
	error	9	6.0x10 ⁸	6.7x10 ⁷		
	total	11	6.4x10 ⁸			
Cell popln.	<u>means</u>	3.2x10 ⁴	3.4x10 ⁴	4.1x10 ⁴		
	treatment	2	2.0x10 ¹⁰	1.0x10 ¹⁰	8.0	**
	error	9	1.1x10 ¹⁰	1.2x10 ⁹		
	total	11	3.1x10 ¹⁰			

Table 19 (contd.)
 EXPERIMENT IV: Effects of different fluence rates of
 blue light on upper and lower epidermes of leaf 6.

means High blue : Mid blue : Low blue

Lower epidermis

SI	<u>means</u>	22.1	21.8	20.7		
	treatment	2	4.40	2.20	2.6	ns
	error	9	7.74	0.86		
	total	11	12.1			
SD (mm ⁻²)	<u>means</u>	85.4	75.4	72.0		
	treatment	2	391	195	2.0	ns
	error	9	879	98		
	total	11	1270			
CD (mm ⁻²)	<u>means</u>	387	344	346		
	treatment	2	4.68x10 ³	2339	1.7	ns
	error	9	1.23x10 ⁴	1366		
	total	11	1.70x10 ⁴			
Stomatal popln.	<u>means</u>	6.8x10 ⁴	6.8x10 ⁴	8.2x10 ⁴		
	treatment	2	5.58x10 ⁸	2.79x10 ⁸	3.7	ns
	error	9	6.67x10 ⁸	7.41x10 ⁷		
	total	11	1.22x10 ⁹			
Cell popln.	<u>means</u>	3.1x10 ⁵	3.1x10 ⁵	4.0x10 ⁵		
	treatment	2	2.05x10 ¹⁰	1.02x10 ¹⁰	10	**
	error	9	9.25x10 ⁹	1.03x10 ⁹		
	total	11	2.97x10 ¹⁰			

Table 20
 EXPERIMENT IV: Effects of different fluence rates of
 blue light on plant height, on petiole length,
 area, biomass and SLA of leaf 6 and on
 pigment content of leaf 8.

means High blue : Mid blue : Low blue

Plant height (mm)	<u>means</u>	77.0	77.3	130			
	treatment	2	1.08×10^4	5416	20	***	
	error	14	3.81×10^3	272			
	total	16	1.46×10^3				

Leaf 6

petiole length (mm)	<u>means</u>	24.0	22.2	29.6			
	treatment	2	159	79.5	37	***	
	error	13	27.9	2.15			
	total	15	186.9				

Leaf area (cm ²)	<u>means</u>	8.3	8.7	11.56			
	treatment	2	37.5	18.8	15	**	
	error	14	16.69	1.19			
	total	16	54.2				

Leaf biomass (mg)	<u>means</u>	23.6	20.6	29.1			
	treatment	2	209	128	37	***	
	error	14	48.4	3.45			
	total	16	257				

SLA (cm ² g ⁻¹)	<u>means</u>	397	422	351			
	treatment	2	1.45×10^4	7260	5.3	**	
	error	14	1.92×10^4	1372			
	total	16	3.37×10^4				

Table 20 (contd.)

EXPERIMENT IV: Effects of different fluence rates of blue light on plant height, on petiole length, area, biomass and SLA of leaf 6 and on pigment content of leaf 8.

means High blue : Mid blue : Low blue

Leaf 8

Chl. a ₁ (mg g ⁻¹ fresh weight)	<u>means</u>	2.55	2.55	2.30		
	treatment	2	0.241	0.120	4.3	*
	error	14	0.385	0.027		
	total	16	0.627			
Chl. a ₂ (mg m ⁻² leaf area)	<u>means</u>	378	420	376		
	treatment	2	6.65x10 ³	3.32x10 ³	3.1	ns
	error	14	1.49x10 ⁴	1.06x10 ³		
	total	16	2.15x10 ⁴			
Chl. a:b ratio	<u>means</u>	2.63	2.68	2.16		
	treatment	2	0.939	0.469	6.9	**
	error	14	0.950	0.068		
	total	16	1.89			
Chl.: Carot. ratio	<u>means</u>	7.79	7.56	7.97		
	treatment	2	0.481	0.24	2.6	ns
	error	14	1.26	0.92		
	total	16	1.74			

Table 21
EXPERIMENT V: Time course of stomatal opening
induced by blue and red light

<u>t</u> <u>min</u>	<u>mg m⁻² s⁻¹</u>	<u>μg m⁻² s⁻¹</u>	<u>gs⁻¹</u> <u>mm s⁻¹</u>	<u>Ci'</u> <u>mg m⁻³</u>
<u>20 μmol m⁻² s⁻¹ Blue light</u>				
0	< 3	-	< 0.2	-
20	26	20	8.5	660
45	5.2	0	1.2	670
65	17	20	4.7	660
85	10	40	2.5	640
200 (stable)	30	40	10.5	660
<u>17 μmol m⁻² s⁻¹ Blue light</u>				
0	< 3	-	< 0.2	-
25	30	0	9.4	670
45	3.3	0	0.7	670
70	21	0	5.3	670
90	10	0	2.2	670
200 (stable)	28	0	8.7	670
0	< 3	-	< 0.2	-
25	30	40	11.4	660
50	9.5	40	2.4	640
70	27	40	9.5	660
<u>30 μmol m⁻² s⁻¹ Red Light</u>				
0	< 3	-	< 0.1	-
30	18	50	8.5	650
60	11	60	3.6	630
120	16.6	60	6.7	650
240 (stable)	17	60	7.1	650
0	< 3	-	< 0.1	-
25	23	230	17.6	620
50	8.7	80	2.6	610
90	19	130	8.9	630
120	13	100	4.8	620
0	< 3	-	< 0.1	-
30	17	110	5.2	620
50	6.4	80	1.5	570
75	17	110	5.3	620
95	9.5	100	2.4	590
115	14	100	4.4	620

Table 22

EXPERIMENT VI: Effects of different light regimes during development on leaf gas exchange.

Plant	(PAR $\mu\text{mol m}^{-2} \text{s}^{-1}$)	Growth Cuvette	$\text{mg m}^{-2} \text{s}^{-1}$	$\mu\text{g m}^{-2} \text{s}^{-1}$	mm s^{-1}	$\text{Ci}' \text{mg m}^{-3}$
<u>PAR fluence rate effects</u>						
A	85	190	22	450	4.4	480
		190	49	530	9.0	530
		80	34	220	6.5	590
B	110	150	37	520	6.4	490
		150	46	520	9.3	530
		150	41	550	7.3	490
C	110	150	39	430	8.5	540
		150	30	350	4.3	510
		150	28	340	4.5	510
D	200	190	40	530	6.1	490
		190	36	530	5.2	470
E	230	150	23	390	4.5	490
		150	25	390	4.5	490
F	230	150	27	400	5.1	500
		150	41	480	13.2	560
		150	40	430	10.5	560

Spectral effects

Growth environment: White plus far-red light ($\phi_c = 0.38$; $\phi_r = 0.19$)

G	110	76	29	250	11.4	600
		95	30	300	10.5	590
		45	23	160	6.1	610
		135	30	550	11.1	530
		95	20	270	4.3	540
		95	20	300	4.5	530
H	110	92	35	380	8.0	590

Growth environment: Blue light - see EXPERIMENT IV

I	130	$\frac{\text{B:R}}{\text{ratio}}$	100	35	330	5.6	550
		0.30					
J	130	0.78	100	47	370	7.8	570
K	130	1.80	100	43	350	9.3	580
			100	30	310	4.9	550

DISCUSSION

Growth Cabinet

During an almost continuous 18 month period, the growth cabinet operated reliably and generally fulfilled its design specification. The two principle problems encountered involved the radiance of the Kolorarc lamps and the transmittance of the cavity windows.

The light output from individual new Kolorarc lamps was neither equal nor constant and the spectral quality also varied. The effect of these differences was minimised by carefully selecting the lamps for each quarter of the cabinet, but after the lamps had aged a few months their output had fallen by about 30%. Thus the fluence rates available were lower than originally intended. Dysprosium-based metal halide lamps (Wotan) have superseded Kolorarcs as the best relatively inexpensive source of high irradiance white light, but these may suffer from similar problems.

Fluence rates were further eroded as fine debris accrued inside the cavity windows. Time did not permit a heat exchanger of the type successfully utilised in the Zeta cabinet to be constructed. The "temporary" system used throughout the period of operation involved pumping water up to the cavity windows and allowing it to drain back to a refrigerated tank via a pair of gate valves, carefully adjusted to maintain a hyperbaric pressure in the windows. This was essential to prevent the water degassing inside the windows as it became heated by the lamps. However, variation in flow rate occasionally allowed the pressure to fall substantially and bubbles formed, scattering a substantial proportion of the light back upwards. The bubbles also tended to leave a fine white film behind them. Algal growth was not a problem, however, as ethanol was added to the water in circulation (ca. 10% v/v). After a year of operation, when the PAR transmittance of the windows had fallen from 90 to 60%, they were dismantled, cleaned and reassembled. The facility will be much enhanced once the proper cooling system is installed.

Gas analysis system

The effectiveness of the humidification system left much to be desired, as the dewpoint varied by as much as 2°C (equivalent to a change in relative humidity of about 10%) through the day, despite attempts to maintain the humidification column at constant temperature and pressure. The cuvette was well-suited to its purpose, although no attempts were made to further optimise the design. The IRGA operated reliably following an initial overhaul, but the hygrometer caused frequent problems as its readings tended to vary with the null point setting (which controls the stable level of condensation on the Peltier-cooled mirror), contrary to the manufacturer's assertion. This problem may have resulted from the necessity of using low flow rates in order to obtain sufficient resolution of the transpiration rate. Almost entirely as a result of problems with the hygrometer, approximately half of the gas exchange experiments initiated had to be abandoned before useful data had been obtained.

Experimental work

The effects of the various treatments on the gross leaf morphology were broadly in accord with previous work. Experiment I indicated that a reduction in PAR fluence rate from 276 to 157 $\mu\text{mol m}^{-2}\text{s}^{-1}$ stimulated leaf expansion; Morgan and Smith's [1981] data showed that although leaf area in the same species increased between 25 and 45, it fell between 45 and 100 $\mu\text{mol m}^{-2}\text{s}^{-1}$. Thus it appears that the classical etiolation response to non-spectral shade (see 2.1) begins at fluence rates somewhere below 100 $\mu\text{mol m}^{-2}\text{s}^{-1}$ in this species. In Experiment IV, where the level of blue light was varied between 42 and 12 $\mu\text{mol m}^{-2}\text{s}^{-1}$ while total PAR was kept constant, leaf expansion was also stimulated by a low relative level of blue light; it is thus likely that cryptochrome is involved in this response. In accord with Morgan and Smith [1981] and Child *et al.* [1981], supplementary far-red had little effect on leaf area in any of the experiments. Previous reports concerning the same species in which phytochrome was implicated in leaf area changes (Holmes and Smith, 1975, 1977c) may have been confounded by other effects of the treatments, particularly related to the level of blue light.

SLA was massively increased at low PAR fluence rate

Gas analysis system

The effectiveness of the humidification system left much to be desired, as the dewpoint varied by as much as 2°C (equivalent to a change in relative humidity of about 10%) through the day, despite attempts to maintain the humidification column at constant temperature and pressure. The cuvette was well-suited to its purpose, although no attempts were made to further optimise the design. The IRGA operated reliably following an initial overhaul, but the hygrometer caused frequent problems as its readings tended to vary with the null point setting (which controls the stable level of condensation on the Peltier-cooled mirror), contrary to the manufacturer's assertion. This problem may have resulted from the necessity of using low flow rates in order to obtain sufficient resolution of the transpiration rate. Almost entirely as a result of problems with the hygrometer, approximately half of the gas exchange experiments initiated had to be abandoned before useful data had been obtained.

Experimental work

The effects of the various treatments on the gross leaf morphology were broadly in accord with previous work. Experiment I indicated that a reduction in PAR fluence rate from 276 to 157 $\mu\text{mol m}^{-2}\text{s}^{-1}$ stimulated leaf expansion; Morgan and Smith's [1981] data showed that although leaf area in the same species increased between 25 and 45, it fell between 45 and 100 $\mu\text{mol m}^{-2}\text{s}^{-1}$. Thus it appears that the classical etiolation response to non-spectral shade (see 2.1) begins at fluence rates somewhere below 100 $\mu\text{mol m}^{-2}\text{s}^{-1}$ in this species. In Experiment IV, where the level of blue light was varied between 42 and 12 $\mu\text{mol m}^{-2}\text{s}^{-1}$ while total PAR was kept constant, leaf expansion was also stimulated by a low relative level of blue light; it is thus likely that cryptochrome is involved in this response. In accord with Morgan and Smith [1981] and Child *et al.* [1981], supplementary far-red had little effect on leaf area in any of the experiments. Previous reports concerning the same species in which phytochrome was implicated in leaf area changes (Holmes and Smith, 1975, 1977c) may have been confounded by other effects of the treatments, particularly related to the level of blue light.

SLA was massively increased at low PAR fluence rate

in Experiment I; Morgan and Smith [1981b] observed a similar but less pronounced trend in the same species. Such a response buffers relative growth rate against changes in fluence rate, and is considered a fundamental characteristic of shade tolerance. Differences in growth habits between species should be borne in mind, however. It has also been found that net assimilation is sometimes enhanced in shade tolerant species by reduced respiration rates (Jarvis, 1964; Grime, 1965; Bjorkman, 1981). The data from Experiment I indicate that Chenopodium album shows a large SLA response at relatively high fluence rates, even though it is a shade-intolerant species. It is evident that SLA, like leaf area itself, bears a subtle relationship to fluence rate which is probably species-dependent.

Regarding the spectral dependence of leaf area and SLA, supplementary far-red light substantially offset the effects of reduced PAR in Experiment I. At the higher fluence rates used in Experiment II, supplementary far-red light induced a similar trend but the differences were not statistically significant. Using lower light levels, Morgan and Smith [1981b] found that the effect of supplementary far-red was rather variable. It would appear that in these responses, differences in ϕ exerted their principal effects at fluence rates nearer typical daylight levels. In Experiment IV, the significant differences in SLA between treatments were not correlated with the B:R ratio, implying that cryptochrome was not involved in contrast to the results for leaf area itself.

Turning to the epidermis, stomatal density, arguably the most potent morphological variable influencing gas exchange physiology, was found to vary five-fold (ca. 50 - 250 stomata mm^{-2}) in the various experiments. In addition to leaf area, the factors which govern stomatal density (namely, SI and total protodermal cell population) were studied intensively.

Most of the results for the first three experiments showed that SI on both epidermes was linearly correlated with ϕ_c , although occasionally an insignificant effect was observed. This is in general accord with the data of Child et al. [1981]. In Experiment III there was little difference in SI between leaves 3 and 5 in each treatment indicating that SI may be independent of the usual change in leaf area observed at successive nodes along the stem (ontogenic drift). Salisbury [1927] reached a similar

conclusion in a comparative study of the English woodland flora. SI in Experiment II was lower on the lower epidermis and higher on the upper epidermis than in Experiment III. This may be due to differences in PAR fluence rate. The data collected in Experiment IV at constant PAR and ϕ indicate a significant effect of the B:R ratio on upper epidermis SI but not on the lower. As the B:R ratio was substantially constant in Experiments II and III, the fluence rate of blue light, rather than PAR or the B:R ratio per se, may have been responsible. However, PAR fluence rate was without effect on SI in Experiment I. In Experiment III the treatment means for leaf 7 were all similar to those for the other two leaves in the no far-red treatment. This be an artifact resulting from incomplete leaf expansion.

The total protodermal cell population, assuming that no division occurred during leaf expansion, was deduced from the final leaf area and estimates of CD in the midrib - lateral vein area of the lamina. Although CD tended to fall with ϕ c, this was not always apparent. The massive effect of PAR fluence rate on CD seen in Experiment I indicates that slight differences in PAR during development might be responsible for these discrepancies, as the lower leaves effectively grew down from the light sources (since the apices were maintained at a constant distance). The correlation between PAR and leaf area seen in this experiment is probably the principal cause of the variation in CD. However, Experiment IV indicated that blue light may be responsible for the expansion effect on CD. The cell population (calculated as CD x leaf area) was not significantly affected by far-red light in most cases. In Experiment I reduced PAR was associated with smaller populations especially on the lower epidermis, whereas in Experiment IV low levels of blue light alone had the oppo site effect. The effect of the PAR difference between Experiments II and III cannot be interpreted because of the apparent effect of ontogenic drift on the cell populations.

The experiments indicated that the total cell population of the epidermis was scarcely affected by supplementary far-red, while SI was strongly reduced. The simplest physiological hypothesis is that protoderm mitosis was unaffected while stomatal induction was enhanced by reduced phytochrome photoequilibria. A fall in stomatal population would be expected, but this parameter (calculated from SD x leaf area) showed no such trend.

Paradoxically, neither cell nor stomatal numbers change, yet the ratio of the two does!

At least three possible explanations exist. Firstly, it is not generally valid to apply parametrical statistics (based on the properties of the normal distribution) directly to ratios, which characteristically have skewed distributions. Although Kleiber and Mohr [1963] applied a mathematical correction to remove this distortion, Schürmann [1959] showed that the skew is insignificant over the commonly encountered range of SI (10 - 30%). Secondly, the calculation of protodermal cell population from leaf area and the densities of stomata and undifferentiated cells may be confounded by the effects of meristemoid initiation. Certainly this may be the case in such species as Commelina where numerous subsidiary cells are present and meristemoids may increase the number of epidermal cells. In Chenopodium however, true subsidiary cells are absent and the activity of the meristemoid is apparently confined to stomatal morphogenesis. Thirdly and most probably, CD and SD in the midrib - lateral vein region of the lamina may not be simply related to the expansion of the leaf as a whole; the data in Figure 96 indicate that the relationship between epidermis and leaf expansion is probably a subtle one. The true populations can only be deduced from density x leaf area data if the former provides an unbiased estimate for the whole leaf.

With so many influential factors, the SD data *themselves* can only be interpreted in very general terms. Leaf 5 in Experiment III yielded SD values consistent with those in Experiment I, with low fluence rates tending to reduce the density more effectively than supplementary far-red, especially on the upper epidermis. Leaf expansion is probably the predominant factor, although cell population may also vary because of changes in the mitotic activity of the protoderm. According to Experiment IV, some of the effects of PAR may be attributable to blue light alone. Ontogenic drift prevents the results for Experiment II being compared directly to the others, but the effect of far-red was similar.

Spectral differences had no apparent effects on stomatal size (Experiment II and Experiment III, leaf 5) and, although stomatal size may have been influenced by leaf expansion, the ratios of stomatal area to leaf area for the two experiments differed by 30%. Thus the stomata apparently do not expand in exact proportion to the leaf

as a consequence ontogenic drift. However, the accuracy of the estimate of stomatal size scarcely justifies any conclusions regarding maximum stomatal pore area. Other possible structural differences (for example, mesophyll anatomy) were not investigated as they were considered unlikely to vary as widely as SD, and probably have less potential significance in gas exchange physiology (see Monteith, 1973).

The data from Experiments II and IV (PAR fluence rates of 360 and 130 $\mu\text{mol m}^{-2}\text{s}^{-1}$ respectively) indicated that neither supplementary far-red light nor the blue : red ratio had large effects on the type or quantity of photosynthetic pigments. However, Experiment I showed that chlorophyll levels were substantially reduced by supplementary far-red at 150 $\mu\text{mol m}^{-2}\text{s}^{-1}$ PAR fluence rate. Earlier work on this species has also shown that far-red tends to reduce chlorophyll content, especially when expressed on an area basis (Holmes and Smith, 1975; Morgan and Smith, 1978; Child *et al.*, 1981), but Fitter and Ashmore [1974] found the reverse in *Veronica persica* grown at *ca.* 10% daylight. Bjorkman [1981] concluded that sun species tended to maintain a fairly constant level of chlorophyll (on an area basis) over a wide range of PAR fluence rates, while the data from Experiment I indicated that chlorophyll levels were substantially lower at 280 than at 150 $\mu\text{mol m}^{-2}\text{s}^{-1}$ PAR. Thus the results from this experiment seem unusual and require verification.

Bjorkman [1981] suggested that the generally reported fall in the Chl a : b ratio at reduced fluence rates may be an acclimation response to leafy shade. Far-red light stimulates only photosystem I, so the imbalance between photosystems I and II under these conditions could be corrected by increasing levels of chlorophyll b which is associated with photosystem II alone. Although phytochrome would apparently be an ideal photoreceptor for this response, it was without effect in Experiments I and II (also Child *et al.*, 1981). According to Experiment IV, the fluence rate of blue light may be the significant factor.

The leaves used in Experiment VI showed similar morphogenic responses to ϕ and PAR as in the growth experiments. In view of the large effects of PAR fluence rate on the distribution and abundance of stomata during development, it is surprising that the gas exchange measurements in Experiment VI showed no significant

effects of PAR fluence rate during foliar development on any of the variables measured. The nastic feedback responses probably masked the differences in stomatal density to such an extent that the cuvette system was unable to detect them. Differences in the B:R ratio during growth were also without apparent effect. Although supplementary far-red during growth tended to reduce SD, the values of g_s recorded for these leaves were relatively high. The small sample size prevents a realistic estimate of the significance of the difference however. The different PAR fluence rates during growth had little effect on the net photosynthetic rate or calculated value of C_i' ; in general, these were a function of the PAR in the cuvette, although no special effort was made to establish the exact relationships. Thus, whatever the effects of fluence rate on light harvesting or carboxylating capacity, the measured parameters of photosynthesis were unaffected. J.S. McLaren (unpublished data) found that the only apparent differences in photosynthesis between Ch. album plants grown under various levels of supplementary far-red were related to the net CO_2 depletion per chlorophyll molecule. In contrast, the morphogenic work reported here showed little effect of far-red light on chlorophyll content, so this work does not support the notion that photosynthetic efficiency is altered.

As discussed in 2.1, $g_{s\max}$ might be expected to have some ecological significance in constraining the maximum rate of photosynthesis achievable under favourable conditions of humidity, temperature and irradiance. Experiment VI provides no information about this aspect as the fluence rates available saturated neither photosynthesis nor stomatal opening.

Under the conditions adopted in Experiment V, the rate of stomatal opening was similar under both red and blue light. Especially rapid opening responses specific to blue light are considered to be restricted to grasses (Johnsson et al., 1976), but Zeiger et al. [1981] showed that precocious stomatal opening before dawn was stimulated by blue light in a species of mallow. Rapid opening may result from a greater ion pumping capacity in relation to the volume of the guard cells, while its spectral sensitivity may simply reflect the absorption spectrum of cryptochrome.

CONCLUSIONS

The growth experiments on Chenopodium album were successful in further defining the role of light in leaf development. Leaf area and SLA were more strongly affected by PAR fluence rate than by purely spectral differences, but at least part of this effect appears to be mediated by cryptochrome rather than the photosynthetic pigments, as variations in the fluence rate of violet-blue light induced a response at constant levels of PAR. Leaf area is a principal factor determining the rate of photosynthesis of the plant as a whole at a given level of PAR. Most growth analyses have concentrated on crop plants which generally have been selected for high relative growth rate; their leaf area is therefore likely to be close to maximum. On the basis of such results, light is usually simply considered to either limit or saturate photosynthesis. There is evidence, however, that shade tolerance in natural populations involves a characteristic ability to offset changes in mean PAR without catastrophic effects on relative growth rate by reducing respiration and increasing the leaf area available for light capture. Once this homeostatic capacity is exceeded, it seems likely that many plants attempt to avoid the presumed obstacle to light by undergoing the classical changes associated with etiolation (reduced leaf area and chlorophyll content, and increased internode extension). Reduced red : far-red ratios, characteristic of leafy shade, apparently induce the stem extension component alone. This may be of considerable ecological significance, but as data are available for only a few species, further speculation regarding the exact roles of cryptochrome and phytochrome action in the natural environment is premature.

Another important factor determining the rate of photosynthesis, at least at high fluence rates, is the ability of the leaf to absorb CO_2 from the atmosphere. However, water loss from the plant must also be minimised in most terrestrial habitats. The evolution of stomata has contributed considerably to the ability of plants to reconcile CO_2 uptake and H_2O loss. Both temporary (nastic) and permanent (morphogenic) phenomena affect the rate of gas exchange.

Stomatal opening is generally stimulated by light but it was apparent from these experiments that the rate of opening in Chenopodium was not strongly wavelength-dependent. Especially rapid opening induced by blue light

has been reported in grasses (Johnsson et al., 1976) and probably reflects the predominant sensory role of cryptochrome in this response, coupled with rapid effects on guard cell turgor in these species. There is unlikely to be an ecological motive for the sensitivity to blue light in particular because, although these wavelengths predominate during twilight, the rate of increase in fluence rate throughout the spectrum is so great that a given SPFR is reached by each part of the spectrum within a few minutes of any other. The stable conductance attained was, however, higher under blue light despite the lower fluence rates used. This is consistent with previously published results.

In addition to the aperture of the stomatal pores, the density of stomata on the epidermis also affects the rate of gas exchange. This density is related to the number of protoderm cells from which the epidermis is formed, the proportion of these converted into stomata (the stomatal index) and the expansion of the leaf.

The abundance of protoderm cells (as indicated by the total cell population of the epidermis, calculated from cell density \times leaf area) was apparently little affected by the level of supplementary far-red light, whereas ontogenic drift and the fluence rates of both PAR and blue light were effective.

Stomatal index was found to be affected predominantly by the red : far-red ratio, high levels of far-red tending to reduce stomatal induction, whereas high fluence rates of blue light tended to increase stomatal index on the upper epidermis. These responses are likely to be mediated by phytochrome and cryptochrome, respectively.

Despite these results, the equivalent estimate for stomatal population failed to show an effect of supplementary far-red light. The explanation of the paradox may be that expansion in the central area of the lamina where the cell densities were estimated was not simply related to the final leaf area. Consequently, the "density \times leaf area" calculations may be biased.

Although the effects of the different light treatments on stomatal density are complex, in this species as in most of those investigated by Salisbury

[1927], the effects of differences in leaf area were greater. Consequently, fluence rate rather than colour plays the predominant role in determining stomatal density, blue light being particularly potent. However, in many herbs ontogenic drift in leaf area along the stem may mask this.

On both leaf area and fresh weight bases, supplementary far-red light was associated with rather lower chlorophyll concentrations. Neither the chlorophyll a : b ratio nor the chlorophyll : carotenoid ratio was substantially affected by the light treatments.

Plants grown at different PAR fluence rates were found to have very similar gas exchange characteristics at the fairly low fluence rates used. Photosynthesis was closely correlated with the PAR fluence rate in the gas analysis cuvette, irrespective of the growth treatment. Differences in the level of blue light during growth were also without substantial effect, but leaves grown in the presence of supplementary far-red light showed somewhat higher conductances.

These insignificant effects in the face of substantially different stomatal densities resulting from the various growth treatments are presumably a reflection of the feedback mechanisms which control stomatal aperture; without these, stomatal density would have a direct effect on conductance. It is interesting that the properties of the control loops themselves appeared to be unaffected. An increase in maximum conductance at light saturation in plants grown at elevated growth fluence rates has been reported elsewhere (Holmgren, 1968); it would be interesting to discover the relationship between this and the effect on stomatal density.

Presumably these photoresponses have an adaptive value, somehow allowing the plant to acclime better to its local environment. Although the characteristics of natural daylight are now quite well known, it is difficult to relate these to the results described in this section. Leaf area changes have a large effect on stomatal density and, above a certain fluence rate, the area is directly correlated with the fluence rate in the environment, and hence with the photosynthetic rate attainable per unit leaf area. Thus the increase in stomatal density at higher PAR fluence rates may permit more rapid gas exchange at

[1927], the effects of differences in leaf area were greater. Consequently, fluence rate rather than colour plays the predominant role in determining stomatal density, blue light being particularly potent. However, in many herbs ontogenic drift in leaf area along the stem may mask this.

On both leaf area and fresh weight bases, supplementary far-red light was associated with rather lower chlorophyll concentrations. Neither the chlorophyll a : b ratio nor the chlorophyll : carotenoid ratio was substantially affected by the light treatments.

Plants grown at different PAR fluence rates were found to have very similar gas exchange characteristics at the fairly low fluence rates used. Photosynthesis was closely correlated with the PAR fluence rate in the gas analysis cuvette, irrespective of the growth treatment. Differences in the level of blue light during growth were also without substantial effect, but leaves grown in the presence of supplementary far-red light showed somewhat higher conductances.

These insignificant effects in the face of substantially different stomatal densities resulting from the various growth treatments are presumably a reflection of the feedback mechanisms which control stomatal aperture; without these, stomatal density would have a direct effect on conductance. It is interesting that the properties of the control loops themselves appeared to be unaffected. An increase in maximum conductance at light saturation in plants grown at elevated growth fluence rates has been reported elsewhere (Holmgren, 1968); it would be interesting to discover the relationship between this and the effect on stomatal density.

Presumably these photoresponses have an adaptive value, somehow allowing the plant to acclime better to its local environment. Although the characteristics of natural daylight are now quite well known, it is difficult to relate these to the results described in this section. Leaf area changes have a large effect on stomatal density and, above a certain fluence rate, the area is directly correlated with the fluence rate in the environment, and hence with the photosynthetic rate attainable per unit leaf area. Thus the increase in stomatal density at higher PAR fluence rates may permit more rapid gas exchange at

still higher fluence rates. In contrast to the situation in the growth cabinet, daytime PAR levels in the natural environment commonly vary by more than an order of magnitude. A photomorphogenic adjustment related to the mean fluence rate might allow more rapid photosynthesis under optimal conditions; water loss could then be reduced over a long period, as the conductance could be maintained at a lower level under adverse conditions without reducing the growth rate. When g_s was determined in Experiment V, however, the fluence rates at which the plants were grown had apparently little effect, possibly because the measurements were carried out below saturating fluence rates. The hypothesis does not explain why stomatal density is not always maintained at as high a level as possible; perhaps peristomatal transpiration is reduced by lower stomatal density. The adaptive significance of phytochrome-mediated control of stomatal induction is also obscure and merits serious investigation under field conditions, by means of both experiments and surveys of natural populations. Before this has been attempted, speculation regarding the role of phytochrome here is unlikely to be fruitful.

SECTION 3

Final discussion and conclusions

FINAL DISCUSSION AND CONCLUSIONS

Meteorological factors, the position of the sun in the sky and terrestrial objects, notably leafy canopies, affect not only the fluence rate but also the colour of daylight. While low fluence rates have long been known to cause etiolation in most green plants (leaf size and chlorophyll content are reduced and the internodes extended as a shade-avoidance strategy), attention has recently been directed to the role of spectral composition in photomorphogenesis. Phytochrome apparently serves to detect the relative levels of red and far-red light; its photochromic properties enable it to produce a photoequilibrium (ϕ) between two stable forms, which is dependent upon the red : far-red fluence ratio rather than the absolute irradiance. The ratio of the two most potent wavelengths (660 nm and 730 nm) is known as \mathfrak{R} .

In this project the characteristics of the natural light environment were studied intensively in order to gain a better understanding of the ecological role of the various plant responses to their light environment. The main daytime value of \mathfrak{R} in the absence of shading was found to be 1.15 (Table 1; Fig. 20), which is in exact agreement with earlier work (Holmes and Smith, 1977a) and corresponds to a calculated photoequilibrium (ϕ_c) of 0.53 (Table 2; Fig. 21). Seasonal variation probably occurs (Fig. 26) since \mathfrak{R} reached a minimum of ca. 1.0 in late winter (February-March) and a maximum of ca. 1.25 six months later. However, the variation in \mathfrak{R} during a single day was of a similar order and the seasonal changes in ambient temperature and photoperiod are probably of much greater physiological significance. In general, cloud cover had little effect on \mathfrak{R} (Table 4), although the spectral composition of daylight varied considerably during the passage of broken cloud, as the solar disc was alternately exposed and obscured (Fig. 24).

Although most previous work has indicated that the effects of cryptochrome (the blue light absorbing photoreceptor) are fluence rate dependent, little attempt has been made to investigate its photochromicity. However, red / blue reversibility has been reported in a fungus (Lüser and Schäfer, 1980), and there is both biochemical and physiological evidence of an interaction between the effects of blue and red light. The mean daytime value of the blue : red fluence ratio was approximately 0.86

(Table 3; Fig. 22) but the effect of cloud cover (Table 4) was substantial.

An association between phytochrome action and the well-known differential transmission of red and far-red light by green leaves has long been suspected (Cumming, 1963) and many now consider the detection of leafy shade to be the principal role of phytochrome. Apparently independently, Jordan [1969] described the use of a similar red / far-red ratio for estimating leaf area index in a tropical rainforest. A good indication of shading based on absolute fluence rate requires simultaneous knowledge of the fluence rate outside the canopy, while fluence ratios are irradiance independent. Subsequently, a close relationship between \bar{J} and leaf area index was reported for wheat, but significant changes in \bar{J} during the leafy phase of several deciduous woodlands were apparently not accompanied by changes in light transmission (Holmes and Smith, 1977b; Tasker and Smith 1977; Tasker, 1977).

In this project the light environment of an oak woodland was studied intensively. \bar{J} and ϕ_c (Figs. 39 and 40) fell substantially on leaf emergence but once again, although \bar{J} increased temporarily in late summer, there was no apparent change in the absolute fluence rate within the wood (Fig. 42). Furthermore, there were no parallel changes in the pigment content (Fig. 57) or optical properties of the leaves or canopy (Fig. 59). Consequently, the observed increases in \bar{J} and ϕ_c in woodlands during late summer are probably entirely due to the simultaneous occurrence of high \bar{J} and ϕ_c values of the incident light. The presence of significant seasonal variation in \bar{J} places a strict limit on the possible accuracy of leafy shade detection via phytochrome; The correlation between \bar{J} and transmittance during the leafy phase (Fig. 60) was poor.

The oak canopy had substantial effects on the light environment beneath; even during the "light phase" the fluence rate was half that outside, while only about a tenth of the photosynthetically useful light reached the woodland floor during the "leafy phase". However, the leaf area indices of deciduous woodland are generally high (>5) and so canopy transmittance to PAR was surprisingly high in view of the strong absorption by individual leaves. This was because the leaves in such a canopy are clumped, forming an optical "sieve" rather than tessalated layers.

The spectral effect of the canopy is similarly reduced. Conversely, according to propagation theory, scattering of light by leaves reduces the overall transmittance and exaggerates the effects of pigments (other factors remaining constant). Consequently, phytochrome photoequilibrium is affected not only by leaf area index and chlorophyll content, but also by the arrangement and reflectance of the leaves. The seasonal variation in \overline{J} values of incident daylight further complicates the relationship between this ratio and leafy shade beneath an open canopy.

The far denser canopy formed by a sugar beet crop was investigated in the following year. Here, transmittance declined rapidly during mid-summer, reaching a minimum of only 0.26% at 680 nm in late September; \overline{J} and ϕ_c fell to ca. 0.04 and 0.12 respectively. Thereafter, wind damage to the canopy was probably responsible for an increase in transmittance and the values of \overline{J} and ϕ_c . The effects of the canopy overwhelmed the seasonal variation in incident \overline{J} , and the mean daytime values of \overline{J} (Fig. 84) closely followed changes in the equivalent transmittance ratio (Fig. 85); the correlation between \overline{J} and the canopy transmittance was close (Fig. 86).

Holmes and Smith (1977b) reported that mean \overline{J} values beneath a wheat canopy were substantially lower under clear than under cloudy skies. This can be attributed to sampling bias against sunflecks which occur periodically and have high \overline{J} values; when the leaves are fairly uniformly distributed, these periods of high \overline{J} must be compensated for by lower values when the solar disc is aligned with leafy areas. As sunflecks do not occur under a dense canopy without gaps, beneath these cloud cover should have no effect on \overline{J} . These conclusions were fully justified by the data collected.

Substantially denser canopies than that of the sugar beet crop are rare in the natural environment. According to Hartmann's [1966] hypothesis regarding the role of phytochrome destruction in the high irradiance response of etiolated plants, most of the original pool will be lost within a single day even at a photoequilibrium of 0.1. The HIR will therefore be abolished rapidly in the natural environment and is unlikely to be ecologically important.

Particular attention was paid to twilight periods in this work, spectra being recorded every two or three

minutes around sunrise and sunset. In addition to the obvious change in fluence rate, the red : far-red ratio tended to fall at dusk and rise again at dawn, presumably modifying ϕ . Phytochrome is known to be involved in the night-break phenomenon of photoperiodism and, as it is thought to modulate development via relative spectral differences largely irrespective of absolute fluence rate, such twilight variations in light quality have been suggested as the effective time signals in photoperiodic control.

The data collected showed that γ and ϕ_c during twilight were significantly affected by solar position (Figs. 20 and 21; Table 6); however, the date of recording had substantial effects too. In the shade light environment, the seasonal changes associated with the leafy phase were at least as significant as those associated with twilight. Consequently, the capacity of phytochrome to provide reliable time signals is very limited under field conditions.

The high proportion of blue light was found to be correlated with solar position during twilight, yet during the day only small changes were apparent. A surprising result was that the relationship persisted beneath leafy canopies (Tables 6, 9 and 10). The blue : red ratio therefore provides a more satisfactory time signal than γ .

The action of blue light in photoperiodism has been considered unimportant, but this is not entirely justified as the conclusion relies on several misconceptions. Firstly, action spectra for the phytochrome-mediated night break response have wrongly been considered typical of the sensitivity throughout the dark period, and thus phytochrome control has become the central dogma of photoperiodism. Secondly, most spectral treatments have been wrongly based on power rather than photon units, and are thus biased against the photochemical efficacy of short wavelengths. Even the original action spectra for the night-break response imply that blue light has a peculiarly variable action in different species; these cannot be accounted for by differences in "chlorophyll screening" as the red region was unaffected. The possible significance of carotenoid screening has not been studied. A further factor contributing to the misconception is that high fluence rates of blue light are difficult to maintain for prolonged periods in the laboratory, and so relatively few

experiments have actually been performed.

When "end-of-day" experiments are considered, the involvement of phytochrome in photoperiodic control is quite unconvincing. Neither Red / far-red reversibility nor antagonism have been demonstrated, and numerous species (notably crucifers) show high sensitivity to blue light, although these may be exceptional. Perhaps the most obvious evidence against phytochrome involvement is irradiance dependence, while phytochrome action is usually irradiance-compensated in the other photoresponses of green plants it is thought to mediate.

In this project, the change in fluence rate during twilight was closely correlated with solar position (Fig. 23) and, even in the presence of a leafy canopy, this effect dwarfed differences between recording dates (Tables 6, 9 and 10). Thus, a fluence rate dependent photoreceptor would be ideally suited to provide a time signal for the photoperiodic system. Action spectra for the flowering responses to light during the end-of-day and end-of-night periods are lacking, but would be useful in defining the likely photoreceptor. Currently, there is very little justification for implicating phytochrome to the exclusion of other, possibly unknown, photoreceptors.

* * *

One of the most closely studied photoresponses of green plants concerns internode extension. Blue light, acting via cryptochrome, tends to reduce the extension rate and the response is fluence rate dependent. However, elongation is also related to the ϕ value established by the treatment and is largely independent of fluence rate in the 600 - 800 nm (red and far-red) range. Phytochrome thus seems to elicit at least part of the etiolation response independently of irradiance. Phytochrome-mediated effects on leaf expansion are fairly small, however, in contrast to those of absolute fluence rate.

A growth cabinet was designed and built in order to study the roles of phytochrome and cryptochrome in leaf development under controlled environmental conditions. Fluence rates approaching those of natural daylight were achieved, making the results relevant to photomorphogenesis in the field. The spectral distribution of the light was varied using coloured filters in combination with

incandescent tungsten-halogen filament lamps or metal halide discharge lamps. Adjustable shelves in the growth chamber allowed the apices of the growing plants to be maintained at a constant distance from the lamps.

The various growth experiments carried out using Chenopodium album confirmed that supplementary far-red, and hence phytochrome, had little effect on final leaf area, while the fluence rate of either PAR or blue light alone apparently modified leaf expansion. However, the final leaf area was negatively correlated with fluence rate, the opposite of the classical etiolation effect. Similar relationships have, however, been reported by other workers. The response may help to buffer the plant's growth rate against changes in PAR fluence rate, leaf area increasing in order to improve photon capture. The leaves probably decrease in size as an austerity measure only when fluence rates fall below a certain tolerance threshold.

Although unaffected by supplementary far-red light, the chlorophyll a : b ratio decreased at low levels of blue light; while it has been suggested that this cryptochrome-controlled response may serve to balance the activity of photosystems I and II under leafy canopy shade where far-red light is predominant, phytochrome would be a vastly superior mediator. While the effects of the various light treatments on the chlorophyll a content of leaves were rather inconsistent, this tended to increase with the fluence rate of blue light and fall at higher levels of far-red.

Stomatal morphogenesis and gas exchange were studied intensively. For a given stomatal pore size, the density of stomata on the epidermis has a direct effect on the conductance of the leaf to CO₂ and water vapour; hence, unless the carboxylation capacity is limiting, such changes will affect the maximum rate of photosynthesis. In this study leaf area was lower at high fluence rates, and stomatal density on both epidermes increased while stomatal size fell because of the simultaneous effect on epidermal expansion. Light is not the only factor affecting expansion, however, and in addition herbaceous species usually show an innate decline in leaf area towards the apex. More densely packed, smaller pores are generally thought to allow easier diffusion of gas, but in the case of epidermal expansion, a more subtle effect on pore shape may complicate matters.

Other possible effects on stomatal density arise from changes in either the total population of leaf protoderm cells or the proportion of these converted to stomata (the stomatal index). In this project the protoderm population was estimated from the stomatal and the undifferentiated cell densities and the leaf area. Reduced blue and PAR fluence rates had significant but opposing effects on the population, while far-red was ineffective. In contrast, the stomatal index was reduced by supplementary far-red but was unaffected by blue or PAR fluence rate. Child *et al.* [1981] reported a smaller SI in the presence of supplementary far-red for the same species at rather lower PAR fluence rates. Stomatal size was apparently unaffected by supplementary far-red light.

It is apparent, therefore, that both the colour and the absolute fluence rate of light are potentially significant factors in controlling leaf expansion and stomatal development in the natural environment. Fluence rate, through its effects on leaf area, is probably the dominant factor determining stomatal density in this species. However, while this response may be of value in acclimation, there is no obvious motive for phytochrome control of stomatal induction.

CO₂ and water vapour gas analysers coupled to a small leaf cuvette were used to investigate the effect of the morphogenic changes on gas exchange. Surprisingly, the steady-state stomatal conductance was not measurably affected by the different PAR fluence rates under which the plants were grown; photosynthetic rates and inter-cellular CO₂ concentrations were also scarcely affected. Plants grown under supplementary far-red light showed, if anything, slightly higher conductances despite their lower stomatal density. These results may indicate that the "feedback" control of stomatal aperture is immune to the presence of different fluence rates during development. The gas exchange work was carried out at fairly low PAR fluence rates ($<200 \mu\text{mol m}^{-2}\text{s}^{-1}$); had higher levels of PAR been available, it would have been interesting to determine whether the growth treatments had any effect on the maximum attainable conductance or photosynthetic rate.

The kinetics of stomatal opening in response to dim red and blue light were similar under the experimental conditions, even though blue light has been proved responsible for early morning opening in the desert species, *Malva* (Zeiger *et al.*, 1981). In general, stomatal

opening is most sensitive to blue light, and it is probably this rather than any spectrally-dependent difference in the rate of opening that restricts the dawn response to the blue region of the spectrum. Rapid stomatal opening has been correlated with shade tolerance in several tree species, so it would be interesting to discover whether photomorphogenic factors are also involved.

APPENDIX I

In order to make the various parameters derived from the natural daylight research readily accessible in graphical form, an algorithm, "FAUKES", was written to take data directly from file and display it on a screen or draw it on paper. The language used was FORTRAN IV and the graphics instructions were carried out by calls to the widely used GINO subroutine library (Computer Aided Design Centre, Cambridge, U.K.). It would have been easy to construct the program to handle this data specifically, but it was obvious that such a facility could be of use to many workers if it were designed with an element of flexibility in mind. In view of the great precision with which modern plotting machines repeatedly can produce line drawings in colour, there would have been little point in producing graphs of such poor quality that they would require tracing before becoming acceptable for publication. Conversely, it was considered that the amount of information the user would have to give the program should be as small as possible, in order to save time. FAUKES was developed on the PDP11/44 machine (Digital Equipment Corp., Maynard, U.S.A.) at the Computer Graphics Centre of the University of Leicester, and is interfaced to an S3663 colour graphics display (Sigma Electronic Systems Ltd., Horsham, U.K.) and a C1012 incremental graph plotter (California Computer Products Inc., Anaheim, U.S.A.).

In its final form, FAUKES is able to accept any simple list of x and y values and will plot them conventionally, although up to fourteen simultaneous variables are permissible. The user is asked how many variables are involved, and the data is read in from Channel 4. This data file consists of data blocks of the form:-

<variable 1> <variable 2> [<variable 3> ... <variable 14>]

Subsequently, the user has four options; he may either abort the program (STOP = 0), ask it to display a crude graph of the relationship between a pair of variables (FAST DISPLAY = 999), display a graphical figure with specified axis labels, legends, etc. (DISPLAY = 2), or draw a copy of the display onto paper (DRAW = 1). Of course, as more than two variables can be involved, the user must specify which should be plotted on the x and y axes. The algorithm finds the maximum and minimum values of these two and the total number of data blocks in the file; it then tabulates them for the user. If FAST DISPLAY has been selected, these maxima and minima are automatically used to position and scale the axes, and the graph is displayed as a series of small triangles connected by straight lines.

Considerable refinement is possible using DISPLAY, however, as the user must provide a number of plotting instructions. In this way the position of each axis is specified, along with its five graduation pips and legend. When drawn onto paper, the figures are half A4 size, so the user must indicate whether the upper or the lower half should be used; wide margins are left around the figure. The user must also specify the symbols to be used (0=none; 1=dots; 2=triangles; 3=inverted triangles; 4=plusses; 5=crosses; 6=squares; 7=diamonds; 8=circles; 9=stars) and whether or not he requires lines to be drawn between points. A useful option for certain kinds of data is to direct the algorithm to divide the data into four discontinuous x classes and calculate the mean and standard error of the data falling within each. Subsequently, the four "error bars" are included in the figure. A further refinement enables FAUKES to plot more than one set of data in the same figure. The user merely has to specify how many data blocks are to be allocated to the

current symbol. If the number of blocks equals or exceeds that in the file, the program proceeds to plot all the data points. If a negative number is entered, any remaining blocks are ignored. The symbol corresponding to each set of points may be given a "key title" which is positioned anywhere on the figure or, if not required, at a point outside the plotting window. After all these instructions have been accepted, the figure is displayed on a colour monitor via a microprocessor interface. Further plotting is possible but the user must first specify whether the screen is to be cleared (or the paper wound on to the next page) or not; subsequent figures can in this way be superimposed.

PROGRAM FAWKES

```

C .....
C ...This program displays and draws 2-dimensional graphs.
C It takes data from channel 4 (comprising any number of
C data units; each unit contains the simultaneous values of
C upto 14 variables).
C The user specifies which variable should be plotted on the x and y
C axes, and whether a hard copy of the figure is required; a number
C of other plotting options are also available.
C .....

COMMON X(14), XPIPS(5), YPIPS(5), IHEAD(20,20), IH(20), XHEAD(20),
AYHEAD(20), ISY(20), ICOL(20), ISET(20), IXLAB(20), IYLAB(20), IC(10),
BIX, IY, T(4), TT(4), N(4), XVERT, YHORI, IUP, ILIN, ISTAT, XPOS, MS, NX,
CININ, YMIN, XMAX, YMAX, ICON, NCH, YINC, XINC
DATA IC/1,1,5,2,1,2,5,7,1,7/

C      initialise the colour display
      CALL S3663

C      initial instructions
1030 CALL PRIN

      IF(ICON.EQ.999)CALL RAPID
      IF(ICON.EQ.2)CALL USER
      IF(ICON.NE.0)GOTO 3678
      CALL DEVEND
      STOP

3678 CONTINUE

C      display or draw the figure
      CALL FIGURE

C      reset the program
      CALL RESET
      GOTO 1030

      END

SUBROUTINE MIN(X, IX, IY, XMIN, XMAX, YMIN, YMAX)

C      This subroutine stores any new maxima or minima

```

REAL X(14)

```
IF(X(IX).LT.XMIN)XMIN=X(IX)
IF(X(IX).GT.XMAX)XMAX=X(IX)
IF(X(IY).GT.YMAX)YMAX=X(IY)
IF(X(IY).LT.YMIN)YMIN=X(IY)
```

RETURN

END

SUBROUTINE AXES

C This subroutine inserts the axes and their labels

```
COMMON X(14),XPIPS(5),YPIPS(5),IHEAD(20,20),IH(20),XHEAD(20),
ATHEAD(20),ISY(20),ICOL(20),ISET(20),IXLAB(20),IYLAB(20),IC(10),
BIX,IY,T(4),TT(4),N(4),XVERT,YHOR,IUP,ILIN,ISTAT,XPOS,NS,NX,
CXMIN,YMIN,XMAX,YMAX,ICON,NCH,YINC,XINC
```

C insert the x and y axis lines

```
CALL PENDEL(1,1.0,0)
CALL WINDO2(10.0,190.0,1.0,249.0)
DO 3777 I=1,2
  CALL MOVTO2(XPIPS(I),YHOR1)
  CALL LINTO2(XPIPS(5),YHOR1)
  CALL LINTO2(XPIPS(1),YHOR1)
  CALL MOVTO2(XVERT,YPIPS(1))
  CALL LINTO2(XVERT,YPIPS(5))
3777 CALL LINTO2(XVERT,YPIPS(1))
```

C insert the legends on each axis

```
CALL CHASIZ(4.0,3.0)
```

C x-axis

```
CALL MOVTO2(XPOS,YPIPS(1))
CALL TRANSF(0)
CALL MOVBY2(20.0,-15.0)
CALL CHAARR(IXLAB,20,2)
CALL TRANSF(1)
```

C y-axis

```
CALL MOVTO2(XPOS,YPIPS(1))
CALL TRANSF(0)
CALL MOVBY2(-25.0,5.0)
CALL CHAARR(IYLAB,20,2)
CALL CHAARR(0.0)
CALL TRANSF(1)
```

C insert and label the five graduation pips on each axis

```
CALL CHASIZ(3.0,3.0)
DO 1000 I=1,5
  CALL MOVTO2(XVERT,YPIPS(I))
  CALL SYMBOL(3)
  CALL TRANSF(0)
  CALL MOVBY2(-23.0,1.0)
  CALL CHAFIX(YPIPS(I),7,2)
  CALL TRANSF(1)
```

```

      CALL NOVTO2(XPIPS(I),YHORI)
      CALL SYMBOL(3)
      CALL TRANSF(0)
      CALL NOVBY2(-13.0,-6.0)
1000  CALL CHAFIX(XPIPS(I),7,2)
      CALL TRANSF(1)

```

```

      RETURN

```

```

      END

```

SUBROUTINE SINDOL(I)

C This subroutine controls the selection of symbols
C for each set of data units.

```

      IF(I.EQ.0)RETURN
      IF(I.NE.1)GOTO 3664
      CALL DOT(0.35)
      RETURN
3664 CALL SYMBOL(I-1)

```

```

      RETURN

```

```

      END

```

SUBROUTINE STAT1

C This subroutine keeps a tally of the sample size, sum of y, and
C sum of y squared in each of the four x classes.

```

      COMMON X(14),XPIPS(5),YPIPS(5),IHEAD(20,20),IH(20),IHEAD(20),
      AYHEAD(20),ISY(20),ICOL(20),ISET(20),IXLAB(20),IYLAB(20),IC(10),
      BIX,IY,T(4),TT(4),N(4),IVERT,YHORI,IUP,ILIN,ISTAT,XPOS,MS,NX,
      CXIN, YHIN, XMAX, YMAX, ICON, NCH, YINC, XINC

```

C find into which x class, if any, the data falls

```

      I=1
1020 XT=(XPIPS(I)+3*XPIPS(I+1))/4
      XB=(XPIPS(I)+3*XPIPS(I+1))/4
      IF(X(IY).LE.XT.AND.X(IY).GE.XB)GOTO1010
      I=I+1
      IF(I.GT.4)RETURN
      GOTO1020

```

```

1010 CONTINUE

```

C update y sample size, sum of y, and sum of y squared for the class

```

      N(I)=N(I)+1
      T(I)=T(I)+X(IY)
      TT(I)=TT(I)+X(IY)**2

```

```

      RETURN

```

```

      END

```

SUBROUTINE STAT2

```

C      This subroutine calculates the standard error in each of the
C      four x classes, and inserts the error bars and class widths
C      in the figure.

      COMMON X(14), XPIPS(5), YPIPS(5), IHEAD(20,20), IH(20), XHEAD(20),
      AYHEAD(20), ISY(20), ICOL(20), ISET(20), IXLAB(20), IYLAB(20), IC(10),
      BIX, IY, T(4), TT(4), N(4), XVERT, YHORI, IUP, ILIN, ISTAT, XPOS, MS, NX,
      CXMIN, YMIN, XMAX, YMAX, ICON, NCH, YINC, XINC

      DO 5000 I=1,4
C      calculate class centre and width
      IF(N(I).LE.1)GOTO 5000
      BRS=(XPIPS(I)+XPIPS(I+1))*0.5
      WD=(BRS+XPIPS(I))*0.5-BRS

C      calculate mean and standard error of mean
      XM=T(I)/N(I)
      VAR=(TT(I)-(T(I)**2)/N(I))/(N(I)-1)
      SE=SQRT(VAR/N(I))

C      insert the error bar and class width in figure
      CALL MOVTO2(BRS,XM-SE)
      CALL LINDY2(0.0,SE*2)
      CALL MOVTO2((BRS-WD),XM)
      CALL LINDY2(WD*2,0.0)

5000 CONTINUE

      RETURN

      END

```

SUBROUTINE PRIME

```

C      This subroutine prompts the user to give initial instructions
C      to the algorithm.

      COMMON X(14), XPIPS(5), YPIPS(5), IHEAD(20,20), IH(20), XHEAD(20),
      AYHEAD(20), ISY(20), ICOL(20), ISET(20), IXLAB(20), IYLAB(20), IC(10),
      BIX, IY, T(4), TT(4), N(4), XVERT, YHORI, IUP, ILIN, ISTAT, XPOS, MS, NX,
      CXMIN, YMIN, XMAX, YMAX, ICON, NCH, YINC, XINC

C      how many variables are there?
      WRITE(5,1263)
1263 FORMAT(1X/' HOW MANY VARIABLES? (2-14) '/')
      READ(5,*)NCH

C      how is the data to be processed?
1050 WRITE(5,1010)
1010 FORMAT(1X/' 0 = STOP PROGRAM',

```

```

      A' 1 = DRAW THE FIGURE BEING DISPLAYED'
      B' 2 = DISPLAY      999 = FAST DISPLAY (AUTOMATIC)'
6010 READ(S,*)ICON

```

```

      IF(ICON.EQ.0)RETURN
1000 IF(ICON.GE.2)GOTO 5060

```

```

C    ... otherwise, switch to plotter
      CALL SEVEND
      CALL CC1012
C    ... and return with the current instructions
      RETURN

```

```

5060 CONTINUE

```

```

C    which variables correspond to the x and y axes?
      WRITE(S,4060)
4060 FORMAT(1X/' WHICH IS THE X VARIABLE & WHICH IS THE Y VARIABLE?')
      READ (S,*)IX,IY

```

```

C    find minimum and maximum of the x and y channels, and number of
C    sets

```

```

      XMAX=-10000
      YMAX=-10000
      XMIN=10000
      YMIN=10000
      NX=0

```

```

7569   READ(4,*,END=7570)(X(I),I=1,NCH)
      NX=NX+1
      CALL MIN(X, IX, IY, XMIN, XMAX, YMIN, YMAX)
      GOTO 7569

```

```

7570 REWIND 4

```

```

C    tabulate
      WRITE (S,1020)XMIN, XMAX, YMIN, YMAX, NX
1020 FORMAT(1X/'      MIN      MAX'/' X',2(F12.5)/' Y',2(F12.5),10X,
11S,' SCANS')
      RETURN
      END

```

SUBROUTINE USER

```

C    This subroutine prompts the user to give the algorithm explicit
C    instructions to generate the figure.

```

```

      COMMON X(14),XPIPS(5),YPIPS(5),IHEAD(20,20),IH(20),XHEAD(20),
      AYHEAD(20),ISY(20),ICOL(20),ISET(20),IXLAB(20),IYLAB(20),IC(10),
      BIX,IY,T(4),TT(4),N(4),XVERT,YHORI,IUP,ILIN,ISTAT,XPOS,MS,NX,
      CXMIN,YMIN,XMAX,YMAX,ICON,NCH,YINC,XINC

```

```

C    in terms of x and y, where should the axes be positioned, and
C    where are the graduation 'pips' required?
      WRITE(S,1030)
1030 FORMAT(1X/' Y AXIS <?> ALONG X & X AXIS <?> ALONG Y '/)

```

```

      READ(S,*)XVERT,YHOR;
      WRITE(S,1040)
1040  FORMAT(1X/' 5 PIPS ALONG X & 5 PIPS ALONG Y AXES AT...'/)
      READ(S,*)XPIPS,YPIPS

C      what are the legends for the axes? ( : marks the mid-point)
      WRITE(S,4667)
4667  FORMAT(1X/' X & Y LEGENDS...'/12X,1H:/)
      READ(S,8466)IXLAS,IYLAB
8466  FORMAT(20A2/20A2)

C      when drawn, should the figure be in the upper half of the page?
C      should the symbols be connected by lines?
C      are error bars required?
      WRITE(S,8233)
8233  FORMAT(1X/' UPPER PLOT? LINES? STATS? <0 OR 1>'/)
      READ(S,*)IUP,ILIN,ISTAT

C      include the legends in the figure.
      XPOS=XPIPS(1)

C      IT is a tally of the data units processed.
      IT=0

C      sets of the plotted data units may be assigned different symbols.
C      MS is a tally of the number of sets
      MS=0

5782      MS=MS+1

C      which symbols are required for this set of how many data units?
C      return if less than one.
      WRITE(S,3773)
3773  FORMAT(1X/' SYMBOL CODE? <0-9> HOW MANY POINTS? <-VE=STOP>'/)
      READ(S,*)ISY(MS),ISET(MS)
      IF(ISET(MS).LT.1)RETURN
C      select corresponding colour
      ICOL(MS)=IC(ISY(MS)+1)

C      what is the legend for this set?
      WRITE(S,3010)
3010  FORMAT(1X/' WHAT IS THE TEXT FOR THE HEADER?'/)
      READ(S,3020)((IHEAD(MS,II),II=1,20)
3020  FORMAT(20A2)

C      where in the figure is the legend for this set to be placed?
      WRITE(S,3030)
3030  FORMAT(1X/' HEADER POSITION (MM)? <60-170 & CA. 110>'/)
      READ(S,*)IXHEAD(MS),IYHEAD(MS)

      IT=IT+ISET(MS)

      IF(IT.GE.NX)RETURN
      GOTO 5782

      END

```

SUBROUTINE RAPID

C This subroutine provides the algorithm with instructions based
C upon parameters of the data rather than asking the user.

```
COMMON X(14),XPIPS(5),YPIPS(5),IHEAD(20,20),IH(20),XHEAD(20),  
ATHEAD(20),ISY(20),ICOL(20),ISET(20),IXLAB(20),IYLAB(20),IC(10),  
BIX,IY,T(4),TT(4),N(4),XVERT,YHORI,IUP,ILIN,ISTAT,XPOS,MS,NX,  
CXMIN,YMIN,XMAX,YMAX,ICON,NCH,YINC,XINC
```

C the axes are placed at the minima of the x and y channels
C no error bars are drawn
C lines are drawn between the symbols
C the figure is drawn at the bottom of the page
C the axes legends are not included
C all the data units are included in a single set
C the 'pips' are inserted at 25% intervals

```
4070 XVERT=XMN  
YHORI=YMIN  
ISTAT=0  
ILIN=1  
IUP=0  
MS=1  
XPOS=-10000  
ISET(1)=NX  
ISY(1)=1  
ICOL(1)=4  
XINC=(XMAX-XMIN)/4.0  
YINC=(YMAX-YMIN)/4.0  
XHEAD(1)=500.0  
YHEAD(1)=500.0  
XPIPS(1)=XMN  
YPIPS(1)=YMIN  
DO 3000 I=2,5  
XPIPS(I)=XPIPS(I-1)+XINC  
3000 YPIPS(I)=YPIPS(I-1)+YINC  
  
RETURN  
  
END
```

SUBROUTINE FIGURE

C This subroutine controls the display or drawing of the figure.

```
COMMON X(14),XPIPS(5),YPIPS(5),IHEAD(20,20),IH(20),XHEAD(20),  
ATHEAD(20),ISY(20),ICOL(20),ISET(20),IXLAB(20),IYLAB(20),IC(10),  
BIX,IY,T(4),TT(4),N(4),XVERT,YHORI,IUP,ILIN,ISTAT,XPOS,MS,NX,  
CXMIN,YMIN,XMAX,YMAX,ICON,NCH,YINC,XINC
```

C set-up the figure space
CALL WINDO2(10.0,190.0,1.0,249.0)
IF(IUP.EQ.1.AND.ICON.EQ.1)CALL SHIFT2(0.0,125.0)
CALL CHASIZ(3.0,3.0)

C write keys to the symbols for each set of data units
DO 7494 MZ=1,MS
CALL MOVTO2(XHEAD(MZ),YHEAD(MZ))
CALL PENSEL(ICOL(MZ),1.0,0)
CALL SIMBOL(ISY(MZ))


```

        CALL MOVBY2(4.0,-2.0)
        DO 6392 II=1,20
6392      IH(II)=IHEAD(RZ,II)
7494      CALL CHAARR(IH,20,2)

C      scale and position the plot
C      ... but leave room for the axes labels
        CALL SHIFT2(60.0,20.0)
C      define the size of the plot
        WITF=110
        HYTE=85
C      plot only those points within the approximate area of the axes
        CALL WINDOW2(95.0,WITF+65.0,15.0,HYTE+25.0)
        IF(IUP.EQ.1.AND.ICON.EQ.1)CALL WINDOW2
A(95.0,WITF+65.0,140.0,HYTE+150.0)
C      scale the coordinate range to fill the plot area
        CALL SCALE2(WITF/(XPIPS(5)-XPIPS(1)),HYTE/(YPIPS(5)-YPIPS(1)))
C      ...and reposition minima to bottom left
        CALL SHIFT2(-1.0*XPIPS(1),-1.0*YPIPS(1))

C      reset the statistics tallies to zero
        CALL TALLY0(T,TT,N)

C      plot the sets of points

C      IT = total number of data units up to end of current set
C      RZ = number of current set
C      IFLAG=1 for first data unit in set; IFLAG=0 for rest
C      I = data unit counter

        IT=ISET(1)
        RZ=1
        IFLAG=1
        I=0
        CALL PENSEL(ICOL(1),1.0,0)
1070      I=I+1
        READ(4,*)(X(IJ),IJ=1,NCH)
        IF(ILIN.EQ.0.OR.IFLAG.EQ.1)CALL MOVTO2(X(IX),X(IY))
        IF(ILIN.EQ.1)CALL LINTO2(X(IX),X(IY))
        CALL SIMBOL(ISTY(RZ))
        IF(ISTAT.EQ.1)CALL STAT1
        IFLAG=0
        IF(I.LT.IT.AND.I.LT.NX)GOTO1070
        IF(ISTAT.EQ.1)CALL STAT2
        IF(I.GE.NX)GOTO7932
        RZ=RZ+1
        IF(ISET(RZ).LT.0)GOTO7932
        IFLAG=1
        IT=IT+ISET(RZ)
        CALL PENSEL(ICOL(RZ),1.0,0)
        GOTO1070

7932 CONTINUE

        REWIND 4

C      insert the axes
        CALL AXES

C      empty the internal buffer memory of the colour display
        IF(ICON.CE.2)CALL S5000Q(-1)

```

RETURN

END

SUBROUTINE RESET

- C This subroutine resets the algorithm for further plots.

```
COMMON X(14),XPIPS(5),YPIPS(5),IHEAD(20,20),IH(20),XHEAD(20),  
ATHEAD(20),ISY(20),ICOL(20),ISET(20),IXLAB(20),IYLAB(20),IC(10),  
SIX,IY,T(4),TT(4),N(4),XVERT,YHORI,IUP,ILIN,ISTAT,XPOS,MS,NX,  
CMIN,YMIN,XMAX,YMAX,ICON,NCH,YINC,XINC
```

- C reset the transformations to unity
CALL TRANSF(2)

- C clear the screen or page if required
WRITE(S,8860)

```
8860 FORMAT(1X/' CLEAR? (0,1)'/)  
READ (S,*)ICLEAR  
IF(ICLEAR.EQ.1)CALL PICCLE
```

```
IF(ICON.GE.2)RETURN
```

```
WRITE(S,3745)
```

```
3745 FORMAT(1X/' THE PLOT OUTPUT FILE IS ON CHANNEL 3...')
```

```
CALL NOVTO2(0.0,0.0)
```

```
CALL DEVEND
```

- C reinitialise the colour display
CALL S3663
CALL DEVICE(2,7)

RETURN

END

SUBROUTINE TALLY0(T,TT,N)

- C This subroutine resets the statistical tallies to zero

```
DIMENSION T(4),TT(4),N(4)
```

```
DO 1746 I=1,4
```

```
T(I)=0
```

```
TT(I)=0
```

```
1746 N(I)=0
```

RETURN

END

RETURN

END

SUBROUTINE RESET

C This subroutine resets the algorithm for further plots.

COMMON X(14),XPIPS(5),YPIPS(5),IHEAD(20,20),IH(20),XHEAD(20),
AYHEAD(20),ISY(20),ICOL(20),ISET(20),IXLAB(20),IYLAB(20),IC(10),
SIX,IY,T(4),TT(4),N(4),IVERT,YHORI,IUP,ILIN,ISTAT,XPOS,MS,NX,
CXIN,YNIN,XMAX,YMAX,ICON,NCH,YINC,XINC

C reset the transformations to unity
CALL TRANSF(2)

C clear the screen or page if required
WRITE(S,8860)

8860 FORMAT(1X/' CLEAR? <0,1>'//)
READ (S,*)ICLEAR
IF(ICLEAR.EQ.1)CALL PICCLE

IF(ICON.GE.2)RETURN

WRITE(S,3745)

3745 FORMAT(1X/' THE PLOT OUTPUT FILE IS ON CHANNEL 3...')

CALL NOVTO2(0.0,0.0)

CALL DEVEND

C reinitialise the colour display
CALL S3663
CALL DEVICE(2,7)

RETURN

END

SUBROUTINE TALLY0(T,TT,N)

C This subroutine resets the statistical tallies to zero

DIMENSION T(4),TT(4),N(4)

DO 1746 I=1,4

T(I)=0

TT(I)=0

1746 N(I)=0

RETURN

END

APPENDIX II

Deriving the SPD in terms of the mean SPFR in discrete wavebands is essentially simple if the sensitivity of the spectroradiometer is known at each wavelength

$$\text{SPFR}_\lambda = \frac{d_\lambda \cdot \lambda}{n \cdot h \cdot c} \cdot m_\lambda \quad \dots\dots\dots(1)$$

where λ is the wavelength

SPFR_λ is the unknown SPFR of the waveband centred at λ

d_λ is the effective chart pen deflection it causes, taking into account the attenuation setting

n is Avogadro's number

h is Planck's constant

c is the velocity of light

m_λ is the multiplication factor ($i_\lambda \cdot D_\lambda$)

where i_λ is the spectral irradiance of the calibration lamp

and D_λ is the effective chart pen deflection it causes

Tasker [1977] used a computer to perform this calculation, but supplied the 41 values of d for each unknown SPD by visually estimating the mean deflection in each waveband and typing the data into a file. In the work reported here, the number of SPDs necessarily recorded demanded that a more rapid and less tedious procedure be developed. Funds were not available to purchase a suitable machine to interface the spectroradiometers directly to a computer, so analogue recording onto x-y chart recorder paper was retained, but the "raw" SPD was transferred to the computer by an electronic digitiser (Freescan, Ferranti Ltd., Edinburgh, U.K.) With the chart paper positioned beneath a transparent template on the digitiser table, the cursor was slid along the plotted SPD line and its position electronically recorded at appropriate intervals. The sensitivity of the spectroradiometers was about 10dB lower in the far-red than in the blue; consequently, when recording SPDs a lower attenuation setting was often switched in to record d at longer wavelengths. In order to handle SPDs recorded at two levels of attenuation, two "record coordinates" buttons were defined; the computer was then able to distinguish between the "maximum attenuation" (defined initially) and "x10" points. Recording the coordinates at fixed wavelength intervals, as had been the custom when using visual read-off was found to be inefficient in practice, so instead the subroutine DIGIT was designed to accept a series of points representing approximate inflections along the curve. Thereafter, DIGIT linearly interpolates between them and solves the equations at nanometer intervals. The data is allocated to 10 nm classes and the mean SPFR in each is calculated from Eq.1 above. DIGIT therefore is the source of the d list; it forms the basis of two programs used to derive most of the SPD information reported here; CALIS was the source of the multiplication factors (Eq.1) subsequently used by SUCAR to derive the SPD of an unknown source.

CALIS first of all copies onto the output file a list of data (taken from Butler et al. [1964] describing the spectral absorbance of Pr and Pfr - see below). It then accepts the digitised calibration SPDs and generates, via DIGIT, lists of multiplication factors, each corresponding to a photomultiplier calibration voltage.

SUCAR selects the appropriate list of factors on the basis of a

code number, and calculates the d_{λ} list (and hence the SPFR list, via Eq.1) and the solar position, via DIGIT and ALAZ respectively. This data is tabulated on output channel 3. The algorithm also derives a number of parameters of the SPDs. The fluence rates corresponding to 400-700 nm (PAR), 410-500 nm (blue), 510-600 nm (green), 610-700 nm (red), 710-800 nm (far-red) are derived by a simple summation; Tasker's [1977] use of Simpson's rule for numerical integration here is erroneous, as this procedure is based upon class boundaries and not class centres. The SPFR ratios at 660/730 nm (3) and 410-500/610-700 nm (blue:red ratio) are also calculated.

The photoequilibrium of phytochrome is calculated in a manner similar to Tasker [1977], but without a running mean. The procedure is based upon the total absorbance of each form of phytochrome through the whole SPD and the quantum efficiency of photoconversion (Hartmann, 1966). The absorbance data (that of Butler *et al.* [1964] for low molecular weight phytochrome) is read in along with the multiplication factors from the output file of CALIB. SUCAR uses all five of the input/output channels permitted by the RSX operating system of the computer, so it is unable to read the data file itself, whereas CALIB has a "spare" input channel which can be assigned to the task. Pratt [1978] showed that the photoequilibrium of less degraded phytochrome never exceeded 75% (instead of 81% calculated by Butler *et al.* [1964]). However, as Pratt and Cundiff [1976] only describe the absorbance in the red and far-red, their data cannot replace that of Butler *et al.* for the purposes of this program; hence, as an approximation, a simple arithmetic correction was applied. The relative cycling rate is also calculated according to the procedure adopted by Johnson and Tasker (1980).

These parameters were tabulated onto output channel 4 in a suitable form to be read directly by FAUKES.

PROGRAM CALIB

```

C .....
C ...This program processes "digitised" calibration spectral scans and
C produces a list of multiplication factors corresponding to the anode
C voltage at which each of the calibrations was carried out.
C Channel 1 input is the spectral irradiance of the calibration lamp.
C Channel 3 input is the spectral absorbance of phytochrome (data of
C Butler et al, 1964).
C .....

      REAL VERT(41),NPL(41),E(82)
      INTEGER NHEAD(7)

      CALL ASSIGN(3,'PHYTO.DAT')
      CALL ASSIGN(1,'NPL.DAT')

C  read the absorbance data from file 'PHYTO.DAT'
      READ(3,*)E

C  ignore the initial 9 lines of the digitiser output file
      READ(2,1000)
      1000 FORMAT(/////////)

C  read the spectral irradiance data for the lamp from file 'NPL.DAT'

```

```

      READ(1,*)NPL
C    tabulate the absorbance data
      WRITE(4,2020)E
2020 FORMAT(10(10(1X,F6.3)/))
C    calculate the multiplication factors for the forty-one 10nm
C    wavebands corresponding to each digitised scan
      3    CONTINUE
C    read the maximum attenuation range factor used for this scan
      READ(2,2010,END=1030)MAXRF
2010 FORMAT(I1)
      CALL DIGIT(VERT,MAXRF)
C    this subroutine is identical to that used by SUCAR
C    calculate the multiplication factors
      DO 1 I=1,41
1    VERT(I)=NPL(I)/VERT(1)
C    tabulate
      DO 2 N=1,40,5
2    WRITE(4,1010)(VERT(I), I=N,N+4)
      WRITE(4,1010)VERT(41)
1010 FORMAT(5(F10.5,1X))
      COT03
1030 STOP
      END

```

```

      READ(1,*)NPL
C   tabulate the absorbance data
      WRITE(4,2020)E
2020 FORMAT(10(10(1X,F6.3)/))
C   calculate the multiplication factors for the forty-one 10nm
C   wavebands corresponding to each digitized scan
3     CONTINUE
C   read the maximum attenuation range factor used for this scan
      READ(2,2010,END=1030)MAXRF
2010 FORMAT(I1)
      CALL DIGIT(VERT,MAXRF)
C   this subroutine is identical to that used by SUGAR
C   calculate the multiplication factors
      DO 1 I=1,41
1     VERT(I)=NPL(I)/VERT(1)
C   tabulate
      DO 2 N=1,40,5
2     WRITE(4,1010)(VERT(I),I=N,N+4)
      WRITE(4,1010)VERT(41)
1010 FORMAT(5(F10.5,1X))
      COT03
1030 STOP
      END

```


PROGRAM SUGAR

```

C -----
C This program processes the "digitised" field data from the natural
C daylight work. Channel 1 input is equivalent to channel 4 output
C from CALIB; Channel 2 input is equivalent to the digitiser output
C plus an initial line of data concerning solar position. Channel 3
C output contains the tabulated SPDs, while Channel 4 output contains
C parameters such as zeta, PAR, etc.
C -----

```

```

      DOUBLE PRECISION DCNT,RA,DECL,GST,AL,AZ
      REAL HEAD(15),VERT(41),FACT(41,9),TOT(6),ER(41),EFR(41)
      INTEGER I(WAVE(41),START,STOP)

```

```

C read Pr and Pfr spectral absorbance data
      READ(1,*)ER,EFR
C read calibration factors
      READ(1,*,END=3337)FACT

```

3337 CONTINUE

```

C set-up wavelengths array
      DO 2000 I=1,41
1000 I(WAVE(I)=(I+39)*10
C calculate 2 * pi
      PI2=6.28318530718*PI

```

```

C read Right Ascension, Declination, and Greenwich Siderial Time
C for 0000 GMT on the day concerned (from Ephemeris tables)
      READ(2,*)RA,DECL,GST
C convert declination angle to radians
      DECL=(DECL/360.0)*PI2

```

```

C step over the initial lines that head the digitiser output files
      READ(2,1090)NVOLT
1090 FORMAT(A1////////)

```

1 CONTINUE

```

C process each SPD separately by iteration
C NVOLT = photomultiplier voltage code
C MAXRF = highest attenuation range factor used
C NHR,NMIN = Greenwich Mean Time

```

```

      READ(2,1020,END=3)NVOLT,MAXRF,NHR,NMIN
1020 FORMAT(2(I1),2(I2))

```

```

C convert time to decimal hours
      DCNT=NHR+NMIN/60.0

```

```

C read the heading line of this SPD data block (scan no., date, etc.)
      READ(2,1080)HEAD
1080 FORMAT(2X,15(A4))

```

```

      CALL ALAZ(RA,DECL,GST,DCNT,AL,AZ)

```

```

      CALL DIGI*(VERT,MAXRF)

```

```

C scale the SPFR bands according to the corresponding sensitivity
C of the instrument, and convert from energy to quantum units
      DO 2 I=1,41

```

```

2   VERT(1)=VERT(1)*FACT(1,NVOLT)*(39+1)*0.08358

C   integrate for PAR, blue, green, red, and far red broadbands
    CALL TOTALE(1,31,VERT,TOT(1))
    CALL TOTALE(2,11,VERT,TOT(2))
    CALL TOTALE(12,21,VERT,TOT(3))
    CALL TOTALE(22,31,VERT,TOT(4))
    CALL TOTALE(32,41,VERT,TOT(5))

C   calculate 660/730 and blue/red ratios
    ZETA=VERT(27)/VERT(34)
    BR=TOT(2)/TOT(4)

    CALL PSTAT(ER,EFR,VERT,PHI,TOT(6))

    CALL DATA(IWAVE,VERT,DCNT,AL,AZ,HEAD)

C   output the parameters of this SPD
    WRITE(4,1040)NMIN,DCNT,AL,AZ,ZETA,PHI,BR,TOT
1040 FORMAT(13,1X,6F9.3/5X,6(F12.5))

    GOTO 1

3   STOP
    END

SUBROUTINE DATA(IWAVE,VERT,DCNT,AL,AZ,HEAD)

C   this subroutine tabulates (beneath the header, decimal CNT and solar
C   position) the SPD data as forty-one 10nm SPFR bands with their
C   wavelengths alongside

    REAL VERT(41),HEAD(15)
    INTEGER IWAVE(41)

    WRITE(3,1000)HEAD,DCNT,AL,AZ
1000 FORMAT(1X,15(A4)/3F8.2)
    DO 2 N=1,40,5
2   WRITE(3,1010)((IWAVE(I),VERT(I),I=N,N+4)
    WRITE(3,1010)IWAVE(41),VERT(41)
1010 FORMAT(5(1X,13,F11.5))

    RETURN
    END

SUBROUTINE TOTALE(START,STOP,VERT,TOT)

C   This subroutine numerically integrates any part of the SPD
C   between 400nm(=1) and 800nm(=41)

    REAL VERT(41)
    INTEGER START,STOP

    TOT=0.0

```

```

      DO 1 I=START,STOP
1     TOT=TOT+VERT(I)
      TOT=TOT*0.01

      RETURN

      END

```

SUBROUTINE PSTAT(ER,EFR,VERT,PHI,CYCLE)

```

C   This subroutine calculates the photoequilibrium and cycling
C   rate of phytochrome

      REAL ER(41),EFR(41),VERT(41)

C   -----
C   after Tasker, 1977
      R=0
      S=0
C   calculate the total absorbance of Pr and of Pfr
      DO 1 I=1,40
        R=R+(VERT(I)*EFR(I))
1     S=S+(VERT(I)*ER(I))
C   calculate the Pfr/Ptot ratio
      PHI=1/(1+0.813*(R/S))
      PHI=(PHI/0.8)*0.75
C   -----

C   calculate the relative cycling rate
      CYCLE=((1-PHI)*S+PHI*R)/100

      RETURN

      END

```

SUBROUTINE DIGIT(VERT,MAXRF)

```

C   This subroutine converts the digitiser data block into
C   forty-one 10nm bands

      REAL VERT(41)
      INTEGER MAXRF,RCODE,RF

C   first coordinate....
      I=1
      N=1
      M=1
      VERT(N)=0
C   X1,Y1 = coordinates of digitised point
C   RCODE = 3 = white button = maximum range factor
C           = 1 = green button = maximum range factor - 1
      READ(2,1030)RCODE,X1,Y1
1030 FORMAT(2X,I1,2(1X,E14.7))
C   .....scale X1 accordingly

```

```

RF=MAXRF
IF(RCODE.EQ.1)RF=RF-1
Y1=Y1+10**RF

```

C subsequent coordinate....

```

2 READ(2,1030)RCODE,X2,Y2
  IF(X2.LE.X1)COTO2
  RF=MAXRF
  IF(RCODE.EQ.1)RF=RF-1
  Y2=Y2+10**RF

```

C linear interpolation and classification

```

  SLOPE=(Y2-Y1)/(X2-X1)
  DIS=Y1-SLOPE*X1
  3 IF(X2.GT.394+1)COTO1
  X1=X2
  Y1=Y2
  COTO2
  1 VERT(N)=((SLOPE*(394+1)+DIS)*0.1)+VERT(N)
  I=I+1
  N=N+1
  IF(I.GT.410)COTO4
  IF(N.LE.10)COTO3
  N=N+1
  VERT(N)=0
  N=1
  COTO3

```

4 CONTINUE

C beyond 303nm, move to beginning of next SPD data block

```

  READ(2,1060)MAXRF
  1060 FORMAT(A1)
  IF(MAXRF.NE.1H-)COTO4
  READ(2,1060)MAXRF

```

RETURN

END

SUBROUTINE ALAZ(RA,DECL,CST,DCNT,AL,AZ)

C This subroutine calculates the position of the sun as
C "azimuth angle" (the angle subtended between sun and north)
C and "solar angle" (the angle subtended between sun and horizon)

DOUBLE PRECISION DLMT,DECL,RA,CST,SLAT,CLAT,
 1DCNT,P12,HA,SALT,AL,CAZ,AZ

C calculate 2 x pi

P12=6.0*DATAN(1.0D0)

C calculate sine and cosine of latitude of site

SLAT=DSIN((52.7833/360.0)*P12)
 CLAT=DCOS((52.7833/360.0)*P12)

C local time = Greenwich time + 4 minutes for every degree east

C (1.23 DEG WEST = -0.0833 HOURS)
 DLMT=DCNT-0.0833

```

C   calculate hour angle (= time since sun was due south)
    HA=((GST+1.002739*DLMT)-(RA+((DCMT/24.0)*0.0656)))*15.0
C   hour angle must be positive
    IF(HA.LT.0.0)HA=HA+360
C   convert to radians
    HA=(HA/360.0)*PI2

C   calculate solar angle
    SALT=(DSIN(DECL)*SLAT)+(DCOS(DECL)*CLAT*DCOS(HA))
    AL=(DASIN(SALT)/PI2)*360.0

C   calculate solar azimuth
    CAZ=(DSIN(DECL)-SLAT*SALT)/(CLAT*DCOS((AL/360.0)*PI2))
    AZ=(DACOS(CAZ)/PI2)*360.0
    IF(DSIN(HA).GT.0.0)AZ=360.0-AZ

    RETURN

    END

```

BIBLIOGRAPHY

- AL-HATTAB, A.H. [1968] Ned. Landbouwhoges. Wageningen 68(12):1-111
- ALLAWAY, W.G. [1981] in "Stomatal Physiology" Jarvis, P.G. and Mansfield, T.A. (eds) Cambridge University Press; pp. 71-85
- ARNOLD, G.P. [1975] in "Light as an Ecological Factor II" Evans, G.C., Bainbridge, R. and Rackham, O. (eds) Blackwell, Oxford; pp. 1-26
- ATKINS, W.R.G., POOLE, H.H. and STANBURY, F.A. [1937] Proc. R. Soc. (B) 121:427-50
- BARRS, H.D. [1971] Ann. Rev. Plant Physiol. 22:223-36
- BARSCH-GOLLNAU, S., RITTERBUSCH, A. and MOHR, H. [1980] Plant Cell Environ. 3:363-70
- BARTLEY, M.R. and FRANKLAND, B. [1982] Nature 300:750-2
- BEGGS, C.J., HOLMES, M.J., JABSEN, M. and SCHAFER, E. [1980] Plant Physiol. 66:615-8
- BERRY, J. and BJORKMAN, O. [1980] Ann. Rev. Plant Physiol. 31:491-543
- BJORKMAN, O. [1981] in "Physiological Plant Ecology" (Encycl. Plant Physiol. (ns) 12a) Lange, O.L., Nobel, P.S., Osmond, C.B. and Ziegler, H. (eds) Springer-Verlag, Berlin; pp. 57-107
- BJORKMAN, O. and HOLMGREN, P. [1963] Physiol. Plant. 16:889-914
- BJORKMAN, O., BOARDMAN, N.K., ANDERSON, J.M., THORNE, S.W., GOODCHILD, D.J. and PYLOTIS, N.A. [1972a] Carnegie Inst. Wash. Yearb. 71:115-35
- BJORKMAN, O., LUDLOW, M.M. and MORROW, P.A. [1972b] Carnegie Inst. Wash. Yearb. 71:115-35
- BLACK, M. and SHUTTLEWORTH, J.E. [1974] Planta 117:57-66
- BLACKMAN, G.E. and RUTTER, A.J. [1948] Ann. Bot. (NS) 11:1-26
- BLACKMAN, G.E. and WILSON, C.L. [1951] Ann. Bot. (NS) 15:373-408
- BOARDMAN, N.K. [1977] Ann. Rev. Plant Physiol. 28:355-77

BODKIN, P.C., SPENCE, D.H.N. and WEEKS, D.C. [1980] New Phytol.
84: 533-42

BOISSARD, J., SPRUIT, C.J.P. and ROLLIN, P. [1968]
Ned. Landbouwhoges. Wageningen 68(17): 1-5

BORTHWICK, H.A., HENDRICKS, S.B. and PARKER, M.W. [1948a]
Botan. Gaz. 110: 103-18

[1948b]
in "Vernalisation and Photoperiodism" Murneck, A.Z. and
Whyte, R.O. (eds) Chronica Botanica, Waltham, U.S.A.;
pp. 71-7

[1952]
Proc. Natl. Acad. Sci. U.S.A. 38: 929-34

BORTHWICK, H.A., HENDRICKS, S.B., SCHNEIDER, M.J., TAYLORSON, R.B.
and TOOLE, V.K. [1969] Proc. Natl. Acad. Sci. U.S.A.
64: 479-86

BORTHWICK, H.A., HENDRICKS, S.B., TOOLE, E.H. and TOOLE, V.K.
[1952] Proc. Natl. Acad. Sci. U.S.A. 38: 662-66

[1954] Botan. Gaz. 115: 205-25

BRENNER, P.H., EL SAEED, E.A.K. and SCOTT, R.K. [1967]
J. Agri. Sci. 69: 283-90

BROWN, J.A.M. and KLEIN, W.H. [1971] Plant Physiol. 47: 393-9

BUNNIK, N.J.J. [1978] Ned. Landbouwhoges. Wageningen
78(1): 1-172

BUNNING, E. [1936] Ber. Deutsch. Botan. Ges. 54: 590-607

BUNNING, E. and NOSER, I [1969] Proc. Natl. Acad. Sci. U.S.A.
62: 1018-22

BUTLER, W.L., HENDRICKS, S.B. and SIEGELMAN, H.W. [1964]
Photochem. Photobiol. 3: 521-28

BUTLER, W.L. and LANE, H.C. [1965] Plant Physiol. 40: 13-17

BUTLER, W.L., LANE, H.C. and SIEGELMAN, H.W. [1963]
Plant Physiol. 38: 514-19

CATNEY, H.M. and BORTHWICK, H.A. Botan. Gaz. 125: 232-6

CHILD, R., MORGAN, D.C. and SMITH, H. [1981] New Phytol.
89: 545-55

CHON, N.P. and BRIGGS, W.R. [1966] Plant Physiol.
41: 1715-24

- COLWELL, J.E. [1974] *Remote Sensing Environ.* 3:175-83
- COSGROVE, D.J. [1981] *Plant Physiol.* 67:584-90
- COWAN, I.R. and MILTHORPE, F.L. [1968] in "Water deficits and Plant Growth I" Kozlowski, T.T. (ed) Academic Press, London; pp. 137-93
- CRESSWELL, E.G. and CRINE, J.P. [1981] *Nature* 291:583-5
- CUMMING, B.G., HENDRICKS, S.B. and BORTHWICK, H.A. [1965] *Canad. J. Bot.* 43:825-53
- CUTTER, E.G. [1978] "Plant Anatomy: I Cells and Tissues" 2nd. Ed. Edward Arnold, London.
- DENGLER, N.G. [1980] *Canad. J. Bot.* 58:717-80
- DEITZER, G., HAYES, R. and JABEN, N. [1979] *Plant Physiol.* 64:1015-21
- DENNISON, D.S. [1981] in "Physiology of Movements" (Encycl. Plant Physiol. (NS) 7) Haupt, W. and Feinleib, M.E. (eds) Springer-Verlag, Berlin; pp. 506-66
- DOWNS, R.J., HENDRICKS, S.B. and BORTHWICK, H.A. [1957] *Botan. Gaz.* 118:199-208
- DUBBE, D.R., FARQUHAR, G.D. and RASCHKE, K. [1978] *Plant Physiol.* 62:413-7
- ELLER, B.M., GLATTLI, R. and FLACH, B. [1981] *Flora* 171:170-85
- EVANS, G.C. [1966] in "Light as an Ecological Factor" Bainbridge, R., Evans, G.C. and Rackham, O. (eds) Blackwell, Oxford; pp. 53-76
- EVANS, L.T. [1975] "Daylength and the flowering of plants" McMillan, Melbourne.
- _____ [1976] *Aust. J. Plant Physiol.* 3:207-17
- EVANS, L.T. and ALLAWAY, W.G. [1972] *Aust. J. Biol. Sci.* 25:885-93
- EVANS, L.T. and KING, R.W. [1969] *Zelt. Pflanzenphysiol.* 60:277-88
- EVANS, L.T., BORTHWICK, H.A. and HENDRICKS, S.B. [1965] *Aust. J. Biol. Sci.* 18:745-62
- EVERETT, M.S. and BRIGGS, W.R. [1970] *Plant Physiol.* 45:679-83
- FARQUHAR, G.D. and SHARKEY, T.D. [1982] *Ann. Rev. Plant Physiol.* 33:317-45

- FEDERER, C.A. and TANNER, C.B. [1966] *Ecology* 47:555-60
- FENNER, M. [1980] *New Phytol.* 84:103-6
- FITTER, A.H. and ASHNORE, C.J. [1974] *New Phytol.* 73:997-1001
- FOX, L.R. and HILLMAN, W.S. [1968] *Plant Physiol.* 43:1799-1804
- FRANKLAND, B. [1981] in "Plants and the Daylight Spectrum"
Smith, H. (ed), Academic Press, London; pp. 187-204
- FRANKLAND, B. and LETANDRE, R.J. [1978] *Photochem. Photobiol.*
27:223-30
- FUNKE, G.L. [1948] in "Vernalisation and Plant Photoperiodism"
Hurneek, A.E. and Whyte, R.O. Waltham, U.S.A.; pp. 79-82
- PUKSHANSKI, L. [1981] in "Plants and the Daylight Spectrum"
Smith, H. (ed), Academic Press, London; pp. 21-42
- GAASTRA, P. [1959] *Nederl. Landbouwk. Gesch. Wageningen*
59(13):1-68
- GABA, V. and BLACK, M. [1979] *Nature* 278:51-4
- GATES, D.M. [1980] "Biophysical Ecology" Springer-Verlag,
New York.
- GAY, A.P. and HURD, R.C. [1975] *New Phytol.* 75:37-46
- GINKEL, C.V. and HAMMANS, J.W.K. [1980a] *Photochem. Photobiol.*
31:377-83
- _____ [1980b] *Photochem. Photobiol.*
31:385-95
- GOLDBERG, B. and KLEIN, W.H. [1977] *Solar Energy* 19:3-13
- GOODFELLOW, S. and BARKHAM, J.P. [1974] *Acta Botan. Neerl.*
23:225-30
- CORSKI, T. [1976] *Naturwissenschaften* 63:530-1
- _____ [1980] *Int. J. Biometeor.* 24:361-5
- CORSKI, T., CORSKA, K. and NOWICK, J. [1977] *Flora* 166:249-60
- CRINE, J.P. [1979] "Plant Strategies and Vegetation Processes"
John Wiley, Chichester, U.K.
- CRINE, J.P. [1981] in "Plants and the Daylight Spectrum"
Smith, H. (ed), Academic Press, London; pp. 159-86
- CUTTMAN, A. [1968] *Appl. Optics.* 7:2377-81

- HACKER, M., HARTMANN, K.M. and MOHR, H. [1964] *Planta* 136:181-6
- HADFIELD, V. [1974] *J. Appl. Ecol.* 11:179-99
- HALL, A.E., CANACHO-B, S.E. and KAUFMANN, M.R. [1975] *Physiol. Plant.* 33:62-5
- HALL, A.E., SCHULZE, E.D. and LANGE, O.L. [1976] in "Water and Plant Life: problems and modern approaches" (Ecological Studies 19) Lange, O.L., Kappen, L. and Schulze, E.D. (eds) Springer-Verlag, Berlin; pp. 169-88
- HANNER, K.C. and BONNER, J. [1938] *Botan. Gaz.* 100:388-431
- HANKE, J. HARTMANN, K.M. and MOHR, H. [1969] *Planta* 86:235-49
- HARTMANN, K.M. [1966] *Photochem. Photobiol.* 5:349-366
- _____ [1967] *Zeit. Naturforsch.* 22b:1172-5
- HEATHCOTE, L. BANBRIDGE, K. and McLAREN, J.S. [1979] *J. Exp. Bot.* 30:347-53
- HENDERSON, S.T. [1977] "Daylight and its Spectrum"
Hilger, Bristol
- HILLMAN, W.S. [1966a] *Plant Physiol.* 41:907-8
- _____ [1966b] *Science* 154:1360-2
- _____ [1967] *Ann. Rev. Plant. Physiol.* 18:301-24
- _____ [1972] in "Phytochrome" Mitrakos, K. and Shropshire, W. (eds), Academic Press, London; pp. 573-86
- HOLLAND, R.W.K. and VINCE, D. [1971] *Planta* 98:232-43
- HOLMES, M.G. [1981] in "Plants and the Daylight Spectrum"
Smith, H. (ed), Academic Press, London; pp. 147-58
- HOLMGREN, P. [1968] *Physiol. Plant.* 21:676-98
- HOLMGREN, P., JARVIS, P.G. and JARVIS, M. [1965] *Physiol. Plant.* 18:557-73
- HOLMES, M.G. and MCCARTNEY, H.A. [1976] in "Light and Plant Development" Smith, H. (ed) Butterworths, London; pp 467-76
- HOLMES, M.G. and SMITH, H. [1975] *Nature* 254:512-4
- _____ [1977a] *Photochem. Photobiol.* 25:533-8

25:539-45 [1977b] Photochem. Photobiol.

25:551-7 [1977c] Photochem. Photobiol.

HOLMES, M.G. and SCHAFER, E. [1981] *Planta* 153:267-72

HOLMES, M.G. and WAGNER, E. [1980] *J. Theor. Biol.* 83:255-65

HOPKINS, W.G. [1971] *Canad. J. Bot.* 49:467-70

HOPKINS, W.G. and HILLMAN, W.S. [1965] *Planta* 65:157-166

HOSHIZAKI, T. and HAMNER, K.C. [1969] *Photochem. Photobiol.*
10:87-96

HSIAO, T.C. [1976] in "Transport in Plants" (Encycl. Plant
Physiol. (NS) 2B) Pitman, N.G. and Lüttge, U. (eds)
Springer-Verlag, Berlin; pp. 195-221

HSIAO, T.C., ALLAWAY, W.G. and EVANS, L.T. [1973] *Plant Physiol.*
51:82-8

HULL, J.N. [1954] *Illum. Eng.* 19:21-8

HUTCHINSON, B.A. and HATT, D.R. [1977] *Agri. Meteorol.* 18:255-65

JAGGARD, K.W., BISCOE, P.V. and LAWRENCE, D.K. [1982] "Chemical
Manipulation of Crop Growth" McLaren, J.S. Butterworths,
London; pp. 139-50

JABBen, M. and DEITZER, G. [1979] *Plant Physiol.* 63:481-5

92:575-84 [1980] *Ber. Deutsch. Botan. Ges.*

JARVIS, P.G. [1964] *J. Ecol.* 52:545-71

JARVIS, P.G. and MORISON, J.I.L. [1981] in "Stomatal Physiology"
Jarvis, P.G. and Mansfield, T.A. (eds) Cambridge University
Press; pp.247-279

JOHNSON, T.B., SALISBURY, F.B. and CONNOR, C.T. [1967]
Science 155:1663-5

JOHNSON, C.B. [1980] *Plant Cell Environ.* 3:45-51

JOHNSON, C.B. and TASKER, R. [1979] *Plant Cell Environ.* 2:259-65

JOHNSON, M.S., ISSAIAS, T., BROGARDN, T. and JOHNSON, A. [1976]
Physiol. Plant. 36:229-32

JORDAN, C.F. [1969] *Ecology* 50:663-6

25:539-45 [1977b] Photochem. Photobiol.

25:551-7 [1977c] Photochem. Photobiol.

HOLMES, H.G. and SCHAFER, E. [1981] *Planta* 153:267-72

HOLMES, H.G. and WAGNER, E. [1980] *J. Theor. Biol.* 83:255-65

HOPKINS, W.G. [1971] *Canad. J. Bot.* 49:467-70

HOPKINS, W.G. and HILLMAN, W.S. [1965] *Planta* 65:157-166

HOSHIZAKI, T. and HANNER, K.C. [1969] *Photochem. Photobiol.*
10:87-96

HSIAO, T.C. [1976] in "Transport in Plants" (Encycl. Plant
Physiol. (NS) 2B) Pitman, H.G. and Lüttge, U. (eds)
Springer-Verlag, Berlin; pp. 195-221

HSIAO, T.C., ALLAWAY, W.G. and EVANS, L.T. [1973] *Plant Physiol.*
51:82-8

HULL, J.N. [1954] *Illum. Eng.* 19:21-8

HUTCHINSON, B.A. and MATT, D.R. [1977] *Agri. Meteorol.* 18:255-65

JAGGARD, K.W., BISCOE, P.V. and LAWRENCE, D.K. [1982] "Chemical
Manipulation of Crop Growth" McLaren, J.S. Butterworths,
London; pp. 139-50

JABBen, M. and DEITZER, G. [1979] *Plant Physiol.* 63:481-5

92:575-84 [1980] *Ber. Deutsch. Botan. Ges.*

JARVIS, P.G. [1964] *J. Ecol.* 52:545-71

JARVIS, P.G. and MORISON, J.I.L. [1981] in "Stomatal Physiology"
Jarvis, P.G. and Mansfield, T.A. (eds) Cambridge University
Press; pp. 247-279

JOHNSON, T.B., SALISBURY, F.B. and CONNOR, C.T. [1967]
Science 155:1663-5

JOHNSON, C.B. [1980] *Plant Cell Environ.* 3:45-51

JOHNSON, C.B. and TASKER, R. [1979] *Plant Cell Environ.* 2:259-65

JOHNSON, M.S., ISSAIAS, T., BROCARD, T. and JOHNSON, A. [1976]
Physiol. Plant. 36:229-32

JORDAN, C.F. [1969] *Ecology* 50:663-6

- JOSE, A. and SCHAFER, E. [1978] 138:25-28
- JOSE, A. and VINCE-PRUE, D. [1977a] *Planta* 135:95-100
-
- [1977b] *Planta* 136:131-4
-
- [1978] *Photochem. Photobiol.*
27:209-16
- KADMAN-ZAHVI, A. and EPHRAT, E. [1976] *Isrl. J. Bot.* 25:11-23
- KARVE, A. [1961] *Zelt. Bot.* 49:47-72
- KASPERBAUER, M.J. [1971] *Plant Physiol.* 47:775-8
- KASPERBAUER, M.J., BORTHWICK, H.A. and HENDRICKS, S.B. [1963]
Botan. Gaz. 124:444-451
- KATAYANA, T.C. [1964] *Jap. J. Bot.* 18:349-83
- KENDRICK, R.E. and HILLMAN, W.S. [1971] *Amer. J. Bot.*
58:424-8
- KENDRICK, R.E. and SPRUIT, C.P.J. [1973] *Photochem. Photobiol.*
18:139-44
- KENDRICK, R.E., SPRUIT, C.J.P. and FRANKLAND, B. [1969]
Planta 88:293-302
- KING, R.W. [1974] *Aust. J. Plant Physiol.* 1:445-57
- KING, R.W. and CUNNING, B.G. [1972] *Planta* 108:39-57
- KING, R.W., SCHAFER, E., THOMAS, B. and VINCE-PRUE, D. [1982]
Plant Cell Environ. 5:395-404
- KING, R.W., VINCE-PRUE, D. and QUAIL, P.H. [1978] *Planta*
141:15-22
- KLEIN, W.H., EDWARDS, J.L. AND SHROPSHIRE, W. [1967]
Plant Physiol. 42:264-70
- KRIZEK, D.T. and ORNROD, D.P. [1980] *Amer. J. Hort. Sci.*
105:936-9
- KUJPER, P.J.C. [1964] *Plant Physiol.* 39:952-5
- KUNNAR, M. [1981] "Spectral Reflectance and Light Interception
by Crop Canopies" PhD Dissertation, Nottingham University.
- LANE, N.C., CATHEY, H.M. and EVANS, L.T. [1965] *Amer. J. Bot.*
52:1006-14
- LANGE, O., LOSCH, R., SCHULZE, E.D. and KAPPEN, L. [1971] *Planta*:
100:76-86

- LECHARNEY, A. and JACQUES, R. [1982] *Plant Cell Environ.* 5:31-6
- LEE, S.M. and CAVERS, P.B. [1981] *Canad. J. Bot.* 59:1776-86
- LICHTENTHALER, H.K., BUSCHMANN, C., DOLL, M., FIETZ, H.-J., BACH, T., KOZEL, U., NEIER, D. and RAHNSDORF, U. [1981] *Photosynth. Res.* 2:115-41
- LLERAS, E. [1977] *Acta Amazonica* 7:473-6
- LOOHIS, W.E. [1965] *Ecology* 46:14-7
- LOSCH, R. and SCHENK, B. [1978] *J. Exp. Bot.* 29:781-7
- LOSER, G. and SCHAFER, E. [1980] in "The Blue Light Syndrome" Senger, H. (ed) Springer-Verlag, Berlin; pp. 244-50
- MANCINELLI, A. [1980] *Photochem. Photobiol.* 32:853-7
- MANSFIELD, T.A. [1965] *Proc. R. Soc. Lond. (B)* 162:567-74
- _____ [1976] *J. Exp. Bot.* 27:559-64
- MANSFIELD, T.A. and HEATH, O.V.S. [1963] *J. Exp. Bot.* 14:334-52
- MANSFIELD, T.A. and MEIDNER, H. [1966] *J. Exp. Bot.* 17:510-21
- MARTIN, E.S. and MEIDNER, H. [1971] *New Phytol.* 70:923-8
- MEIDNER, H. [1975] *J. Exp. Bot.* 26:666-73
- _____ [1976] *J. Exp. Bot.* 27:172-4
- MEIDNER, H. and MANSFIELD, T.A. [1968] (eds) "Physiology of Stomata" McGraw-Hill, Maidenhead, U.K.
- MEIDNER, H. and SHERIFF, D.W. [1976] "Water and Plants" Blackie, Glasgow.
- MEIJER, G. [1959] *Acta Botan. Neerl.* 8:189-246
- _____ [1968] *Acta Botan. Neerl.* 17:9-14
- MOHR, H. [1957] *Planta* 49:389-405
- _____ [1972] "Lectures on Photomorphogenesis" Springer-Verlag, Berlin.
- MOHR, H., DRUMM, H., SCHMIDT, R. and STEINITZ, B. [1979] *Planta* 146:369-76
- MONSI, N. and SAEKI, T. *Jap. J. Bot.* 14:22-52
- MONTEITH, J.L. [1973] "Principles of Environmental Physics" Edward Arnold, London.

- _____ [1975] in "Light and Plant Development"
Smith, H. (ed) Butterworths, London; pp. 447-460
- MORGAN, D.C. [1977] "The Function of Phytochrome in the Natural Environment" PhD Dissertation, Nottingham University.
- MORGAN, D.C., CHILD, R. and SMITH, H. [1981] *Planta* 151:497-8
- MORGAN, D.C., O'BRIEN, T. and SMITH, H. [1980] *Planta* 150:95-101
- MORGAN, D.C. and SMITH, H. [1978a] *Planta* 141:187-94
- _____ [1978b] *Nature* 273:534-6
- _____ [1979] *Planta* 145:253-8
- _____ [1981a] in "Encyclopedia of
Plant Physiology" (NS) 12A Lange, O.L., Nobel, P.S.,
Osmond, C.B. and Ziegler, H. (eds) Springer-Verlag,
Berlin; pp. 109-34
- _____ [1981b] *New Phytol.* 88:239-48
- MOSS, R.A. and LOONIS [1952] *Plant Physiol.* 27:370-91
- NOURAVIEZ, I. [1958] *Bull. Soc. Bot. France.* 105:467-75
- McARTHUR, R.H. and WILSON, E.D. [1967] "The theory of island
biogeography" Princeton University Press.
- MCCARTNEY, H.A. [1975] "Spectral distribution of solar
radiation within and above crops" PhD Dissertation,
Nottingham University.
- McCree, K.J. [1972a] *Agri. Meteorol.* 9:191-216
- _____ [1972b] *Agri. Meteorol.* 10:443-53
- MCCULLOUGH, J.M. and SHROPSHIRE, W. [1970]
Plant Cell Physiol. 11:139-48
- McLAREN, J.S. and SMITH, H. [1978] *Plant Cell Environ.* 1:61-7
- McROBBIE, E.A.C. [1981] in "Stomatal Physiology" Jarvis, P.G.
and Mansfield, T.A. (eds) Cambridge University Press;
pp. 51-70
- NANDA, K.K. and HANNER, K.C. [1958] *Botan. Gaz.* 120:14-25
- NORMAN, J.M. and TANNER, C.B. [1969] *Agron. J.* 61:847-9
- OCAWA, T. ISHIKAWA, H., SHIMADA, K. and SHIBATA, K. [1978]
Planta 142:61-5

- OUTLAW, W.H., MAYNE, B.C., ZENGER, U. and MANCHESTER, J. [1981]
Plant Physiol. 67:12-16
- OUTLAW, W.H., MANCHESTER, J., DICANELLI, C.A., RANDALL, D.D.,
RAPP, B. and VEITH, G.N. [1979] Proc. Natl. Acad. Sci. U.S.A.
76:6371-5
- PALEVITZ, B.A. [1981] in "Stomatal Physiology" Jarvis, P.G.
and Mansfield, T.A. (eds) Cambridge University Press;
pp. 1-23
- PARKER, H.W., HENDRICKS, S.B. and BORTHWICK, H.A. [1950]
Botan. Gaz. 111:242-52
- PARKER, H.W., HENDRICKS, S.B., BORTHWICK, H.A. and SCULLY, M.J.
[1945] Science 102:152-5
-
- [1946] Botan. Gaz. 108:1-26
- PATTERSON, D.J. [1982] Weed Sci. 30:25-30
- PENFOUND, W.T. [1931] Am. J. Bot. 18:558-72
- PITTENDRIGH, C.S. [1980] in "Biological Clocks in Seasonal
Reproductive Cycles" Follett, B.K. and Follett, D.E.
(eds) John Wright, Bristol; pp. 1-35
- PITTENDRIGH, C.S. and CALDAROLA, P.C. [1973] Proc. Natl. Acad.
Sci. U.S.A. 70:2697-701
- POPE, D.J. and LLOYD, P.S. [1975] in Evans et al. [1975],
pp. 383-408
- POPP, H.W. [1926] Amer. J. Bot. 13:706-36
- PRATT, L.H. [1978] Photochem. Photobiol. 27:81-105
- _____ [1982] Ann. Rev. Plant Physiol. 33:557-582
- PRATT, L.H. and CUNDIFF [1975] Photochem. Photobiol. 21:91-7
- QUAIL, P.H., MARNE, D. and SCHAFER, E. [1973] Nature 245:189-91
- RABIDEAU, C.S. FRENCH, C.S. and HOLT, A.S. [1946]
Amer. J. Bot. 33:769-77
- RASCHKE, K. [1972] Plant Physiol. 49:229-34
- _____ [1975a] Ann. Rev. Plant Physiol. 26:309-40
- _____ [1975b] Planta 125:243-59
- RAVEN, J. [1981] in "Plants and the Daylight Spectrum"
Smith, N. (ed), Academic Press, London; pp. 375-90

- RICHARDSON, S.D. [1959] *Forestry* 32:126-37
- RITTER, A., WAGNER, E. and HOLMES, N.G. [1981] *Planta* 153:556-60
- ROBERTSON, C.W. [1966] *Ecology* 47:640-43
- ROBINSON, N. [1966] "Solar Radiation" Elsevier, New York.
- ROODENBURG, J.W. [1940] *Rec. Trav. Bot. Neerl.* 27:301-74
- ROTH-BEJERANO, N. and ITAI, C. [1981] *Physiol. Plant.* 52:201-6
- ROZENBURG, G.V. [1966] "Twilight: a study in atmospheric optics" Plenum Press, New York.
- SALISBURY, E.J. [1916] *J. Ecol.* 4:83-117
- _____ [1927] *Phil. Trans. R. Soc. Lond. (B)* 216:1-65
- SALISBURY, F.B. [1963] "The Flowering Process" Pergamon, Oxford.
- _____ [1981a] *Plant Physiol.* 67:1230-8
- _____ [1981b] in "Encyclopedia of Plant Physiology" (NS) 12A Lange, O.L., Nobel, P.S., Osmond, C.B. and Ziegler, H. (eds) Springer-Verlag, Berlin; pp. 135-62
- SARKAR, H.K. and SONG, P.-S. [1982] *Photochem. Photobiol.* 35:243-6
- SAWHNEY, R. [1977a] *Planta* 133:97-102
- _____ [1977b] *Planta* 133:103-6
- _____ [1977c] *Planta* 133:107-9
- SCHAFER, E. [1975] *J. Math. Biol.* 2:41-56
- SCHAFER, E. and MOHR, H. [1974] *J. Math. Biol.* 1:9-15
- SCHNEIDER, M.J., BORTHWICK, H.A. and HENDRICKS, S.B. [1967] *Amer. J. Bot.* 54:1241-49
- SCHNEIDER, M.J. and STINSON, W.R. [1971] *Plant Physiol.* 12:312-5
- _____ [1972] *Proc. Natl. Acad. Sci. U.S.A.* 69:2150-4
- SCHOUGH, P.C., ZINSOU, C. and SIBI, M. [1980] *J. Exp. Bot.* 31:1211-6
- SCHULZE, E.D., LANGE, O., BUSCHBON, U., KAPPEN, L. and EVENARI, M. [1972] *Planta* 108:239-70

- SCHURMANN, B. [1959] *Flora* 147:471-520
- SENGER, H. [1980] (ed) "The Blue Light Syndrome" Springer-Verlag, Berlin.
- SESTAK, Z., CATSKY, J. and JARVIS, P.G. [1971] (eds) "Plant Photosynthetic Production: Manual of Methods" Junk, The Hague.
- SHARKEY, T.D. and RASCHKE, K. [1981a] *Plant Physiol.* 68:1170-4
 _____ [1981b] *Plant Physiol.* 68:33-40
- SINCLAIR, T., HOFFER, R.M. and SCHREIBER, M.M. [1971] *Agron. J.* 63:864-68
- SINCLAIR, T. and LENON, E. [1973] *Solar Energy* 15:89-97
- SHELL, C.S.G. and LANG, A.R.G. [1976] *Agri. Met.* 16:161-70
- SHROPSHIRE, W. [1972] in "Phytochrome" Shropshire, W. and Mitrakos, K. Academic Press, London; pp. 161-84
 _____ [1973] *Solar Energy* 15:99-105
- SHUTTLEWORTH, J.E. and BLACK, M. [1977] *Planta* 135:51-5
- SMITH, N. [1970] *Nature* 227:665-668
 _____ [1974] in "Seed Ecology" Heydecker, W. (ed) Butterworths, London; pp. 219-31
 _____ [1975] "Phytochrome and Photomorphogenesis" McGraw-Hill, Maidenhead, U.K.
 _____ [1980] in "Plants and their Atmospheric Environment" Grace, J., Ford, E.D. and Jarvis, P.G. (eds) Blackwell, Oxford; pp. 93-110
 _____ [1981a] in "Plants and the Daylight Spectrum" Smith, N. (ed), Academic Press, London; pp. 499-508
 _____ [1981b] *Nature* 293:163-5
 _____ [1982] *Ann. Rev. Plant. Physiol.* 33:481-518
- SMITH, N. and HOLMES, M.G. [1977] *Photochem. Photobiol.* 25:547-50
- SPENCE, D.N.N. [1981] in "Plants and the Daylight Spectrum" Smith, N. (ed), Academic Press, London; pp. 245-276
- STOLWIJK, J.A.J. [1954] *Nederl. Landbouwhogeschool. Wageningen* 34(3):181-244

- STOLWIJK, J.A.J. and ZEEVAART, J.A.D. [1955]
Proc. Kon. Ned. Acad. Wet. (Series C) 58:386-96
- STRUTT, J.W. [1871] Phil. Mag. 41:107-20 & 274-79
- TAKIMOTO, A. and HANNER, K.C. [1965a] Plant Physiol. 40:859-64
_____ [1965b] Plant Physiol. 40:859-64
- TAKIMOTO, A. and IKEDA, K. [1960] Botan. Mag. Tokyo 73:175-81
_____ [1961] Plant Cell Physiol. 2:213-29
- TAKIMOTO, A. and NAITO, Y. [1962] Botan. Mag. Tokyo 75:255-63
- TASKER, R. [1977] "Phytochrome and the Light Environment of Woodlands" PhD. Dissertation, Nottingham University.
- TASKER, R. and SMITH, H. [1977] Photochem. Photobiol. 26:487-91
- TAYLOR, A.N. and KERR, G.P. [1941] J. Opt. Soc. Amer. 31:3-8
- THOMAS, B. [1981] in "Plants and the Daylight Spectrum"
Smith, H. (ed) Academic Press, London; pp. 443-59
- THOMAS, B. and DICKENSON, H.C. [1979] Planta 146:545-50
- TRAVIS, A.J. and MANSFIELD, T.A. [1979] Plant Cell Environ. 2:319-23
- TUCKER, D.J. and MANSFIELD, T.A. [1972] Planta 102:140-51
- TURNER, N.R. and VINCE, D. [1969] Planta 84:368-82
- van der VEEN, R. and NEIJER, C. [1959] "Light and Plant Growth"
Philips Technical Library, Eindhoven.
- VEZINA, P.E. and BOULTER, D.W.K. [1966] Canad. J. Bot. 44:1267-84
- VINCE-PRUE, D. [1975] "Photoperiodism in Plants" McGraw-Hill,
Maldenhead, U.K.
_____ [1977] Planta 133:149-56
_____ [1979] in "La Physiologie de la Floraison"
Champagnat, P. and Jacques, R. (eds) CNRS, Paris;
pp. 91-127
_____ [1981] in "Plants and the Daylight Spectrum"
Smith, H. (ed) Academic Press, London; pp. 223-42
- WAGNER, E. and NONN, H. [1966] Photochem. Photobiol. 5:397-406

- WARRINGTON, I.J. and MITCHELL, K.J. [1976]
Agri. Meteorol. 16: 247-62
- WATSON, P. and SMITH, N. [1982] Planta 154: 121-7
- WETHERELL, D.F. and KOUKKARI, W.L. [1970] Plant Physiol. 46: 350-1
- WILD, A. [1979] Ber. Deutch. Botan. Ges. 92: 341-64
- WILDERMANN, A., DRUMM, H., SCHAFER, E. and MOHR, H. [1978]
Planta 141: 211-16
- WITHROW, R.B. and BENEDICT, H.M. [1936] Plant Physiol. 11: 225-249
- WOODS, D.B. and TURNER, N.C. [1972] New Phytol. 70: 77-84
- WOOLLEY, J.T. [1971] Plant Physiol. 47: 656-62
- WOOLLEY, J.T. and STROLLER, E.W. [1978] Plant Physiol. 61: 597-600
- YOCUM, C.S. ALLEN, L.N. and LEMON, E.R. [1964] Agron. J. 56: 249-53
- YOUNG, J.E. [1975] in "Light as an Ecological Factor II"
Evans, G.C., Bainbridge, R. and Rackham, O. (eds) Blackwell,
Oxford; pp. 135-60
- ZAVITOVSKI, J. [1982] Agri. Meteorol. 25: 245-55
- ZEDERBAUR, C. [1908] Forest Quart. 6: 255-62
- ZEIGER, E. and HEPLER, P.K. [1977] Science 196: 887-9
- ZEIGER, E., ARMOND, P. and MELIS, A. [1981] Plant Physiol. 67: 17-20
- ZEIGER, E., BLOOM, A.J. and HEPLER, P.K. [1978] What's New in Plant
Physiology, Gaithersburg 9: 29-32
- ZEIGER, E., FIELD, C. and MOONEY, H.A. [1981] in "Plants and the
Daylight Spectrum" Smith, H. (ed); pp. 391-407